



**University
of Antwerp**

Faculty of Pharmaceutical, Biomedical and Veterinary Sciences

Department Biomedical Sciences

The new epigenetic driver role of PPAR α and mitochondria in metabolic dysfunction associated liver disease (MASLD), paving the way towards new therapeutics and diagnostic biomarkers

De nieuwe sturende rol van PPAR α en mitochondriën in de epigenetische regulatie van metabole disfunctie geassocieerde leverziekte (MASLD), een stap dichterbij nieuwe therapeutica en diagnostische biomarkers

Thesis submitted in fulfillment of the requirements for the degree of Doctor in Biochemistry and Biotechnology at the University of Antwerp, defended by

Claudia Theys

Promotor: Prof. Dr. Wim Vanden Berghe

Laboratory of Protein Science, Proteomics and Epigenetic Signaling (PPES)
Antwerp, 2024

Disclaimer

The author allows to consult and copy parts of this work for personal use. Further reproduction or transmission in any form or by any means, without the prior permission of the author is strictly forbidden.

Internal Doctoral Committee

Promotor

Prof. dr. Wim Vanden Berghe
*Laboratory of Protein Science, Proteomics and Epigenetic Signaling (PPES),
Department of Biomedical Sciences, University of Antwerp*

Internal members

Prof. dr. Rosa Rademakers (Chair)
*Applied and Translational Neurogenomics, VIB Center for molecular Neurology,
University of Antwerp*

Prof. dr. Anja Verhulst (Jury-member)
Pathophysiology, Department of Biomedical Sciences, University of Antwerp

Table of Contents

Acknowledgments	3
List of Abbreviations	7
Summary	11
Samenvatting	13
Introduction	17
<i>Chapter 1: PPARα in the epigenetic driver seat of NAFLD: new therapeutic opportunities for epigenetic drugs?</i>	23
<i>Chapter 2: Mitochondrial dysfunctions and MASLD progression: cause or consequence?</i>	49
Thesis Outline and Research Objectives	71
Results	75
<i>Chapter 3: Loss of PPARα function promotes epigenetic dysregulation of lipid homeostasis driving ferroptosis and pyroptosis lipotoxicity in Metabolic Dysfunction Associated Steatotic Liver Disease (MASLD)</i>	77
<i>Chapter 4: Optimisation of mitochondrial DNA methylation detection in an in vitro MASLD model</i>	125
<i>Chapter 5: Mitochondrial GpC and CpG DNA hypermethylation cause metabolic stress induced mitophagy and cholestophagy</i>	145
General Discussion and Future Perspectives	187
<i>Chapter 6: General discussion and future perspectives</i>	187
Academic Curriculum Vitae	201

Acknowledgements

First of all, Woohoo, I made it!!!

Ze zeggen wel eens dat het leven een rollercoaster is. Vier jaar geleden ben ik vol enthousiasme in het karretje genaamd 'PhD' gestapt en wist ik nog niet waar ik aan begon. Wel, nu kan ik zeggen dat mijn PhD bestond uit de ene looping en twister na de andere waardoor je niet meer goed weet wat boven en onder is of waar je gaat uitkomen. Maar op één of andere manier kwam het toch samen in een recht pad naar de finish. Het was een avontuur dat ik nooit meer opnieuw ga beleven en waarvan ik niet de finish had gehaald zonder fantastische mensen rondom mij. Zij hebben mijn hand vastgehouden tijdens deze rit, mij aangemoedigd wanneer ik het even niet meer zag zitten en occasioneel hun oren afgedekt wanneer mijn geschreeuw (aka frustaties) wat te veel werden.

Als eerste zou ik graag mijn promotor **Wim Vanden Berghe** willen bedanken, die mij de kans gegeven heeft om een PhD te starten in PPES. Jouw (meestal nogal ambitieuze) ideeën, open minded kijk naar wetenschap en data, aanmoediging voor nieuwe uitdagingen zoals presenteren op congressen of FWO beurzen schrijven en verdedigen, hebben mij altijd gestimuleerd om out of the box te denken en mijn grenzen te verleggen. Jou te pakken krijgen was soms een uitdaging en om jouw structuur in de chaos of uiteenzettingen op papier bij een brainstorm sessie te begrijpen, heb ik nog een PhD van 4 jaar nodig. Maar puntje bij paaltje was de feedback er altijd en ben ik dankbaar voor de hulp en aanmoediging om het beste uit mijn doctoraat te halen.

I would also like to thank the members of my internal jury, **Prof. Dr. Rosa Rademakers** and **Prof. Dr. Anja Verhulst**. Thank you for the feedback, encouragement and discussion throughout my research project. I'm convinced that the multidisciplinary look on my data, brought my research to a higher level by challenging me to look at it in different ways.

Daarnaast zijn er ook verschillende mensen in het epigenetics team die ik heel graag wil bedanken. Als eerste de mensen van de original squad waarmee ik mijn avontuur begonnen ben, **Emilie, Claudina en Claudio**. **Emilie**, nog voor ik begon aan mijn PhD avontuur, in de voorbereiding van mijn eerste FWO verdediging, heb je mij gesteund en aan mijn zijde gestaan. Je stond altijd open voor een babbeltje, een peptalk als ik het even niet meer zag zitten of een kleine brainstorm over mijn data als ik door het bos de bomen niet meer zag. Ik ben ervan overtuigd dat zonder jouw steun en aanmoediging ik hier vandaag niet had gestaan. Daarom nogmaals dankjewel om een fantastische collega te zijn en mij de weg te wijzen in het doolhof van een doctoraat. **Claudina**, je bent een sterke vrouw die veel bordjes tegelijk in de lucht moet houden. Je hebt een hart van goud en hebt altijd het beste voor met iedereen. Al wil ik je toch nog meegeven om jezelf niet te vergeten in deze chaos. Je verdient het zo hard om gelukkig te zijn, gewaardeerd te worden en te doen waar je energie en plezier uit haalt. Daarom hoop ik met heel mijn hart dat het vervolg van jouw traject iets rustiger en vol plezier mag verlopen. **Claudio**, bedankt voor de herinneringen aan ons dagelijks gelach, gezang in de lift, taal cursus by Claudio tijdens de afwas, ijsjesdates en steun als ik het moeilijk had. Na twee jaar heb ik het plezier gehad om de volgende top collega/bureaubuddy te mogen ontmoeten. **Amber**, Je hebt geen gemakkelijke start gehad van jouw PhD en mag daarom trots zijn op wat je tot nu toe al bereikt hebt. Ik ben ervan overtuigd dat jouw passie voor jouw project en drive om te werken, meer dan voldoende zijn om nog mooie dingen te bereiken in jouw

traject. Daarnaast wil ik jou ook nog bedanken voor het luisterend oor, de aanmoediging en de toffe thee/koffie momentjes waar ik altijd even mijn hart kon luchten of frustraties kon bespreken. Je bent de cheerleader die iedereen eigenlijk nodig zou hebben in heel het traject. Dus dankjewel daarvoor en koester deze eigenschap voor altijd want het gaat je veel mooie dingen brengen in de toekomst. Tot slot, geef ik jou nog 1 raad mee. Onthoud dat het 'maar' een job is en vergeet niet om ook te genieten en te ontspannen (en dat kan nu dubbel met jullie nieuwe huisje 😊). Last but definitely not least, **Laura**. You are just an amazing woman and an example for me on how a work-life balance should be. It is incredible how you combine the passion for your job and science, with a family and just enjoying life. I got to know you as a very kind, supporting and hard working woman that I'm sure of can accomplish everything in life. Thank you for being the best addition to the group I could ever wish for in my last year. I wish you all the best of luck in your next adventure and really hope you find as much joy and passion in your next job!

Dan zijn er nog een paar mensen van het PPES team die niet kunnen ontbreken. **Karen** en **Eva**, ik kan niet de ene zonder de andere benoemen want jullie zijn HET practicum team, maar toch wil ik jullie afzonderlijk bedanken. **Eva**, je hebt het misschien niet door gehad, maar ik kijk op en heb heel veel respect voor hoe jij in het leven staat. Jouw passie voor studenten en jouw job in het algemeen, de assertiviteit en toch enorme steun die je kan geven en jouw relativeringsvermogen zijn voor mij een voorbeeld. Het is iets wat ik in mijn achterhoofd zal houden en ook hoop te bereiken. Je was als student een top practicum begeleidster en vervolgens de houvast en persoon waar je altijd naar toe kon tijdens mijn PhD, dus dankjewel daarvoor. **Karen**, jij stond altijd klaar voor een babbeltje, roddeltje of gewoon eens goed lachen wanneer ik het nodig had. Als jij erbij was kon ik mijn stress altijd wat vergeten en (meestal) eens goed lachen omdat je je mond voorbij had gepraat en er de meest oprechte, maar droge opmerking uit kwam. I just LOVE it! Ik wist altijd wat ik aan jou had en hoe je over dingen dacht zonder een blad voor de mond te nemen. Eén van je mooiste eigenschappen vind ik persoonlijk. Dus dankjewel om mij de relaxpill te geven die ik af en toe (lees: vaak) nodig had. **Joey**, hoe stress niet in jouw woordenboek stond, daar zal ik altijd jaloers op zijn. Ik begrijp nog altijd niet hoe iemand zo chill kan zijn en toch alles voor elkaar kan krijgen op een manier dat ik zelf niet beter zou kunnen. Hoedje af voor dat. Bedankt om mij regelmatig te herinneren aan 'Het komt allemaal wel goed, ge moet zo niet stressen'. Want door de chille manier waarop je dat altijd zei en meende, werd ik ook echt terug rustig. **Herald**, je stond altijd klaar voor vragen en hulp in het labo. Een hele dikke merci daarvoor. Vanaf nu beloof ik dat ik jou niet meer zal lastig vallen met vragen of mails voor (achterstallige) bestellingen. Verzorg je voeten/achillespees goed en niet meer te zot bij badminton/airsoft/padel/... **Ruben**, nooit gedacht dat zo veel droge woord-mopjes en Lord Of The Rings facts uit één persoon konden komen. Je ben een uniek persoon met een hart van goud die altijd klaar staat voor iedereen en daarom alle geluk van de wereld verdient. Dankjewel om altijd te helpen met al mijn vragen, hulp in het labo of gewoon even te ontspannen met een tof babbeltje. Al begreep ik jouw geeky kantje niet altijd, het was wel een plezier om jou met zo veel passie over iets te zien vertellen. Daarom bedankt om mij toch een beetje bij te leren over deze hele (voor mij nieuwe) wereld. **Zainab**, jij was als een zonnetje dat altijd klaar stond met een lach en daardoor altijd een positieve sfeer bracht in het labo. Ik wens jou nog heel veel succes bij Pfizer en al jouw toekomstige uitdagingen. **Hanne**, ik ben blij dat ik toch voor even nog jouw collega kon zijn op PPES. Je stond altijd klaar om te luisteren of te helpen waar nodig. De manier waarop jij een labo volledig hebt geleid naast een leger aan studenten is bewonderingswaardig. Ik hoop dat je nu wat meer rust gevonden hebt in je job en dat je die voor

altijd mag ervaren want dat verdien je. Hopelijk kan ik op een dag ook naar jouw doctoraatsverdediging komen en jou zien stralen. **Bregje**, je hebt alle capaciteiten die een doctoraatsstudent nodig heeft. Je bent een doorzetter, goedlachs en behulpzaam. Dus geloof in jezelf en ga voor jouw doelen en dan ben ik er zeker van dat je alles gaat bereiken wat je wilt. **Silke**, twee labo's combineren is geen gemakkelijke taak, maar ik ben er zeker van dat jij dat kan. Nog heel veel succes in de rest van je doctoraat! **Xaveer** en **Andy**, bedankt voor alle discussies en feedback tijdens de labmeetings.

Dankjewel voor alle feedback en steun aan het GOA team **Evelien, Cedric, Rik, Shivani** en **Tammy**. Samen zijn we begonnen aan dit pittige project en hebben we vele eindeloze vergaderingen doorstaan. Ik hoop dat jullie allemaal een fantastisch doctoraat mogen afleggen en wens jullie veel succes in jullie verdere uitdagingen.

Thank you to all the international people from Cuba, Poland, Ecuador, Thailand and Turkey that I have met during my PhD. I appreciate the tropical and enthusiast atmosphere you all brought to the lab and I'm grateful to have learned so much about all the different cultures.

Dan rest er mij alleen nog een dikke dankjewel aan alle familie en vrienden die mij gedurende heel dit traject gesteund hebben. **Kaat, An, Gert, Alexander** en **Pablo** jullie zijn al sinds dag één mijn grootste cheerleaders. Jullie stonden altijd klaar met een wijntje om een nieuwe milestone die ik bereikt had te vieren of een luisterend oor wanneer ik mijn frustraties even kwijt moest. Dankjewel om er altijd te zijn voor mij en de beste vrienden te zijn die ik kon wensen. Ik zou zeggen het volgende wijntje om dit te vieren, tracteer ik! **Flo, Loucka** en **Lene**, jullie zijn niet gewoon vrienden, maar sister from other misters. Bij jullie kan ik altijd volledig mezelf zijn zonder blad voor de mond en gewoon laten zien hoe het echt met mij gaat. Elke keer dat ik jullie zie ben ik terug in de kampbubble, waar ik alles kan vergeten en gewoon oneindig kan lachen en plezier maken dus dankjewel daarvoor. **Capo** en **Melanie, Kevin en Lien** momentjes samen met jullie zijn altijd een feest vol gelach en ontspanning waardoor ik even kon ontsnappen uit mijn PhD gekte. Dankjewel voor zo veel begrip en aanmoediging tijdens heel mijn traject. Jullie zijn vrienden met een hart van goud. **Britt, Ellen** en **Popskie**, de weg hier naar toe was ongetwijfeld nooit hetzelfde geweest zonder jullie. Zonder al het lachen, gieren, brullen en occasionele kater had ik nooit zo een plezier gehad tijdens mijn studie en nooit begonnen aan dit volgend avontuur. Dankjewel om er toen zo een fantastische tijd van te maken en mij nu zo te steunen tijdens dit avontuur! **Mama en papa**, als er iemand in mij gelooft met oneindige trots, dan zijn jullie het wel. Dankjewel om mij alle kansen te bieden waarmee ik het allerbeste in mijzelf naar boven kon halen en mij gaandeweg op elke seconde te steunen. Jullie zijn mijn rots in de branding en zonder jullie had ik hier niet gestaan. Woorden schieten te kort om mijn dankbaarheid en liefde voor jullie uit te drukken. **Laura/Peet**, ik ben zo oneindig trots en blij dat jij mijn zus bent. Al heel mijn leven ben je een voorbeeld waar ik naar op kijk en die mij bij elke stap helpt en steunt om het beste pad te bewandelen. Ook tijdens dit avontuur stond je altijd voor me klaar, luisterde zonder te oordelen en begreep zonder veel woorden wat ik wou zeggen wanneer niemand dit kon. Zonder deze onvoorwaardelijke steun, begrip en liefde had ik hier niet gestaan dus daar ben ik je oneindig dankbaar voor. WE DID IT! **Bram/Sjarel**, je bent een uniek persoon met zo veel capaciteiten die je zelf maar al te vaak onderschat. Ik ben je enorm dankbaar dat je mij altijd gesteund hebt, mij aangemoedigd hebt om door te blijven gaan en eraan herinnerd dat ik het WEL kon. Geloof in jezelf en dan ben ik er zeker van dat je alles kan bereiken wat je maar wilt. **Arno** en **Delphine**, ook een dikke dankjewel aan jullie

om mij te steunen en mee te leven naar dit moment. Ik had mij geen betere aanvulling aan de familie kunnen wensen. **Tante struif** en **Coachie**, ook jullie verdienen zeker een plekje in het dankwoord. Gedurende heel het traject hebben jullie mij aangemoedigd als jullie eigen dochter. Daarom ben ik dan ook heel blij dat ik dit moment ook met jullie kan delen en vieren. **Carine, Ivo** en **Kristof** vanaf de eerste dag dat ik jullie ontmoet heb, voelde ik mij welkom en thuis. Ik had mij geen betere schoonfamilie kunnen wensen en het doet mij dan ook veel deugd om te zien dat ik jullie als schoondochter/zus ook trots heb kunnen maken.

Tot slot is er nog één persoon die ik niet genoeg kan bedanken voor zijn eeuwige liefde en steun, **Mathias**. Ik ben je oneindig dankbaar voor alle momenten waarop je mij gesteund, getroost of aangemoedigd hebt. Je stond altijd klaar met een knuffel, luisterend oor, bemoedigend woord of hielp mij om alles te relativeren en mijn perfectionisme te temperen wanneer ik het te ver pushte. Met andere woorden, ik kon mij geen betere partner aan mijn zijde wensen. Zonder jou had ik hier vandaag niet gestaan en na dit avontuur ben ik meer dan ooit overtuigd dat met jou aan mijn zijde, ik ALLES kan bereiken. I love you! Alle deuren staan nu open, dus tijd voor het zonnetje om terug te stralen en lots of happy happy joy joy!

Pompebak out 😊

List of Abbreviations

3'UTR	3'-untranslated region
5caC	5-carboxycytosine
5fC	5-formylcytosine
5hmC	5-hydroxymethylcytosine
5meC	5-methylcytosine
6-mA	N ⁶ methyldeoxyadenosine
8-OHdG	8-hydroxy-2'-deoxyguanosine
Acetyl-CoA	Acetyl coenzyme A
AF-1	Activation function one
AF-2	Activation function two
ALT	Alanine aminotransferase
AMPK	AMP-activated protein kinase
AST	Aspartate aminotransferase
Atg8	Autophagy related protein 8
BA	Bile acid
BMIQ	Beta mixture interquartile matrix method
BSA	Bovine serum albumin
CA	Cholic acid
CaMK	Ca ²⁺ /CaM kinase
CAP	Controlled attenuation parameter
CDAHFD	Choline-deficient, L-amino acid-defined, high-fat diet
CDCA	Chenodeoxycholic acid
DAMPs	Danger-associated molecular patterns
DB	Delta beta
DCA	Deoxycholic acid
DEG	Differentially expressed genes
DNMT	DNA methyltransferase
DNMT1	DNA methyltransferase I
Drp1	Dynamin-related protein 1
DTT	1,4- dithiothreitol
E2f8	E2F Transcription Factor 8
ER	Endoplasm reticulum
ETC	Electron transport chain
FA	Fatty acid
FFA	Free fatty acids
FGF21	Fibroblast growth factor 21
Fis1	Fission 1
FXR	Farnesoid X receptor
GABP α	GA-binding protein α
GPx	Glutathione peroxidase
GSH	Gluthathione
H&E	Haematoxylin-eosin
HAT	Histone acetyl transferase
HCC	Hepatocellular carcinoma

HDAC	Histone deacetylase
HDAC1	Histone deacetylase 1
HepG2	Human hepatoma cells
HFD	High fat diet
HMT	Histone methyltransferase
HR	Hinge region
HSP	Heavy strand promotor
IMM	Inner mitochondrial membrane
IRE1 α	Inositol-requiring enzyme 1 α
JMJD	Jumonji C-domain-containing histone demethylases
JMJD3	Jumonji D3
JNK	c-Jun N-terminal kinase
KDM	Lysine demethylase
KMT	Lysine methyltransferase
LBD	Ligand-binding domain
LC3	Microtubule-associated protein 1A/1B light chain
LCA	Lithocholic acid
LKB1	Liver Kinase B1
LSP	Light strand promotor
MAPK	p38 mitogen activated protein kinase
MASH	Metabolic Dysfunction Associated Steatohepatitis
MASLD	Metabolic Dysfunction Associated Steatotic Liver Disease
MCviPI mutant	Catalytically inactive mitochondrial DNMT that induces GpC methylation
MCviPI	Mitochondrial DNMT that induces GpC methylation
Mff	Mitochondrial fission factor
Mfn1	Mitofusion-1
Mfn2	Mitofusin-2
MiD49	Mitochondrial dynamics proteins of 49 kDa
MiD51	Mitochondrial dynamics proteins of 51 kDa
miRNA	microRNA
MLS	Mitochondrial localisation signal
MPP	Mitochondrial-processing peptidases
MSssl	Mitochondrial DNMT that induces CpG methylation
mtDNA	Mitochondrial DNA
mt-ND6	Mitochondrially encoded NADH dehydrogenase 6
MTP	Mitochondrial trifunctional protein
mtSSB	Mitochondrial single stranded DNA binding protein
NAFLD	Non-alcoholic fatty liver disease
NCR	Non-coding region
ND2/4/5/6	NADH dehydrogenase 2/4/5/6
NES	Nuclear export signal
NFATC	Nuclear factor of activated T cells
NFE2L2	Nuclear factor erythroid-derived 2-like 2
NLRP3	NOD-like receptor family pyrin domain containing 3
NRF-1	Nuclear respiratory factors 1
NRF2	Nuclear factor erythroid-derived 2-related factor 2
NRF-2 α	Nuclear respiratory factors 2 α
OA	Oleic acid

OCR	Oxygen consumption rate
O _H	Origin of heavy strand replication
O _L	Origin of light strand replication
Oligo	Oligomycin
OMM	Outer mitochondrial membrane
Opa1	Optic atrophy 1
OXPHOS	Oxidative phosphorylation pathway
PA	Palmitic acid
PBS	Phosphate-buffered saline
PCG1- α	Peroxisome proliferator-activated receptor gamma coactivator 1-alpha
PINK1	Putative kinase 1
PKA	Protein kinase A
PNPLA3	Patatin-like phospholipase domain-containing 3
POLRMT	Mitochondrial RNA polymerase
POLy	DNA polymerase gamma
PPARGC1 α	Peroxisome proliferator-activated receptor-gamma coactivator 1 α
PPAR α	Peroxisome proliferator-activated receptor- α
PPRE	Peroxisome proliferator response element
PRMT	Arginine histone methyltransferase
PRMT6	Arginine methyltransferase 6
PXR	Pregnane X receptor
qPCR	Quantitative polymerase chain reaction
RB1	Retinoblastoma tumor suppressor gene
ROS	Reactive oxygen species
Rot/AA	Rotenone and antimycin A
RXR	Retinoid X receptor
SAB	SH3 homology associated BTK-binding protein
SAM	S-adenosyl methionine
SIRT	Sirtuin
SIRT1	Sirtuin 1
SOD	Superoxide dismutase
T2DM	Type 2 diabetes mellitus
TBW	Total body weight
TCA	Tricarboxylic acid
TDG	Thymine-DNA-glycosylase
TEFM	Transcription elongation factor
TET	Ten-eleven translocation enzymes
TFAM	Mitochondrial transcription factor A
TFB2M	Dimethyl adenosine transferase 2 mitochondrial protein
TK2	Thymidine kinase
Uhrf1	Ubiquitin Like With PHD And Ring Finger Domains 1
UPR	Unfolded protein response
VCTE	Vibration-controlled transient elastography
VDR	Vitamin D receptor
WT	Wild type
XBP1	X-box binding protein 1

Summary

Metabolic dysfunction associated fatty liver disease (MASLD), previously known as non-alcoholic fatty liver disease (NAFLD), is a growing global health burden with an estimated prevalence of 20-30% in Europe. It consists of a spectrum of liver disorders ranging from steatosis, characterized by an accumulation of lipid droplets that eventually cause lipotoxicity and inflammation, and thereby progresses into metabolic dysfunction associated steatohepatitis (MASH). The latter predisposes patients for further cirrhosis and hepatocarcinoma. Unfortunately, there is still no FDA-approved treatment for MASLD and therefore changes in lifestyle including diet and exercise remain the current treatment strategy. However this is difficult to maintain, leading to a lot of relapsing patients. The unsatisfactory results of previous MASLD therapeutics in clinical trials, is due to the lack of diagnostic biomarkers that allow to stratify patients and thereby give a right prognosis, but also the multifactorial nature of the disease. Thus, there is an urgent need for a full characterization of the molecular targets that have a key role in the progression of the disease, in order to target multiple aspects of the disease. Two of these interesting targets are the nuclear receptor PPAR α and mitochondria. As elaborated in detail in Chapter 1 and 2, they have a key role in lipid metabolism and are also closely related to inflammation. Moreover, recent research, especially cancer research, has shown that mitochondrial DNA methylation can be used as a biomarker and interactions of PPAR α with epigenetic enzymes can regulate lipid metabolism in liver and colon. These new insights give opportunities for epigenetic diagnostic biomarker and therapeutic research in the battle against MASLD. Therefore in this PhD work, we further characterized the epigenetic “driver” or “passenger” functions of PPAR α in the epigenetic progression of MASLD and the role of mitochondrial methylation in the process of mitochondrial dysfunction in MASLD.

In Chapter 3, we investigated whether the epigenetic reprogramming of the lipid metabolism in MASLD, including PPAR α target genes, is a PPAR α dependent or independent process. PPAR α function is lost in the progression of MASLD, inducing a reprogramming of the lipid metabolism. However PPAR α agonists gave unsatisfactory results in clinical trials, suggesting that the loss of PPAR α induces more reprogramming than just the loss of a transcription factor. Therefore we compared genome-wide DNA methylation and transcriptome changes in livers of wild type (WT) and hepatocyte-specific PPAR α knock out (KO) mice, receiving control chow diet versus MASLD promoting high fat diet (CDAHFD). We demonstrated that the diet-induced PPAR α loss of function induced a similar epigenetic and transcriptional reprogramming of the lipid and bile acid metabolism towards a MASLD disease signature, as a genetic knock out on a chow/CDAHFD diet. Furthermore, we showed that the loss of function of this one PPAR α hub, induced a shock wave of transcription changes of lipid transcription factors and epigenetic enzymes that induces the epigenetic progression towards lipotoxic ferroptosis and pyroptosis, closely related to MASLD fibrosis. This epigenetic reprogramming of the lipid and bile acid metabolism, included hypermethylation of a lot of PPAR α target genes, which suggests an epigenetic driver role of PPAR α in the epigenetic reprogramming of MASLD and may aid in the search towards new diagnostic epigenetic biomarkers for patient stratification.

In Chapter 4 and 5, we investigated the role of mitochondrial methylation in both mitochondrial dysfunction and MASLD. In Chapter 4 we first optimised Nanopore episequencing of the mitochondrial DNA (mtDNA). We demonstrated that regular DNA extraction followed by pre-processing of the samples including fragmentation and size selection, generated enough material to sequence 'pure' mtDNA without nuclear DNA contamination and with a coverage high enough to correctly estimate methylation percentages. The mtDNA showed overall more CpG than GpC methylation in mitochondrial encoded tRNAs and OXPHOS genes. Although the overall percentage of mitochondrial methylation were low, the percentage of methylation in a characterized *in vitro* steatosis model, showed higher methylation percentages in genes related to the electron transport cycle (ETC). Therefore, in chapter 5 we further characterized the role of mitochondrial CpG and GpC methylation in mitochondrial dysfunction related to MASLD. MtDNA is organised in circular nucleoids, lacking histones and transcribed from only three promoters generating polycistronic RNA transcripts. This organisation is very different from the nuclear DNA and therefore raises questions about the functional role of mtDNA methylation in mitochondrial dysfunction. Therefore we characterized different mitochondrial aspects including morphology, respiratory activity, metabolic competence as well as gene expression and DNA methylation changes in both an established *in vitro* steatosis and untreated cell model upon overexpression of either a CpG or GpC mitochondrial-specific DNA methyltransferase. We demonstrated that an increase of 20% in mitochondrial GpC or CpG methylation promotes metabolic stress-induced mitophagy or cholestophagy. Moreover, mitochondrial GpC methylation changes bile acid metabolic gene expression via epigenetic mito-nuclear communication, promoting mitochondrial swelling and cholestophagy, associated with a MASLD disease signature. Whereas, both CpG and GpC methylation induce an overactivation of mitochondrial respiration, that can not be further increased upon free fatty acid treatment and thereby induces lipid accumulation and morphological changes promoting mitophagy. Together, these functional changes are closely related to mitochondrial dysfunction in MASLD and raise new opportunities for mitochondrial methylation in therapeutic research.

Altogether, the results of this thesis show promising new insights for PPAR α and mitochondrial focused epigenetic research in MASLD, with potential for new (combination) therapeutic and diagnostic biomarkers. Nevertheless, to fully exploit PPAR α and mitochondrial epigenetic drugs and biomarkers to tackle the progression of MASLD, multiple hurdles still need to be overcome. For example, although strong associations were found, the regulatory mechanisms could not yet be defined. How can the loss of PPAR α function and epigenetic reprogramming be linked to each other? Can this epigenetic reprogramming be used as a diagnostic biomarker? Also, mitochondrial methylation has shown to induce changes in mitochondrial functioning, but do these changes have therapeutic possibilities for MASLD? Can mitochondrial methylation be used as biomarker for MASLD stratifications? These issues, together with recommendations for future follow-up studies, are discussed in the final part of the thesis.

Samenvatting

Metabole disfunctie geassocieerde vette leverziekte (MASLD), voorheen bekend als niet-alcoholische vette leverziekte (NAFLD), is een groeiende wereldwijde gezondheidsbelasting met een geschatte prevalentie van 20-30% in Europa. Het bestaat uit een spectrum van leveraandoeningen variërend van steatose, gekenmerkt door een ophoping van vetdruppels die uiteindelijk lipotoxiciteit en ontsteking veroorzaken en daardoor overgaan in metabole dysfunctie steatohepatitis (MASH). Deze laatste aandoening maakt patiënten vatbaar voor verdere cirrose en hepatocarcinoom. Helaas is er nog steeds geen door de FDA goedgekeurde behandeling voor MASLD en daarom blijven veranderingen in levensstijl, waaronder dieet en lichaamsbeweging, de huidige behandelingsstrategie. Dit is echter moeilijk vol te houden, waardoor veel patiënten hervallen. De onbevredigende resultaten van eerdere MASLD-therapieën in klinische studies zijn te wijten aan het gebrek aan diagnostische biomarkers die het mogelijk maken om patiënten te stratificeren en zo een juiste prognose te geven, maar ook aan de multifactoriële aard van de ziekte. Daarom is er nood aan een volledige karakterisering van de eiwitten die een sleutelrol spelen in de progressie van de ziekte, zodat meerdere aspecten van de ziekte tegelijk aangepakt kunnen worden. Twee van deze interessante doelwitten zijn de nucleaire receptor PPAR α en mitochondriën. Zoals gedetailleerd omschreven in hoofdstuk 1 en 2, hebben beide een sleutelrol in het vetmetabolisme en zijn ze ook nauw gerelateerd aan ontstekingen. Bovendien heeft recent onderzoek, met name kankeronderzoek, aangetoond dat mitochondriale DNA-methylatie kan worden gebruikt als biomarker en dat interacties van PPAR α met epigenetische enzymen het lipidenmetabolisme in lever en dikke darm kunnen reguleren. Deze nieuwe inzichten bieden mogelijkheden voor epigenetische diagnostische biomarkers en therapeutisch onderzoek in de strijd tegen MASLD. Daarom hebben we in dit doctoraatsonderzoek de epigenetische "driver" of "passenger" functies van PPAR α in de epigenetische progressie van MASLD en de rol van mitochondriale methylering in het proces van mitochondriale disfunctie in MASLD verder gekarakteriseerd.

In hoofdstuk 3 hebben we onderzocht of de epigenetische herprogrammering van het vetmetabolisme in MASLD, inclusief PPAR α -targetgenen, een PPAR α -afhankelijk of -onafhankelijk proces is. De functie van PPAR α gaat verloren in de progressie van MASLD, wat een herprogrammering van het lipidenmetabolisme induceert. PPAR α agonisten gaven echter onbevredigende resultaten in klinische studies, wat suggereert dat het verlies van PPAR α meer herprogrammering induceert dan alleen het verlies van een transcriptiefactor. Daarom vergeleken we genomwijde DNA-methylatie en transcriptoomveranderingen in levers van wild-type (WT) en hepatocyt-specifieke PPAR α knock-out (KO) muizen, die een controle dieet kregen versus een MASLD bevorderend vetrijk dieet (CDAHFD). We toonden aan dat het verlies van PPAR α functie geïnduceerd door het dieet een vergelijkbare epigenetische en transcriptionele herprogrammering van het vet- en galzuurmetabolisme naar een MASLD-ziektesignatuur vertoonde, als een genetische knock-out op een chow/CDAHFD dieet. Verder toonden we aan dat het verlies van functie van deze ene PPAR α hub een schokgolf van transcriptieveranderingen in lipidetranscriptiefactoren en epigenetische enzymen veroorzaakt, die de epigenetische progressie in de richting van lipotoxische ferroptose en pyroptose, nauw verwant aan MASLD-fibrose, induceert. Deze epigenetische

herprogramming van het vet- en galzuurmetabolisme omvatte hypermethylering van veel PPAR α -targetgenen, wat suggereert dat PPAR α een epigenetische rol speelt in de epigenetische herprogramming van MASLD en kan helpen in de zoektocht naar nieuwe diagnostische epigenetische biomarkers voor patiëntstratificatie.

In hoofdstuk 4 en 5 onderzochten we de rol van mitochondriale methylering in zowel mitochondriale disfunctie als MASLD. In hoofdstuk 4 hebben we epiNanopore sequencing van het mitochondriaal DNA (mtDNA) geoptimaliseerd. We toonden aan dat gewone DNA-extractie gevolgd door een voorbehandeling van de stalen, inclusief fragmentatie en selectie op grootte, voldoende materiaal genereerde om 'puur' mtDNA te sequencen zonder nucleaire DNA-verontreiniging en met een dekking die hoog genoeg was om het percentage methylering correct te schatten. Het mtDNA vertoonde over het algemeen meer CpG- dan GpC-methylering in mitochondriaal gecodeerde tRNA's en OXPHOS-genen. Hoewel het totale mitochondriale methylering percentage laag was, toonde het gekarakteriseerd *in vitro* steatosemodel een hoger methylering percentage in genen van de elektronentransportcyclus (ETC) dan het onbehandelde staal. Daarom hebben we in hoofdstuk 5 de rol van mitochondriale CpG en GpC methylering in mitochondriale disfunctie gerelateerd aan MASLD verder gekarakteriseerd. MtDNA is cirkelvormig, georganiseerd in nucleoïden, zonder histonen en transcriptie vindt plaats vanuit slechts drie promotors die polycistronische RNA-transcripten genereren. Deze organisatie verschilt sterk van het nucleaire DNA en roept daarom vragen op over de functionele rol van mtDNA-methylering in mitochondriale disfunctie. Daarom hebben we verschillende mitochondriale aspecten gekarakteriseerd, waaronder morfologie, respiratie, metabolische competentie, genexpressie en veranderingen in DNA-methylering in een *in vitro* steatose- en onbehandeld celmodel met een overexpressie van een CpG- of GpC-specifiek mitochondriale methyltransferase. We toonden aan dat een toename van 20% in mitochondriale GpC of CpG methylering metabole stress-geïnduceerde mitofagie of cholestofagie bevordert. Bovendien verandert mitochondriale GpC-methylering de galzuurmetabolische genexpressie via epigenetische mito-nucleaire communicatie, wat mitochondriale zwelling en cholestofagie veroorzaakt, geassocieerd met een MASLD-ziektesignatuur. Terwijl zowel CpG- als GpC-methylering een overactivering van de mitochondriale respiratie induceren, die niet verder kan worden verhoogd bij behandeling met vrije vetzuren en daardoor vetophoping en morfologische veranderingen induceert die mitofagie bevorderen. Samen zijn deze functionele veranderingen nauw gerelateerd aan mitochondriale disfunctie in MASLD en bieden ze nieuwe mogelijkheden voor mitochondriale methylering in therapeutisch onderzoek.

Samen, laten de resultaten van dit proefschrift veelbelovende nieuwe inzichten zien voor PPAR α en mitochondriaal gericht epigenetisch onderzoek in MASLD, met potentieel voor nieuwe (combinatie) therapeutische en diagnostische biomarkers. Niettemin, om PPAR α en mitochondriale epigenetische geneesmiddelen en biomarkers volledig te benutten om de progressie van MASLD aan te pakken, moeten er nog meerdere hordes genomen worden. Hoewel er bijvoorbeeld sterke associaties werden gevonden, konden de regulerende mechanismen nog niet worden gedefinieerd. Hoe kunnen het verlies van de PPAR α -functie en epigenetische herprogramming met elkaar in verband worden gebracht? Kan deze epigenetische herprogramming worden gebruikt als diagnostische biomarker? Ook is aangetoond dat mitochondriale methylering veranderingen teweegbrengt in de mitochondriale functie, maar hebben deze veranderingen therapeutische mogelijkheden voor MASLD? Kan mitochondriale methylering gebruikt worden als biomarker voor

MASLD-stratificatie? Deze vragen, samen met aanbevelingen voor toekomstige vervolgstudies, worden besproken in het laatste hoofdstuk van dit proefschrift.

GENERAL INTRODUCTION

CHAPTER I:

PPAR α in the epigenetic driver seat of NAFLD: new therapeutic opportunities for epigenetic drugs?

CHAPTER II:

Mitochondrial dysfunctions and MASLD progression: cause or consequence?

Introduction

Introduction

Metabolic diseases are becoming a big health threat worldwide. The number of patients are steadily increasing and more deaths are reported. Remarkably, Chew et al. showed that nonalcoholic fatty liver disease (NAFLD) had the highest prevalence in 2019 amongst the other studied metabolic diseases, type 2 diabetes mellitus (T2DM) and hypertension¹. NAFLD, recently re-named and re-defined as Metabolic Dysfunction Associated Steatotic Liver Disease (MASLD)², is known as a growing epidemic mimicking the growing incidence in obesity and diabetes mellitus in Western diet-consuming countries. The estimated prevalence of MASLD is currently 20-30% in Europe. Moreover, it is the most common cause of chronic liver disease worldwide^{3,4}. MASLD consists of a spectrum of liver disorders, ranging from isolated steatosis to Metabolic Dysfunction Associated Steatohepatitis (MASH) and fibrosis (Figure 1). The majority of patients have isolated steatosis which is often considered benign in nature, whereas MASH predisposes to complications such as fibrosis, cirrhosis and hepatocellular carcinoma (HCC), as well as extrahepatic diseases, especially cardiovascular disease⁵⁻⁷. Knowing the mechanism behind the pathological progression of MASLD is crucial, but incomplete at present.

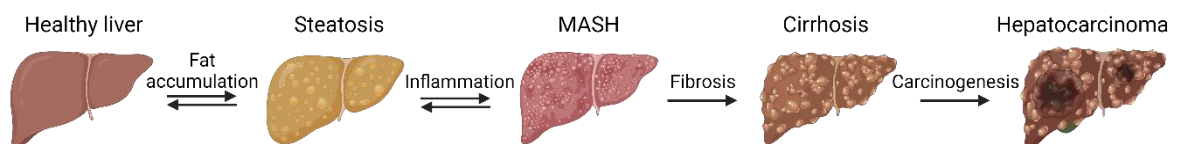


Figure 1: The progression of MASLD. A healthy liver can progress into a steatotic liver by the constant influx of lipids. Over time, this can induce lipotoxicity leading to inflammation in the hepatocytes and progression to the second stage called Metabolic Dysfunction Associated Steatohepatitis (MASH). The latter can predispose patients for further fibrosis that can progress into cirrhosis or even hepatocarcinoma.

The majority of patients with MASLD are asymptomatic, although some of them may present symptoms like fatigue, right upper quadrant discomfort, hepatomegaly, acanthosis nigricans or lipomatosis. Therefore, MASLD is very often discovered due to abnormal liver function tests (alanine aminotransferase (ALT) and aspartate aminotransferase (AST) levels) or incidental findings of hepatic steatosis on radiologic abdominal scans during medical evaluations for other reasons⁸. In these liver function test, MASLD patients generally show elevated ALT levels, where MASH patients generally have higher ALT levels than steatosis patients^{8,9}. When this first indication of liver malfunctioning is discovered, various imaging modalities can be used to support the diagnosis of MASLD including ultrasound, computed tomography, vibration-controlled transient elastography (VCTE) (Fibroscan) that provides a controlled attenuation parameter (CAP), and magnetic resonance imaging. However, the results of these tests can not distinguish between simple steatosis and MASH. The gold standard to diagnose the different stages of MASLD (Steatosis vs. MASH) is an invasive liver biopsy that allows to assess inflammation and the grade of fibrosis¹⁰. Simple steatosis is defined as the presence of $\geq 5\%$ hepatic steatosis without further evidence of hepatocellular injury in the form of hepatocyte ballooning¹¹. MASH is distinguished from isolated hepatic steatosis by the presence of hepatocellular injury characterized by the presence of lobular inflammation and hepatocellular ballooning independent of the presence or absence of fibrosis¹². However, several

Introduction

limitations have been associated with these liver biopsies including sampling variability due to uneven distribution of MASH histological lesions, inter and intra-observer variability and risk for complications which may all lead to misdiagnosis and staging inaccuracies^{8,10}. Therefore there is an urgent need for non-invasive biomarkers that allow correct stratification of the patients into MASH or non-MASH.

The development of MASLD is a complex process that is not completely understood. Today, it is generally accepted that the interplay between environmental factors, genetics and epigenetics plays a crucial role in the development of MASLD (Figure 2).

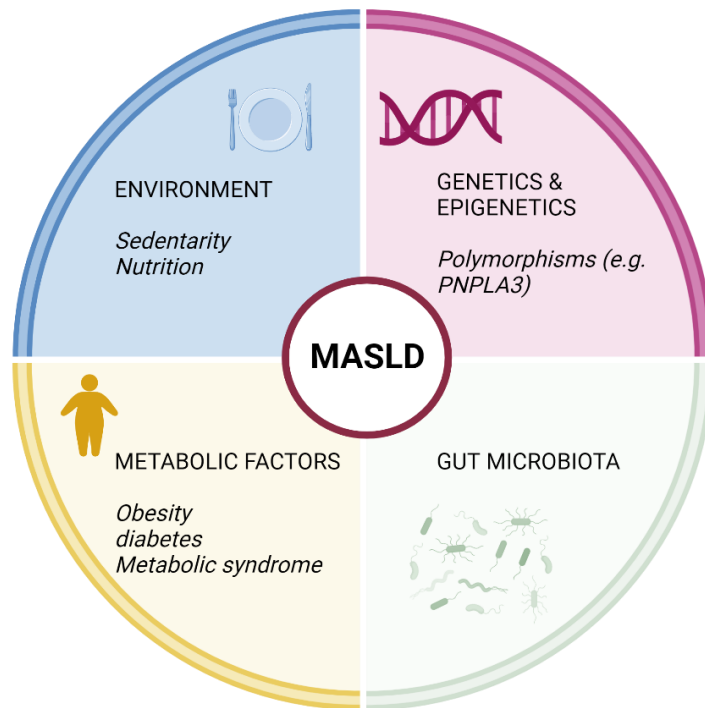


Figure 2: Factors contributing to the development of metabolic dysfunction associated steatotic liver disease (MASLD). Metabolic syndrome, obesity and diabetes are closely related to the increasing prevalence of MASLD. In addition, genetic background but also epigenetics which is largely affected by both genetics and environmental factors including diet and a sedentary lifestyle, strongly influence disease progression and development. More recently, gut microbiota has emerged as an important key player in MASLD. Abbreviations: metabolic dysfunction associated steatotic liver disease (MASLD); patatin-like phospholipase domain-containing 3 (PNPLA3). Adapted from Fougerat et al.¹³

More specifically, environmental factors including a lipid rich diet and the lack of exercise are largely linked to the development of MASLD¹⁴. Therefore the only treatment for MASLD that is currently recommended consists of a change in lifestyle, including a change in diet and a lot of exercise. In some cases where changes in diet or exercise are impossible or not effective, this first line treatment will be combined with drugs (e.g. antidiabetic drugs including Pioglitazone) that can effectively regulate glucose and lipid metabolism to reduce liver inflammation and fibrosis¹⁵. Several studies have shown that a reduction of 5% of total body weight (TBW) is needed to decrease hepatic steatosis, over 7% for inflammation resolution, and over 10% to resolve/stabilize fibrosis¹⁶⁻¹⁹. However this is difficult to achieve and maintain for patients and therefore many relapse²⁰. Besides, MASLD has also been diagnosed in lean patients without obesity or diabetes, for whom this treatment is less appropriate²¹. Furthermore, genetic mutations have also been linked to

Introduction

development of MASLD. For example mutations in the patatin-like phospholipase domain-containing 3 (PNPLA3) gene is considered a hallmark for the development of MASLD^{22,23}. However, neither environmental factors nor genetic factors alone can give a satisfactory explanation for the high prevalence of MASLD. Interestingly, epigenetics integrate both environmental exposures and genetic predisposition and have an important contribution to transcriptional network changes²⁴. Therefore researchers are now also searching for epigenetic factors contributing to the development and progression of MASLD. Although global DNA hypomethylation, hypermethylation of peroxisome proliferator-activated receptor- α (PPAR α) gene (promoter) sequences and hypermethylation of the mitochondrial ND6 gene have been associated with MASLD, little is known about the key players and mechanism behind this epigenetic regulation²⁵⁻²⁷. Therefore current drug research is mostly focused on agents targeting lipid metabolism, inflammatory or fibrotic pathways, i.e. lipid lowering agents (e.g. statins), antioxidants (e.g. vitamin E) and agents activating key players in the lipid metabolism (e.g. PPAR α , SIRT1, AMPK). However, these agents show variable therapeutic benefits and mostly target only one aspect of the disease. Hence, therapeutic research would benefit by a better understanding of the different regulatory epigenetic aspects of MASLD which could be targeted in future (combination) therapies²⁸. Therefore, this PhD thesis will focus on epigenetic regulation mechanisms of two key players in the progression of MASLD: the nuclear receptor PPAR α and the mitochondria. Although both are involved in lipid metabolism and MASLD disease etiology, their contribution in epigenetic dysfunctions in MASLD progression is not fully understood.

PPAR α loss of function following DNA hypermethylation and gene silencing is recognized as a key hallmark in the pathogenesis of MASLD^{26,29}. Nevertheless, PPAR α specific activating ligands (agonists) (e.g. fibrates) have shown disappointing results in clinical trials³⁰. Since PPAR α target genes related to lipid metabolism also reveal strong DNA methylation variation in MASLD, recent research has shifted focus towards identification of key players in this epigenetic regulation. Indeed, new reports demonstrate direct or indirect interactions of PPAR α with epigenetic enzymes to control the lipid metabolism, which opens new perspectives for novel epigenetic drug discovery pipelines against MASLD. Therefore in chapter I, I will summarize the current knowledge on epigenetic regulation of PPAR α in MASLD, as well as PPAR α interacting epigenetic enzymes and associations with downstream epigenetic target genes.

Mitochondrial dysfunction has been described as a crucial driving force in the progression of MASLD. Indeed, mitochondria are dynamic organelles that can adapt their role in lipid metabolism (e.g. β -oxidation and OXPHOS pathway) to the metabolic needs of the cell. However upon lipid overload in MASLD, excessive influx of lipids in mitochondria will threaten their metabolic plasticity leading to mitochondrial dysfunction, ROS generation, inflammation and ER stress which are all hallmarks of MASLD progression³¹. Despite this strong evidence, linking mitochondrial dysfunction and MASLD progression, the regulatory mechanisms that drive the structural and metabolic changes in mitochondria in the different stages of MASLD remain poorly understood. Since new nanopore based sequencing technologies now allow to study mitochondrial DNA methylation, this creates new opportunities to evaluate the possible contribution of mitochondrial epigenetics in MASLD. Therefore I will summarize in chapter II the overall regulation of mitochondrial physiology, as well as the current knowledge about mitochondrial DNA methylation and the functional and epigenetic role of mitochondria in MASLD progression.

Introduction

CHAPTER I

PPAR α in the epigenetic driver seat of NAFLD: new therapeutic opportunities for epigenetic drugs?

Published as: **Theys C**, Lauwers D, Perez-Novo C, Vanden Berghe W. PPAR α in the Epigenetic Driver Seat of NAFLD: New Therapeutic Opportunities for Epigenetic Drugs? *Biomedicines*. 2022 Nov 25;10(12):3041. doi: 10.3390/biomedicines10123041. PMID: 36551797; PMCID: PMC9775974.

Important remark: NAFLD nomenclature changed into metabolic dysfunction associated steatotic liver disease (MASLD) after publication of this review. However the article was kept in its original form in this PhD work.

Introduction: Chapter 1

PPAR α in the epigenetic driver seat of NAFLD: new therapeutic opportunities for epigenetic drugs?

1.1 The peroxisome proliferator activated receptor alpha – PPAR α

1.1.1 Structure and regulation of PPAR α

PPAR α is a nuclear receptor which is part of the PPAR family consisting of three members: PPAR α , PPAR β/δ and PPAR γ . These three receptors are expressed from different genes and each isotype is highly expressed in different tissue^{32,33}. PPAR α is largely expressed in the liver and brown adipose tissue, followed by the heart and the kidneys. PPAR β/δ is ubiquitously expressed in tissues with high peroxisomal and mitochondrial β -oxidative activity including skeletal muscle. PPAR γ is mainly expressed in white adipose tissue³³. Since PPAR α is highly expressed in the liver and a key regulator of the lipid metabolism, it is an interesting target in the research of NAFLD.

The *PPARA* gene consists of eight exons and it is mapped to chromosome 22 in humans and chromosome 15 in the mouse. It encodes for the PPAR α protein which is 468 amino acid residues long (Figure 3). This protein contains five functional domains, from A to F. First, at the N-amino terminal there is the A/B domain or the activation function one (AF-1) domain. This domain works independently without binding of a ligand. Second, next to the AF-1 domain there is the C-domain or DNA-binding domain (DBD) containing two highly conserved zinc finger-like motifs. Binding of the receptor to the peroxisome proliferator response element (PPRE) sequence of target genes will be promoted by these zinc finger-like motifs. Third is the D-domain or hinge region (HR) that connects the C-domain with the E/F domain. Last, at the C-terminus there is the E/F domain or ligand-binding domain (LBD) with the activation function two (AF-2). Ligands can bind to the LBD leading to stabilization and recruitment of co-factors by AF-2. The co-regulators can bind to PPAR α with their LXXLL domain³⁴.

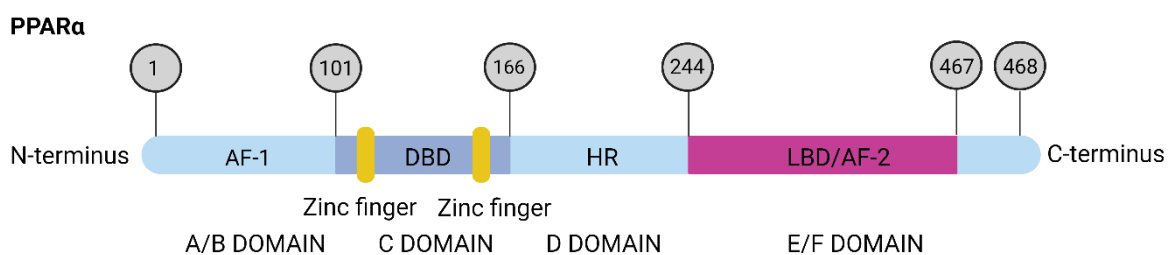


Figure 3: Schematic view of the protein structure of PPAR α and domain function. First there is the A/B domain or the activation function one (AF-1) domain which works without ligand binding, next there is the C-domain or DNA-binding domain (DBD) containing two highly conserved zinc finger-like motifs shown in yellow. Following is the hinge region connecting the C domain with the last E/F domain known as the ligand-binding domain (LBD) with the activation function two (AF-2).

Generally, the ligands of PPAR α are divided into two main groups: one group of natural ligands and another of synthetic ligands. The natural ligands consist of endogenous (e.g., free fatty acids, derived from the lipid metabolism) and exogenous (e.g., resveratrol, derived from the diet or medicinal plants) molecules^{35,36}.

In the cell, the absence of PPAR α ligands leads to inactivation of the receptor by co-repressors. After ligand binding, the co-repressors will be replaced by co-activators resulting in the heterodimerization with retinoid X receptor (RXR). This complex can bind to specific PPREs resulting in the transcription of its target genes^{33,37}. Most of these target genes are involved in lipid metabolism or fatty acid (FA) catabolism, including genes involved in FA binding, transport, degradation via mitochondrial or peroxisomal oxidation. Other pathways include ketogenesis, amino acid metabolism, xenobiotic metabolism, glucose metabolism and inflammation^{38,39} (Table 1).

Table 1: List of verified PPAR α target genes^{38,39} with their corresponding function divided in subcategories.

Target gene	Official Gene symbol	Gene function
<i>Lipid metabolism/ Fatty acid (FA) catabolism</i>		
FA transport protein (FATP)	SLC27A1	Fatty acid transport
Fatty acid translocase (FAT/CD36)	CD36	Uptake of long-chain FAs and oxidized LDL
Acyl-CoA synthetase	ACS	Catalyzes FA metabolism by converting inactive FAs into active acyl CoA derivatives
Fatty acid binding protein	FABP	Intracellular lipid trafficking
Acyl-CoA binding protein (ACBP)	DBI	Fatty acyl CoA esters transport
Solute Carrier Family 25 Member 20	SLC25A20	Fatty acyl CoA esters transport
Carnitine palmitoyltransferase 1	CPT1A	Catalyzes the transfer of a longchain fatty acyl group from CoA to carnitine
Carnitine palmitoyltransferase 2	CPT2	Conjugates the FA back to CoA for subsequent β -oxidation
Medium-chain acyl-CoA dehydrogenase (MCAD)	ACADM	Mitochondrial FA β -oxidation
Long-chain acyl-CoA dehydrogenase (LCAD)	ACADL	Mitochondrial FA β -oxidation
Very long chain acyl-CoA dehydrogenase (VLCAD)	ACADVL	Mitochondrial FA β -oxidation
Dodecenoyl-CoA δ -isomerase	ECI1	Mitochondrial FA β -oxidation of unsaturated and saturated FAs
Carnitine palmitoyltransferase 1B	CPT1B	Mitochondrial FA β -oxidation

Introduction: Chapter 1

Uncoupling Protein 3 (SLC25A9)	UCP3	Mitochondrial anion carrier protein enabling reduction of mitochondrial membrane potential and FA export under lipid stress
Acyl-CoA oxidase	ACOX	Peroxisomal β -oxidation
Bifunctional enzyme (BIEN)	EHHADH	Peroxisomal β -oxidation
Peroxisomal 3-ketoacylCoA thiolase	ACAA1	Peroxisomal β -oxidation
Peroxisomal membrane protein 11A	PEX11A	Peroxisomal β -oxidation
Acyl-CoA Oxidase 1	ACOX1	Peroxisomal β -oxidation
Cytochrome P450 4A	CYP4A	Microsomal FA ω -hydroxylation
Cytochrome P450 Family 1 Subfamily A Member 1	CYP1A1	Microsomal ω -hydroxylation of polyunsaturated fatty acids (PUFA)
Lipoprotein lipase	LPL	Hydrolysis of TGs
Angiopoietin-like protein 4	ANGPTL4	Inhibitor of LPL activity
Perilipin 2	PLIN2	Lipid binding for lipid droplet formation
Adaptor Related Protein Complex 2 Subunit Alpha 2	AP2A2	Lipolysis
Apolipoprotein AI	APOA1	Plasma HDL metabolism
Apolipoprotein AII	APOA2	Plasma HDL metabolism
Apolipoprotein A-V	APOA5	Plasma TG metabolism
Apolipoprotein C-III	APOC3	Plasma HDL Metabolism
FA desaturase 2 (Fads2)	FADS2	Lipogenesis
Stearoyl-CoA desaturase (Scd1)	SCD	Lipogenesis
Malic enzyme (Mod1)	ME1	Lipogenesis
Phosphatidate phosphatase (Lpin2)	LPIN2	Lipogenesis
Acetyl-CoA carboxylase (ACC)	ACACA	Lipogenesis
Fatty acid synthase (FAS)	FASN	Lipogenesis
Retinol Saturase	RETSAT	Retinol metabolism and lipogenesis
KLF Transcription Factor 10 (TIEG1)	KLF10	Regulates the circadian expression of genes involved in lipogenesis, gluconeogenesis, and glycolysis
KLF Transcription Factor 11 (TIEG2)	KLF11	Promoting the effects of TGF- β on cell growth/Inhibition of gluconeogenesis and promoting FA oxidation
<i>Bile acid/cholesterol metabolism</i>		
Solute Carrier Family 10 Member 2	SLC10A2	Bile acid reuptake
Liver X receptor a (LXRa)	NR1H3	Cholesterol metabolism

Introduction: Chapter 1

Cholesterol 7 α -hydroxylase (Cyp7a1)	CYP7A1	Bile acid metabolism
Cholesterol 27 α -hydroxylase (Cyp27a1)	CYP27A1	Bile acid metabolism
Sterol-12 α -hydroxylase	CYP8B1	Bile acid metabolism
NPC1 Like Intracellular Cholesterol Transporter 1	NPC1L1	Cholesterol uptake
UDP Glucuronosyltransferase Family 1 Member A9	UGT1A9	Bile acid metabolism
UDP Glucuronosyltransferase Family 2 Member B4	UGT2B4	Bile acid metabolism
Sulfotransferase Family 2A Member 1	SULT2A1	Bile acid metabolism
PDZ Domain Containing 1	PDZK1	Cholesterol metabolism
Fatty Acid Binding Protein 6	FABP6	Intracellular FA and bile acid trafficking
<i>Glucose metabolism</i>		
Phosphoenolpyruvate carboxykinase (Pck1)	PKC1	Gluconeogenesis
Glycerol-3-phosphate dehydrogenase (GPDH)	GDP	Metabolic conversion of glycerol into glucose
Glycerol kinase	GK	Metabolic conversion of glycerol into glucose
Glycerol transporters aquaporins 3	AQA3	Metabolic conversion of glycerol into glucose
Glycerol transporters aquaporins 9	AQA9	Metabolic conversion of glycerol into glucose
Pyruvate dehydrogenase kinase isoform 4 (Pdk4)	PDK4	Glucose oxidation
Glycogen synthase 2 (Gys-2)	GYS2	Glycogen synthesis
UDP-glucose 6-dehydrogenase	UGDH	Glucose oxidation
<i>Cellular stress/inflammation</i>		
Heme Oxygenase 1	HMOX1	Anti-oxidant, protects against programmed cell death by catabolizing free heme
Thioredoxin	TXN	Catalyzes redox reactions in response to nitric oxide
CAMP Responsive Element Binding Protein 3 Like 3	CREB3L3	Transcription factor involved in acute inflammatory response and maintenance of lipid metabolism

Mitogen-Activated Protein Kinase Kinase Kinase 8	MAP3K8	Activation of the MAPK/ERK pathway in macrophages
Complement C3	C3	Activation of complement system that modulates inflammatory response
<i>Xenobiotic metabolism</i>		
Aryl Hydrocarbon Receptor	AHR	Xenobiotic metabolism
ATP Binding Cassette Subfamily G Member 2	ABCG2	Xenobiotic transporter
Cytochrome P450 Family 3 Subfamily A Member 4	CYP3A4	Xenobiotic metabolism
Cytochrome P450 Family 2 Subfamily C Member 8	CYP2C8	Xenobiotic metabolism
<i>Amino acid metabolism</i>		
Glutamic-pyruvic transaminase (ALT1)	GPT	Transamination of alanine and 2-oxoglutarate into pyruvate and glutamate
<i>Ketogenesis</i>		
Mitochondrial 3-hydroxy3-methylglutaryl-CoA synthase (mHMGCoAS)	HMGCS2	Ketogenesis
Fibroblast growth factor 21	FGF21	Metabolic fuel homeostasis during ketosis
<i>Others</i>		
Solute Carrier Family 29 Member 1	SLC29A1	Nucleoside transporter
Rev-erb α	NR1D1	Repressor of gene transcription
Transferrin	TF	Iron binding

1.2 Epigenetic regulation of PPAR α in NAFLD

1.2.1 Epigenetics

Epigenetics is the study of reversible changes in gene expression that can be inherited through cell division, but are not caused by DNA sequence alterations⁴⁰. Epigenetic modifications consist of DNA methylation, histone modifications, and microRNAs⁴¹.

First, DNA methylation is known as the addition of a methyl group (-CH₃) on the fifth carbon of the pyrimidine ring in cytosine, generating 5-methylcytosine (5meC). This process is managed by DNA methyltransferases (DNMTs) and is most often found in CpG islands of the promotor region. Hence, CpG island hypermethylation typically results in the inhibition of gene transcription. The family of DNMTs consists of three isoforms: DNMT1 which maintains the DNA methylation pattern during DNA replication, and DNMT3a and DNMT3b responsible for de novo methylation^{42,43}. Since DNA methylation is a dynamic process depending on environmental cues and biological context, this methylgroup can also be removed. The first step in active DNA demethylation consists of the hydroxylation of 5meC to 5-hydroxymethylcytosine (5hmC) mediated by DNA dioxygenases known as ten-eleven translocation (TET) enzymes. These enzymes are also responsible for the further

sequential oxidation of 5hmC to 5-formylcytosine (5fC), and 5-carboxycytosine (5caC). Final DNA demethylation will then occur in a two-step manner. First 5fC and 5caC will be excised by thymine-DNA-glycosylase (TDG) followed by a replacement with an unmodified cytosine due to the base excision repair mechanism^{44,45}. The TET family consist of three members: TET1, TET2, and TET3. All TET proteins have the same catalytic activity but are expressed in different tissues and related to different biological processes. TET1 is highly expressed in embryonic stem cells (ESC) and primordial germ cells, TET2 is also expressed in ESC, while TET3 is expressed in oocytes, zygotes and neurons. Both TET1 and TET2 are important for the correct differentiation of ESC^{44,46}. Besides, is TET2 also important for the hematopoietic stem cell differentiation⁴⁷. The TET3 protein is important for the complete erase of 5meC of the paternal genome after fertilization and the correct neuronal differentiation^{48,49}. Although the study of TET enzymes is mostly done in ESC, the correct expression of these enzymes in differentiated tissues has also been proven to be important. TET2 mutations have been associated with myeloid malignancies and aberrant expression due to changes in the steroid hormone regulation. While aberrant expression of TET1 has been related to a worse outcome of reproductive-related cancers^{44,47,50}.

Second, histone modifications consist of post-translational acetylation (lysine), methylation (lysine/arginine), and phosphorylation (threonine/serine) of the N-terminal tail of the different histones H2A, H2B, H3 and H4^{42,43}. These modifications are catalyzed by histone modifying enzymes that can be divided in three classes: writers, readers and erasers. Writers are enzymes that can add modifications to the histone tails including histone methyltransferases (HMTs; including lysine methyltransferases (KMTs) e.g. EZH2 and arginine histone methyltransferases (PRMTs) e.g. PRMT5), histone acetyl transferases (HATs) and ubiquitin ligases. These modifications can then be removed by erasers including lysine demethylases ((KDMs) e.g. JMJD3), histone deacetylases (HDACs) and deubiquitinating enzymes^{43,51,52}. Since histones are responsible for the conformation and stability of the DNA, specific combinations of these modifications promotes the binding of specific protein complexes known as readers. Depending on the protein complexes, this will result in activation or silencing of gene transcription^{42,43}.

Third, microRNAs (miRNAs) suppress mRNA translation by altering protein expression. MicroRNAs are endogenous, short (approximately 18-25 nucleotides), non-coding RNA molecules with an important post-transcriptional, regulatory role. They target the 3'-untranslated region (3'UTR) of specific mRNA leading to inhibited translation or mRNA degradation⁵³. The following section will discuss the epigenetic alterations in NAFLD with a focus on PPAR α .

1.2.2 Methylation state of PPAR α is a biomarker of NAFLD development

Overall, NAFLD patients show aberrant DNA methylation levels (5meC) correlating with the severity of the disease. More specifically, compared to controls a low hepatic global DNA methylation level is present in NAFLD patients which further decreases when mild inflammation and moderate fibrosis are occurring²⁵. Moreover NAFLD patients with mild versus severe fibrosis can be distinguished based on lower methylation of specific CpGs in pro-fibrogenic genes in NAFLD patients with severe fibrosis⁵⁴. Besides methylation, Pirola et al. reported that NAFLD patients also show a significant loss of non-nuclear hydroxymethylation (5hmC) based on immune-specific assays. This non-nuclear 5hmC is probably located at the mitochondria. Hepatic nuclear 5hmC in livers of NAFLD patients is however not significantly altered compared to controls or different stages of the disease. Interestingly, they also found a positive correlation of 5hmC with

mitochondrial DNA copy number and an inverse correlation with peroxisome proliferator-activated receptor-gamma coactivator 1 α (PPARGC1 α) mRNA levels⁵⁵. Since PPARGC1 α is a major modulator of mitochondrial biogenesis and NAFLD is associated with changes in PPARGC1 α expression, mitochondrial function and copy number⁵⁵⁻⁵⁷. This suggests that besides 5meC, 5hmC may also contribute to the pathogenesis of NAFLD by regulation of mitochondrial biogenesis and PPARGC1A expression.

Further evidence of the crucial role of epigenetic regulation in the development of NAFLD can be found in rodent studies using different diets. DNA methylation can be influenced by diet nutrients such as choline, methionine, and betaine. These components are considered “methyl-donors” promoting DNA methylation^{58,59}. Supplementation of these methyl-donors can lead to an increase in the hepatic outflow of triglycerides⁶⁰. For example, betaine is a methyl donor generally existing in food, such as spinach and shrimps, that plays an important role in the prevention and therapy of liver diseases including NAFLD⁶¹. Interestingly, the DNA methylation pattern of PPAR α can be modified by betaine resulting in improved triglycerides content^{60,62,63}. Reciprocally, deficiency of methyl-donors results in triglyceride accumulation by overexpression of genes associated with fatty acid synthesis leading to a NAFLD-like situation⁶⁴. Besides methyl-donors, also lipids and fructose influence DNA methylation. For example, the offspring of female mice fed a high fat diet (HFD) before and during gestation and lactation, followed by a HFD after weaning develop NAFLD with increased methylation of PPAR α in offspring. Similarly, offspring of female rats put on a high fructose diet revealed increased methylation of key metabolic genes including PPAR α ^{65,66}. Both studies indicate that a bad maternal environment can epigenetically predispose the offspring for metabolic diseases, including NAFLD^{65,66}. Besides indicates all the previous data, that the nuclear receptor PPAR α a key factor is in the epigenetic regulation of NAFLD.

Interestingly, both altered DNA methylation and hydroxymethylation patterns have been observed at the PPAR α gene locus in NAFLD conditions. More specifically, PPAR α is hypermethylated in an *in vitro* and *in vivo* steatosis model leading to lower PPAR α gene expression and protein levels²⁶. This is similar to NAFLD patients showing gradually decreasing PPAR α expression levels, with each advanced stage of NAFLD²⁹. Besides methylation, also hydroxymethylation has been shown to influence PPAR α expression in NAFLD. Wang et al.⁶⁷ proved that TET1 can directly bind to the promotor region of PPAR α mediating hydroxymethylation. This might suggest that TET1 has a protective effect against NAFLD by demethylating and thus increasing hydroxymethylation of PPAR α , promoting fatty acid oxidation. Moreover, TET1 knockout mice resulted in a higher degree of liver steatosis and lower levels of PPAR α and its target genes⁶⁷.

Since DNA hypermethylation of the PPAR α gene is linked to the development of NAFLD, researchers have tried to alleviate NAFLD progression by inhibiting DNA methylation of the PPAR α gene by natural herbal compounds. For example, curcumin, a traditional Chinese and Indian medicine isolated from turmeric (*Curcuma longa*) was shown to reverse the NAFLD phenotype *in vitro* and *in vivo* by reducing methylation of several genes including DNMT1 and PPAR α , resulting in increased PPAR α expression^{26,68,69}.

1.2.3 Histone modifications at the promotor region of PPAR α related to the development of NAFLD

Another layer of gene expression regulation by epigenetic modifications are histone modifications. These modifications can alter chromatin structure and thus the accessibility for transcription factors^{42,43}. A growing body of literature has investigated histone methylation and acetylation in NAFLD leading to changes in PPAR α expression.

Previous studies have shown that a deficiency in histone demethylase Jhdm2a (also known as JMJD1A) induces the development of hallmarks of metabolic syndrome including hyperlipidemia and obesity. Jhdm2a is responsible for the demethylation of H3K9 and can thereby regulate the expression of multiple genes^{70,71}. Interestingly, Tateishi et al., found that in skeletal muscle cells, this change in lipid metabolism was due to a direct binding of Jhdm2a to PPAR α . More specifically, Jhdm2a knockout mice had an increased level of the inhibitory H3K9me2 modification at the promotor region of PPAR α which triggered decreased PPAR α expression and downstream PPAR α target genes involved in lipid metabolism including fatty acid oxidation⁷¹. Besides, hepatic transcriptome profiling of HFD-induced NAFLD mice revealed an altered expression of genes encoding jumonji C-domain-containing histone demethylases (JMJD) that can regulate histone trimethylation (e.g., H3K9me3 and H3K4me3)⁷². Accordingly, in lipid-accumulated hepatocytes H3K9me3 and H3K4me3 levels diminished at the promotor region of PPAR α and hepatic lipid catabolism gene networks resulting in their reduced expression⁷². Besides lysine methyltransferase, also arginine methyltransferase (PRMT5) activity has been associated with inhibition of PPAR α functions upon HFD⁷³. PRMT5 is part of the arginine methyltransferase family (PRMT) consisting of three subfamilies which differ in their ability to carry out monomethylation, asymmetric demethylation (type I), monomethylation or symmetric demethylation (type II) or exclusively monomethylation (Type III)⁷⁴. PRMT5 is a known type II arginine methyltransferase that dimethylates histones H2AR3⁷⁵, H4R3⁷⁶ and H3R8⁷⁷ but also non histone proteins including SREBP1 and AKT kinase^{73,78}. Huang et al. showed that a HFD induces the activation of AKT kinase by PRMT5, which will further phosphorylate and inhibit PPAR α functions. This will lead to an inhibition of mitochondrial β -oxidation and aggravation of high fat diet induced hepatic steatosis⁷³. All these studies indicate that the epigenetic regulation by histone methylation are putative hallmarks for the development of NAFLD and the regulation of PPAR α .

Furthermore, increased histone acetylation levels have also been observed in an *in vitro* steatosis model and contribute to the development of NAFLD⁷⁹. Accordingly, HDAC-inhibitors such as sodium butyrate can alleviate HFD-induced NAFLD by increasing β -oxidation. This could be explained by restoring the acetylation pattern and expression of PPAR α . More specifically, sodium butyrate enhances the H3K9Ac modification at the PPAR α gene promoter²⁸.

Altogether, although data on histone modifications in metabolic diseases including NAFLD and key players such as PPAR α remain fragmentary, the current data already highlights the importance of histone methylation and acetylation regulation of PPAR α in the development of NAFLD. Future studies will need to further untangle the histone modification landscape of NAFLD.

1.2.4 PPAR α targeting microRNAs contribute to NAFLD development

Previous studies have shown that several miRNAs are upregulated in NAFLD patients, as well as in experimental *in vitro* and *in vivo* NAFLD models⁸⁰. Today, miRNAs are considered as important

posttranscriptional modulators in NAFLD pathology, which can mimic gene silencing. Some of these altered miRNAs target nuclear receptors, including PPAR α ⁸⁰. For example, miR-200, miR-20b, miR181-a, miR-30a-3p, miR519d, miR-21 and miR-22 are elevated in NAFLD and target directly PPAR α mRNA⁸¹⁻⁸⁷. The working mechanism of these miRNAs leading to aggravation of NAFLD is approximately the same. They all bind to the 3'UTR of PPAR α mRNA resulting in PPAR α mRNA degradation, decreased protein expression and disturbed lipid metabolism, leading to aggravation of an NAFLD phenotype. Moreover, the induced expression of specific miRNAs (miR-20b, miR181-a, miR-30a-3p and miR-22) in FFA-treated hepatocytes increases the intracellular lipid content upon reduction of PPAR α mRNA levels and decreased protein expression^{81,82,84,85}. Moreover, even in colorectal cancer derived liver metastasis, deregulated PPAR targeting miRNAs have been observed⁸⁸.

Therefore, antagomirs targeting specific miRNAs underlying hepatocellular steatosis are investigated as potential therapeutic agents to treat NAFLD. Since inhibition of miR-34a in a mice model improved hepatic steatosis by increasing PPAR α levels promoting lipid oxidation⁸⁹, targeting miR-34a/PPAR α signaling holds promise as an interesting future strategy for clinical miRNA therapeutic applications against NAFLD. Of special note, the antagomir circRNA_0046366 could antagonize miR-34a and restore PPAR α expression which could alleviate NAFLD in an *in vitro* and *in vivo* model^{90,91}.

Further evidence for the involvement of miRNAs in NAFLD development can be found in one of the cells natural rescue mechanisms for the disease. More specifically it has been demonstrated that the increased lipid accumulation in the liver of NAFLD patients triggers protein folding stress in the endoplasmic reticulum (ER). Subsequently, more unfolded proteins accumulate in the ER leading to the activation of the unfolded protein response (UPR)⁹²⁻⁹⁴. The most conserved UPR pathway that has been proven to be important for NAFLD is the inositol-requiring enzyme 1 α (IRE1 α)/ X-box binding protein 1 (XBP1) pathway⁹². IRE1 α is a stress sensor, activated by ER stress, which splices the mRNA of the XBP1 via its RNase activity. This spliced XBP1 will then activate the gene expression of a subset of UPR-associated regulators^{95,96}. Wang et al. further showed that IRE1 α is responsible for the degradation of specific miRNAs including miR-200 and miR-34. These miRNAs can target the mRNA of nuclear receptors such as PPAR α mRNA as discussed above. The decrease of these miRNAs targeting PPAR α mRNA by a deficiency of IRE1 α leads to exacerbated hepatic steatosis in both *in vivo* and *in vitro* diet induced NAFLD models⁸⁷. In conclusion, miRNA regulation is strongly modulated by protein folding stress responses during lipid homeostasis.

1.3 Epigenetic interaction partners in crime in PPAR α dependent liver pathologies

Besides epigenetic control mechanisms of PPAR α protein expression, epigenetic enzymes can also modulate PPAR α functions as direct interaction partners during NAFLD progression. Hence better characterization of epigenetic binding partners of PPAR α may offer new therapeutic perspectives for epigenetic drugs in NAFLD treatment.

1.3.1 PPAR α interactions with histone modifying enzymes

1.3.1.1 SIRT1

Sirtuins (SIRT) are conserved NAD⁺ dependent class III histone deacylases, highly dependent on the cellular metabolism. Hence, they are considered as cellular sensors of energy status in response to diet and environment to protect against metabolic stress. In mammals there are seven sirtuins,

SIRT1-7 located to different cellular components^{97,98}. Several sirtuins play a key regulatory role in both fasting and NAFLD conditions. First of all, the nuclear SIRT1 induces a metabolic switch during fasting conditions to restore the energy balance in the cell. Therefore it will deacetylate several transcription factors in the liver, heart, adipocytes and skeletal muscle that induce an increase in fatty acid use and gluconeogenesis to decrease glycolysis and fatty acid synthesis. In the mitochondria, upregulation of SIRT3 and downregulation of SIRT4 will, increase fatty acid oxidation and oxidative stress during fasting^{98,99}. Therefore it is not surprising that SIRT1, SIRT3 and SIRT6 have been reported to protect against fatty liver disease by controlling the expression of lipogenic enzymes, mitochondrial function and stimulation of fatty acid oxidation respectively¹⁰⁰.

Of particular interest, several research teams have demonstrated an interaction and reciprocal transcriptional crosstalk between PPAR α and histone deacetylase SIRT1 (Figure 4). On one side, one of the major regulatory targets of SIRT1 is the PPAR α signaling pathway. Hence SIRT1 activity is required to activate transcription of PPAR α target genes including FGF21 in the liver¹⁰¹. Besides, it has been reported that natural compounds and drugs used for treatment of NAFLD targeting the PPAR α signaling pathway, are depending on SIRT1 activity¹⁰²⁻¹⁰⁴. Moreover, in both adipocytes and hepatocytes, it has been shown that depletion of SIRT1 reduces the expression of several PPAR α target genes related to lipid metabolism and mitochondrial biogenesis^{105,106}. Reciprocally, PPAR α agonists including fenofibrate, WY1643 and GW7647 or fasting increased expression of PPAR α have been reported to promote SIRT1 activity¹⁰⁷⁻¹¹⁰. Whether these effects are mediated via direct interaction between PPAR α and SIRT1 or require an indirect interaction via the deacetylation of Peroxisome proliferator-activated receptor gamma coactivator 1-alpha (PGC1- α), is not yet fully understood. First, the direct interaction between SIRT1 and PPAR α has been shown to affect the expression of both SIRT1 and PPAR α target genes depending on the cell type. Gong et al. showed with a luciferase assay in adipocytes that under high fat conditions PPAR α and SIRT1 form a direct interaction, when both genes are overexpressed¹¹¹. This interaction induces osteogenic differentiation via the SIRT1 dependent pathway. Further, this direct interaction has also been confirmed in the heart by Villarroya et al. where the interaction of PPAR α and SIRT1 under a high fat diet reduces the binding of PPAR α with the RXR receptor and p65. This reduced interaction leads to an upregulation of the PPAR α pro-inflammatory target genes and downregulation of FAO in the heart¹¹². According to Oka et al., the change in interaction partner of PPAR α is due to imperfect PPAR responsive element (PPRE) binding sites that make the interaction of PPAR α with the RXR α receptor unstable^{113,114}. Subsequently, when PPAR α is upregulated under stress conditions (i.e. heart failure or a HFD), PPAR α is able to bind to other proteins including RXR and SIRT1¹¹³⁻¹¹⁵. The direct interaction of PPAR α and SIRT1 has also been proven by coimmunoprecipitation in the liver¹⁰⁶. Interestingly, in the liver, the interaction between PPAR α and SIRT1 is increased when PPAR α is activated and abolished when PPAR α is poly(ADP-ribosyl)ation by PARP1¹¹⁶. Since PPAR α and SIRT1 are downregulated and PARP1 upregulated in NAFLD patients, the study of this interaction is of high importance for the treatment of the disease^{29,116,117}.

Besides its direct interaction, SIRT1 also indirectly activates PPAR α functions via the AMPK-Sirt1-Pgc-1 α signaling pathway. AMPK and SIRT1 are both metabolic energy sensors that form a positive feedback loop, to finetune the cellular energy metabolism status¹¹⁸. More specifically, AMPK can be activated by SIRT1 through the deacetylation of liver Kinase B1 (LKB1), while SIRT1 is activated by AMPK through the synthesis of NAD⁺^{119,120}. Subsequently, activated SIRT1 can deacetylate and

activate PCG1- α , while AMPK enhances its activity by phosphorylation^{106,121,122}. This deacetylated PCG1- α has been reported to function as a coactivator of PPAR α , leading to activation of several PPAR α target genes involved in the lipid metabolism, mitochondrial biogenesis and (anti)-inflammatory pathways^{121,123–126}. All these pathways have been described for their role in the development and progression of metabolic diseases, indicating the importance of this pathway for the treatment of several metabolic diseases including diabetes and NAFLD^{127–129}.

1.3.1.2 JMJD3

The jumonji D3 (JMJD3) is a histone lysine demethylase that belongs to the KDM6 family and epigenetically activates genes by demethylating the repressive histone H3K27-me3 mark¹³⁰. The JMJD3 has an established role in development, differentiation, immunity and extending lifespan in response to mild mitochondrial stress^{130,131}. However recently it has also proven its role in the initiation of autophagy and metabolic regulation by the interaction with PPAR α ^{132,133} (Figure 4).

Autophagy is an essential catabolic process for cellular survival and energy homeostasis under nutrient deprivation^{134,135}. It recycles cytoplasmic components (e.g. organelles) to new building blocks (e.g. amino acids) for cellular renovation and provides free fatty acids for β -oxidation by degrading intracellular lipid stores for energy production¹³⁵. Byun, S et al. firstly reported a role of JMJD3 in the activation of autophagy under starvation by an interaction with PPAR α . Upon fasting, FGF21 (Fibroblast growth factor 21) signaling is activated which induces phosphorylation of JMJD3 at Thr-1044 by PKA (Protein kinase A). This will lead to activation of JMJD3, increasing its nuclear localization and interaction with PPAR α to transcriptionally activate autophagy¹³². Dysregulation of autophagy has been linked to several diseases including NAFLD¹³⁶. Moreover the expression of both JMJD3 and PPAR α is decreased in NAFLD patients^{29,132}. However to determine whether there is a causal link between the FGF21-JMJD3-PPAR α axis leading to decreased expression of autophagy genes and the development of NAFLD further investigation is necessary. In addition to autophagy, an interaction between JMJD3, PPAR α and SIRT1 also activates mitochondrial fatty acid β -oxidation¹³³. Under fasting conditions, PPAR α recruits both JMJD3 and SIRT1 to activate β -oxidation genes. Next, SIRT1 will be phosphorylated at Ser434 upon PKA activation, inducing the formation of the JMJD3-SIRT1-PPAR α complex at PPRE of β -oxidation network genes. This interaction is abolished when one of the genes is downregulated, indicating a strong positive autoregulatory loop. Moreover, liver specific downregulation of JMJD3 impairs mitochondrial β -oxidation, liver steatosis and glucose and insulin intolerance in mice fed a normal chow diet¹³³.

Both studies indicate an interesting link between the epigenetic enzyme JMJD3 and PPAR α at the crossroad of autophagy and β -oxidation in NAFLD, which could be targeted by epigenetic drugs.

1.3.2 PPAR α interactions with DNA modifying enzymes

1.3.2.1 TET enzymes

Pang et al. observed an association of decreased expression of TET1 and TET2 with increased methylation of PPAR α in the mice embryos of mothers fed a HFD during gestation¹³⁷. Reciprocally, PPAR α activation induces demethylation of its target genes, including *fgf21* and several genes of the β -oxidation both during the perinatal period induced by milk lipids or in adolescent rats induced by a HFD^{138–141}. Moreover mouse livers of mice treated with the PPAR α agonist WY-14643 show a demethylation of the growth arrest DNA damage-inducible beta (*GADD45b*) gene¹⁴². Although it is not sure how PPAR α induces this demethylation, Yuan et al. reported increased expression of TET2

and TET3 during lactation together with a possibly interaction of PPAR α with the TET2 enzyme¹³⁹ (Figure 5). Besides, it has been shown that ascorbic acid, a cofactor for TET enzymes, is necessary to induce proper demethylation of PPAR α target genes, including *fgf21*, in offspring¹⁴³.

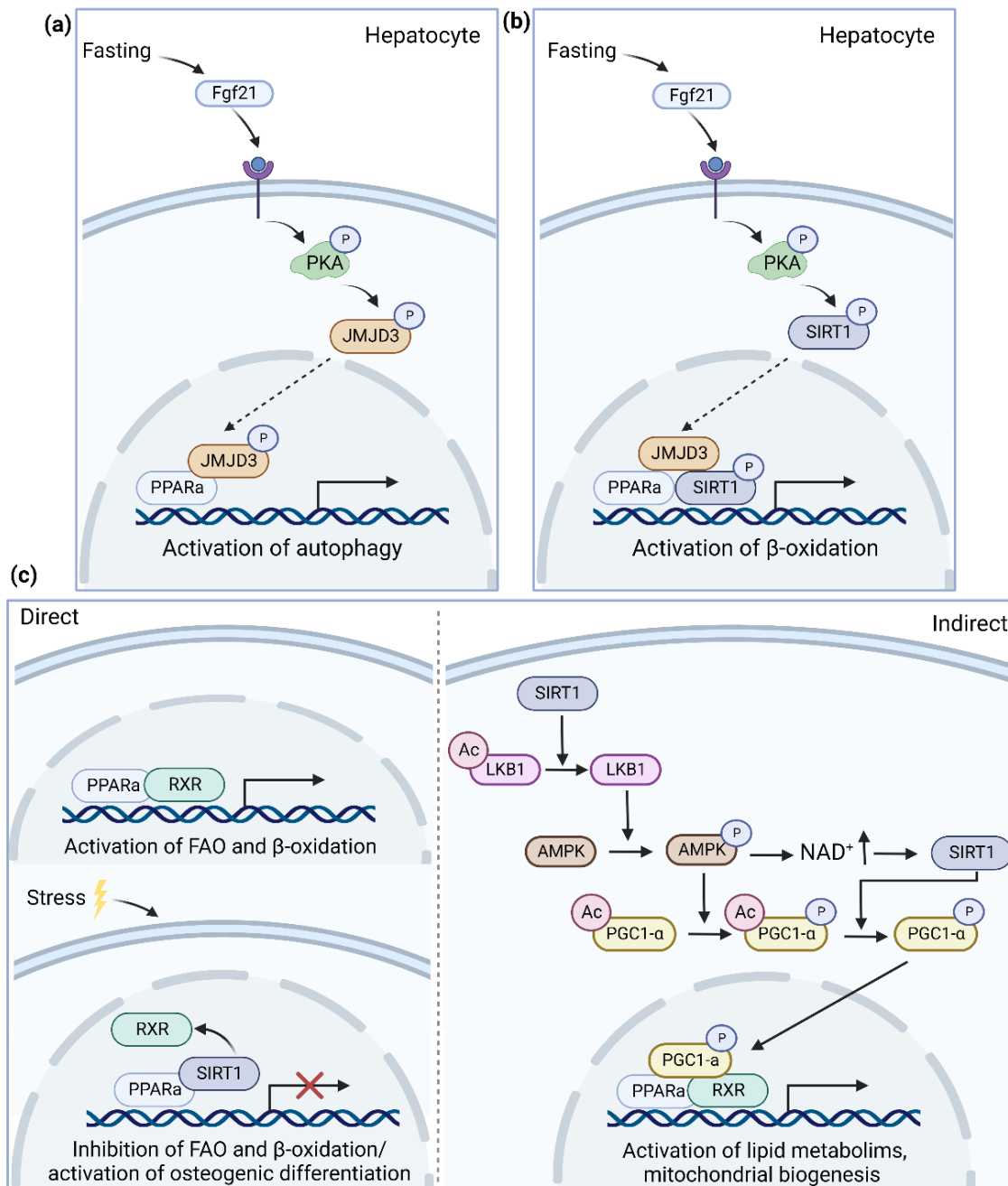


Figure 4: Overview of possible pathways leading to a direct interaction of PPAR α with histone modifying enzymes regulating diverse pathways. **(a)** JMJD3 can activate autophagy under starvation by an interaction with PPAR α **(b)** PPAR α has been described to recruit both JMJD3 and SIRT1 to activate β -oxidation genes under fasting conditions **(c)** It is not clear yet if the bidirectional regulation of PPAR α and SIRT1 target genes is regulated by the direct interaction between PPAR α and SIRT1 or the indirect interaction via the deacetylation of PGC1- α . Abbreviations: peroxisome proliferator-activated receptor- α , PPAR α ; Fibroblast growth factor 21, Fgf21; Protein kinase A, PKA; Jumonji D3, JMJD3; Sirtuin 1, SIRT1; retinoid X receptor, RXR; Liver Kinase B1, LKB1; AMP-activated protein kinase, AMPK; Peroxisome proliferator-activated receptor gamma coactivator 1-alpha, PGC1- α

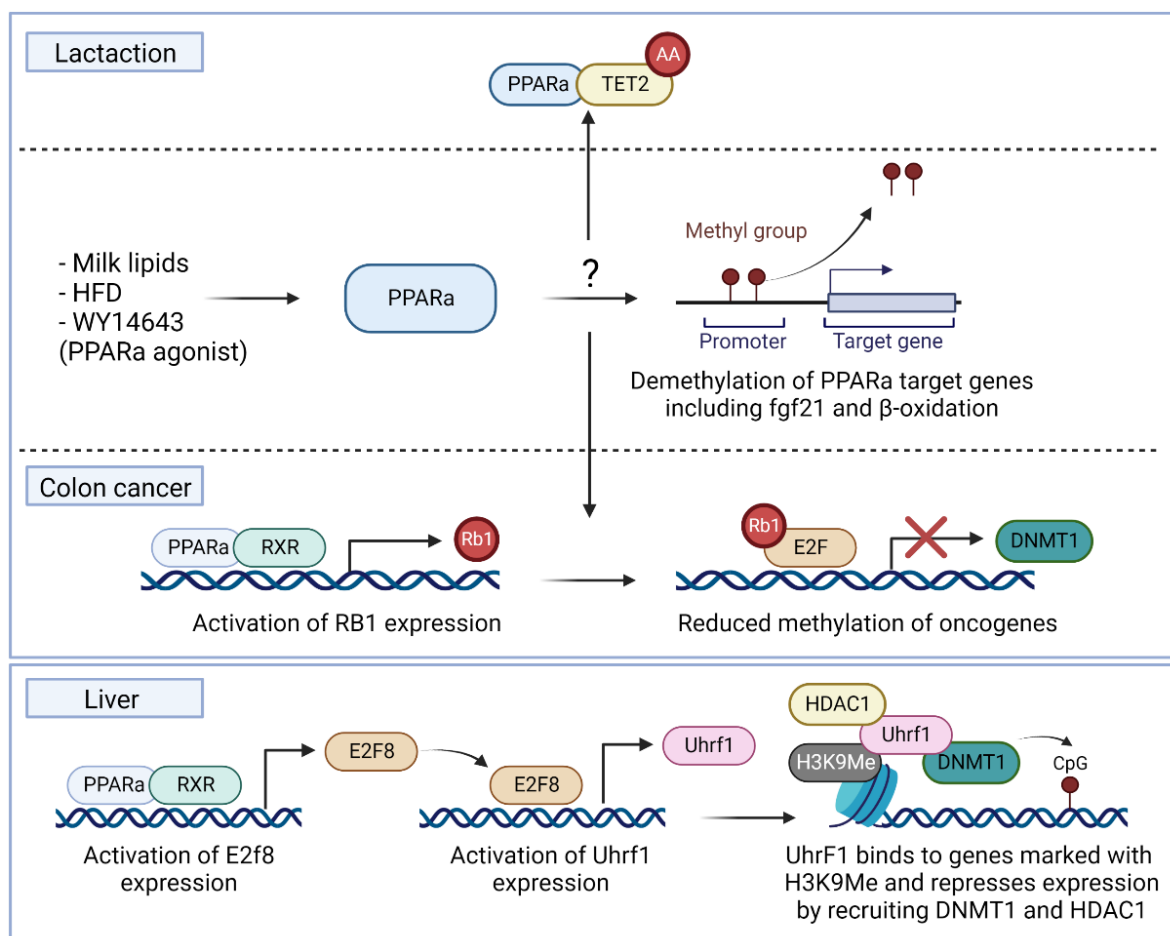


Figure 5: Overview of PPAR α as an epigenetic regulatory driver regulating expression of its target genes by interacting with DNA modifying enzymes. Possible pathways for demethylation could be a direct interaction with TET2 as found during lactation or by inhibiting DNMT1 via the RB1/E2F pathway due to the activation of Rb1 expression by PPAR α as found in colon cancer. Besides can PPAR α activate the expression of the epigenetic regulator Uhrf1 by inducing the expression of the E2f8 transcription factor. Uhrf1 is known to recruit DNMT1 to target genes with a H3K9me3 histone mark leading to hypermethylation and downregulation. Abbreviations: peroxisome proliferator-activated receptor- α , PPAR α ; tet methylcytosine dioxygenase 2, TET2; Fibroblast growth factor 21, Fgf21; High fat diet, HFD; retinoid X receptor, RXR; retinoblastoma tumor suppressor gene, RB1; E2F transcription factor, E2F; DNA methyltransferase I, DNMT1; E2F Transcription Factor 8, E2f8; Ubiquitin Like With PHD And Ring Finger Domains 1, Uhrf1; Histone deacetylase 1, HDAC1.

1.3.2.2 DNMT enzymes

Besides interactions of PPAR α and TET enzymes in early development, associations of PPAR α inhibition with increased expression of DNA methyltransferase I (DNMT1) and protein arginine methyltransferase 6 (PRMT6) have already been demonstrated in colon cancer and liver^{144,145}. More specifically Luo et al. reported that in colon cancer due to the downregulation of PPAR α , less RB1 protein will be expressed. Considering the repressive role of RB1 on E2F transactivation and the E2F binding sites in the DNMT1 and PRMT6 promoters this will induce an upregulation of DNMT1 and PRMT6^{144,146}. Following decreased expression of tumor suppressor genes and the development of more severe colon cancer¹⁴⁴ (Figure 5). This inhibitory role of PPAR α on DNMT1 has also been confirmed by Kong et al. showing an inhibition of DNMT1 followed by an activation of the tumor suppressor gene CDKN2A due to lower methylation, induced by a treatment with the PPAR α agonist fenofibrate¹⁴⁵. Besides has Aibara et. al reported that in the liver PPAR α activation causes

hepatocyte proliferation by the activation of DNMT1 via the expression of another E2F transcription factor called E2f8. This E2f8 transcription factor is known to induce the expression of the epigenetic regulator Uhrf1, which binds to target genes with a H3K9me3 histone mark and recruits DNMT1 and HDAC1 to regulate expression¹⁴⁷. These studies establish an interesting functional epigenetic regulatory driver role of PPAR α to epigenetically regulate targets by activating transcription factors regulating the activity of DNMT1 (Figure 5). Moreover Hervouet et al. suggested a direct interaction of PPAR α with DNMT1¹⁴⁸. In mice, a high fat diet induced NAFLD phenotype was also accompanied with a decreased expression of DNMT3a and DNMT3b¹⁴⁹. Further molecular characterization of possible interactions of PPAR α with DNMTs and TET enzymes may reveal new therapeutic targets for epigenetic drugs against NAFLD.

1.4 Conclusion and future perspectives

Since the discovery of PPAR α in 1990, this nuclear receptor is known as a master regulator of the metabolism because of its regulatory role in the lipid metabolism¹⁵⁰. Therefore it has been an attractive therapeutic target in the research for a therapy of NAFLD. However although various epigenetic enzyme interaction partners (SIRT1, JMJD3, TET, DNMT1) already have been identified for PPAR α , there remains a research gap which addresses the role of PPAR α as an epigenetic driver in NAFLD progression. As summarized in this review some clear associations and interactions of PPAR α with epigenetic modifying enzymes are involved in metabolism. However the mechanistic pathways behind these associations are incomplete and need further research. Especially because epigenetic modifications are reversible and dynamic during development and progression of NAFLD and therefore combination therapies of epigenetic drugs with currently investigated PPAR agonists-antagonists hold promise for future drug discovery pipelines against NAFLD. Since there is still no FDA approved therapy for NAFLD, a lot of drugs under investigation include PPAR α agonists. The first type of agonists tested were fibrates, which showed promising results in preclinical trials, but this was not translated in the clinical trials with NAFLD and NASH patients^{151–154} (reviewed in³⁰). Another PPAR α agonist called Pemafibrate is approved and marketed in Japan for treatment of dyslipidemia^{155,156}. Although this drug shows promising results based on blood-based markers of NAFLD (e.g. ALT, AST, TG), histological liver outcomes are missing^{30,157}. Therefore it needs further investigation for the treatment of NAFLD patients in clinical trials. Dual or pan PPAR agonists show more promising results as potential treatment. Especially the pan PPAR agonist lanifibranor, which is currently further investigated in a phase III clinical trial with NASH patients^{30,158}. Besides targeting the three PPAR isoforms, it could also be interesting in the future to combine PPAR α agonists with epigenetic drugs. For example, currently investigated epigenetic drugs vitamin E and resveratrol which inhibit DNMT1 expression and activating SIRT1 respectively, may also affect the epigenetic regulation of PPAR α in NAFLD as shown in this review^{159,160}. Therefore a better functional molecular characterization of epigenetic interaction partners of PPAR α may provide novel mechanistic insights for innovative therapeutic targeting strategies which can restore lipid energy homeostasis and ameliorate NAFLD.

1.5 References

1. Chew, N. *et al.* Global burden of metabolic diseases: data from Global Burden of Disease 2000-2019. A consortium of metabolic disease. *Eur Heart J* **44**, (2023).
2. Rinella, M. E. *et al.* A multi-society Delphi consensus statement on new fatty liver disease nomenclature. *J Hepatol* (2023) doi:10.1016/j.jhep.2023.06.003.
3. Loomba, R. & Sanyal, A. J. The global NAFLD epidemic. *Nat Rev Gastroenterol Hepatol* **10**, 686–690 (2013).
4. Younossi, Z. M. *et al.* Global epidemiology of nonalcoholic fatty liver disease-Meta-analytic assessment of prevalence, incidence, and outcomes. *Hepatology* **64**, 73–84 (2016).
5. Hyun, J. & Jung, Y. DNA Methylation in Nonalcoholic Fatty Liver Disease. *Int J Mol Sci* **21**, (2020).
6. Chalasani, N. *et al.* The diagnosis and management of nonalcoholic fatty liver disease: Practice guidance from the American Association for the Study of Liver Diseases. *Hepatology* **67**, 328–357 (2018).
7. Stepanova, M. & Younossi, Z. M. Independent association between nonalcoholic fatty liver disease and cardiovascular disease in the US population. *Clin Gastroenterol Hepatol* **10**, 646–650 (2012).
8. Pouwels, S. *et al.* Non-alcoholic fatty liver disease (NAFLD): a review of pathophysiology, clinical management and effects of weight loss. *BMC Endocr Disord* **22**, 63 (2022).
9. Hadizadeh, F., Faghihimani, E. & Adibi, P. Nonalcoholic fatty liver disease: Diagnostic biomarkers. *World J Gastrointest Pathophysiol* **8**, 11 (2017).
10. Cotter, T. G. & Rinella, M. Nonalcoholic Fatty Liver Disease 2020: The State of the Disease. *Gastroenterology* **158**, 1851–1864 (2020).
11. Kleiner, D. E. *et al.* Design and validation of a histological scoring system for nonalcoholic fatty liver disease. *Hepatology* **41**, 1313–1321 (2005).
12. Chalasani, N. *et al.* The diagnosis and management of nonalcoholic fatty liver disease: Practice guidance from the American Association for the Study of Liver Diseases. *Hepatology* **67**, 328–357 (2018).
13. Fougerat, A., Montagner, A., Loiseau, N., Guillou, H. & Wahli, W. Peroxisome Proliferator-Activated Receptors and Their Novel Ligands as Candidates for the Treatment of Non-Alcoholic Fatty Liver Disease. *Cells* **9**, 1638 (2020).
14. Romero-Gomez, M., Zelber-Sagi, S. & Trenell, M. Treatment of NAFLD with diet, physical activity and exercise. *J Hepatol* **67**, 829–846 (2017).
15. Rong, L. *et al.* Advancements in the treatment of non-alcoholic fatty liver disease (NAFLD). *Front Endocrinol (Lausanne)* **13**, (2023).
16. Golabi, P. *et al.* Effectiveness of exercise in hepatic fat mobilization in non-alcoholic fatty liver disease: Systematic review. *World J Gastroenterol* **22**, 6318 (2016).

17. Koutoukidis, D. A. *et al.* Association of Weight Loss Interventions With Changes in Biomarkers of Nonalcoholic Fatty Liver Disease. *JAMA Intern Med* **179**, 1262 (2019).
18. Katsagoni, C. N. *et al.* Improvements in clinical characteristics of patients with non-alcoholic fatty liver disease, after an intervention based on the Mediterranean lifestyle: a randomised controlled clinical trial. *British Journal of Nutrition* **120**, 164–175 (2018).
19. Younossi, Z. M., Corey, K. E. & Lim, J. K. AGA Clinical Practice Update on Lifestyle Modification Using Diet and Exercise to Achieve Weight Loss in the Management of Nonalcoholic Fatty Liver Disease: Expert Review. *Gastroenterology* **160**, 912–918 (2021).
20. Vilar-Gomez, E. *et al.* Weight Loss Through Lifestyle Modification Significantly Reduces Features of Nonalcoholic Steatohepatitis. *Gastroenterology* **149**, 367–78 e5; quiz e14-5 (2015).
21. Kim, H. J. *et al.* Metabolic significance of nonalcoholic fatty liver disease in nonobese, nondiabetic adults. *Arch Intern Med* **164**, 2169–2175 (2004).
22. Schwimmer, J. B. *et al.* Heritability of nonalcoholic fatty liver disease. *Gastroenterology* **136**, 1585–1592 (2009).
23. Romeo, S. *et al.* Genetic variation in PNPLA3 confers susceptibility to nonalcoholic fatty liver disease. *Nat Genet* **40**, 1461–1465 (2008).
24. Rodríguez-Sanabria, J. S., Escutia-Gutiérrez, R., Rosas-Campos, R., Armendáriz-Borunda, J. S. & Sandoval-Rodríguez, A. An Update in Epigenetics in Metabolic-Associated Fatty Liver Disease. *Front Med (Lausanne)* **8**, (2022).
25. Lai, Z. *et al.* Association of Hepatic Global DNA Methylation and Serum One-Carbon Metabolites with Histological Severity in Patients with NAFLD. *Obesity (Silver Spring)* **28**, 197–205 (2020).
26. Li, Y. Y. *et al.* Fatty liver mediated by peroxisome proliferator-activated receptor-alpha DNA methylation can be reversed by a methylation inhibitor and curcumin. *J Dig Dis* **19**, 421–430 (2018).
27. Pirola, C. J. *et al.* Epigenetic modification of liver mitochondrial DNA is associated with histological severity of nonalcoholic fatty liver disease. *Gut* **62**, 1356–1363 (2013).
28. Sun, B. *et al.* Sodium Butyrate Ameliorates High-Fat-Diet-Induced Non-alcoholic Fatty Liver Disease through Peroxisome Proliferator-Activated Receptor alpha-Mediated Activation of beta Oxidation and Suppression of Inflammation. *J Agric Food Chem* **66**, 7633–7642 (2018).
29. Francque, S. *et al.* PPARalpha gene expression correlates with severity and histological treatment response in patients with non-alcoholic steatohepatitis. *J Hepatol* **63**, 164–173 (2015).
30. Lange, N. F., Graf, V., Caussy, C. & Dufour, J. F. PPAR-Targeted Therapies in the Treatment of Non-Alcoholic Fatty Liver Disease in Diabetic Patients. *Int J Mol Sci* **23**, (2022).
31. Amorim, R., Magalhães, C. C., Borges, F., Oliveira, P. J. & Teixeira, J. From Non-Alcoholic Fatty Liver to Hepatocellular Carcinoma: A Story of (Mal)Adapted Mitochondria. *Biology (Basel)* **12**, 595 (2023).
32. Bugge, A. & Mandrup, S. Molecular Mechanisms and Genome-Wide Aspects of PPAR Subtype Specific Transactivation. *PPAR Res* **2010**, (2010).

33. Poulsen, L., Siersbaek, M. & Mandrup, S. PPARs: fatty acid sensors controlling metabolism. *Semin Cell Dev Biol* **23**, 631–639 (2012).
34. Tahri-Joutey, M. *et al.* Mechanisms Mediating the Regulation of Peroxisomal Fatty Acid Beta-Oxidation by PPARalpha. *Int J Mol Sci* **22**, (2021).
35. Kliewer, S. A. *et al.* Fatty acids and eicosanoids regulate gene expression through direct interactions with peroxisome proliferator-activated receptors alpha and gamma. *Proc Natl Acad Sci U S A* **94**, 4318–4323 (1997).
36. Rimando, A. M. *et al.* Evaluation of PPARalpha activation by known blueberry constituents. *J Sci Food Agric* **96**, 1666–1671 (2016).
37. Liss, K. H. & Finck, B. N. PPARs and nonalcoholic fatty liver disease. *Biochimie* **136**, 65–74 (2017).
38. Bougarne, N. *et al.* Molecular Actions of PPARalpha in Lipid Metabolism and Inflammation. *Endocr Rev* **39**, 760–802 (2018).
39. Fang, L. *et al.* PPARgene: A Database of Experimentally Verified and Computationally Predicted PPAR Target Genes. *PPAR Res* **2016**, 1–6 (2016).
40. Berger, S. L., Kouzarides, T., Shiekhattar, R. & Shilatifard, A. An operational definition of epigenetics. *Genes Dev* **23**, 781–783 (2009).
41. Zhang, L., Lu, Q. & Chang, C. Epigenetics in Health and Disease. *Adv Exp Med Biol* **1253**, 3–55 (2020).
42. Moran-Salvador, E. & Mann, J. Epigenetics and Liver Fibrosis. *Cell Mol Gastroenterol Hepatol* **4**, 125–134 (2017).
43. Claveria-Cabello, A. *et al.* Epigenetics in Liver Fibrosis: Could HDACs be a Therapeutic Target? *Cells* **9**, (2020).
44. Melamed, P., Yosefzon, Y., David, C., Tsukerman, A. & Pnueli, L. Tet Enzymes, Variants, and Differential Effects on Function. *Front Cell Dev Biol* **6**, 22 (2018).
45. Ito, S. *et al.* Tet proteins can convert 5-methylcytosine to 5-formylcytosine and 5-carboxylcytosine. *Science (1979)* **333**, 1300–1303 (2011).
46. Koh, K. P. *et al.* Tet1 and Tet2 regulate 5-hydroxymethylcytosine production and cell lineage specification in mouse embryonic stem cells. *Cell Stem Cell* **8**, 200–213 (2011).
47. Delhommeau, F. *et al.* Mutation in TET2 in myeloid cancers. *N Engl J Med* **360**, 2289–2301 (2009).
48. Gu, T. P. *et al.* The role of Tet3 DNA dioxygenase in epigenetic reprogramming by oocytes. *Nature* **477**, 606–610 (2011).
49. Iqbal, K., Jin, S. G., Pfeifer, G. P. & Szabo, P. E. Reprogramming of the paternal genome upon fertilization involves genome-wide oxidation of 5-methylcytosine. *Proc Natl Acad Sci U S A* **108**, 3642–3647 (2011).
50. Good, C. R. *et al.* A novel isoform of TET1 that lacks a CXXC domain is overexpressed in cancer. *Nucleic Acids Res* **45**, 8269–8281 (2017).

51. Gong, F. & Miller, K. M. Histone methylation and the DNA damage response. *Mutat Res Rev Mutat Res* **780**, 37–47 (2019).
52. Ramarao-Milne, P. *et al.* Histone Modifying Enzymes in Gynaecological Cancers. *Cancers (Basel)* **13**, (2021).
53. Bartel, D. P. MicroRNAs: genomics, biogenesis, mechanism, and function. *Cell* **116**, 281–297 (2004).
54. Zeybel, M. *et al.* Differential DNA methylation of genes involved in fibrosis progression in non-alcoholic fatty liver disease and alcoholic liver disease. *Clin Epigenetics* **7**, 25 (2015).
55. Pirola, C. J. *et al.* Epigenetic Modifications in the Biology of Nonalcoholic Fatty Liver Disease: The Role of DNA Hydroxymethylation and TET Proteins. *Medicine (Baltimore)* **94**, e1480 (2015).
56. Sunny, N. E., Bril, F. & Cusi, K. Mitochondrial Adaptation in Nonalcoholic Fatty Liver Disease: Novel Mechanisms and Treatment Strategies. *Trends Endocrinol Metab* **28**, 250–260 (2017).
57. Sookoian, S. *et al.* Epigenetic regulation of insulin resistance in nonalcoholic fatty liver disease: impact of liver methylation of the peroxisome proliferator-activated receptor gamma coactivator 1alpha promoter. *Hepatology* **52**, 1992–2000 (2010).
58. Lombardi, R., Iuculano, F., Pallini, G., Fargion, S. & Fracanzani, A. L. Nutrients, Genetic Factors, and Their Interaction in Non-Alcoholic Fatty Liver Disease and Cardiovascular Disease. *Int J Mol Sci* **21**, (2020).
59. Wang, L. *et al.* Betaine supplement alleviates hepatic triglyceride accumulation of apolipoprotein E deficient mice via reducing methylation of peroxisomal proliferator-activated receptor alpha promoter. *Lipids Health Dis* **12**, 34 (2013).
60. Wang, L. J. *et al.* Betaine attenuates hepatic steatosis by reducing methylation of the MTP promoter and elevating genomic methylation in mice fed a high-fat diet. *J Nutr Biochem* **25**, 329–336 (2014).
61. Wang, C., Ma, C., Gong, L., Dai, S. & Li, Y. Preventive and therapeutic role of betaine in liver disease: A review on molecular mechanisms. *Eur J Pharmacol* **912**, 174604 (2021).
62. Xu, L. *et al.* Betaine alleviates hepatic lipid accumulation via enhancing hepatic lipid export and fatty acid oxidation in rats fed with a high-fat diet--CORRIGENDUM. *Br J Nutr* **114**, 995–996 (2015).
63. Cordero, P., Gomez-Uriz, A. M., Campion, J., Milagro, F. I. & Martinez, J. A. Dietary supplementation with methyl donors reduces fatty liver and modifies the fatty acid synthase DNA methylation profile in rats fed an obesogenic diet. *Genes Nutr* **8**, 105–113 (2013).
64. Pooya, S. *et al.* Methyl donor deficiency impairs fatty acid oxidation through PGC-1alpha hypomethylation and decreased ER-alpha, ERR-alpha, and HNF-4alpha in the rat liver. *J Hepatol* **57**, 344–351 (2012).
65. Pruis, M. G. *et al.* Maternal western diet primes non-alcoholic fatty liver disease in adult mouse offspring. *Acta Physiol (Oxf)* **210**, 215–227 (2014).

66. Ando, Y. *et al.* Maternal high-fructose corn syrup consumption causes insulin resistance and hyperlipidemia in offspring via DNA methylation of the Pparalpha promoter region. *J Nutr Biochem* **103**, 108951 (2022).
67. Wang, J. *et al.* TET1 promotes fatty acid oxidation and inhibits NAFLD progression by hydroxymethylation of PPARalpha promoter. *Nutr Metab (Lond)* **17**, 46 (2020).
68. Lestari, M. L. & Indrayanto, G. Curcumin. *Profiles Drug Subst Excip Relat Methodol* **39**, 113–204 (2014).
69. Prasad, S., Gupta, S. C., Tyagi, A. K. & Aggarwal, B. B. Curcumin, a component of golden spice: from bedside to bench and back. *Biotechnol Adv* **32**, 1053–1064 (2014).
70. Inagaki, T. *et al.* Obesity and metabolic syndrome in histone demethylase JHDM2a-deficient mice. *Genes Cells* **14**, 991–1001 (2009).
71. Tateishi, K., Okada, Y., Kallin, E. M. & Zhang, Y. Role of Jhdm2a in regulating metabolic gene expression and obesity resistance. *Nature* **458**, 757–761 (2009).
72. Jun, H. J., Kim, J., Hoang, M. H. & Lee, S. J. Hepatic lipid accumulation alters global histone h3 lysine 9 and 4 trimethylation in the peroxisome proliferator-activated receptor alpha network. *PLoS One* **7**, e44345 (2012).
73. Huang, L. *et al.* Inhibition of protein arginine methyltransferase 5 enhances hepatic mitochondrial biogenesis. *J Biol Chem* **293**, 10884–10894 (2018).
74. Bedford, M. T. & Clarke, S. G. Protein arginine methylation in mammals: who, what, and why. *Mol Cell* **33**, 1–13 (2009).
75. Tee, W. W. *et al.* Prmt5 is essential for early mouse development and acts in the cytoplasm to maintain ES cell pluripotency. *Genes Dev* **24**, 2772–2777 (2010).
76. Fabbriozio, E. *et al.* Negative regulation of transcription by the type II arginine methyltransferase PRMT5. *EMBO Rep* **3**, 641–645 (2002).
77. Pal, S., Vishwanath, S. N., Erdjument-Bromage, H., Tempst, P. & Sif, S. Human SWI/SNF-associated PRMT5 methylates histone H3 arginine 8 and negatively regulates expression of ST7 and NM23 tumor suppressor genes. *Mol Cell Biol* **24**, 9630–9645 (2004).
78. Liu, L. *et al.* Arginine Methylation of SREBP1a via PRMT5 Promotes De Novo Lipogenesis and Tumor Growth. *Cancer Res* **76**, 1260–1272 (2016).
79. Chung, S., Hwang, J. T., Park, J. H. & Choi, H. K. Free fatty acid-induced histone acetyltransferase activity accelerates lipid accumulation in HepG2 cells. *Nutr Res Pract* **13**, 196–204 (2019).
80. Lopez-Sanchez, G. N., Dominguez-Perez, M., Uribe, M., Chavez-Tapia, N. C. & Nuno-Lambarri, N. Non-alcoholic fatty liver disease and microRNAs expression, how it affects the development and progression of the disease. *Ann Hepatol* **21**, 100212 (2021).

81. Huang, R. *et al.* Upregulation of miR-181a impairs lipid metabolism by targeting PPARalpha expression in nonalcoholic fatty liver disease. *Biochem Biophys Res Commun* **508**, 1252–1258 (2019).
82. Wang, D. R. *et al.* Suppression of miR-30a-3p Attenuates Hepatic Steatosis in Non-alcoholic Fatty Liver Disease. *Biochem Genet* **58**, 691–704 (2020).
83. Martinelli, R. *et al.* miR-519d overexpression is associated with human obesity. *Obesity (Silver Spring)* **18**, 2170–2176 (2010).
84. Yang, Z. *et al.* MiR-22 modulates the expression of lipogenesis-related genes and promotes hepatic steatosis in vitro. *FEBS Open Bio* **11**, 322–332 (2021).
85. Lee, Y. H. *et al.* Hepatic MIR20B promotes nonalcoholic fatty liver disease by suppressing PPARA. *Elife* **10**, (2021).
86. Rodrigues, P. M., Rodrigues, C. M. P. & Castro, R. E. Modulation of liver steatosis by miR-21/PPARalpha. *Cell Death Discov* **4**, 9 (2018).
87. Wang, J. M. *et al.* IRE1alpha prevents hepatic steatosis by processing and promoting the degradation of select microRNAs. *Sci Signal* **11**, (2018).
88. Liu, J. *et al.* Epigenetic Alternations of MicroRNAs and DNA Methylation Contribute to Liver Metastasis of Colorectal Cancer. *Dig Dis Sci* **64**, 1523–1534 (2019).
89. Ding, J. *et al.* Effect of miR-34a in regulating steatosis by targeting PPARalpha expression in nonalcoholic fatty liver disease. *Sci Rep* **5**, 13729 (2015).
90. Guo, X. Y. *et al.* circRNA_0046366 inhibits hepatocellular steatosis by normalization of PPAR signaling. *World J Gastroenterol* **24**, 323–337 (2018).
91. Torres, L. F., Cogliati, B. & Otton, R. Green Tea Prevents NAFLD by Modulation of miR-34a and miR-194 Expression in a High-Fat Diet Mouse Model. *Oxid Med Cell Longev* **2019**, 4168380 (2019).
92. Zhang, K. *et al.* The unfolded protein response transducer IRE1alpha prevents ER stress-induced hepatic steatosis. *EMBO J* **30**, 1357–1375 (2011).
93. Zhang, K. & Kaufman, R. J. From endoplasmic-reticulum stress to the inflammatory response. *Nature* **454**, 455–462 (2008).
94. Ron, D. & Walter, P. Signal integration in the endoplasmic reticulum unfolded protein response. *Nat Rev Mol Cell Biol* **8**, 519–529 (2007).
95. Hollien, J. *et al.* Regulated Ire1-dependent decay of messenger RNAs in mammalian cells. *J Cell Biol* **186**, 323–331 (2009).
96. Hollien, J. & Weissman, J. S. Decay of endoplasmic reticulum-localized mRNAs during the unfolded protein response. *Science (1979)* **313**, 104–107 (2006).
97. Michan, S. & Sinclair, D. Sirtuins in mammals: insights into their biological function. *Biochem J* **404**, 1–13 (2007).

98. Chang, H. C. & Guarente, L. SIRT1 and other sirtuins in metabolism. *Trends in Endocrinology and Metabolism* **25**, 138–145 (2014).
99. Laurent, G. *et al.* SIRT4 represses peroxisome proliferator-activated receptor alpha activity to suppress hepatic fat oxidation. *Mol Cell Biol* **33**, 4552–4561 (2013).
100. Watroba, M. & Szukiewicz, D. Sirtuins at the Service of Healthy Longevity. *Front Physiol* **12**, (2021).
101. McCarty, M. F. Practical prospects for boosting hepatic production of the ‘pro-longevity’ hormone FGF21. *Horm Mol Biol Clin Investig* **30**, (2015).
102. Zhang, L. *et al.* Administration of isoliquiritigenin prevents nonalcoholic fatty liver disease through a novel IQGAP2-CREB-SIRT1 axis. *Phytother Res* **35**, 3898–3915 (2021).
103. Hua, Y. Q., Zeng, Y., Xu, J. & Xu, X. L. Naringenin alleviates nonalcoholic steatohepatitis in middle-aged Apoe(-/-)mice: role of SIRT1. *Phytomedicine* **81**, 153412 (2021).
104. Suga, T. *et al.* Ipragliflozin-induced improvement of liver steatosis in obese mice may involve sirtuin signaling. *World J Hepatol* **12**, 350–362 (2020).
105. Majeed, Y. *et al.* SIRT1 promotes lipid metabolism and mitochondrial biogenesis in adipocytes and coordinates adipogenesis by targeting key enzymatic pathways. *Sci Rep* **11**, 8177 (2021).
106. Purushotham, A. *et al.* Hepatocyte-specific deletion of SIRT1 alters fatty acid metabolism and results in hepatic steatosis and inflammation. *Cell Metab* **9**, 327–338 (2009).
107. Wang, W. *et al.* PPARalpha agonist fenofibrate attenuates TNF-alpha-induced CD40 expression in 3T3-L1 adipocytes via the SIRT1-dependent signaling pathway. *Exp Cell Res* **319**, 1523–1533 (2013).
108. Pantazi, E. *et al.* PPARalpha Agonist WY-14643 Induces SIRT1 Activity in Rat Fatty Liver Ischemia-Reperfusion Injury. *Biomed Res Int* **2015**, 894679 (2015).
109. Sandoval-Rodriguez, A. *et al.* Pirfenidone Is an Agonistic Ligand for PPARalpha and Improves NASH by Activation of SIRT1/LKB1/pAMPK. *Hepatol Commun* **4**, 434–449 (2020).
110. Hayashida, S. *et al.* Fasting promotes the expression of SIRT1, an NAD⁺-dependent protein deacetylase, via activation of PPARalpha in mice. *Mol Cell Biochem* **339**, 285–292 (2010).
111. Gong, K. *et al.* Peroxisome Proliferator-Activated Receptor alpha Facilitates Osteogenic Differentiation in MC3T3-E1 Cells via the Sirtuin 1-Dependent Signaling Pathway. *Mol Cells* **40**, 393–400 (2017).
112. Villarroya, J. *et al.* Sirt1 mediates the effects of a short-term high-fat diet on the heart. *J Nutr Biochem* **26**, 1328–1337 (2015).
113. Oka, S. *et al.* PPARalpha-Sirt1 complex mediates cardiac hypertrophy and failure through suppression of the ERR transcriptional pathway. *Cell Metab* **14**, 598–611 (2011).
114. Oka, S. *et al.* Peroxisome Proliferator Activated Receptor-alpha Association With Silent Information Regulator 1 Suppresses Cardiac Fatty Acid Metabolism in the Failing Heart. *Circ Heart Fail* **8**, 1123–1132 (2015).

115. Planavila, A., Iglesias, R., Giral, M. & Villarroya, F. Sirt1 acts in association with PPARalpha to protect the heart from hypertrophy, metabolic dysregulation, and inflammation. *Cardiovasc Res* **90**, 276–284 (2011).
116. Huang, K. *et al.* PARP1-mediated PPARalpha poly(ADP-ribosyl)ation suppresses fatty acid oxidation in non-alcoholic fatty liver disease. *J Hepatol* **66**, 962–977 (2017).
117. Wu, T., Liu, Y. H., Fu, Y. C., Liu, X. M. & Zhou, X. H. Direct evidence of sirtuin downregulation in the liver of non-alcoholic fatty liver disease patients. *Ann Clin Lab Sci* **44**, 410–418 (2014).
118. Ruderman, N. B. *et al.* AMPK and SIRT1: a long-standing partnership? *Am J Physiol Endocrinol Metab* **298**, E751-60 (2010).
119. Lan, F., Cacicedo, J. M., Ruderman, N. & Ido, Y. SIRT1 modulation of the acetylation status, cytosolic localization, and activity of LKB1. Possible role in AMP-activated protein kinase activation. *J Biol Chem* **283**, 27628–27635 (2008).
120. Canto, C. *et al.* AMPK regulates energy expenditure by modulating NAD⁺ metabolism and SIRT1 activity. *Nature* **458**, 1056–1060 (2009).
121. Fernandez-Marcos, P. J. & Auwerx, J. Regulation of PGC-1alpha, a nodal regulator of mitochondrial biogenesis. *Am J Clin Nutr* **93**, 884S–90 (2011).
122. Canto, C. & Auwerx, J. PGC-1alpha, SIRT1 and AMPK, an energy sensing network that controls energy expenditure. *Curr Opin Lipidol* **20**, 98–105 (2009).
123. Finkel, T., Deng, C. X. & Mostoslavsky, R. Recent progress in the biology and physiology of sirtuins. *Nature* **460**, 587–591 (2009).
124. Vega, R. B., Huss, J. M. & Kelly, D. P. The coactivator PGC-1 cooperates with peroxisome proliferator-activated receptor alpha in transcriptional control of nuclear genes encoding mitochondrial fatty acid oxidation enzymes. *Mol Cell Biol* **20**, 1868–1876 (2000).
125. Jiang, Y. *et al.* Elucidation of SIRT-1/PGC-1alpha-associated mitochondrial dysfunction and autophagy in nonalcoholic fatty liver disease. *Lipids Health Dis* **20**, 40 (2021).
126. Kauppinen, A., Suuronen, T., Ojala, J., Kaarniranta, K. & Salminen, A. Antagonistic crosstalk between NF-kappaB and SIRT1 in the regulation of inflammation and metabolic disorders. *Cell Signal* **25**, 1939–1948 (2013).
127. Yao, W. *et al.* Icaritin ameliorates endothelial dysfunction in type 1 diabetic rats by suppressing ER stress via the PPARalpha/Sirt1/AMPKalpha pathway. *J Cell Physiol* **236**, 1889–1902 (2021).
128. Chen, X. Y. *et al.* LB100 ameliorates nonalcoholic fatty liver disease via the AMPK/Sirt1 pathway. *World J Gastroenterol* **25**, 6607–6618 (2019).
129. Yang, X. *et al.* The diabetes medication canagliflozin promotes mitochondrial remodelling of adipocyte via the AMPK-Sirt1-Pgc-1alpha signalling pathway. *Adipocyte* **9**, 484–494 (2020).
130. Shi, Y. Histone lysine demethylases: emerging roles in development, physiology and disease. *Nat Rev Genet* **8**, 829–833 (2007).

131. Merkwirth, C. *et al.* Two Conserved Histone Demethylases Regulate Mitochondrial Stress-Induced Longevity. *Cell* **165**, 1209–1223 (2016).
132. Byun, S. *et al.* Fasting-induced FGF21 signaling activates hepatic autophagy and lipid degradation via JMJD3 histone demethylase. *Nat Commun* **11**, 807 (2020).
133. Seok, S. *et al.* Fasting-induced JMJD3 histone demethylase epigenetically activates mitochondrial fatty acid beta-oxidation. *J Clin Invest* **128**, 3144–3159 (2018).
134. Mizushima, N. & Komatsu, M. Autophagy: renovation of cells and tissues. *Cell* **147**, 728–741 (2011).
135. Singh, R. *et al.* Autophagy regulates lipid metabolism. *Nature* **458**, 1131–1135 (2009).
136. Czaja, M. J. Function of Autophagy in Nonalcoholic Fatty Liver Disease. *Dig Dis Sci* **61**, 1304–1313 (2016).
137. Pang, H. *et al.* Gestational high-fat diet impaired demethylation of Pparalpha and induced obesity of offspring. *J Cell Mol Med* **25**, 5404–5416 (2021).
138. Hashimoto, K. & Ogawa, Y. Epigenetic Switching and Neonatal Nutritional Environment. *Adv Exp Med Biol* **1012**, 19–25 (2018).
139. Yuan, X. *et al.* Epigenetic modulation of Fgf21 in the perinatal mouse liver ameliorates diet-induced obesity in adulthood. *Nat Commun* **9**, 636 (2018).
140. Ehara, T. *et al.* Ligand-activated PPARalpha-dependent DNA demethylation regulates the fatty acid beta-oxidation genes in the postnatal liver. *Diabetes* **64**, 775–784 (2015).
141. Moody, L., Xu, G. B., Chen, H. & Pan, Y. X. Epigenetic regulation of carnitine palmitoyltransferase 1 (Cpt1a) by high fat diet. *Biochim Biophys Acta Gene Regul Mech* **1862**, 141–152 (2019).
142. Kim, J. H., Wahyudi, L. D., Kim, K. K. & Gonzalez, F. J. PPARalpha activation drives demethylation of the CpG islands of the Gadd45b promoter in the mouse liver. *Biochem Biophys Res Commun* **476**, 293–298 (2016).
143. Kawahori, K. *et al.* Ascorbic acid during the suckling period is required for proper DNA demethylation in the liver. *Sci Rep* **10**, 21228 (2020).
144. Luo, Y. *et al.* Intestinal PPARalpha Protects Against Colon Carcinogenesis via Regulation of Methyltransferases DNMT1 and PRMT6. *Gastroenterology* **157**, 744–759 e4 (2019).
145. Kong, R., Wang, N., Han, W., Bao, W. & Lu, J. Fenofibrate Exerts Antitumor Effects in Colon Cancer via Regulation of DNMT1 and CDKN2A. *PPAR Res* **2021**, 6663782 (2021).
146. McCabe, M. T., Davis, J. N. & Day, M. L. Regulation of DNA methyltransferase 1 by the pRb/E2F1 pathway. *Cancer Res* **65**, 3624–3632 (2005).
147. Aibara, D. *et al.* Gene repression through epigenetic modulation by PPARA enhances hepatocellular proliferation. *iScience* **25**, 104196 (2022).
148. Hervouet, E., Vallette, F. M. & Cartron, P. F. Dnmt1/Transcription factor interactions: an alternative mechanism of DNA methylation inheritance. *Genes Cancer* **1**, 434–443 (2010).

149. Dahlhoff, C. *et al.* Hepatic methionine homeostasis is conserved in C57BL/6N mice on high-fat diet despite major changes in hepatic one-carbon metabolism. *PLoS One* **8**, e57387 (2013).
150. Issemann, I. & Green, S. Activation of a member of the steroid hormone receptor superfamily by peroxisome proliferators. *Nature* **347**, 645–650 (1990).
151. Nikam, A. *et al.* The PPARalpha Agonist Fenofibrate Prevents Formation of Protein Aggregates (Mallory-Denk bodies) in a Murine Model of Steatohepatitis-like Hepatotoxicity. *Sci Rep* **8**, 12964 (2018).
152. Rodriguez-Vilarrupla, A. *et al.* PPARalpha activation improves endothelial dysfunction and reduces fibrosis and portal pressure in cirrhotic rats. *J Hepatol* **56**, 1033–1039 (2012).
153. Basaranoglu, M., Acbay, O. & Sonsuz, A. A controlled trial of gemfibrozil in the treatment of patients with nonalcoholic steatohepatitis. *J Hepatol* **31**, 384 (1999).
154. Fernandez-Miranda, C. *et al.* A pilot trial of fenofibrate for the treatment of non-alcoholic fatty liver disease. *Dig Liver Dis* **40**, 200–205 (2008).
155. Ida, S., Kaneko, R. & Murata, K. Efficacy and safety of pemafibrate administration in patients with dyslipidemia: a systematic review and meta-analysis. *Cardiovasc Diabetol* **18**, 38 (2019).
156. Blair, H. A. Pemafibrate: First Global Approval. *Drugs* **77**, 1805–1810 (2017).
157. Ishibashi, S. *et al.* Effects of K-877, a novel selective PPARalpha modulator (SPPARMalpha), in dyslipidaemic patients: A randomized, double blind, active- and placebo-controlled, phase 2 trial. *Atherosclerosis* **249**, 36–43 (2016).
158. Boubia, B. *et al.* Design, Synthesis, and Evaluation of a Novel Series of Indole Sulfonamide Peroxisome Proliferator Activated Receptor (PPAR) alpha/gamma/delta Triple Activators: Discovery of Lanifibranor, a New Antifibrotic Clinical Candidate. *J Med Chem* **61**, 2246–2265 (2018).
159. Remely, M. *et al.* Vitamin E Modifies High-Fat Diet-Induced Increase of DNA Strand Breaks, and Changes in Expression and DNA Methylation of Dnmt1 and MLH1 in C57BL/6J Male Mice. *Nutrients* **9**, (2017).
160. Zhou, R. *et al.* Resveratrol Ameliorates Lipid Droplet Accumulation in Liver Through a SIRT1/ ATF6-Dependent Mechanism. *Cell Physiol Biochem* **51**, 2397–2420 (2018).

CHAPTER II

*Mitochondrial dysfunctions and MASLD progression: cause
or consequence?*

Mitochondrial dysfunctions and NAFLD progression: cause or consequence

2.1 Mitochondrial DNA structure

Mitochondria are crucial organelles for the maintenance of the cellular metabolic homeostasis and are responsible for the bulk of the cell's energy requirements by the production of ATP. This ATP production is regulated via the oxidative phosphorylation pathway (OXPHOS) carried out by the electron transport chain (ETC) and ATP synthase in the inner mitochondrial membrane. A process driven by glucose uptake, β -oxidation of fatty acids and amino acids uptake¹. Besides, mitochondria are important for regulating Ca^{2+} homeostasis in control of apoptosis². Interestingly, these processes are not fully regulated by nuclear gene expression, because the mitochondria own their own mitochondrial DNA (mtDNA). A cell contains multiple mitochondria with each mitochondrion containing 2-10 copies of its own mtDNA³.

In contrast to the nuclear DNA, the mitochondrial DNA (mtDNA) is a 16,5 kb circular dsDNA molecule lacking introns and packed into nucleoprotein complexes, called nucleoids^{4,5} (Figure 1). It consists of a heavy (H) and a light (L) chain that can be distinguished based on the GC content^{6,7}. The mtDNA encodes 22 tRNAs, 2 rRNAs and 13 mRNAs that encode for essential proteins of the OXPHOS pathway^{5,8}. In the 16,5 kb there is only one non-coding region (NCR) of 1,1kb containing the heavy (HSP1 and HSP2) and light strand promoters (LSP), as well as the origin of heavy strand replication (O_H). A large part of this NCR forms a three strand loop structure of 650nt, called the D-loop. Although the D-loop and NCR are used interchangeably, this is not fully correct since the D-loop does not span the entire NCR⁹. Between the two promoters (HSP and LSP) there are several binding sites for the core transcription factor, mitochondrial transcription factor A (TFAM), to initiate transcription.

2.2 Mitochondrial transcription and replication

Mitochondrial transcription starts by the formation of the transcription initiation complex consisting of TFAM, dimethyl adenosine transferase 2 mitochondrial protein (TFB2M) and mitochondrial RNA polymerase (POLRMT) at one of the three different promoters. Although it is known that formation of this complex initiates the synthesis of a polycistronic RNA that is further processed into single mRNAs, the mechanism of this assembly is still not fully understood^{5,10}. Currently, the proposed mechanism is based on footprinting and cross-linking studies which revealed TFAM binding to the LSP, followed by POLRMT binding to form a pre-initiation complex. Next, TFB2M will be recruited to start the transcription. However there is still no high affinity TFAM site found in the HSP1 promoter, indicating that transcription initiation could be different in this promoter¹¹⁻¹⁴. Besides, other studies indicate that TFB2M and POLRMT can form a complex that can bind and catalyze promoter specific transcription when recruited by TFAM¹⁵. Hence to fully understand mitochondrial control of gene expression, more research is necessary to understand the mechanism of transcription complex formation on the three different promoters.

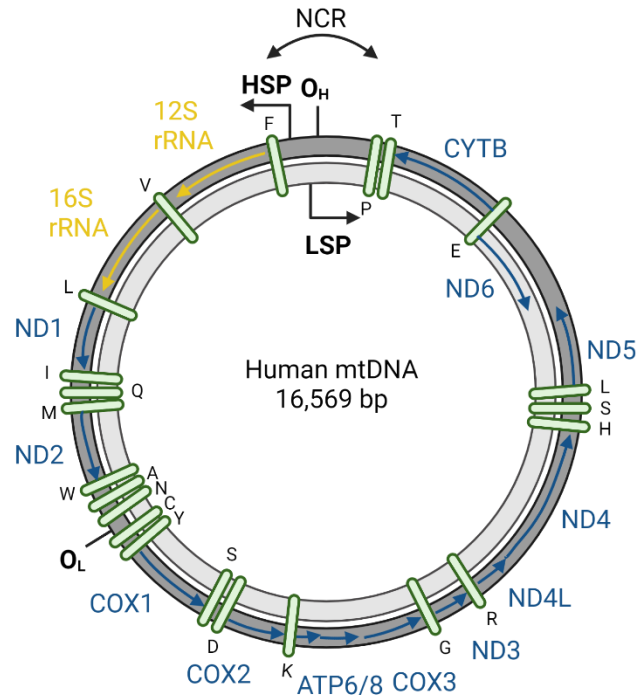


Figure 1: Mitochondrial DNA structure. Mitochondrial DNA consists of a heavy (dark grey) and light (light grey) strand coding for rRNAs (yellow), mRNAs (blue) and tRNAs (green). Transcription is bidirectional and initiated in the D-loop control region which is part of the non-coding region (NCR), starting from the three promoters (HSP1, HSP2 (showed as HSP) and LSP). Abbreviations: OH, origin of heavy strand replication; OL, origin of light strand replication, HSP, heavy strand promoter; LSP, light strand promoter.

Transcription starting from the H strand encodes 12 mRNAs of OXPHOS proteins, 2 rRNAs and 14 tRNAs. The L strand only drives transcription of 1 mRNA of an OXPHOS protein (ND6), 8 tRNAs and primers needed for replication starting from the O_H. These primers can be used by DNA polymerase gamma (POL γ) to start mtDNA replication from the O_H unidirectionally. A minimal mtDNA replisome has been defined and consist of the hexameric helicase TWINKLE, POL γ and the tetrameric mitochondrial single stranded DNA binding protein (mtSSB)^{16,17}. During replication, TWINKLE will first unwind the leading strand in a 5' to 3' direction, that can then be replicated by POL γ . mtSSB is responsible for binding and stabilizing ssDNA until it is replicated by POL γ . Origin of light strand replication (O_L) is reached when almost two-thirds of the leading strand is replicated. When O_L is reached, replication of the lagging strand will be started in the other direction of the H-strand by the formation of a hairpin structure that recruits POLRMT for primer synthesis to initiate replication^{18,19}. It has been described that the switch between transcription and replication relies on the transcription of the transcription elongation factor (TEFM)²⁰.

Both replication and translation require a lot of proteins that are mostly encoded in the nuclear DNA. Hence, except for the 37 proteins that are encoded on the mtDNA, the other mitochondrial proteins (~1000 proteins) are encoded on the nuclear DNA^{5,9}. Expression of these nuclear encoded mitochondrial genes (including TFAM, POLRMT and TFB2M) are mostly controlled by the nuclear transcription factors nuclear respiratory factors 1 and 2 α (NRF-1, NRF-2 α), the latter also known as GA-binding protein α (GABP α). After transcription in the nucleus, these proteins are translated in the cytoplasm and transported into the mitochondria. Of note, it has been shown that some

nuclear transcription factors can also be imported into the mitochondria and directly regulate mitochondrial transcription²¹.

2.3 Mitochondrial DNA methylation in general and MASLD

Methylation of the mitochondrial DNA was already discovered more than forty years ago in loach embryos, mouse and hamster samples²²⁻²⁴. Although some researchers afterwards questioned the presence of mitochondrial methylation, Rebelo et al.²⁵ and Shock et al.²⁶ both resparked the interest and research to mitochondrial methylation. Rebelo et al. proved that mtDNA methylation is regulated by the level of TFAM occupancy, influencing the packaging and replication of the mtDNA and therefore influences the accessibility of the mtDNA to DNA methyltransferases (DNMTs)²⁵. Shock et al. showed that mitochondrial DNMT1, an isoform of DNMT1, expression is upregulated by nuclear transcription factors NRF1 and PGC1 α and can directly migrate to the mitochondria by a conserved mitochondrial targeting sequence. In the mitochondria, DNMT1 can bind and methylate the D-loop region and thereby can regulate the expression of *MT-ND6* and *MT-ND1* genes in a gene specific manner²⁷. Since both researchers could identify mitochondrial methylation and prove functional effects, mitochondrial methylation became more generally accepted and triggered more follow-up studies focusing on additional mitochondrial methylation patterns with newer epigenetic sequencing techniques including Nanopore sequencing.

Generally, these studies showed that mitochondrial methylation can be detected, especially in the D-loop region, in different disease models including cancer and cardiovascular, neurodegenerative and metabolic diseases which has been extensively reviewed by Stoccoro et al.²⁸ Of special interest, in MASLD patients, Pirola et al. has shown that the mitochondrially encoded NADH dehydrogenase 6 (mt-ND6) region, translated into the ND6 dehydrogenase which is part of the complex I of the ETC, is hypermethylated. This hypermethylation results in a downregulation of ND6 dehydrogenase and therefore a malfunctioning of the OXPHOS pathway²⁹. Besides, Chen et al. showed that in rats a methyl donor deficient (MDD) diet induces differential methylation of nuclear encoded mitochondrial genes leading to changes in mitochondrial metabolism and other genes related to MASLD³⁰. Other studies have found associations between mtDNA methylation and MASLD associated diseases including cardiovascular diseases, diabetes and obesity (reviewed in³¹). These studies mostly showed methylation of the D-loop region associated with changes in mitochondrial gene transcription and copy number³¹⁻³⁴.

Of particular interest, besides mitochondrial presence of DNMT1 isoforms, demonstrated by Shock et al., also de novo DNMT3A and DNMT3B and TET enzymes could be detected in the mitochondria^{27,35-41}. Furthermore, functional DNMT knockdown studies revealed that absence of DNMTs changes mtDNA methylation^{42,43}. Interestingly, methylation of the mtDNA has been mostly linked to changes in copy number or mitochondrial gene expression depending on the cell type and context of cytosine methylation⁴⁴⁻⁵⁰. However, it remains poorly understood how specific mtDNA methylation changes regulate mitochondrial functions. This is because there are several differences between the nuclear epigenetic machinery and the epigenetic modifications of the mtDNA. For example, the mitochondrial amount of non-CpG methylation, including N⁶-methyldeoxyadenosine (6-mA) methylation, is much higher than standard nuclear CpG methylation⁵¹⁻⁵³. Bellizzi et al. further showed that also GpC methylation can be found in the D-loop⁵⁴. Therefore it is important that in the future more research is focused on the different changes in mitochondrial methylation in both CpG and non-CpG context in the different stages of MASLD. Moreover, the global amount of

mtDNA methylation is much lower as compared to the nuclear DNA methylation and not symmetrical on both strands: in general the L-strand has an overall higher percentage of methylation, and depending on cell and methylation type mtDNA methylation affects gene expression or mtDNA replication^{42–44,54–57}. Besides, similar as the nuclear genome, 5-hydroxymethylation has also been detected near gene start sites, although in a more dynamic cell type specific pattern⁵⁸. All these studies reflect the high complexity of mtDNA methylation dynamics and suggest different regulation of mitochondrial epigenetics as compared to the nuclear epigenetic machinery.

Furthermore, besides direct methylation of the mtDNA, it has been recently suggested that more research should look into the interplay between (posttranslational) modifications of mitochondrial packaging molecules (proteins, metabolites) and mtDNA gene expression. Although mtDNA lacks histones, it is packed in the mitochondrial matrix into a mtDNA-protein complex called a nucleoid. The core protein responsible for the packaging of the mtDNA is TFAM⁵⁹. As shown above, is TFAM also responsible for mtDNA transcription and mtDNA maintenance regulating the mitochondrial copy number, emphasizing the crucial role of TFAM in mitochondrial homeostasis^{5,10,60,61}. Interestingly, it has been reported that this protein gets post-translationally modified, similarly like the post-translation modifications on histones in the nuclear DNA. TFAM has been reported to be phosphorylated and acetylated, affecting its binding affinity to mtDNA and thereby regulating mitochondrial transcription and replication (biogenesis)^{62–64}. Taking into account high levels of acetyl-coA and methyl-donor metabolites present in the mitochondria, posttranslational acetylation-methylation modification of mitochondrial substrates has taken center stage^{65,66}. Besides, TFAM has also been reported to be O-linked glycosylated, which reduces its activity⁶⁷. Since Rebelo *et al.* showed that an unbalanced expression of TFAM, either low or high, directly regulates the amount of methylation by changing the packaging and accessibility of the mtDNA to DNMTs, it is interesting to further study the impact of post-translation modifications of TFAM on mtDNA methylation⁶⁸. Finally, also post-translation modifications of nucleoid associated proteins including helicase TWINKLE, POLγ, mtSSB, POLRMT etc. may need further consideration.

2.4 Mito-nuclear communication influences both mitochondrial and nuclear epigenetics and function

Since mitochondrial function and thus ATP production is relying on both transcription of nuclear encoded and mitochondrial encoded genes, there is an important bidirectional communication between the nucleus and the mitochondria to maintain mitochondrial homeostasis. This bidirectional signalling is called mito-nuclear communication and influences both transcription and methylation of both DNAs^{69–73}. Mito-nuclear communication consists of anterograde communication from the nucleus to the mitochondria and reciprocally retrograde communication from the mitochondria to the nucleus.

Since most of the mitochondrial proteins are encoded on the nuclear genome, anterograde communication is necessary to maintain mitochondrial homeostasis and adapt mitochondrial function to changing environments. This process is regulated by nuclear receptors, transcription factors and co-activators and co-repressors that are encoded on the nuclear genome and expressed in relation to changing environments e.g. exercise or cold⁷⁴. Expression of nuclear encoded mitochondrial genes is mostly regulated by the nuclear transcription factors NRF1 and NRF2 α (also known as GA-binding protein α ; GABP α). Most of the genes involved in the OXPHOS pathway,

mitochondrial replication and transcription are regulated by NRF1⁷⁵⁻⁷⁸. Besides, mitochondrially encoded proteins are regulated by co-activators and nuclear receptors. The main co-activator is PPAR γ co-activator 1 α (PGC1- α) which can be upregulated by an increase of AMPK activity or an increase in Ca²⁺^{74,79}. Once activated, this co-activator can further stimulate NRF and various PPAR and ERR nuclear receptors that control protein expression of genes involved in mitochondrial biogenesis, OXPHOS pathway, TCA cycle and fatty acid oxidation⁸⁰⁻⁸².

Retrograde communication is activated by the release of different metabolites from the mitochondria that will activate gene expression in the nucleus to protect against mitochondrial dysfunction⁸³. Depending on the trigger, the reaction of the nucleus can be classified in three groups: energetic stress response, Ca²⁺-dependent stress responses and the ROS dependent responses. Energy deprivation characterized by the loss of ATP synthesis will lead to the activation of mitochondrial biogenesis and mitochondrial quality control in the form of mitophagy. This activation is orchestrated by the activity of AMPK or mTOR, leading to an adaptation of the metabolism to manage energy deficits^{84,85}. Release of Ca²⁺ by a decrease in membrane potential due to a dysfunction in the OXPHOS pathway or mtDNA mutations will activate calcium metabolic and glycolytic genes in the nucleus via two mechanisms^{86,87}. First, the activation of calcineurin induces nuclear translocation of NF- κ B or nuclear factor of activated T cells (NFATC)^{88,89}. Alternatively, Ca²⁺ can activate several kinases including c-Jun N-terminal kinase (JNK), p38 mitogen activated protein kinase (MAPK), Ca²⁺/CaM kinases (CaMKs) which will activate other transcription factors to stimulate calcium metabolism, insulin signalling, glucose metabolism and cell proliferation⁷⁴. Accumulation of ROS by defective ETC that is not deleterious to the cell, will activate the antioxidant system and detoxifying enzymes in mitochondria and the cytosol. This process is managed by different transcription factors including the activation of nuclear factor erythroid-derived 2-related factor 2 (NRF2), also known as nuclear factor erythroid-derived 2-like 2 (NFE2L2), that activates the transcription of different genes in the antioxidant system⁹⁰. Besides, ROS will also activate PGC1- α expression via AMPK or JNK activation, to increase mitochondrial biogenesis and reprogram energy metabolism^{91,92}.

Besides the exchange of metabolites as a consequence of changes in cellular metabolic needs or mitochondrial dysfunction, mito-nuclear communication is also epigenetically regulated. First of all, mitochondrial function depends on a lot of mitochondrial genes that are encoded by the nuclear genome⁹³. Some of these mitochondrial gene promoters have been reported to be methylated and therefore differentially expressed. For example Poly can be hypermethylated, leading to a downregulation that directly effects mitochondrial replication and thus copy number^{94,95}. Besides, it has been reported that thymidine kinase (TK2), responsible for the salvage pathway of deoxynucleotide synthesis in the mitochondria, can be hypermethylated in human hearts affected by dilated cardiomyopathy. This hypermethylation induces a downregulation of TK2 protein and therefore induces mtDNA depletion^{96,97}. More research is necessary to investigate other types of epigenetic modifications including the effects of histone modifications or miRNAs on nuclear encoded mitochondrial genes, but these examples strongly indicate the importance of nuclear epigenetics in the anterograde communication. Reciprocally, mitochondrial metabolism does also effect nuclear epigenetics. Mitochondrial metabolism is responsible for the production of ATP, citrate, s-adenosyl methionine (SAM), α -ketoglutarate, acetyl coenzyme A (acetyl-CoA), succinate and fumarate. These metabolites all regulate the activity of different epigenetic enzymes as reviewed by Castegna et al.⁶⁹ and therefore influence nuclear DNA methylation. For example ATP

is an important metabolite for histone phosphorylation⁹⁸, SAM is the main methyl donor⁹⁹, acetyl-CoA is used by histone acetyl transferases for histone acetylation¹⁰⁰, α -ketoglutarate is substrate of demethylating ten eleven translocation (TET) enzymes¹⁰¹ and succinate and fumarate are competitive inhibitors of the jumonjiC domain-containing histone demethylases and the TET enzymes¹⁰². Not unexpectedly, mtDNA copy number has been reported to influence nuclear DNA methylation and therefore gene expression of different genes that impact human health¹⁰³. Along the same line, removal of mtDNA or changes in mtDNA haplogroups has been associated with changes in nuclear DNA methylation levels^{104–106}.

All together the mito-nuclear communication shows a complex interplay between the mitochondria and the nucleus that is both epigenetically and metabolically regulated for maintenance of cellular health. Despite some clear indications of the dual mito-nuclear interactions, there remains a lot to be discovered about the regulation and function of this interplay in different disease-health conditions.

2.5 Mitochondrial functional changes in MASLD

There are three important mitochondrial processes to maintain lipid and mitochondrial homeostasis: mitochondrial fatty acid oxidation, mitochondrial biogenesis and mitochondrial autophagy. Disruption or changes in activation of these processes induces mitochondrial dysfunction which is recognized as an important driver in the progression of MASLD^{107,108}. However, the full mechanistic story behind this strong association remains poorly understood and requires further investigation.

2.5.1 Mitochondrial Fatty acid oxidation (FAO)

Mitochondria are known to play an important role in fatty acid catabolism, through β -oxidation of fatty acids, generating acetyl-CoA. Next, acetyl-CoA is converted in the tricarboxylic acid (TCA) cycle in the mitochondrial matrix to CO_2 and H_2O ¹¹⁰. Besides, the TCA cycle generates electron donors NADH_2 and FADH_2 , that can be transported through complexes I to IV of the ETC to create a proton gradient over the inner mitochondrial membrane. Finally, this proton gradient is used by the last complex V of the ETC to generate ATP, completing the OXPHOS pathway¹¹¹. In MASLD, this process of FAO will initially be hyperactivated in the mitochondria aiming to reduce hepatic lipotoxicity. This increase in β -oxidation will subsequently also induce an increase in activity of the TCA and OXPHOS cycle which increases oxidative stress. As such, prolonged overactivation will eventually induce mitochondrial dysfunction, leading to a downregulation of the β -oxidation, ETC activity and an accumulation of triglycerides in the hepatocytes, correlating with MASLD progression^{112–114}. Of special note, the deletion of the protein catalysing the last three steps of the β -oxidation named mitochondrial trifunctional protein (MTP), results in steatosis development in mice. Since this can be rescued by the modulation of MTP, these results emphasize the important role of the FAO in MASLD^{115,116}.

Besides mitochondrial dysfunction, this FAO hyperactivation also leads to an accumulation of reactive oxygen species (ROS). A small percentage of electrons will leak out of the ETC cycle and can directly interact with oxygen to form superoxide radicals¹¹⁷. Initially mitochondria can overcome this increase in ROS with their antioxidant system that is activated by retrograde communication as shown previously, but eventually it will overwhelm the antioxidant system and lead to oxidative stress which is an important hallmark of MASLD. ROS are known to damage the

mitochondrial membrane, mtDNA and ETC constituents inducing a further increase in ROS production, generating a vicious cycle^{118–120}. Moreover, the mitochondrial membrane damage and the subsequent necrosis leads to the accumulation of DNA-enriched mitochondria-derived danger-associated molecular patterns (DAMPs) including mtDNA, that can activate the innate immune system leading to an inflammatory response^{107,121–123}. Besides, ROS accumulation will also

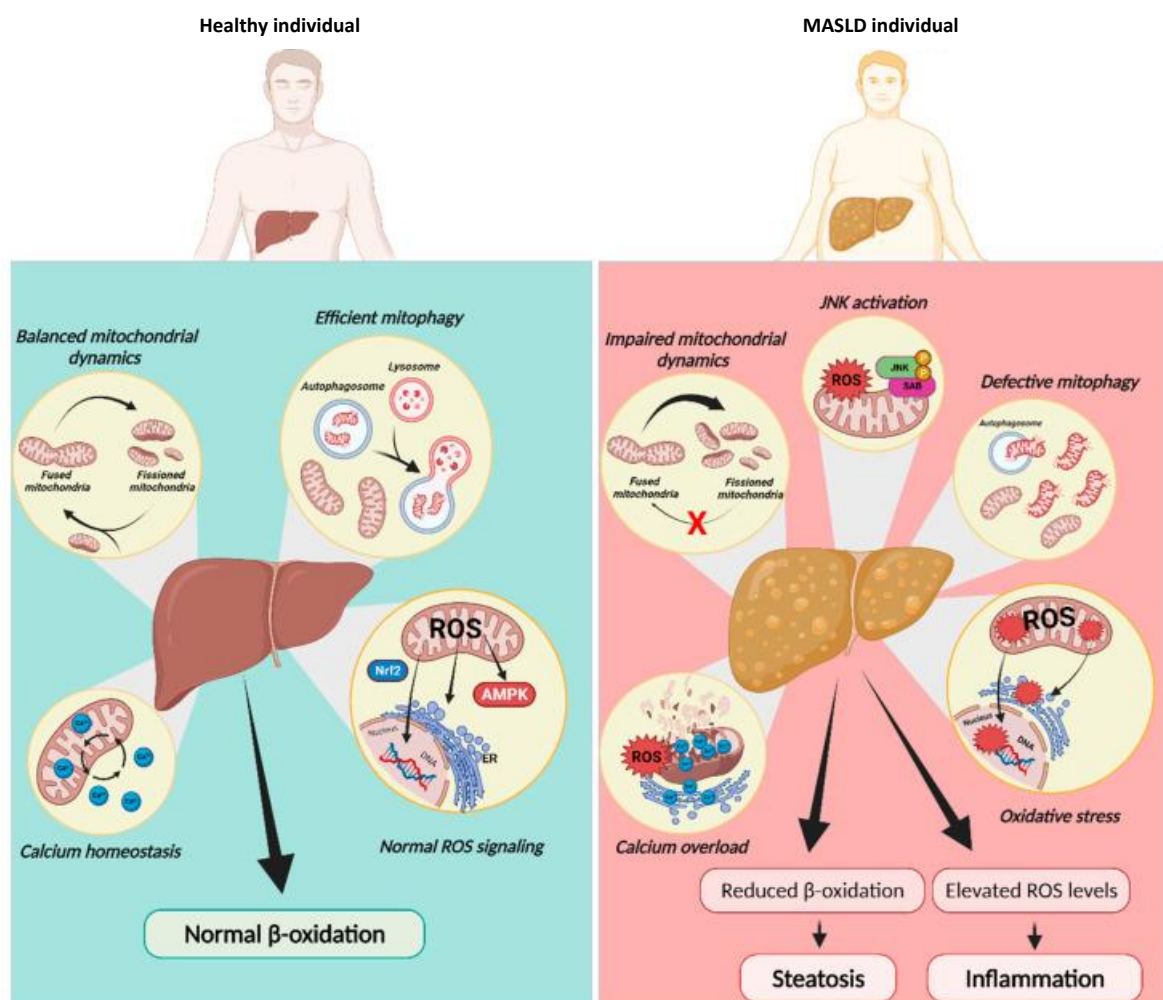


Figure 2: Overview mitochondrial dysfunction in MASLD. In healthy individuals there is a balance between the mitochondrial dynamic processes (fission and fusion) and mitochondrial mitophagy and a balanced intake of lipids. Thereby generating normal ROS signaling that can be processed by the mitochondrial antioxidant system, normal calcium homeostasis and normal β -oxidation. However in MASLD patients the constant influx of lipids will eventually induce mitochondrial dysfunction including reduced β -oxidation and malfunctioning of the ETC cycle. This will induce an accumulation of ROS that can further induce oxidative stress, calcium overload, ER stress and JNK activation. Besides will this mitochondrial dysfunction effect mitochondrial dynamics and mitophagy leading to accumulation of damaged mitochondria. Altogether this will induce inflammation and accumulation of triglycerides in the liver. Abbreviations: ER, endoplasmic reticulum; JNK, c-Jun N-terminal kinase; SAB, SH3 homology associated BTK-binding protein; ROS, reactive oxygen species (Adapted from Amorim et al.¹⁰⁹)

directly initiate inflammation by the activation of inflammatory signalling pathways such as the NF- κ B and JNK pathways, as well as overexpression of TNF synthesis and other cytokines that induce

apoptosis and necroptosis^{122,124,125}. Furthermore, ROS production and the lipid overload will also affect the endoplasmic reticulum, leading to endoplasmic stress, which will trigger a series of stress related responses known as the unfolded protein response (UPR) which is another hallmark of MASLD^{126,127}.

In summary both the overactivation of FAO and ROS production due to the constant influx of lipids in MASLD, lead to mitochondrial dysfunction and loss of mitochondrial plasticity. This is represented as ultrastructurally damaged mitochondria, ROS-mediated mtDNA damage, release of mtDNA and activation of inflammation in MASLD patients^{125,128,129}. Moreover, MASLD patients show elevated expression of antioxidants (e.g. superoxide dismutase (SOD), glutathione (GSH), glutathione peroxidase (GPx)) and byproducts of DNA oxidation including 8-hydroxy-2'-deoxyguanosine (8-OHdG)), which further corroborate the importance of mitochondrial homeostasis to attenuate progression of MASLD^{129,130}.

2.5.2 Mitochondrial dynamics and biogenesis

Mitochondrial dynamics is also described as the fusion and fission of the mitochondria¹³¹. Both processes together with mitochondrial biogenesis, also known as mitochondrial replication, are important to maintain mitochondrial homeostasis and essential to overcome cellular stress by mitochondrial dysfunction^{132,133}. The process of mitochondrial fusion is known as the mix of contents of partially damaged mitochondria to generate a new mitochondria that can compensate and balance out the previous mitochondrial dysfunctions. Reciprocally, mitochondrial fission, creates new mitochondria by separating the oxidative stress induced damaged mitochondria from the healthy ones^{128,134}. Once the balance between fusion and fission is disrupted by intracellular stress and external factors, this will result in mitochondrial fragmentation¹³⁵.

Proteins involved in mitochondrial fission are mitochondrial fission 1 (Fis1), dynamin-related protein 1 (Drp1), mitochondrial fission factor (Mff), mitochondrial dynamics proteins of 49 kDa and 51 kDa (MiD49 and MiD51). Drp1 is responsible for the fission of the OMM, the other proteins (Fis1 on the outer mitochondrial membrane (OMM); and Mff and MiDs on the mitochondrial tubules) will recruit Drp1 to the OMM¹³⁶. Several studies have shown that the expression of Drp1 is increased in animal MASH models, indicating mitochondrial fragmentation¹³⁷⁻¹³⁹. This increase in mitochondrial fission has also been confirmed by electron microscopy in animals subjected to a HFD^{138,140}. Interestingly, transgenic inhibition of mitochondrial fission in mice was protective against liver steatosis, which shows the therapeutic potential of decreasing mitochondrial fission in MASLD patients¹³⁸.

Proteins involved in mitochondrial fusion are: mitofusion-1 (Mfn1) and mitofusin-2 (Mfn2), optic atrophy 1 (Opa1). Mfn1 and Mfn2 are responsible for the fusion of the OMM, while Opa1 regulates the fusion of the inner mitochondrial membrane (IMM)¹⁴¹. Moreover, plays Opa1 a crucial role in maintaining the balance between mitochondrial fusion and fission. The IMM bound long isoform of Opa1 (L-Opa1), can be cleaved into short isoforms (S-Opa1) by mitochondrial-processing peptidases (MPP). L-Opa1 is required for fusion, while S-Opa1 limits fusion and promotes fission^{133,142}. In contrast to mitochondrial fission, mitochondrial fusion is downregulated in MASLD. A study by Gong et al. showed that hepatocytes of HFD-fed mice have a reduced expression of Mfn1 associated with MASH¹⁴³. Several *in vitro* and *in vivo* studies also showed a decrease in Mfn2 expression associated with increased inflammation, triglyceride concentration and fibrosis that is abolished upon re-expression of Mfn2¹⁴⁴⁻¹⁴⁷. Moreover, diminished levels of Mfn2 have been detected in the livers of MASH patients¹⁴⁸.

2.5.3 Mitochondrial autophagy, known as mitophagy

Mitophagy is a form of autophagy that specifically isolates and degrades damaged mitochondria. This protects the cell from the accumulation of ROS due to damaged mitochondria and maintains cellular redox balance¹⁴⁹. The process of mitophagy is regulated by different autophagy receptors that both bind to the ubiquitinated cargo molecule and autophagy related protein 8 (Atg8) or microtubule-associated protein 1A/1B light chain (LC3). This process can be E3 ligase PARKIN- putative kinase 1 (PINK1) dependent or PARKIN independent. First The PINK1- PARKIN dependent mitophagy pathway is most studied and consists of the binding of PINK1 to damaged depolarized mitochondria, thereby recruiting PARKIN. The binding of PARKIN will lead to phosphorylation of the OMM proteins that will bind to autophagy receptors that on their turn can bind to LC3 on the membrane of the autophagosomes, initiating mitophagy. The PARKIN independent pathway is regulated by autophagy receptors proteins that are mitochondrial membrane proteins. When these receptor proteins are activated, they can directly bind with LC3 to initiate the mitophagy pathway. Besides, lipids including cardiolipin or other E3 ligases including Mul1 can also initiate mitophagy by direct binding to LC3 or binding to PINK1¹⁵⁰. As described in paragraph 5.1.1 mitochondrial respiration is increased in MASLD, inducing the generation of ROS. This is reflected in enlarged and swollen hepatocellular mitochondria with the loss of cristae in MASH patients¹⁵¹⁻¹⁵³. Therefore, it is not surprising that the removal of damaged mitochondria through mitophagy is seen as a protective mechanism against long-term MASLD development. Moreover, several *in vivo* and *in vitro studies* found that the mitophagy process is perturbed in MASLD-related phenotypes¹⁵⁴⁻¹⁶¹. Although increased expression of mitophagy promoting proteins Bnip-3^{158,162}, Sirt3¹⁵⁸ and Parkin¹⁵⁷ revealed protection against MASLD, the molecular mechanisms involved in mitophagy regulation during the different stages of MASLD remain poorly understood and require further investigation.

2.6 References

1. Tang, J. X., Thompson, K., Taylor, R. W. & Oláhová, M. Mitochondrial OXPHOS Biogenesis: Co-Regulation of Protein Synthesis, Import, and Assembly Pathways. *Int J Mol Sci* **21**, 3820 (2020).
2. Rossi, A., Pizzo, P. & Filadi, R. Calcium, mitochondria and cell metabolism: A functional triangle in bioenergetics. *Biochimica et Biophysica Acta (BBA) - Molecular Cell Research* **1866**, 1068–1078 (2019).
3. Cavelier, L., Johannisson, A. & Gyllensten, U. Analysis of mtDNA Copy Number and Composition of Single Mitochondrial Particles Using Flow Cytometry and PCR. *Exp Cell Res* **259**, 79–85 (2000).
4. SATOH, M. Organization of multiple nucleoids and DNA molecules in mitochondria of a human cell. *Exp Cell Res* **196**, 137–140 (1991).
5. Basu, U., Bostwick, A. M., Das, K., Dittenhafer-Reed, K. E. & Patel, S. S. Structure, mechanism, and regulation of mitochondrial DNA transcription initiation. *Journal of Biological Chemistry* **295**, 18406–18425 (2020).
6. Wells, R. D. & Larson, J. E. Buoyant Density Studies on Natural and Synthetic Deoxyribonucleic Acids in Neutral and Alkaline Solutions. *Journal of Biological Chemistry* **247**, 3405–3409 (1972).
7. Shokolenko, I. & Alexeyev, M. Mitochondrial DNA: Consensuses and Controversies. *DNA* **2**, 131–148 (2022).
8. Anderson, S. *et al.* Sequence and organization of the human mitochondrial genome. *Nature* **290**, 457–465 (1981).
9. Nicholls, T. J. & Minczuk, M. In D-loop: 40years of mitochondrial 7S DNA. *Exp Gerontol* **56**, 175–181 (2014).
10. Bouda, E., Stapon, A. & Garcia-Diaz, M. Mechanisms of mammalian mitochondrial transcription. *Protein Science* **28**, 1594–1605 (2019).
11. Morozov, Y. I. *et al.* A novel intermediate in transcription initiation by human mitochondrial RNA polymerase. *Nucleic Acids Res* **42**, 3884–3893 (2014).
12. Fisher, R. P. & Clayton, D. A. A transcription factor required for promoter recognition by human mitochondrial RNA polymerase. Accurate initiation at the heavy- and light-strand promoters dissected and reconstituted in vitro. *J Biol Chem* **260**, 11330–8 (1985).
13. Fisher, R. P. & Clayton, D. A. Purification and Characterization of Human Mitochondrial Transcription Factor 1. *Mol Cell Biol* **8**, 3496–3509 (1988).
14. Uchida, A. *et al.* Unexpected sequences and structures of mtDNA required for efficient transcription from the first heavy-strand promoter. *Elife* **6**, (2017).
15. Ramachandran, A., Basu, U., Sultana, S., Nandakumar, D. & Patel, S. S. Human mitochondrial transcription factors TFAM and TFB2M work synergistically in promoter melting during transcription initiation. *Nucleic Acids Res* **45**, 861–874 (2017).

16. Wanrooij, S. & Falkenberg, M. The human mitochondrial replication fork in health and disease. *Biochimica et Biophysica Acta (BBA) - Bioenergetics* **1797**, 1378–1388 (2010).
17. Korhonen, J. A., Pham, X. H., Pellegrini, M. & Falkenberg, M. Reconstitution of a minimal mtDNA replisome in vitro. *EMBO J* **23**, 2423–2429 (2004).
18. Filograna, R., Mennuni, M., Alsina, D. & Larsson, N. Mitochondrial DNA copy number in human disease: the more the better? *FEBS Lett* **595**, 976–1002 (2021).
19. Doimo, M., Pfeiffer, A., Wanrooij, P. H. & Wanrooij, S. mtDNA replication, maintenance, and nucleoid organization. in *The Human Mitochondrial Genome* 3–33 (Elsevier, 2020). doi:10.1016/B978-0-12-819656-4.00001-2.
20. Agaronyan, K., Morozov, Y. I., Anikin, M. & Temiakov, D. Replication-transcription switch in human mitochondria. *Science (1979)* **347**, 548–551 (2015).
21. Leigh-Brown, S., Enriquez, J. & Odom, D. T. Nuclear transcription factors in mammalian mitochondria. *Genome Biol* **11**, 215 (2010).
22. Vanyushin, B. F., Kiryanov, G. I., Kudryashova, I. B. & Belozersky, A. N. DNA-methylase in loach embryos (*Misgurnus fossilis*). *FEBS Lett* **15**, 313–316 (1971).
23. Nass, M. M. K. Differential methylation of mitochondrial and nuclear DNA in cultured mouse, hamster and virus-transformed hamster cells In vivo and in vitro methylation. *J Mol Biol* **80**, 155–175 (1973).
24. Cummings, D. J., Tait, A. & Goddard, J. M. Methylated bases in DNA from *Paramecium aurelia*. *Biochimica et Biophysica Acta (BBA) - Nucleic Acids and Protein Synthesis* **374**, 1–11 (1974).
25. Rebelo, A. P., Williams, S. L. & Moraes, C. T. In vivo methylation of mtDNA reveals the dynamics of protein–mtDNA interactions. *Nucleic Acids Res* **37**, 6701–6715 (2009).
26. Shock, L. S., Thakkar, P. V., Peterson, E. J., Moran, R. G. & Taylor, S. M. DNA methyltransferase 1, cytosine methylation, and cytosine hydroxymethylation in mammalian mitochondria. *Proceedings of the National Academy of Sciences* **108**, 3630–3635 (2011).
27. Shock, L. S., Thakkar, P. V., Peterson, E. J., Moran, R. G. & Taylor, S. M. DNA methyltransferase 1, cytosine methylation, and cytosine hydroxymethylation in mammalian mitochondria. *Proceedings of the National Academy of Sciences* **108**, 3630–3635 (2011).
28. Stoccoro, A. & Coppedè, F. Mitochondrial DNA Methylation and Human Diseases. *Int J Mol Sci* **22**, 4594 (2021).
29. Pirola, C. J. *et al.* Epigenetic modification of liver mitochondrial DNA is associated with histological severity of nonalcoholic fatty liver disease. *Gut* **62**, 1356–1363 (2013).
30. Chen, G. *et al.* Identification of master genes involved in liver key functions through transcriptomics and epigenomics of methyl donor deficiency in rat: Relevance to nonalcoholic liver disease. *Mol Nutr Food Res* **59**, 293–302 (2015).

31. Stoccoro, A. & Coppedè, F. Mitochondrial DNA Methylation and Human Diseases. *Int J Mol Sci* **22**, 4594 (2021).
32. Zheng, L. D. *et al.* Insulin resistance is associated with epigenetic and genetic regulation of mitochondrial DNA in obese humans. *Clin Epigenetics* **7**, 60 (2015).
33. Kowluru, R. A. Retinopathy in a Diet-Induced Type 2 Diabetic Rat Model and Role of Epigenetic Modifications. *Diabetes* **69**, 689–698 (2020).
34. Corsi, S. *et al.* Platelet mitochondrial DNA methylation predicts future cardiovascular outcome in adults with overweight and obesity. *Clin Epigenetics* **12**, 29 (2020).
35. Dzitoyeva, S., Chen, H. & Manev, H. Effect of aging on 5-hydroxymethylcytosine in brain mitochondria. *Neurobiol Aging* **33**, 2881–2891 (2012).
36. Chestnut, B. A. *et al.* Epigenetic Regulation of Motor Neuron Cell Death through DNA Methylation. *The Journal of Neuroscience* **31**, 16619–16636 (2011).
37. Bellizzi, D. *et al.* The Control Region of Mitochondrial DNA Shows an Unusual CpG and Non-CpG Methylation Pattern. *DNA Research* **20**, 537–547 (2013).
38. Saini, S. K., Mangalhar, K. C., Prakasam, G. & Bamezai, R. N. K. DNA Methyltransferase1 (DNMT1) Isoform3 methylates mitochondrial genome and modulates its biology. *Sci Rep* **7**, 1525 (2017).
39. Wong, M., Gertz, B., Chestnut, B. A. & Martin, L. J. Mitochondrial DNMT3A and DNA methylation in skeletal muscle and CNS of transgenic mouse models of ALS. *Front Cell Neurosci* **7**, (2013).
40. Dou, X. *et al.* The strand-biased mitochondrial DNA methylome and its regulation by DNMT3A. *Genome Res* **29**, 1622–1634 (2019).
41. Chen, H., Dzitoyeva, S. & Manev, H. Effect of valproic acid on mitochondrial epigenetics. *Eur J Pharmacol* **690**, 51–59 (2012).
42. Dou, X. *et al.* The strand-biased mitochondrial DNA methylome and its regulation by DNMT3A. *Genome Res* **29**, 1622–1634 (2019).
43. Patil, V. *et al.* Human mitochondrial DNA is extensively methylated in a non-CpG context. *Nucleic Acids Res* **47**, 10072–10085 (2019).
44. van der Wijst, M. G. P., van Tilburg, A. Y., Ruiters, M. H. J. & Rots, M. G. Experimental mitochondria-targeted DNA methylation identifies GpC methylation, not CpG methylation, as potential regulator of mitochondrial gene expression. *Sci Rep* **7**, 177 (2017).
45. GAO, J., WEN, S., ZHOU, H. & FENG, S. De-methylation of displacement loop of mitochondrial DNA is associated with increased mitochondrial copy number and nicotinamide adenine dinucleotide subunit 2 expression in colorectal cancer. *Mol Med Rep* **12**, 7033–7038 (2015).
46. Janssen, B. G. *et al.* Placental mitochondrial methylation and exposure to airborne particulate matter in the early life environment: An ENVIR ON AGE birth cohort study. *Epigenetics* **10**, 536–544 (2015).

47. Yang, H. Correlation between increased ND2 expression and demethylated displacement loop of mtDNA in colorectal cancer. *Mol Med Rep* (2012) doi:10.3892/mmr.2012.870.
48. Sanyal, T., Bhattacharjee, P., Bhattacharjee, S. & Bhattacharjee, P. Hypomethylation of mitochondrial D-loop and ND6 with increased mitochondrial DNA copy number in the arsenic-exposed population. *Toxicology* **408**, 54–61 (2018).
49. Bianchessi, V. *et al.* Methylation profiling by bisulfite sequencing analysis of the mtDNA Non-Coding Region in replicative and senescent Endothelial Cells. *Mitochondrion* **27**, 40–47 (2016).
50. Yu, D. *et al.* Mitochondrial DNA Hypomethylation Is a Biomarker Associated with Induced Senescence in Human Fetal Heart Mesenchymal Stem Cells. *Stem Cells Int* **2017**, 1–12 (2017).
51. Hao, Z. *et al.* N6-Deoxyadenosine Methylation in Mammalian Mitochondrial DNA. *Mol Cell* **78**, 382-395.e8 (2020).
52. Koh, C. W. Q. *et al.* Single-nucleotide-resolution sequencing of human N 6-methyldeoxyadenosine reveals strand-asymmetric clusters associated with SSBP1 on the mitochondrial genome. *Nucleic Acids Res* **46**, 11659–11670 (2018).
53. Xiao, C.-L. *et al.* N6-Methyladenine DNA Modification in the Human Genome. *Mol Cell* **71**, 306-318.e7 (2018).
54. Bellizzi, D. *et al.* The Control Region of Mitochondrial DNA Shows an Unusual CpG and Non-CpG Methylation Pattern. *DNA Research* **20**, 537–547 (2013).
55. Lima, C. B. & Sirard, M. Mitoeigenetics: Methylation of mitochondrial DNA is strand-biased in bovine oocytes and embryos. *Reproduction in Domestic Animals* **55**, 1455–1458 (2020).
56. Sun, Z. *et al.* High-Resolution Enzymatic Mapping of Genomic 5-Hydroxymethylcytosine in Mouse Embryonic Stem Cells. *Cell Rep* **3**, 567–576 (2013).
57. Goldsmith, C. *et al.* Low biological fluctuation of mitochondrial CpG and non-CpG methylation at the single-molecule level. *Sci Rep* **11**, 8032 (2021).
58. Ghosh, S., Sengupta, S. & Scaria, V. Hydroxymethyl cytosine marks in the human mitochondrial genome are dynamic in nature. *Mitochondrion* **27**, 25–31 (2016).
59. Lee, S. R. & Han, J. Mitochondrial Nucleoid: Shield and Switch of the Mitochondrial Genome. *Oxid Med Cell Longev* **2017**, 1–15 (2017).
60. Ekstrand, M. I. Mitochondrial transcription factor A regulates mtDNA copy number in mammals. *Hum Mol Genet* **13**, 935–944 (2004).
61. Larsson, N.-G. *et al.* Mitochondrial transcription factor A is necessary for mtDNA maintenance and embryogenesis in mice. *Nat Genet* **18**, 231–236 (1998).
62. Zhao, Y. *et al.* PDE2 Inhibits PKA-Mediated Phosphorylation of TFAM to Promote Mitochondrial Ca²⁺-Induced Colorectal Cancer Growth. *Front Oncol* **11**, (2021).
63. King, G. A. *et al.* Acetylation and phosphorylation of human TFAM regulate TFAM–DNA interactions via contrasting mechanisms. *Nucleic Acids Res* **46**, 3633–3642 (2018).

64. Lu, B. *et al.* Phosphorylation of Human TFAM in Mitochondria Impairs DNA Binding and Promotes Degradation by the AAA+ Lon Protease. *Mol Cell* **49**, 121–132 (2013).
65. Małeckki, J. M., Davydova, E. & Falnes, P. Ø. Protein methylation in mitochondria. *Journal of Biological Chemistry* **298**, 101791 (2022).
66. Baeza, J., Smallegan, M. J. & Denu, J. M. Mechanisms and Dynamics of Protein Acetylation in Mitochondria. *Trends Biochem Sci* **41**, 231–244 (2016).
67. Suarez, J. *et al.* Alterations in mitochondrial function and cytosolic calcium induced by hyperglycemia are restored by mitochondrial transcription factor A in cardiomyocytes. *American Journal of Physiology-Cell Physiology* **295**, C1561–C1568 (2008).
68. Rebelo, A. P., Williams, S. L. & Moraes, C. T. In vivo methylation of mtDNA reveals the dynamics of protein–mtDNA interactions. *Nucleic Acids Res* **37**, 6701–6715 (2009).
69. Castegna, A., Iacobazzi, V. & Infantino, V. The mitochondrial side of epigenetics. *Physiol Genomics* **47**, 299–307 (2015).
70. Vivian, C. J. *et al.* Mitochondrial Genomic Backgrounds Affect Nuclear DNA Methylation and Gene Expression. *Cancer Res* **77**, 6202–6214 (2017).
71. Bellizzi, D., D’Aquila, P., Giordano, M., Montesanto, A. & Passarino, G. Global DNA methylation levels are modulated by mitochondrial DNA variants. *Epigenomics* **4**, 17–27 (2012).
72. Smiraglia, D., Kulawiec, M., Bistulfi, G. L., Ghoshal, S. & Singh, K. K. A novel role for mitochondria in regulating epigenetic modifications in the nucleus. *Cancer Biol Ther* **7**, 1182–1190 (2008).
73. Shaughnessy, D. T. *et al.* Mitochondria, Energetics, Epigenetics, and Cellular Responses to Stress. *Environ Health Perspect* **122**, 1271–1278 (2014).
74. Quirós, P. M., Mottis, A. & Auwerx, J. Mitonuclear communication in homeostasis and stress. *Nat Rev Mol Cell Biol* **17**, 213–226 (2016).
75. Blesa, J. R., Prieto-Ruiz, J. A., Hernández, J. M. & Hernández-Yago, J. NRF-2 transcription factor is required for human TOMM20 gene expression. *Gene* **391**, 198–208 (2007).
76. Gleyzer, N., Vercauteren, K. & Scarpulla, R. C. Control of Mitochondrial Transcription Specificity Factors (TFB1M and TFB2M) by Nuclear Respiratory Factors (NRF-1 and NRF-2) and PGC-1 Family Coactivators. *Mol Cell Biol* **25**, 1354–1366 (2005).
77. Virbasius, J. V & Scarpulla, R. C. Activation of the human mitochondrial transcriptionfactor A gene by nuclear respiratory factors: a potential regulatory linkbetween nuclear and mitochondrial gene expression in organellebiogenesis. *Proceedings of the National Academy of Sciences* **91**, 1309–1313 (1994).
78. Dhar, S. S., Ongwijitwat, S. & Wong-Riley, M. T. T. Nuclear Respiratory Factor 1 Regulates All Ten Nuclear-encoded Subunits of Cytochrome c Oxidase in Neurons. *Journal of Biological Chemistry* **283**, 3120–3129 (2008).

79. Fernandez-Marcos, P. J. & Auwerx, J. Regulation of PGC-1 α , a nodal regulator of mitochondrial biogenesis. *Am J Clin Nutr* **93**, 884S-890S (2011).
80. Poulsen, L. la C., Siersbæk, M. & Mandrup, S. PPARs: Fatty acid sensors controlling metabolism. *Semin Cell Dev Biol* **23**, 631–639 (2012).
81. Fan, W. & Evans, R. PPARs and ERRs: molecular mediators of mitochondrial metabolism. *Curr Opin Cell Biol* **33**, 49–54 (2015).
82. Scarpulla, R. C. Metabolic control of mitochondrial biogenesis through the PGC-1 family regulatory network. *Biochimica et Biophysica Acta (BBA) - Molecular Cell Research* **1813**, 1269–1278 (2011).
83. Jazwinski, S. M. The retrograde response: When mitochondrial quality control is not enough. *Biochimica et Biophysica Acta (BBA) - Molecular Cell Research* **1833**, 400–409 (2013).
84. Herzig, S. & Shaw, R. J. AMPK: guardian of metabolism and mitochondrial homeostasis. *Nat Rev Mol Cell Biol* **19**, 121–135 (2018).
85. Lerner, C. *et al.* Reduced mammalian target of rapamycin activity facilitates mitochondrial retrograde signaling and increases life span in normal human fibroblasts. *Aging Cell* **12**, 966–977 (2013).
86. Wrogemann, K., Jacobson, B. E. & Blanchaer, M. C. On the mechanism of a calcium-associated defect of oxidative phosphorylation in progressive muscular dystrophy. *Arch Biochem Biophys* **159**, 267–278 (1973).
87. Trevelyan, A. J. *et al.* Mitochondrial DNA mutations affect calcium handling in differentiated neurons. *Brain* **133**, 787–796 (2010).
88. Biswas, G., Anandatheerthavarada, H. K., Zaidi, M. & Avadhani, N. G. Mitochondria to nucleus stress signaling. *Journal of Cell Biology* **161**, 507–519 (2003).
89. Crabtree, G. R. Calcium, Calcineurin, and the Control of Transcription. *Journal of Biological Chemistry* **276**, 2313–2316 (2001).
90. Nguyen, T., Nioi, P. & Pickett, C. B. The Nrf2-Antioxidant Response Element Signaling Pathway and Its Activation by Oxidative Stress. *Journal of Biological Chemistry* **284**, 13291–13295 (2009).
91. Marino, A. *et al.* AMP-activated protein kinase: A remarkable contributor to preserve a healthy heart against ROS injury. *Free Radic Biol Med* **166**, 238–254 (2021).
92. Chae, S. *et al.* A Systems Approach for Decoding Mitochondrial Retrograde Signaling Pathways. *Sci Signal* **6**, (2013).
93. Sieber, F., Duchêne, A.-M. & Maréchal-Drouard, L. Mitochondrial RNA Import. in 145–190 (2011). doi:10.1016/B978-0-12-386043-9.00004-9.
94. Lee, W. *et al.* Mitochondrial DNA copy number is regulated by DNA methylation and demethylation of POLGA in stem and cancer cells and their differentiated progeny. *Cell Death Dis* **6**, e1664–e1664 (2015).

95. Kelly, R. D. W., Mahmud, A., McKenzie, M., Trounce, I. A. & St John, J. C. Mitochondrial DNA copy number is regulated in a tissue specific manner by DNA methylation of the nuclear-encoded DNA polymerase gamma A. *Nucleic Acids Res* **40**, 10124–10138 (2012).
96. Koczor, C. A. *et al.* Thymidine kinase and mtDNA depletion in human cardiomyopathy: epigenetic and translational evidence for energy starvation. *Physiol Genomics* **45**, 590–596 (2013).
97. Copeland, W. C. Defects in mitochondrial DNA replication and human disease. *Crit Rev Biochem Mol Biol* **47**, 64–74 (2012).
98. Wallace, D. C. & Fan, W. Energetics, epigenetics, mitochondrial genetics. *Mitochondrion* **10**, 12–31 (2010).
99. Lu, S. C. & Mato, J. M. S-adenosylmethionine in Liver Health, Injury, and Cancer. *Physiol Rev* **92**, 1515–1542 (2012).
100. Shen, Y., Wei, W. & Zhou, D.-X. Histone Acetylation Enzymes Coordinate Metabolism and Gene Expression. *Trends Plant Sci* **20**, 614–621 (2015).
101. Joshi, K., Liu, S., Breslin S.J., P. & Zhang, J. Mechanisms that regulate the activities of TET proteins. *Cellular and Molecular Life Sciences* **79**, 363 (2022).
102. Salminen, A., Kauppinen, A., Hiltunen, M. & Kaarniranta, K. Krebs cycle intermediates regulate DNA and histone methylation: Epigenetic impact on the aging process. *Ageing Res Rev* **16**, 45–65 (2014).
103. Castellani, C. A. *et al.* Mitochondrial DNA copy number can influence mortality and cardiovascular disease via methylation of nuclear DNA CpGs. *Genome Med* **12**, 84 (2020).
104. Smiraglia, D., Kulawiec, M., Bistulfi, G. L., Ghoshal, S. & Singh, K. K. A novel role for mitochondria in regulating epigenetic modifications in the nucleus. *Cancer Biol Ther* **7**, 1182–1190 (2008).
105. Bellizzi, D., D’Aquila, P., Giordano, M., Montesanto, A. & Passarino, G. Global DNA methylation levels are modulated by mitochondrial DNA variants. *Epigenomics* **4**, 17–27 (2012).
106. Vivian, C. J. *et al.* Mitochondrial Genomic Backgrounds Affect Nuclear DNA Methylation and Gene Expression. *Cancer Res* **77**, 6202–6214 (2017).
107. Amorim, R., Magalhães, C. C., Borges, F., Oliveira, P. J. & Teixeira, J. From Non-Alcoholic Fatty Liver to Hepatocellular Carcinoma: A Story of (Mal)Adapted Mitochondria. *Biology (Basel)* **12**, 595 (2023).
108. Ramanathan, R., Ali, A. H. & Ibdah, J. A. Mitochondrial Dysfunction Plays Central Role in Nonalcoholic Fatty Liver Disease. *Int J Mol Sci* **23**, 7280 (2022).
109. Amorim, R., Magalhães, C. C., Borges, F., Oliveira, P. J. & Teixeira, J. From Non-Alcoholic Fatty Liver to Hepatocellular Carcinoma: A Story of (Mal)Adapted Mitochondria. *Biology (Basel)* **12**, 595 (2023).
110. Houten, S. M., Violante, S., Ventura, F. V. & Wanders, R. J. A. The Biochemistry and Physiology of Mitochondrial Fatty Acid β -Oxidation and Its Genetic Disorders. *Annu Rev Physiol* **78**, 23–44 (2016).
111. Nolfi-Donagan, D., Braganza, A. & Shiva, S. Mitochondrial electron transport chain: Oxidative phosphorylation, oxidant production, and methods of measurement. *Redox Biol* **37**, 101674 (2020).

112. Pérez-Carreras, M. Defective hepatic mitochondrial respiratory chain in patients with nonalcoholic steatohepatitis. *Hepatology* **38**, 999–1007 (2003).
113. Moore, M. P. *et al.* Compromised hepatic mitochondrial fatty acid oxidation and reduced markers of mitochondrial turnover in human NAFLD. *Hepatology* **76**, 1452–1465 (2022).
114. Koliaki, C. *et al.* Adaptation of Hepatic Mitochondrial Function in Humans with Non-Alcoholic Fatty Liver Is Lost in Steatohepatitis. *Cell Metab* **21**, 739–746 (2015).
115. Nassir, F., Arndt, J. J., Johnson, S. A. & Ibdah, J. A. Regulation of mitochondrial trifunctional protein modulates nonalcoholic fatty liver disease in mice. *J Lipid Res* **59**, 967–973 (2018).
116. Ibdah, J. A. *et al.* Lack of mitochondrial trifunctional protein in mice causes neonatal hypoglycemia and sudden death. *Journal of Clinical Investigation* **107**, 1403–1409 (2001).
117. Zhao, R., Jiang, S., Zhang, L. & Yu, Z. Mitochondrial electron transport chain, ROS generation and uncoupling (Review). *Int J Mol Med* (2019) doi:10.3892/ijmm.2019.4188.
118. Prasun, P., Ginevic, I. & Oishi, K. Mitochondrial dysfunction in nonalcoholic fatty liver disease and alcohol related liver disease. *Transl Gastroenterol Hepatol* **6**, 4–4 (2021).
119. Bessone, F., Razori, M. V. & Roma, M. G. Molecular pathways of nonalcoholic fatty liver disease development and progression. *Cellular and Molecular Life Sciences* **76**, 99–128 (2019).
120. Masarone, M. *et al.* Role of Oxidative Stress in Pathophysiology of Nonalcoholic Fatty Liver Disease. *Oxid Med Cell Longev* **2018**, 1–14 (2018).
121. Garcia-Martinez, I. *et al.* Hepatocyte mitochondrial DNA drives nonalcoholic steatohepatitis by activation of TLR9. *Journal of Clinical Investigation* **126**, 859–864 (2016).
122. Lee, J., Park, J.-S. & Roh, Y. S. Molecular insights into the role of mitochondria in non-alcoholic fatty liver disease. *Arch Pharm Res* **42**, 935–946 (2019).
123. Elsheikh, A. *et al.* Drug Antigenicity, Immunogenicity, and Costimulatory Signaling: Evidence for Formation of a Functional Antigen through Immune Cell Metabolism. *The Journal of Immunology* **185**, 6448–6460 (2010).
124. Pessayre, D., Mansouri, A. & Fromenty, B. V. Mitochondrial dysfunction in steatohepatitis. *American Journal of Physiology-Gastrointestinal and Liver Physiology* **282**, G193–G199 (2002).
125. Feldstein, A. Novel Insights into the Pathophysiology of Nonalcoholic Fatty Liver Disease. *Semin Liver Dis* **30**, 391–401 (2010).
126. Chen, Q., Allegood, J. C., Thompson, J., Toldo, S. & Lesnefsky, E. J. Increased Mitochondrial ROS Generation from Complex III Causes Mitochondrial Damage and Increases Endoplasmic Reticulum Stress. *The FASEB Journal* **33**, (2019).
127. Arroyave-Ospina, J. C., Wu, Z., Geng, Y. & Moshage, H. Role of Oxidative Stress in the Pathogenesis of Non-Alcoholic Fatty Liver Disease: Implications for Prevention and Therapy. *Antioxidants* **10**, 174 (2021).

128. Inzaugarat, M. E., Wree, A. & Feldstein, A. E. Hepatocyte mitochondrial DNA released in microparticles and toll-like receptor 9 activation: A link between lipotoxicity and inflammation during nonalcoholic steatohepatitis. *Hepatology* **64**, 669–671 (2016).
129. Sanyal, A. J. *et al.* Nonalcoholic steatohepatitis: Association of insulin resistance and mitochondrial abnormalities. *Gastroenterology* **120**, 1183–1192 (2001).
130. Perlemuter, G. *et al.* Increase in liver antioxidant enzyme activities in non-alcoholic fatty liver disease. *Liver International* **25**, 946–953 (2005).
131. Scott, I. & Youle, R. J. Mitochondrial fission and fusion. *Essays Biochem* **47**, 85–98 (2010).
132. Larson-Casey, J. L., He, C. & Carter, A. B. Mitochondrial quality control in pulmonary fibrosis. *Redox Biol* **33**, 101426 (2020).
133. Li, R., Toan, S. & Zhou, H. Role of mitochondrial quality control in the pathogenesis of nonalcoholic fatty liver disease. *Aging* **12**, 6467–6485 (2020).
134. Ding, M. *et al.* Dynamin-related protein 1-mediated mitochondrial fission contributes to post-traumatic cardiac dysfunction in rats and the protective effect of melatonin. *J Pineal Res* **64**, e12447 (2018).
135. Sumneang, N., Siri-Angkul, N., Kumfu, S., Chattipakorn, S. C. & Chattipakorn, N. The effects of iron overload on mitochondrial function, mitochondrial dynamics, and ferroptosis in cardiomyocytes. *Arch Biochem Biophys* **680**, 108241 (2020).
136. Losón, O. C., Song, Z., Chen, H. & Chan, D. C. Fis1, Mff, MiD49, and MiD51 mediate Drp1 recruitment in mitochondrial fission. *Mol Biol Cell* **24**, 659–667 (2013).
137. Du, J. *et al.* Pro-Inflammatory CXCR3 Impairs Mitochondrial Function in Experimental Non-Alcoholic Steatohepatitis. *Theranostics* **7**, 4192–4203 (2017).
138. Galloway, C. A., Lee, H., Brookes, P. S. & Yoon, Y. Decreasing mitochondrial fission alleviates hepatic steatosis in a murine model of nonalcoholic fatty liver disease. *American Journal of Physiology-Gastrointestinal and Liver Physiology* **307**, G632–G641 (2014).
139. Stevanović, J., Beleza, J., Coxito, P., Ascensão, A. & Magalhães, J. Physical exercise and liver “fitness”: Role of mitochondrial function and epigenetics-related mechanisms in non-alcoholic fatty liver disease. *Mol Metab* **32**, 1–14 (2020).
140. Piacentini, M. *et al.* Non-alcoholic fatty liver disease severity is modulated by transglutaminase type 2. *Cell Death Dis* **9**, 257 (2018).
141. Infantino, V., Todisco, S. & Convertini, P. Mitochondrial physiology: An overview. in *Mitochondrial Intoxication* 1–27 (Elsevier, 2023). doi:10.1016/B978-0-323-88462-4.00001-8.
142. Ge, Y. *et al.* Two forms of Opa1 cooperate to complete fusion of the mitochondrial inner-membrane. *Elife* **9**, (2020).
143. Gong, F., Gao, L. & Ding, T. IDH2 protects against nonalcoholic steatohepatitis by alleviating dyslipidemia regulated by oxidative stress. *Biochem Biophys Res Commun* **514**, 593–600 (2019).

144. Hernández-Alvarez, M. I. *et al.* Deficient Endoplasmic Reticulum-Mitochondrial Phosphatidylserine Transfer Causes Liver Disease. *Cell* **177**, 881–895.e17 (2019).
145. Sebastián, D. *et al.* Mitofusin 2 (Mfn2) links mitochondrial and endoplasmic reticulum function with insulin signaling and is essential for normal glucose homeostasis. *Proceedings of the National Academy of Sciences* **109**, 5523–5528 (2012).
146. Zhang, L., Seitz, L. C., Abramczyk, A. M. & Chan, C. Synergistic effect of cAMP and palmitate in promoting altered mitochondrial function and cell death in HepG2 cells. *Exp Cell Res* **316**, 716–727 (2010).
147. Legaki, A.-I. *et al.* Hepatocyte Mitochondrial Dynamics and Bioenergetics in Obesity-Related Non-Alcoholic Fatty Liver Disease. *Curr Obes Rep* **11**, 126–143 (2022).
148. Bach, D. *et al.* Mitofusin-2 Determines Mitochondrial Network Architecture and Mitochondrial Metabolism. *Journal of Biological Chemistry* **278**, 17190–17197 (2003).
149. Willems, P. H. G. M., Rossignol, R., Dieteren, C. E. J., Murphy, M. P. & Koopman, W. J. H. Redox Homeostasis and Mitochondrial Dynamics. *Cell Metab* **22**, 207–218 (2015).
150. Ma, X., McKeen, T., Zhang, J. & Ding, W.-X. Role and Mechanisms of Mitophagy in Liver Diseases. *Cells* **9**, 837 (2020).
151. Caldwell, S. H. *et al.* Mitochondrial abnormalities in non-alcoholic steatohepatitis. *J Hepatol* **31**, 430–434 (1999).
152. Sanyal, A. J. *et al.* Nonalcoholic steatohepatitis: Association of insulin resistance and mitochondrial abnormalities. *Gastroenterology* **120**, 1183–1192 (2001).
153. Pérez-Carreras, M. *et al.* Defective hepatic mitochondrial respiratory chain in patients with nonalcoholic steatohepatitis. *Hepatology* **38**, 999–1007 (2003).
154. Lin, D. *et al.* Wolfberries potentiate mitophagy and enhance mitochondrial biogenesis leading to prevention of hepatic steatosis in obese mice: The role of AMP-activated protein kinase α 2 subunit. *Mol Nutr Food Res* **58**, 1005–1015 (2014).
155. Gong, L. *et al.* Akebia saponin D alleviates hepatic steatosis through BNip3 induced mitophagy. *J Pharmacol Sci* **136**, 189–195 (2018).
156. Yu, X. *et al.* Liraglutide ameliorates non-alcoholic steatohepatitis by inhibiting NLRP3 inflammasome and pyroptosis activation via mitophagy. *Eur J Pharmacol* **864**, 172715 (2019).
157. Liu, P. *et al.* Frataxin-Mediated PINK1-Parkin-Dependent Mitophagy in Hepatic Steatosis: The Protective Effects of Quercetin. *Mol Nutr Food Res* **62**, 1800164 (2018).
158. Li, R. *et al.* Therapeutic effect of Sirtuin 3 on ameliorating nonalcoholic fatty liver disease: The role of the ERK-CREB pathway and Bnip3-mediated mitophagy. *Redox Biol* **18**, 229–243 (2018).
159. Lee, D. H. *et al.* Peroxiredoxin 6 Confers Protection Against Nonalcoholic Fatty Liver Disease Through Maintaining Mitochondrial Function. *Antioxid Redox Signal* **31**, 387–402 (2019).

160. Zhou, T., Chang, L., Luo, Y., Zhou, Y. & Zhang, J. Mst1 inhibition attenuates non-alcoholic fatty liver disease via reversing Parkin-related mitophagy. *Redox Biol* **21**, 101120 (2019).
161. Wang, L. *et al.* ALCAT1 controls mitochondrial etiology of fatty liver diseases, linking defective mitophagy to steatosis. *Hepatology* **61**, 486–496 (2015).
162. Glick, D. *et al.* BNip3 Regulates Mitochondrial Function and Lipid Metabolism in the Liver. *Mol Cell Biol* **32**, 2570–2584 (2012).

THESIS OUTLINE AND RESEARCH OBJECTIVES

Thesis outline and research objectives

Thesis outline and research objectives

As outlined in the introductory chapters, metabolic dysfunction associated steatotic liver disease (MASLD) is a complex disease with many possible risk factors and a heterogeneous patient population. Due to the multifactorial nature of the disease, it is challenging to develop therapeutics that effect multiple aspects of the disease progression and define biomarkers that allow the correct stratification of patients. In this regard, epigenetic modifications provide an interesting opportunity, because they are directly associated with environmental and genetic risk factors and are responsible for reprogramming of multiple transcription networks. Indeed, different epigenetic signatures have been correlated with MASLD disease progression. However, the regulatory networks responsible for this epigenetic reprogramming, are not fully defined yet. Thus, there is an urgent need to explore the role of master regulators of MASLD disease progression in the epigenetic progression of the disease, that can be therapeutically targeted.

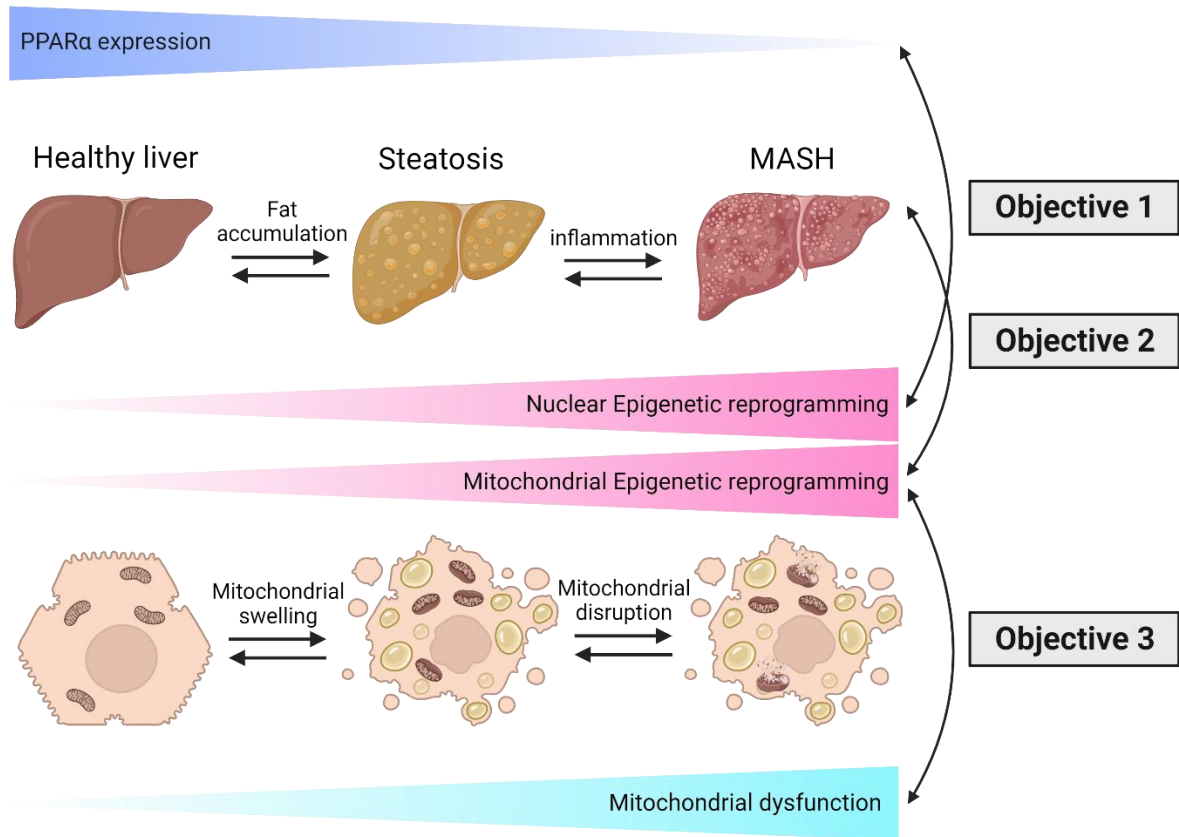
In this thesis, we aimed to characterize the epigenetic “driver” or “passenger” functions of the key regulatory factor of lipid metabolism, the nuclear receptor PPAR α and the role of mitochondrial DNA (mtDNA) methylation in MASLD associated mitochondrial dysfunction. In particular, the following objectives are discussed in the results section of this PhD work.

The **first objective** was to define the role of PPAR α loss of function during the epigenetic dysregulation in MASLD. Does PPAR α have a profound regulatory role in the epigenetic dysregulation in MASLD or is it not reciprocally regulated? PPAR α has recently shown to epigenetically regulate lipid metabolism when activated. This regulation is established by a direct interaction with epigenetic enzymes in different tissues including liver and colon. To define if a similar epigenetic reprogramming is directly linked to the loss of function of PPAR α in MASLD progression, we combined genome-wide DNA methylation profiling with transcriptome sequencing in wild type (WT) and hepatocyte-specific PPAR α knock out (KO) mice, receiving control chow diet versus MASLD promoting high fat diet (CDAHFD) in **Chapter 3**.

The **second objective** was to establish a sequencing protocol that allows to correctly call for methylation in the mtDNA and to define if MASLD is linked to a mtDNA methylation signature. MtDNA methylation has gained new interest over the last years, because it has proven to be a biomarker in cancer research and associated with mitochondrial gene expression and copy number changes. However correctly estimating the methylation percentages of mtDNA has been challenging. Therefore in **Chapter 4** we tested different mitochondrial or mtDNA extraction methods that allow for further Nanopore episequencing. Finally, we analysed mtDNA methylation of one untreated and one characterised *in vitro* steatosis model with Nanopore episequencing. Since differences in methylation percentage could be defined in the steatosis model compared to the untreated cells, the **third objective** of this thesis was to define the functional role of mtDNA methylation in mitochondrial dysfunction and thereby assess a new functional role of mtDNA methylation in MASLD. Therefore in **Chapter 5**, we characterized different morphological features and aspects of mitochondrial functioning in mitochondrial CpG or GpC DNMT overexpressing cell lines, left untreated or after a FFA treatment inducing steatosis. We used Seahorse respiration measurements, electron microscopy, Adipored lipid staining, RNA sequencing and Nanopore

Thesis outline and research objectives

episequencing to compare changes in expression that could explain the characterized mitochondrial dysfunctions associated with mtDNA methylation. Moreover, by genome-wide DNA methylation profiling we could explore the role of mito-nuclear communication in mitochondrial dysfunction induced by mtDNA methylation.



RESULTS

CHAPTER III:

Loss of PPAR α function promotes epigenetic dysregulation of lipid homeostasis driving ferroptosis and pyroptosis lipotoxicity in Metabolic Dysfunction Associated Steatotic Liver Disease (MASLD)

CHAPTER IV:

Optimisation of mitochondrial DNA methylation detection in an in vitro MASLD model

CHAPTER V:

Mitochondrial GpC and CpG DNA hypermethylation cause metabolic stress-induced mitophagy and cholestophagy

CHAPTER III

Loss of PPAR α function promotes epigenetic dysregulation of lipid homeostasis driving ferroptosis and pyroptosis lipotoxicity in Metabolic Dysfunction Associated Steatotic Liver Disease (MASLD)

Chapter 3

Loss of PPAR α function promotes epigenetic dysregulation of lipid homeostasis driving ferroptosis and pyroptosis lipotoxicity in Metabolic Dysfunction Associated Steatotic Liver Disease (MASLD)

Claudia Theys¹, Tineke Vanderhaeghen^{2,3}, Evelien Van Dijck⁴, Cedric Peleman^{5,7}, Anne Scheepers⁴, Joe Ibrahim⁴, Ligia Mateiu⁴, Steven Timmermans^{2,3}, Tom Vanden Berghe^{2,3,7}, Sven M Francque^{5,6}, Wim Van Hul⁴, Claude Libert^{2,3}, Wim Vanden Berghe¹

¹ Protein Chemistry, Proteomics and Epigenetic Signaling (PPES), Department of Biomedical Sciences, University of Antwerp, Antwerp, Belgium.

² Center for Inflammation Research, VIB, Ghent, Belgium.

³ Department of Biomedical Molecular Biology, Ghent University, Ghent, Belgium

⁴ Center of Medical Genetics, University of Antwerp, Antwerp, Belgium

⁵ Laboratory of Experimental Medicine and Pediatrics, Infla-Med Centre of Excellence, University of Antwerp, Universiteitsplein 1, 2610, Antwerp, Belgium.

⁶ Department of Gastroenterology and Hepatology, Antwerp University Hospital, Drie Eikenstraat 655, 2650, Edegem, Belgium.

⁷ Pathophysiology lab, Infla-Med Centre of Excellence, Department of Biomedical Sciences, University of Antwerp, Antwerp, Belgium.

*Corresponding author: wim.vandenbergh@uantwerpen.be

Conflict of Interest: The authors declare no conflict of interest

Accepted for publication in Frontiers Molecular Medicine, DOI: 10.3389/fmmed.2023.1283170

3.1 Abstract

Metabolic Dysfunction Associated Steatotic Liver Disease (MASLD) is a growing epidemic with an estimated prevalence of 20-30% in Europe and the most common cause of chronic liver disease worldwide. The onset and progression of MASLD are orchestrated by an interplay of the metabolic environment with genetic and epigenetic factors. Emerging evidence suggests altered DNA methylation pattern as a major determinant of MASLD pathogenesis coinciding with progressive DNA hypermethylation and gene silencing of the liver-specific nuclear receptor PPAR α , a key regulator of lipid metabolism. To investigate how PPAR α loss of function contributes to epigenetic dysregulation in MASLD pathology, we studied DNA methylation changes in liver biopsies of WT and hepatocyte-specific PPAR α KO mice, following a 6-week CDAHFD (choline-deficient, L-amino acid-defined, high-fat diet) or chow diet. Interestingly, genetic loss of PPAR α function in hepatocyte-specific KO mice could be phenocopied by a 6-week CDAHFD diet in WT mice which promotes epigenetic silencing of PPAR α function via DNA hypermethylation, similar to MASLD pathology. Remarkably, genetic and lipid diet-induced loss of PPAR α function triggers compensatory activation of multiple lipid sensing transcription factors and epigenetic writer-eraser-reader proteins, which promotes the epigenetic transition from lipid metabolic stress towards ferroptosis and pyroptosis lipid hepatotoxicity pathways associated with advanced MASLD. In conclusion, we show that PPAR α function is essential to support lipid homeostasis and to suppress the epigenetic progression of ferroptosis-pyroptosis lipid damage associated pathways towards MASLD fibrosis.

Keywords: PPAR α , MASLD, Epigenetics, Lipid metabolism, Bile acid metabolism, Ferroptosis, Pyroptosis

3.2 Introduction

Non-alcoholic fatty liver disease (NAFLD), recently re-named and re-defined as Metabolic Dysfunction Associated Steatotic Liver Disease (MASLD)¹, is a growing epidemic, paralleling the increase of obesity in western diet consuming countries. MASLD shares, in part, the common pathogenesis of metabolic syndrome including obesity, hyperlipidaemia, insulin resistance, mitochondrial damage, oxidative stress response, and the release of inflammatory cytokines. It has an estimated prevalence of 20-30% in Europe and is the most common cause of chronic liver disease worldwide²⁻⁴. MASLD consists of a spectrum of liver disorders ranging from isolated steatosis to Metabolic Dysfunction Associated Steatohepatitis (MASH) which predisposes patients to progressive fibrosis, cirrhosis and hepatocarcinoma but also extrahepatic diseases, especially cardiovascular diseases^{5,6}. Dysregulation of insulin secretion and dyslipidaemia due to obesity and other lifestyle variables are the primary contributors to the establishment of MASLD. Although the prevalence keeps growing, there is still no FDA-approved treatment for MASLD. Therefore, with no drugs available, the mainstay of MASLD management remains lifestyle changes with exercise and dietary modifications^{7,8}.

The onset and progression of MASLD are orchestrated by an interplay of metabolic environment with genetic and epigenetic (lifestyle, environment) factors^{9,10}. An accumulating body of studies revealed progressive DNA methylation changes across different stages of MASLD pathogenesis, although the underlying mechanisms remain poorly understood¹¹⁻¹⁸. DNA methylation signatures that can affect gene expression are influenced by environmental and lifestyle experiences such as diet, obesity and physical activity and are reversible^{9,19,20}. Hence, DNA methylation signatures and modifiers in MASLD may provide the basis for developing biomarkers indicating the onset and progression of MASLD and therapeutics for MASLD. More specifically, MASLD patients show global hepatic DNA hypomethylation in parallel with increasing hepatic inflammation grade, disease progression and increased hypermethylation of the promotor sequence of the nuclear receptor peroxisome proliferator-activated receptor- α (PPAR α) gene²¹⁻²³. Whether loss of PPAR α function is a cause or consequence of epigenetic dysregulation in MASLD pathology requires further investigation.

PPAR α is part of the PPAR nuclear receptor family that consists of three isoforms: PPAR α , PPAR β and PPAR γ . All three isoforms are involved in lipid metabolism, but are most abundantly expressed in liver, skeletal muscle and adipocytes respectively²⁴⁻²⁷. Since PPAR α is abundantly expressed in the liver, known as a key regulator of lipid metabolism, and downregulated in MASLD patients correlating with the disease stage, several agonists have been therapeutically evaluated over the years²⁸⁻³³. However, PPAR α agonists that only target PPAR α failed to show convincingly positive results in clinical trials^{32,34,35}. Therefore, research is currently more shifting towards drugs targeting multiple therapeutic targets, *i.e.*, pan-PPAR agonists (*e.g.*, Lanifibranor), but also epigenetic modulators (*e.g.* vitamine E)^{36,37}. Both have already shown promising results in clinical trials of MASLD patients, suggesting a crucial role for PPAR interplay with epigenetic control mechanisms in the development of MASLD³⁶⁻³⁸. Indeed, recent papers demonstrate significant demethylation of PPAR α target metabolic genes upon activation of PPAR α ³⁹⁻⁴². Besides, PPAR α interactions with epigenetic enzymes have already been identified in different tissues including liver and colon⁴³⁻⁴⁵. To further characterize epigenetic “driver” or “passenger” functions of PPAR α in MASLD, we compared genome-wide DNA methylation and transcriptome changes in livers of wild type (WT)

and hepatocyte-specific PPAR α knock out (KO) mice, receiving control chow diet versus MASLD promoting high fat diet (CDAHFD). Characterisation of genome-wide DNA methylation and gene expression changes might provide new insights in PPAR α -dependent (epigenetic driver) versus independent (epigenetic passenger) functions, with potential clinical relevance in precision medicine for disease management and staging of MASLD progression.

3.3 Material and Methods

3.3.1 Mouse model

PPAR α KO C57BL/6J (PPAR $\alpha^{fl/fl}$ AlbuminCre $^{Tg/+}$) mice and WT C57BL/6J (PPAR $\alpha^{fl/fl}$ AlbuminCre $^{+/+}$) mice (IRC-VIB, UGent) were housed in a temperature-controlled, specific pathogen free (SPF) air-conditioned animal house with 14/10h light/dark cycles and received food and water *ad libitum*. 7-week old male hepatocyte-specific PPAR α KO and WT mice were fed either a chow diet (normal standard diet, containing 9% energy from fat, 58% from carbohydrates, and 33% from protein) or a CDAHFD (choline-deficient L-amino acid defined high-fat diet, A06071302, New Brunswick, NJ USA, containing 62% energy from fat, 20% from carbohydrates, and 18% from protein) for 6 weeks *ad libitum* creating 4 different treatment groups of 3 mice. At 13 weeks, the mice (n=12) were sacrificed by cervical dislocation after anaesthesia with ketamine and xylazine diluted in phosphate-buffered saline (PBS) (2:2:6). Liver samples were immediately snap frozen and stored at -80°C for further analysis. The animal experiments were approved by the institutional ethics committee for animal welfare of the Faculty of Sciences, Ghent University, Belgium (EC2021-071).

3.3.2 Histology

The liver was excised from euthanized mice and washed in PBS. Excised liver was fixed in 4% paraformaldehyde overnight at 4°C, dehydrated and embedded in paraffin. The excised tissue sections of 5 μ m were cut and stained with haematoxylin-eosin (H&E) using standard protocols.

Liver sections were also stained using Masson's Trichrome staining kit (HT15, Sigma-Aldrich), following the manufacturer's protocol. In short, liver slices were deparaffinized and hydrated using BIDI. Next, the liver slices were treated with the mordant preheated Bouin's solution for 30 min at 60°C. Then, the slices were washed and stained with Weigert's iron haematoxylin at room temperature. After washing and rinsing, the liver slices were stained with Biebrich Scarlet-Acid Fuchsin. After rinsing the tissue slices, the slices were put in a Phosphotungstic/phosphomolybdic Acid solution followed by an Aniline Blue solution and 1% acetic acid. Finally, the liver slices were dipped once in 70% ethanol and 90% ethanol followed by washing the liver slices with 100% ethanol and xylene before mounting the liver slices.

Semiquantitative histopathological scoring and differentiation between normal liver tissue, steatosis and MASH were performed in a blinded manner by an experienced histopathologists according to the steatosis a Clinical Research Network and Steatosis-Activity-Fibrosis NASH scoring systems^{46,47}.

3.3.3 RNA extraction

Total RNA was extracted from the livers of the mice after tissue disruption with the TissueRuptor (Qiagen) with the RNeasy kit (Qiagen, 75162), according to the manufacturer's protocol. Afterwards RNA quantity was determined using QubitTM RNA Broad Range Assay kit with the aid of

the Invitrogen Qubit™ Fluorometer (Thermo Fisher Scientific, USA). The extracted RNA was stored at -80°C until further analysis.

3.3.4 RNA sequencing

Total isolated RNA of the livers of 3 mice of each treatment group were sent to Novogene Leading Edge Genomic Services & Solutions for RNA sequencing analysis on the Novaseq6000 platform. In brief, messenger RNA was purified from total RNA using poly-T oligo-attached magnetic beads. After fragmentation, the first strand cDNA was synthesized using random hexamer primers, followed by the second strand cDNA synthesis and library construction. The library was checked with Qubit and real-time PCR for quantification and bioanalyzer for size distribution detection. Quantified libraries were pooled and sequenced on Illumina platforms, according to effective library concentration and data amount. The quality of the raw sequencing reads was evaluated using FastQC (v0.11.5)⁴⁸ and subsequent alignment to genome reference consortium mouse build 38 (GRCm38) was performed with the STAR (v.2.7.3a) tool⁴⁹. Differential gene expression and pathway analysis were performed using DESeq2 R package software⁵⁰ and the Omics Playground tool (v2.8.12) platform, which was also used for further visualisation. RNA sequencing was validated by qPCR and deposited in the NCBI GEO database with accession number GSE238201.

3.3.5 Quantitative polymerase chain reaction (qPCR)

After RNA extraction, total RNA was converted into cDNA with the iScript™ cDNA Synthesis Kit (BioRad, 1708890) according to the manufacturer's protocol. Next, qPCR analysis was performed using the PowerUp SYBR™ green PCR master mix (Thermo Fisher Scientific, USA) according to the manufacturer's instructions. In brief, a 20 µL reaction volume mix per sample was prepared containing 10 µL PowerUp SYBR Green Master Mix, 0.4 µM forward and reverse primer (Supplementary Table 1), and nuclease-free water. The following PCR program was applied on the Rotor-Gene Q qPCR machine of Qiagen: 50°C for 2 min, 95°C for 2 min, 40 cycles denaturation (95°C, 15 s) and annealing/extension (60°C, 1 min), and dissociation (60–95°C). Each sample was run in triplicate. The mean value of the triplicates was taken to calculate the $\Delta\Delta C_t$ -values using GAPDH and YWHAZ as the normalisation genes. PPAR α and DNMT1 primer sequences (Supplementary Table 1) were designed by Primer3 and synthesized by Integrated DNA Technologies (IDT, USA). Statistical analysis was carried out using a One-Way ANOVA test with Tukey's correction for multiple comparisons. P-value < 0.05 was considered statistically significant.

3.3.6 Protein extraction and western immunoblot analysis

For western blot analysis, liver tissue was disrupted with the TissueRuptor (Qiagen). Next, cells were lysed in 0.5 mL 1x RIPA lysis buffer (150 mM NaCl, 0.1% Triton x-100, 0.1% SDS, 50 mM Tris-HCl pH 8 supplemented with protease inhibitor cocktail (Sigma-Aldrich, Germany) on ice for 15 min. Afterwards cells were briefly sonicated and centrifugated at 13,000 rpm for 15 min at 4°C. Next, supernatant with soluble protein extract was transferred to new Eppendorf tubes and used for protein quantification with Pierce™ BCA Protein Assay Kit (Thermo Fisher Scientific, USA). After protein extraction, SDS-PAGE was performed to separate proteins on a 6-12% gradient Bis-Tris gel. First, samples were mixed with Laemmli buffer (Biorad, USA) and 50 mM 1,4- dithiothreitol (DTT) and then heated at 70 °C for 10 min to denature the protein. Afterwards, both the samples and protein ladder (BenchMark™ Protein Ladder, Thermo Fisher Scientific, USA) were loaded on the Bis-Tris gel at a protein concentration of 10 µg/well (PPAR α , DNMT1, NRF2) or 100µg/well (Caspase-1

and NLRP3). Electrophoresis was performed in a Mini-PROTEAN Tetra Cell System (Biorad, USA) using a high molecular weight buffer (100 mM MOPS, 100 mM Tris, 0.2% SDS, 2 mM EDTA, 5 mM sodium bisulphite). Afterwards, the proteins were transferred to pre-wet nitrocellulose membranes (Cytiva, USA) for 1 hour at 4°C on 250 mA. After blocking the membranes in 5% milk /TBST blocking buffer for 1 hour at room temperature, the primary antibodies anti-PPAR α (Abcam, #ab126285) and anti-DNMT1 (Imgenex, #60B1220.2), anti-NLRP3 (Bio-connect, #AG-20B-0014-C100), anti-Caspase-1 (Bio-connect, AG-20B-0048-C100) and anti-NRF2 (Proteintech, #16396-1-AP) were diluted (1:1000) in the blocking buffer and incubated overnight at 4°C. The next day, membranes were washed three times with TBST and incubated with HRP-conjugated anti-rabbit secondary antibody (PPAR α , DNMT1 and NRF2) or HRP-conjugated anti-mouse secondary antibody (NLRP3 and Caspase-1) diluted in blocking buffer (1:2000) for 1 hour at room temperature. Anti-GAPDH antibody (Bioké #5174S, diluted 1:1000) in blocking buffer was used as loading control. Protein detection was performed on the Amersham imager 680 (Cytiva, USA) using SuperSignal™ West Pico PLUS Chemiluminescent Substrate (Thermo Fisher Scientific, 34577) and quantified using Image-J software. Statistical analysis was carried out using a One-Way ANOVA test with Tukey's correction for multiple comparisons. P-value < 0.05 was considered statistically significant.

3.3.7 Lipid peroxidation-MDA assay

Liver tissue was disrupted with the TissueLyser II (Qiagen) on 20Hz for 5 min at 4°C in 1mL PBS. Afterwards 100 μ L of the tissue lysate was pipetted in a 96 well plate for MDA quantification and the remaining sample was used for further protein quantification with the Pierce™ BCA Protein Assay Kit (Thermo Fisher Scientific, USA) according to the manufacturer's protocol. At the same time, a 1:2 serial dilution of 1,1,3,3-tetramethoxypropane (0-20 μ M) in MiliQ was made to form a standard curve of MDA under acidic conditions. Subsequently, a working solutions consisting of 0.5mg N-methyl phenyl indol (NMPI), 0.2 mL Acetonitrile and 0.08 mL Methanol was added per 100 μ L of sample or standard. Afterwards, 75 μ L of 37% chloric acid was added to the reaction and the samples were incubated for 45min at 70°C. Next, the reaction was stopped by a centrifugation for 10min at 15000rpm at 4°C and the amount of carbocyanine dye formed during this reaction of MDA with NMPI, was measured at 595 nm using the 2103 EnVision™ Multilabel Plate Reader (Perkin Elmer, USA). The final concentration of MDA was further corrected for protein concentration. Statistical analysis was carried out using a One-Way ANOVA test with Dunnett's correction for multiple comparisons. P-value < 0.05 was considered statistically significant.

3.3.8 Methylation analysis

Whole-genome methylation profiling was performed on the livers of 3 mice of each treatment group using the Infinium Mouse Methylation BeadChip array (Illumina, San Diego, CA, USA) at the Centre for Medical Genetics (Antwerp University Hospital (UZA), University of Antwerp). Genomic DNA (gDNA) was extracted from the livers using the Dneasy Blood & Tissue Kit (Qiagen, 69504, Courtaboeuf, France) according to the manufacturer's protocol. DNA concentration and purity were determined by the Qubit 4 Fluorometer (Thermo Fisher Scientific, Q33238). Next, 750 ng DNA was bisulphite converted with the EZ DNA Methylation Kit (Zymo Research, D5001/D5002, Irvine, CA, USA) according to the manufacturer's instructions. Successful bisulphite conversion was confirmed by PCR with the PyroMark PCR kit (Qiagen) in a region of the Line1 gene (Supplementary Table 2). The resulting PCR products were run on a 2% agarose gel. This converted DNA was then further hybridized with the Illumina Infinium Mouse Methylation BeadChip (Illumina, San Diego, CA, USA)

according to the manufacturer's instructions. In brief, converted DNA was amplified overnight and fragmented enzymatically. Precipitated DNA was resuspended in hybridisation buffer and dispensed onto the BeadChips. The hybridisation procedure was performed at 48°C overnight using an Illumina Hybridisation oven. After hybridisation, free DNA was washed away, and single nucleotide extension followed by fluorescent readout was performed. The BeadChips were imaged using an Illumina iScan (Illumina, San Diego, CA, USA). The platform interrogates more than 285,000 methylation sites per sample at single-nucleotide resolution. Annotations for the interrogated sites were taken from Illumina's BeadChip array manifest based on genome build mm10. Raw intensity data from IDAT files was read and processed in R (v. 4.2.0) via the Enmix package and beta values were normalised with the Enmix D method⁵¹. Data pre-processing consisted of masking probes with poor design, control probes, and non-cg and non-ch probes. Detection p-values were inferred using SeSAME's pOOBAH (p-value with out-of-band array hybridization) algorithm. Probes with detection p-values > 0.01 or more than 10% of NA values were filtered out. No samples had more than 10% missing values, thus all were considered for further analysis. Further probe-type bias adjustment was applied with the Regression on Correlated Probes method⁵². The difference in signal intensity between the two-colour channels (dye bias correction) was corrected for using a flexible exponential-normal mixture distribution model. Background correction was done using the Out-Of-Band algorithm. To identify significantly differentially methylated CpGs between the different groups of mice, the Wilcoxon rank-sum test with a Bonferroni correction ($p < 0.01$) for the total amount of CpGs in the Mouse Methylation BeadChip was used. Further Metascape pathway analysis of genes with a delta beta (DB) > |0.1| and FDR < 0.05 was performed with the online Metascape Web tool⁵³. Methylation data was deposited in the NCBI GEO database with accession number GSE238173.

3.3.9 Pyrosequencing analysis

Pyrosequencing was used to validate methylation of the RETSAT and Eci1 promotor identified by BeadChip analysis. The sequences of the promotor region of the RETSAT and Eci1 gene were retrieved from the Ensemble website (<http://genome.ucsc.edu/>). Primers were designed based on this sequence and the PyroMark Assay Design Software 2.0.2. (Qiagen) (Supplementary Table 1). Genomic DNA (gDNA) was extracted from the livers using the Dneasy Blood & Tissue Kit (Qiagen, 69504, Courtaboeuf, France) according to the manufacturer's protocol. DNA concentration and purity was determined by the Qubit 4 Fluorometer (Thermo Fisher Scientific, Q33238). Next, 750 ng DNA was bisulphite converted with the EZ DNA Methylation Kit (Zymo Research, D5001/D5002, Irvine, CA, USA) according to the manufacturer's instructions. Successful bisulphite conversion was confirmed by PCR with the PyroMark PCR kit (Qiagen) in a region of the Line1 gene (Supplementary Table 2). The resulting PCR products were run on a 2% agarose gel. After successful bisulphite conversion, a PCR was performed with the PyroMark PCR kit (Qiagen) and a forward and biotinylated reverse primer specific to a cytosine in the promotor region of the RETSAT and Eci1 gene. Afterwards 20µL of this biotinylated product was further used for pyrosequencing using the PyroMark Q24 system (Qiagen) and PyroMark Q24 advanced reagent kit (Qiagen) in combination with a sequencing primer covering 1 CpG according to the manufacturer's protocol. Analysis was performed using the Pyromark Q24 Advanced software (version 3.0) for detection and quantification of methylation patterns in the target regions. The only values that were reported to be technically reliable by the PyroMark Q24 Software 2.0.8 (Qiagen) were used for statistical

analysis. The One-Way ANOVA was performed to assess differential methylation of RETSAT and Eci1 gene between different treatment groups.

3.4 Results

3.4.1 *Hepatocyte-specific PPAR α KO and high fat diet disrupt bile and fatty acid metabolism and promote MASLD/MASH like gene expression signatures and histopathology features*

PPAR α , a key player of lipid metabolism and energy homeostasis, is typically downregulated in the livers of MASLD patients²⁸. To characterize the functional role of PPAR α in MASLD development, we studied a hepatocyte-specific PPAR α KO mouse model following a 6-week CDAHFD (HFD) to simulate liver pathological properties of a prolonged western diet. First, lack of PPAR α expression in PPAR α KO liver samples was confirmed at the RNA and protein level by qPCR and western blot analysis respectively (Figure 1A-B). QPCR and western analysis clearly confirm lack of significant PPAR α expression in PPAR α KO liver samples as expected (some background *Ppara* mRNA residual transcription may originate from traces of non-hepatocytes (mainly from stellate cells) present in the liver biopsies⁵⁴). Interestingly, RNAseq transcriptome profiling revealed high similarities in transcription profiles of PPAR α KO mice on chow diet versus WT mice following 6-week CDAHFD diet. This suggests that a CDAHFD partially phenocopies loss of hepatocyte function of PPAR α , closely resembling a genetic PPAR α KO approach (Figure 1C, Supplementary Figure 1). Along the same line, GO gene set enrichment analysis confirms mitochondrial dysfunctions due to multiple changes in bile and fatty acid metabolism, amino acid catabolism and inflammation, in response to CDAHFD and upon genetic PPAR α KO or combinations thereof (Figure 1D).

In line with reduced PPAR α expression reported in MASLD/MASH patients, both the qPCR and western blot also reveal decreased PPAR α expression in the WT mice following 6-week CDAHFD diet²³. The latter suggests that a high fat diet may gradually decrease PPAR α expression and as such progressively phenocopies the transcriptome signature of a genetic hepatocyte-specific PPAR α KO model. Furthermore, liver sections were scored based on the Clinical Research Network and Steatosis-Activity-Fibrosis NASH scoring systems to assess the disease stage of the mice (Figure 2A, Supplementary Table 2)^{46,55}. These results show that 6-week CDAHFD in WT and PPAR KO mice, both result in MASH features including steatosis, ballooning, lobular inflammation and fibrosis, similar to liver histopathology in MASH patients. Interestingly, PPAR α KO mice on a normal chow diet already reveal MASLD features such as accumulation of lipid droplets.

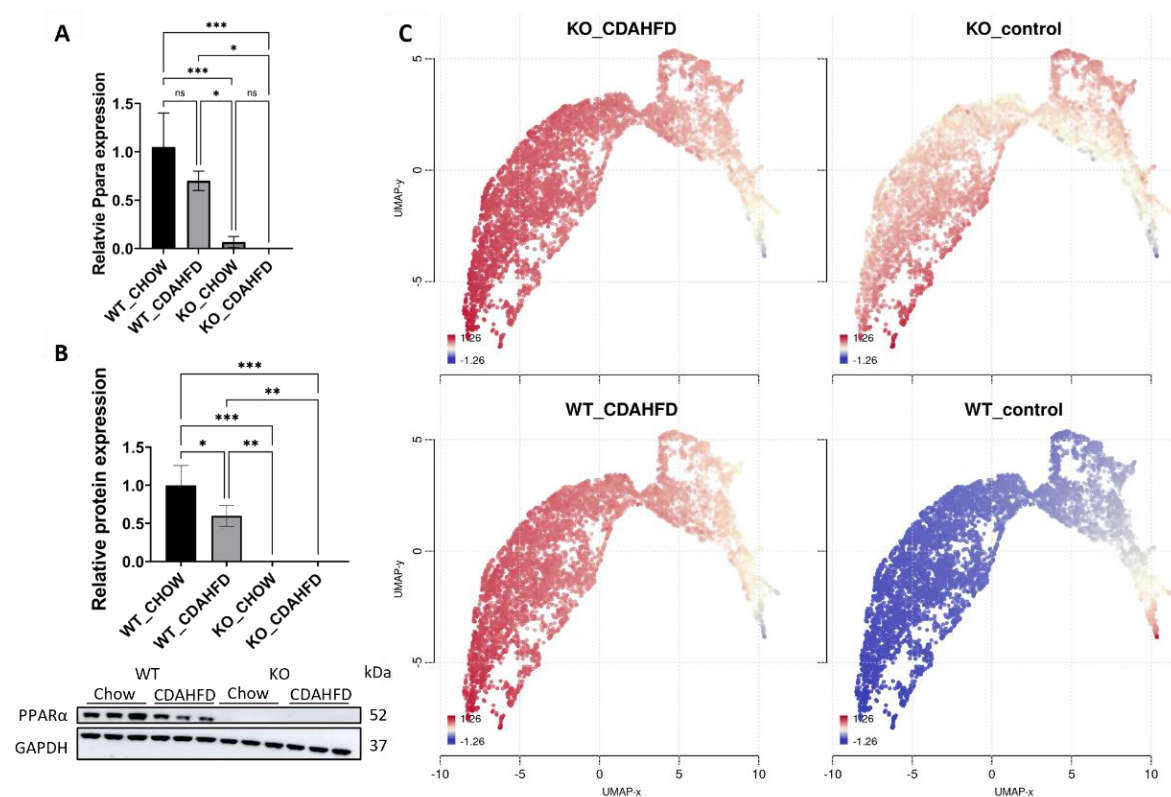
To further characterize whether these histopathological changes also correlate with a MASLD/MASH disease signature in patients, we cross compared our gene expression profiles with the publicly available MASLD/MASH transcriptome signature of liver biopsies of a patient cohort with varying degrees of MASLD (GSE126848⁵⁶) (Supplementary Table 3). The cohort consisted of 14 healthy normal-weight individuals with a body mass index of 18.5-25kg/m², 15 NAFL (old nomenclature since the study was performed before the decision to change the name of the disease) and 16 NASH patients. NAFLD was diagnosed on the basis of ultrasonographic evidence of hepatic steatosis, elevated liver enzymes, and compatible liver histology based on a liver biopsy. For all participants, exclusion criteria included diabetes and excessive alcohol intake (>20/12 g/day for men/women). Interestingly, the hepatocyte-specific PPAR α KO mouse model on both a chow and 6-week CDAHFD diet as well as WT mice after a 6-week CDAHFD diet, reveal a similar

hyperactivated MASLD/MASH transcriptome signature, which confirms the involvement of a PPAR α loss of function and disrupted fatty acid metabolism in the MASLD/MASH disease aetiology (Figure 2B). Accordingly, the MASLD/MASH heatmap of GSE126848 also phenocopies the PPAR α loss of function transcription signature of the hepatocyte-specific PPAR α KO mouse model (Figure 2C).

3.4.2 Genetic and diet-induced PPAR α loss of function trigger lipid metabolic stress by DNA hypermethylation of PPAR α target genes

Besides similarities in lipid metabolic gene expression changes between CDAHFD diet WT and chow/CDAHFD PPAR α KO mice, genetically and diet-induced PPAR α loss of function also regulate overlapping bile and fatty acid responsive transcription factors, nuclear receptors and epigenetic writer-reader-eraser proteins, including multiple DNA (hydroxy)methylating enzymes and DNA Methyl-binding factors (Figure 3A-B). For example, weakly increased RNA and protein expression levels of DNMT1 can be observed in PPAR α KO and CDAHFD diet conditions (Figure 3C-D). Remarkably, Homer motif analysis revealed that several of these differentially expressed transcription factors and DNA Methyl-binding proteins themselves contain PPAR α binding motifs (PPRE) motifs. Since these proteins can directly regulate epigenetic enzymes, these results suggest that epigenetic enzyme expression and activity too might be under lipidomic PPAR α control (Supplementary Table 5).

Since altered DNA methylation has been identified as a key determinant of MASLD pathogenesis^{21,57-61}, we next applied Infinium mouse methylation Beadchip array studies to map genome-wide DNA methylation changes in liver biopsies of WT and hepatocyte-specific PPAR α KO mice, following 6-week chow or CDAHFD diet.



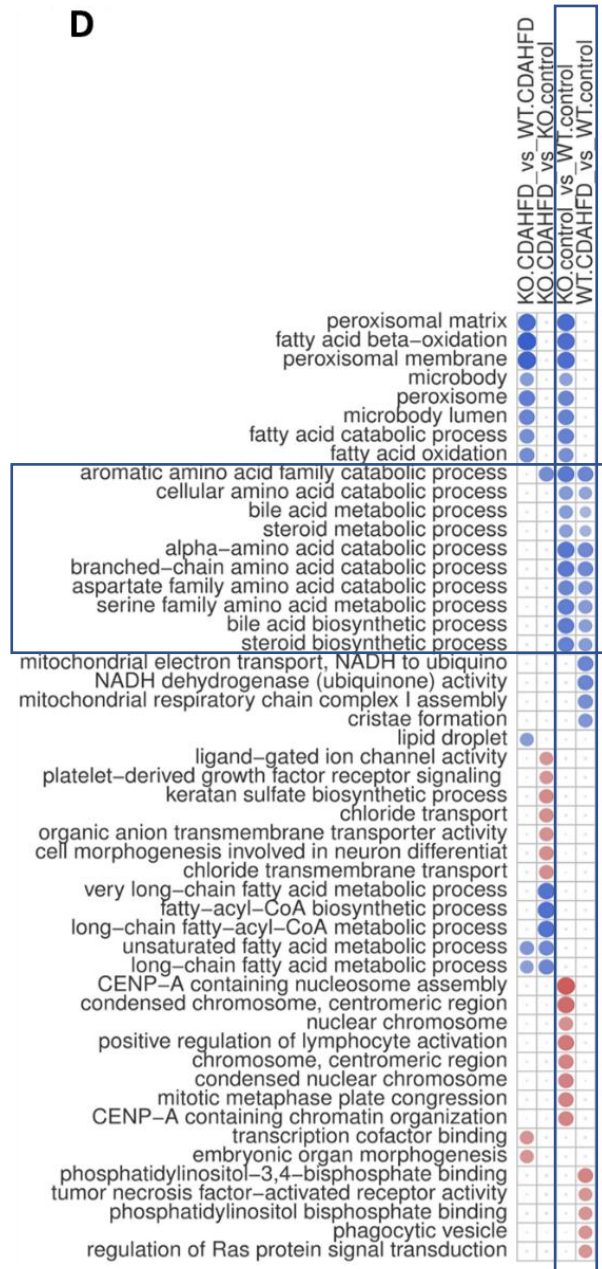
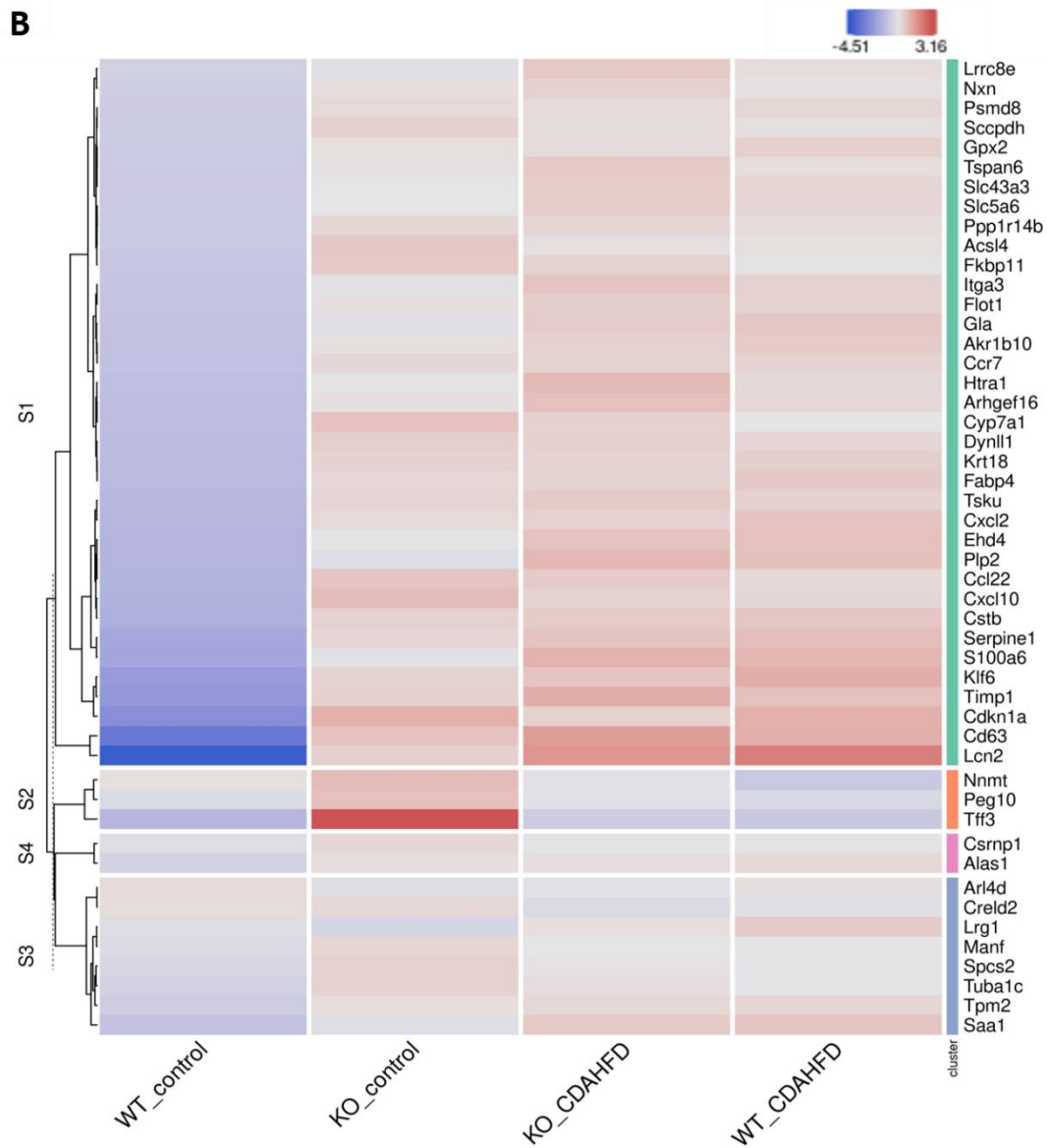
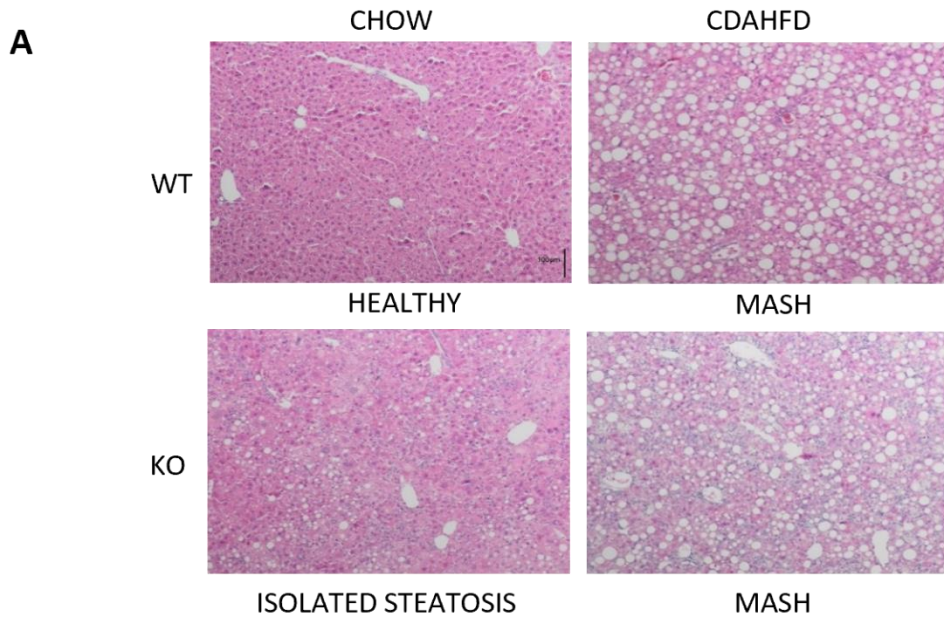


Figure 1: **A)** Relative *Ppara* mRNA expression in *PPARα* WT and KO mice after a 6-week chow or CDAHFD. **B)** Western blot detection and quantification of *PPARα* and *GAPDH* expression levels after a 6-week chow or CDAHFD in WT and KO mice. Data are plotted as the mean \pm s.d., $n=3$ biologically independent replicates. (* $p < 0.05$, ** $p < 0.01$ *** $p < 0.001$) **C)** UMAP representation of gene clustering based on geneset co-expression in *PPARα* WT and KO mice after a 6-week chow or CDAHFD **D)** GO activation matrix representation of pathway enrichment analysis of significantly up- or downregulated pathways in both comparisons of KO mice versus WT mice on a chow or CDAHFD respectively. The size of the circles in the GO activation matrix corresponds to their relative activation, and are coloured according to their upregulation (red) or downregulation (blue) in the contrast profile ($meta.q < 0.05$).



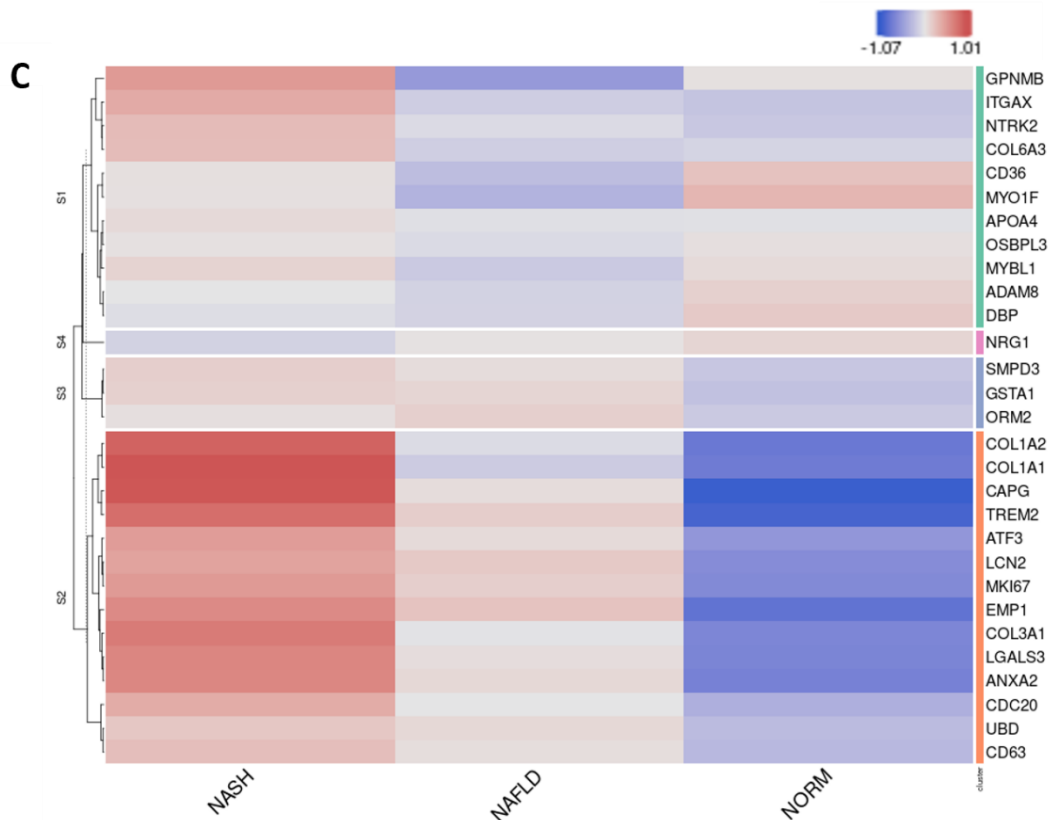
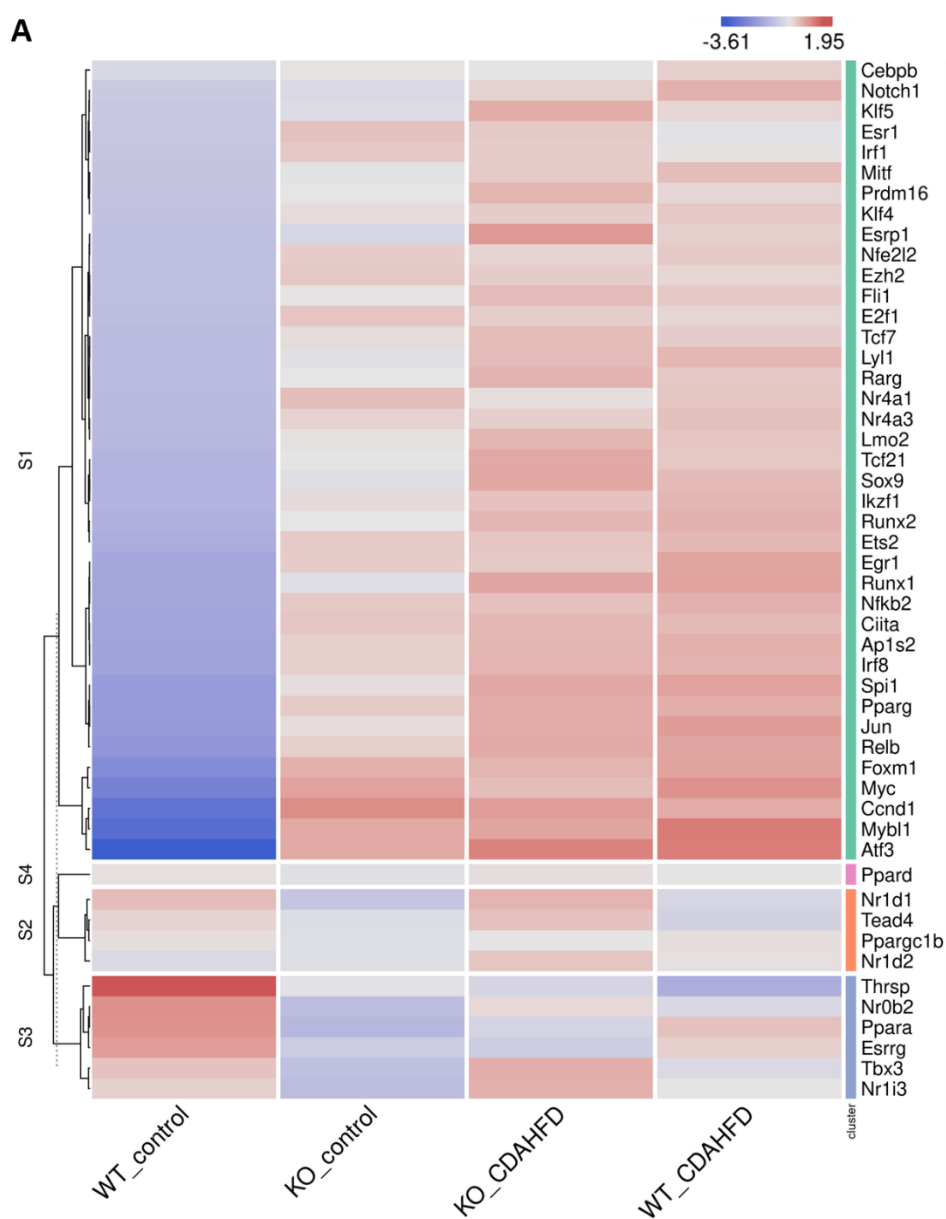


Figure 2: **A)** H&E staining of liver sections of WT and hepatocyte PPAR α KO mice after following 6-week chow or CDAHFD **B)** Heatmap representation of MASLD signature in KO or WT mice after 6-week chow or CDAHFD (n=3). **C)** Heatmap representation of PPAR α KO signature in MASLD (NAFLD) and MASH (NASH) patients of the GEO dataset GSE126848

As shown in Figure 4, the WT mice on a CDAHFD show predominant hypermethylation of the promoter region and gene body of PPAR α compared to the WT mice on a chow diet, which could explain the gradual silencing of PPAR α expression following a 6-week CDAHFD diet (Supplementary Figure 2). Besides, both genetically and diet-induced PPAR α loss of function trigger massive - partially redundant - DNA methylation changes in genes involved in fatty acid and bile acid metabolism, nuclear hormone (steroid) receptor and inflammatory cytokine pathways, according to Metascape enrichment analysis⁵³ (Figure 5A-B). Remarkably, TRRUST motif analysis of hypermethylated genes in PPAR α KO mice shows highly significant enrichment of PPRE (Figure 5C), which is still significantly enriched in WT CDAHFD mice which only partially express PPAR α protein (Figure 5D). Along the same line, the cross-comparison of a list of PPAR α target genes (Supplementary Table 4) with our lists of differentially methylated genes, identified various common hypermethylated target genes in the PPAR α KO mice, following chow or CDAHFD diet, whereas CDAHFD diet in WT liver cells with partially decreased PPAR α expression shows a mixed hypo/hypermethylation pattern (Supplementary Figure 3). Although most of the selected hypermethylated genes involved in fatty acid or bile acid metabolism, including PPAR α metabolic target genes, are downregulated in the hepatocyte-specific PPAR α KO mice and WT mice on a CDAHFD with a partial expression of PPAR α , few genes are upregulated (Figure 5E). Of special note, bisulfite converted DNA assay does not allow discrimination between DNA methylation and hydroxymethylation changes that have been associated with gene silencing and gene activation

responses respectively. Indeed, PPAR α regulatory functions have recently been described for both DNA methylation as well as hydroxymethylation and may need a more detailed in-depth molecular investigation⁶².

To further validate our epic array hypermethylation data, we applied bisulfite pyrosequencing of PPAR α target genes *RETSAT* and *Eci1*, which are according to the EPIC data both hypermethylated by a diet-induced or genetic KO of PPAR α (delta beta KO_chow vs WT_chow: 0,48-0,29; KO_CDAHFD vs WT_CDAHFD: 0,17-0,14; WT_CDAHFD vs WT_chow: 0,31 -0,18). Moreover, these genes are involved in retinol metabolism and beta oxidation respectively and thereby control lipid metabolism^{63,64}. As shown in Figure 5F relative DNA methylation is strongly increased when PPAR α is knocked out, or modestly increased upon CDAHFD diet in WT mice with partially decreased PPAR α expression. These results suggest that PPAR α targeting of lipid metabolic genes may be essential to protect against epigenetic DNA methylation modifications.



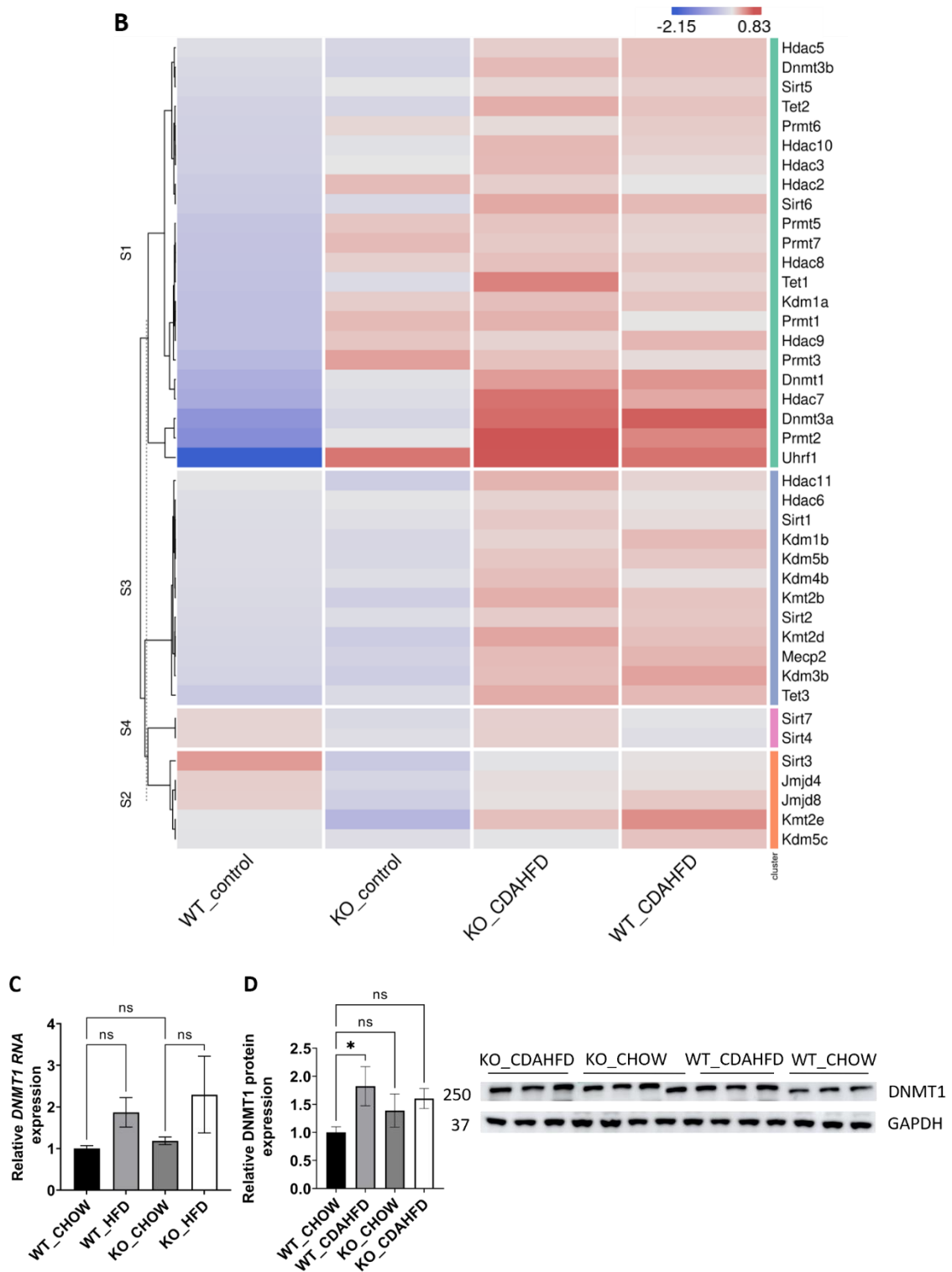


Figure 3: Heatmap representation of differentially expressed **A**) transcription factors and nuclear receptors or **B**) epigenetic writers-readers-eraser proteins in KO or WT mice after 6-week chow or CDAHFD ($n=3$). **C**) qPCR and **D**) western blot detection and quantification of DNMT1 and GAPDH expression levels after 6-week chow or CDAHFD in WT and KO mice. Data are plotted as the mean \pm s.d., $n=3$ biologically independent replicates. (ns $p > 0.05$, * $p < 0.05$, ** $p < 0.01$ *** $p < 0.001$)

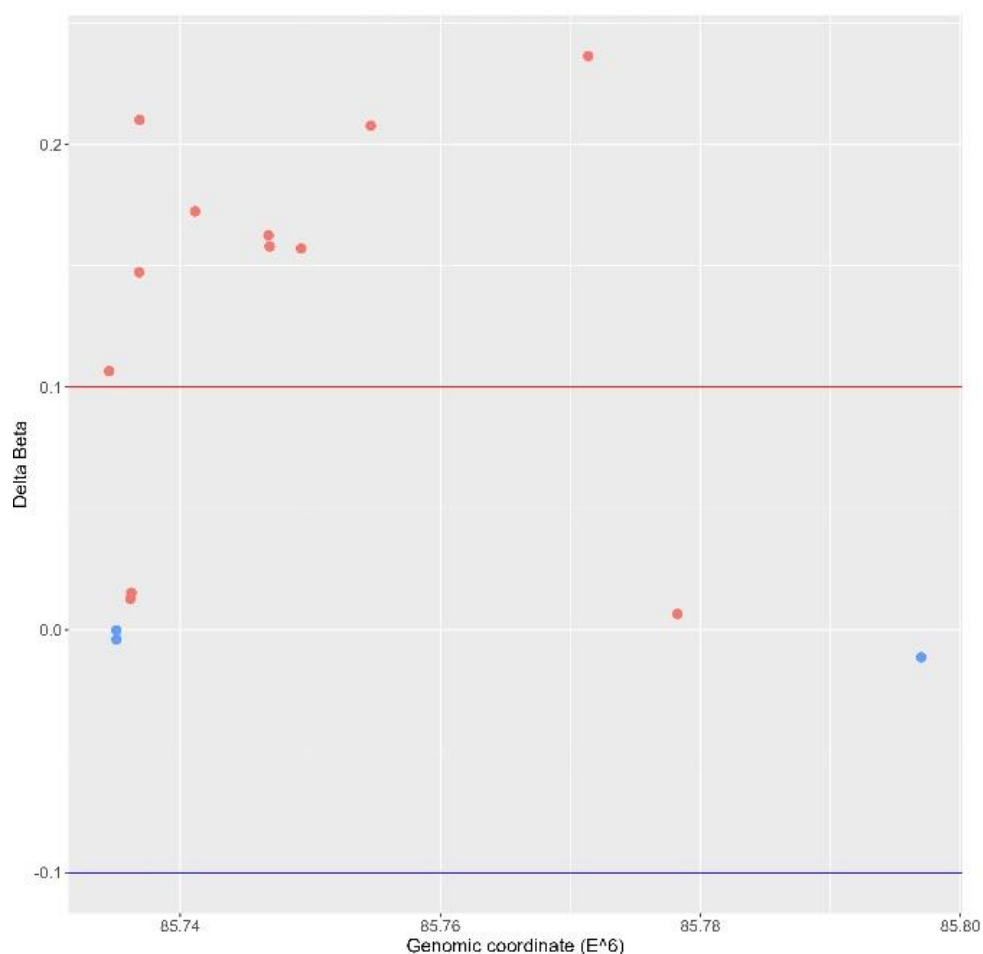


Figure 4: Genomic scatterplot of delta beta values of hypo-(blue) and hypermethylated (red) probes in the promoter region of the $PPAR\alpha$ gene in the WT group on a 6-week CDAHFD compared to the WT mice on 6-week chow diet. The red and blue line define the delta beta cut-off for biologically relevant hyper- or hypomethylation, respectively.

Furthermore, these results could also be confirmed in Epic Beadchip DNA methylation array data of MASLD liver biopsies of MASH patients (n=2 males and 3 females) (GSE241366) with histologically confirmed advanced fibrosis in comparison to healthy tissue controls (n=3 females), which reveal similar enrichment of differentially methylated genes involved in lipid metabolism (fatty acid, bile acid) with $PPAR\alpha$ as one of the top enriched TF motifs in general (Figure 6A) and especially of the hypermethylated genes (p -value < 0.05) (Figure 6B). Altogether this suggests that $PPAR\alpha$ protects against epigenetic DNA (hyper)methylation of lipid metabolic genes involved in the progression of MASLD.

Of special note, in line with the fact that $PPAR\alpha$ can also indirectly regulate genes via transrepression of other bound transcription factors such as $NF\kappa B^{65-67}$, we also observe multiple epigenetic changes of $NF\kappa B$ -driven (XBP1, $NF\kappa B1$, RelA) inflammatory target genes in the mouse/patient samples, which may further contribute to lipid-inflammation tissue damage in MASLD (Figure 5C, 6A-B).

3.4.3 Genetic and diet-induced PPAR α loss of function triggers epigenetic transition from lipid metabolic homeostasis to lipotoxic ferroptosis and pyroptosis in MASLD

Lipotoxic hepatocyte injury is a primary event in MASH, characterized by excess triglyceride accumulation stored as lipid droplets in the cytosol of hepatocytes, which is deemed the first stage of MASLD. Hepatic steatosis may further develop into MASH, fibrosis, cirrhosis and eventually hepatocellular carcinoma without timely interventions. Recent evidence suggests that hepatic ferroptosis and pyroptosis play an important role in this lipotoxic pathological progression of MASLD⁶⁸⁻⁷¹.

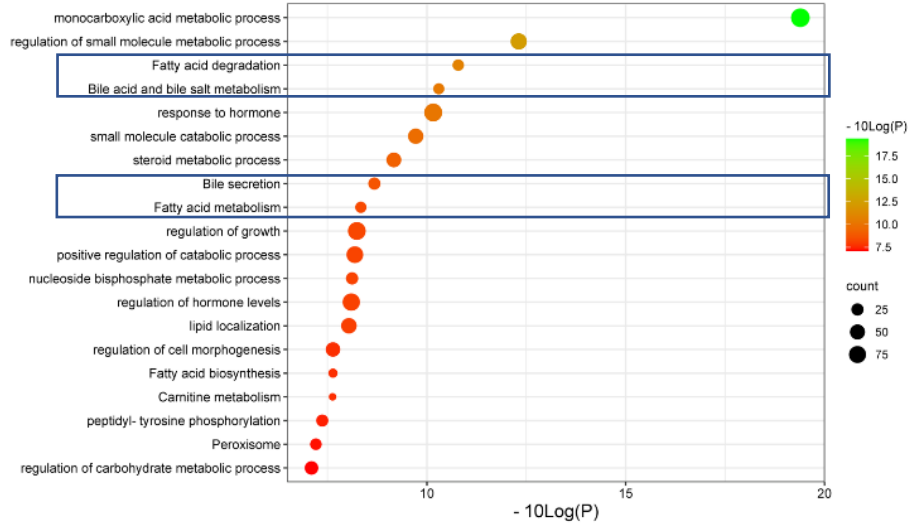
Ferroptosis, a recently recognized nonapoptotic form of regulated cell death that is characterized by iron-dependent lipid peroxidation, was recently confirmed to be the initial cell death process that triggers MASH^{69,70,72} (Supplementary Figure 4). Besides, new results identify hepatocyte pyroptosis and release of NOD-like receptor family pyrin domain containing 3 (NLRP3) inflammasome components as an additional mechanism to propagate liver injury and liver fibrosis development in MASH progression⁷³⁻⁷⁶ (Supplementary Figure 5). As the liver is a “first pass” organ, continually challenged with diverse microbial particles from the intestine as well as endogenous metabolic stress signals (fatty acid, bile acid), hepatocytes are capable of undergoing NLRP3-mediated pyroptotic cell death and release extracellular NLRP3 inflammasome complexes into the extracellular space. These extracellular inflammasomes can be internalized by hepatic stellate cells leading to their activation and subsequent liver fibrogenesis^{71,74,77-79}.

To evaluate whether PPAR α loss may impact ferroptosis/pyroptosis pathways in MASLD/MASH, we next performed a cross comparison of our gene expression mouse data with publicly available ferroptosis/pyroptosis RNAseq based transcriptome datasets⁸⁰⁻⁸⁶. Remarkably, both genetic and diet-induced PPAR α loss reveal strong hyperactivation of lipotoxic ferroptosis/pyroptosis signatures (Figure 7). Indeed, further protein level analysis confirmed a significant upregulation of the nuclear factor E2 related factor 2 (Nrf2/NFE2L2), a key regulator of the ferroptosis^{87,88} and pyroptosis⁸⁹ pathways, in PPAR α KO mice on chow diet and WT or KO mice on CDAHFD diet (Figure 8). Moreover, a significant upregulation of malondialdehyde (MDA), which represents increased lipid peroxidation, was found under a CDAHFD in both the KO and WT mice, in line with observations in MASLD/MASH patient samples⁶⁹. Furthermore, protein validation of Caspase 1 and NLRP3 showed that a genetic and diet-induced PPAR α loss induce an upregulation of NLRP3. However Caspase 1 is not further cleaved in its catalytic domains p10 and p20, indicating that PPAR α loss increases sensitivity for pyroptosis without inducing further pyroptotic cell death. Of special note, when cross comparing differentially methylated target genes of advanced MASH (versus healthy liver biopsies), with both ferroptosis/pyroptosis genesets, we could identify various novel epigenetic biomarkers of ferroptosis/pyroptosis lipotoxicity (Figure 9, Supplementary Table 6).

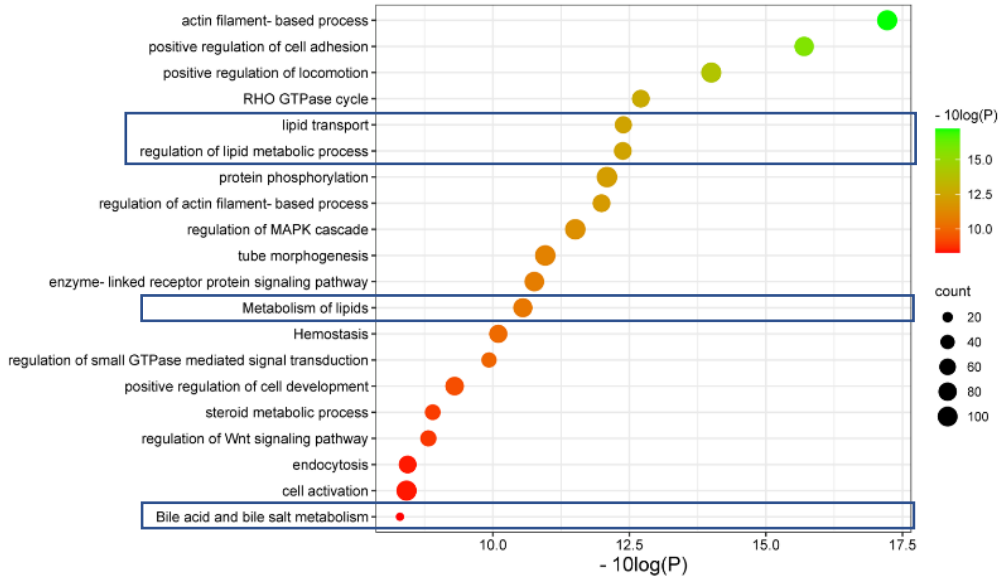
Altogether, these results suggest that PPAR α function is essential to prevent the epigenetic transition from lipid homeostasis to MASH/MASLD lipotoxicity. In addition, epigenetic ferroptosis/pyroptosis biomarkers might hold promise as new precision medicine tools in MASLD/MASH disease management and patient stratification of lipotoxic liver damage.

Results: Chapter 3

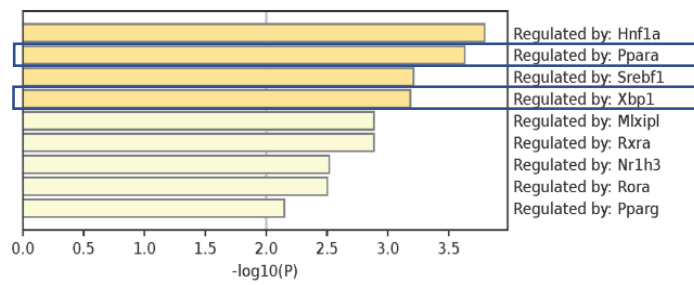
A



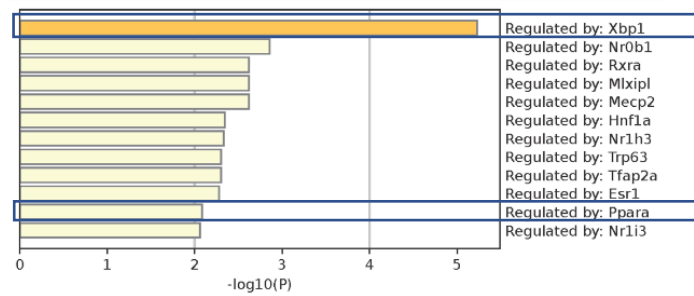
B



C



D



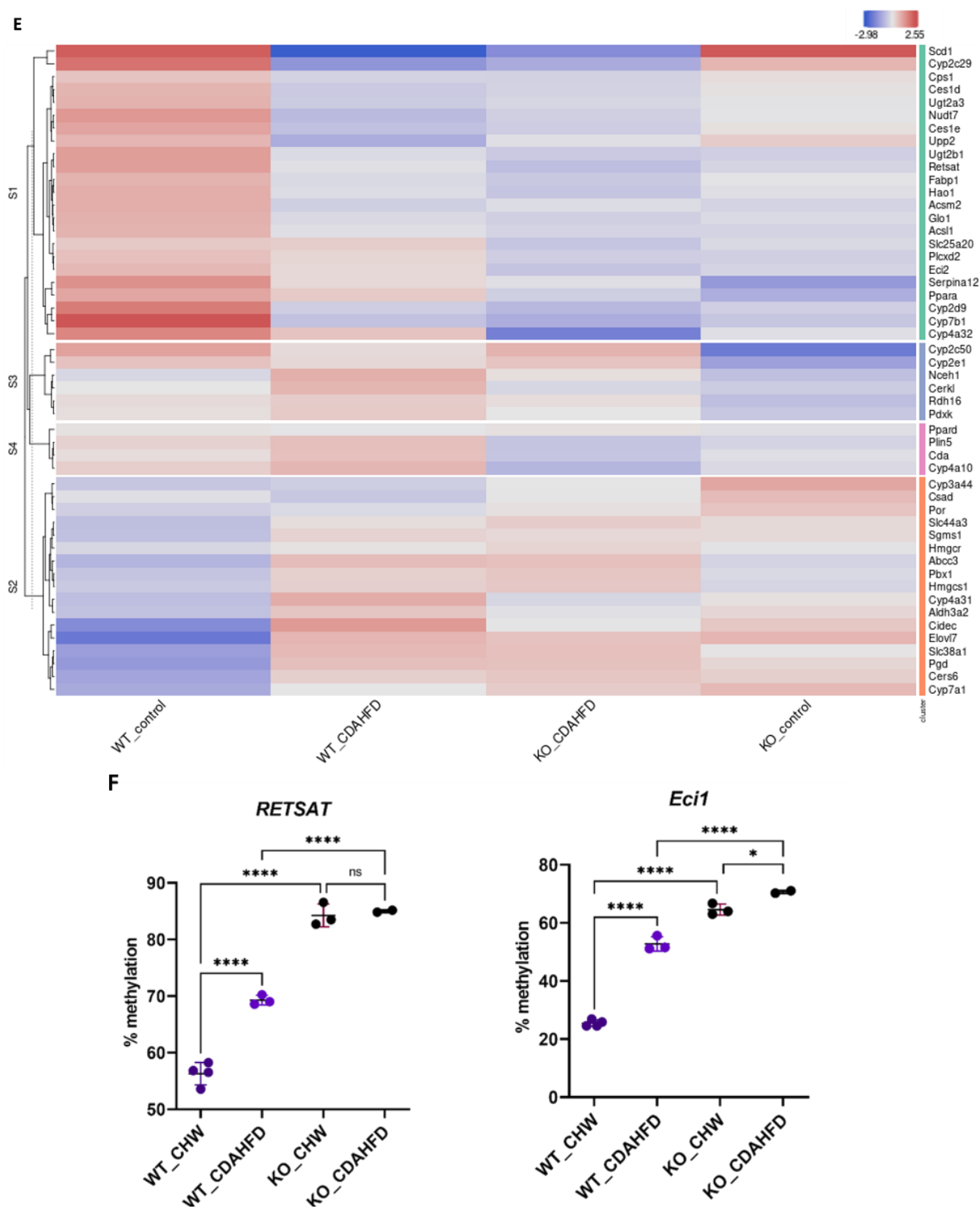


Figure 5: Metascope pathway analysis of differentially methylated genes in **A**) KO mice compared to WT mice on a chow diet ($FDR < 0.05$; $DB > 0.15$) and **B**) WT mice on a CDAHFD compared to a chow diet ($FDR < 0.05$; $DB > 0.25$). TRRUST transcription factor analysis of differentially hypermethylated genes in **C**) KO mice compared to WT mice on a chow diet ($FDR < 0.05$; $DB > 0.15$) **D**) WT mice on a CDAHFD compared to a chow diet ($FDR < 0.05$; $DB > 0.25$). **E**) Heatmap representation of the expression of genes involved in lipid or bile acid metabolic pathways that are hypermethylated in WT mice on a CDAHFD and KO mice on a control chow diet compared to WT mice on a control chow diet. **F**) Pyrosequencing validation of two PPARα target genes (ns $p > 0.05$, * $p < 0.05$, **** $p < 0.0001$).

Results: Chapter 3

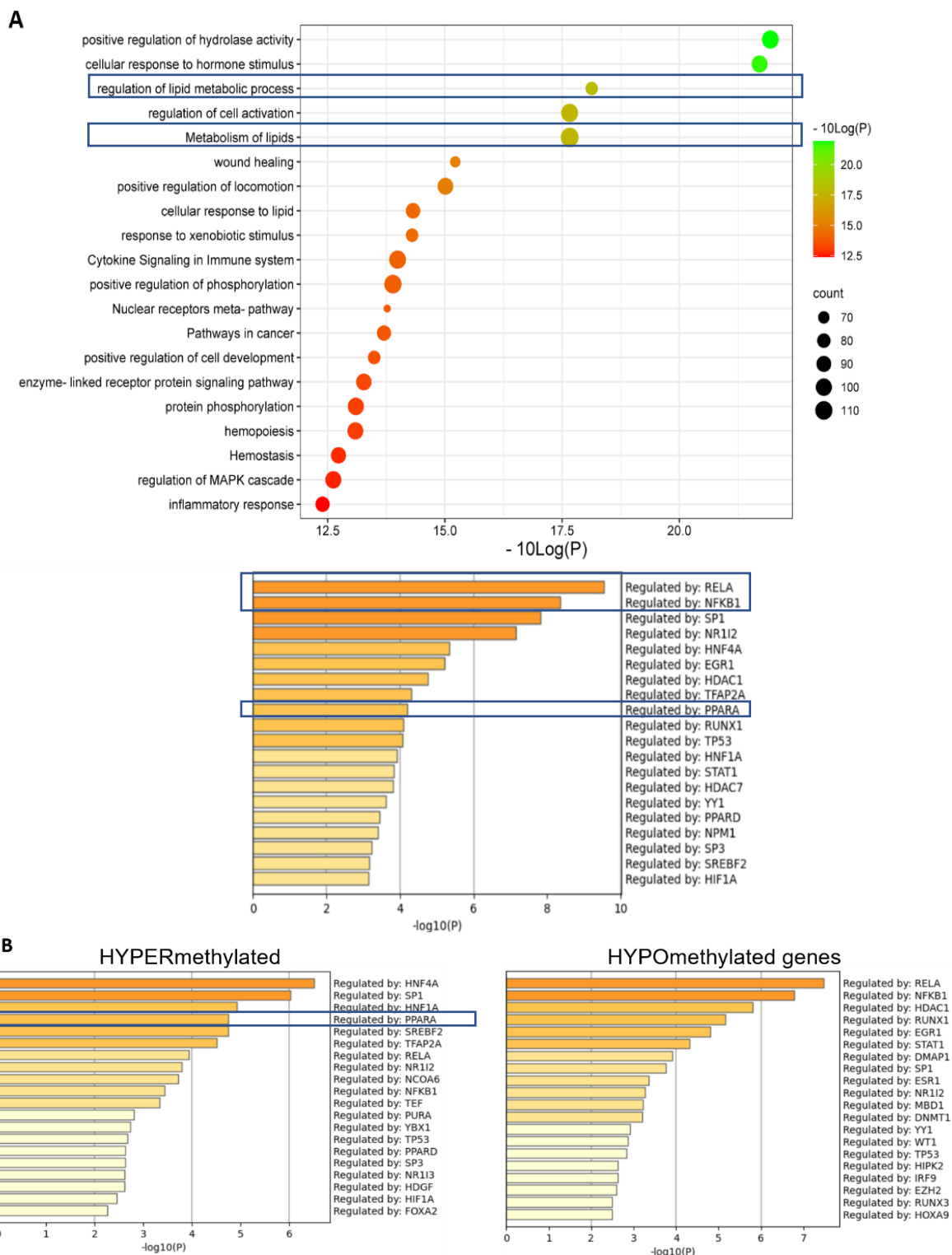


Figure 6: **A**) Metascape pathway analysis (top) and TRRUST transcription factor analysis (bottom) of significant differentially methylated genes in MASH patients with advanced fibrosis versus healthy individuals **B**) TRRUST transcription factor analysis of significant hypermethylated and hypomethylated genes in MASH patients with advanced fibrosis versus healthy individuals. (p -value < 0.05 ; $DB < |0.3|$).

Results: Chapter 3

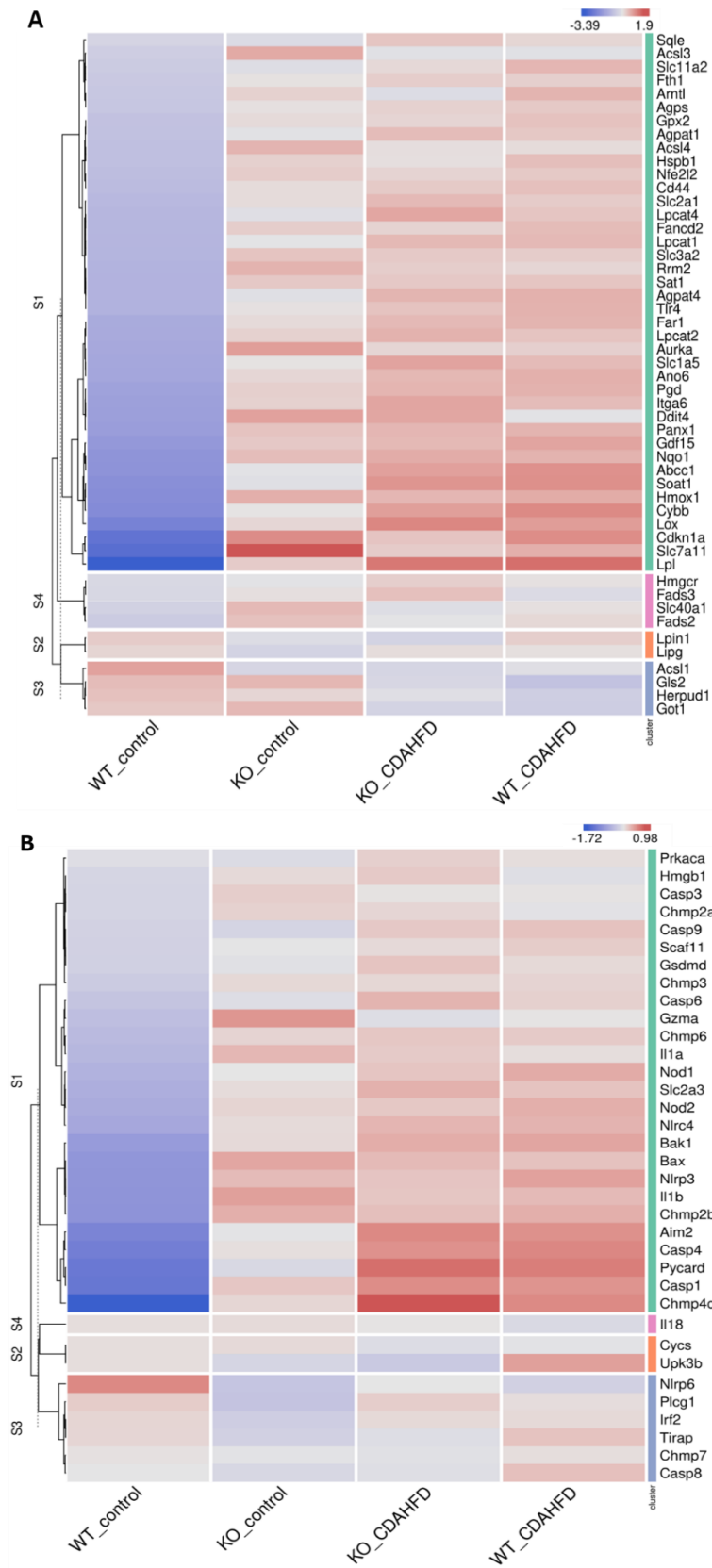


Figure 7: Heatmap representation of **A)** ferroptosis and **B)** pyroptosis signature in WT or PPAR α KO mice on a 6-week chow or CDAHFD.

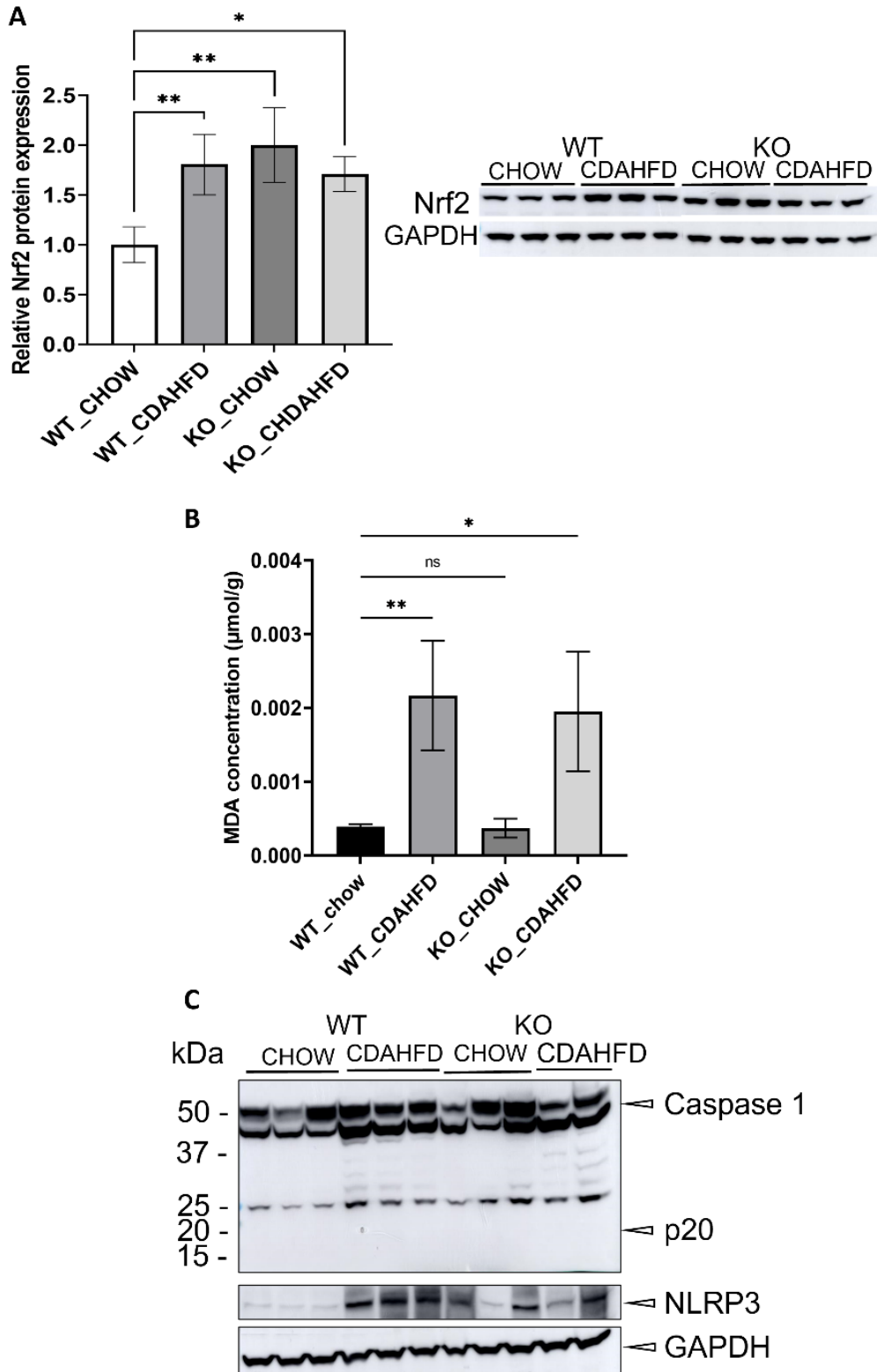


Figure 8: A) Western blot detection and quantification of NRF2 and GAPDH protein expression levels and B) MDA concentration in liver samples of WT and KO mice after a 6-week chow or CDAHFD C) Western blot detection of Caspase 1, NLRP3 and GAPDH in WT and KO mice after a 6-week chow or CDAHFD. Data are plotted as the mean \pm s.d (ns $p > 0.05$, * $p < 0.05$, ** $p < 0.01$ *** $p < 0.001$).

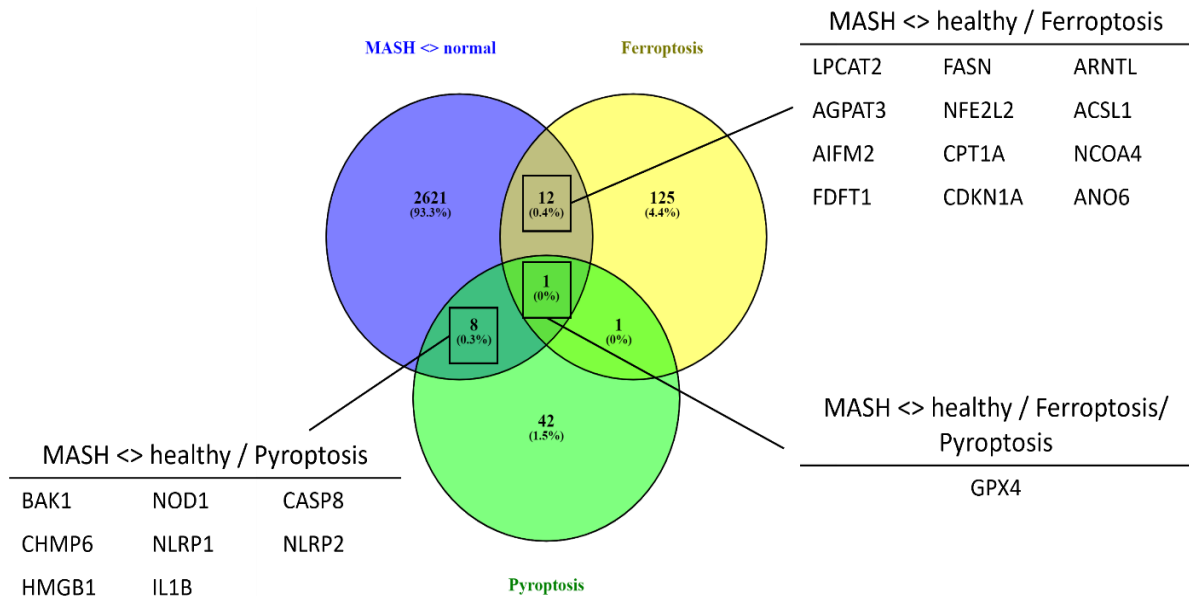


Figure 9: Venn diagram showing the overlap between significant differentially methylated genes in MASH patients compared to normal liver controls and a ferroptosis or pyroptosis signature (p -value <0.05 , $DB > |0.3|$).

3.5 Discussion

The nuclear receptor PPAR α is a critical regulator of lipid metabolism and MASLD progression. Surprisingly, PPAR α ligands have only shown limited therapeutic benefits against MASLD in (pre)clinical trial studies^{32,34,35}. Of special note, recent evidence suggests a possible involvement of epigenetic silencing mechanisms in PPAR α functions in MASLD progression which may counteract therapeutic actions of PPAR ligands⁶². In this respect, to further characterise reciprocal crosstalk of epigenetic regulatory mechanisms with PPAR α functions in lipid metabolism and MASLD progression, we have cross compared DNA methylation and gene expression patterns of chow or CDAHFD hepatocyte-specific PPAR α KO mice versus liver biopsies of MASLD/MASH patient samples.

Upon comparing gene expression changes of liver biopsies of hepatocyte-specific PPAR α KO mice versus WT mice following 6-week chow diet, or WT mice following 6-week CDAHFD, we observed strong similarities in transcriptome signatures with the CDAHFD WT mice. This reveals that CDAHFD phenocopies to some extent a genetic KO of PPAR α liver functions. QPCR and western blot analysis of PPAR α expression indeed confirmed a lack of PPAR α protein expression, whereas CDAHFD revealed significantly decreased PPAR α expression as compared to chow diet fed WT mice. Moreover, in line with the gene expression profiles in mice, publicly available gene expression datasets of liver biopsies of MASLD/MASH patients show high similarities with the PPAR α KO transcriptome signature, which reveals loss of PPAR α function in these patients. This is in line with reduced PPAR α expression levels which have been observed in MASH/MASLD patients²³. Reciprocally, we observed that transcriptome profiles of CDAHFD fed WT and PPAR α KO mice also show high similarity to a MASLD/MASH patient signature, which suggests that CDAHFD fed WT and PPAR α KO mice are clinically relevant mouse models for molecular biochemical investigation of MASH/MASLD disease. In line with these results, histological staining of liver biopsies confirmed increased frequency of lipid droplets in chow fed PPAR α KO mice (stage 2, isolated steatosis), as

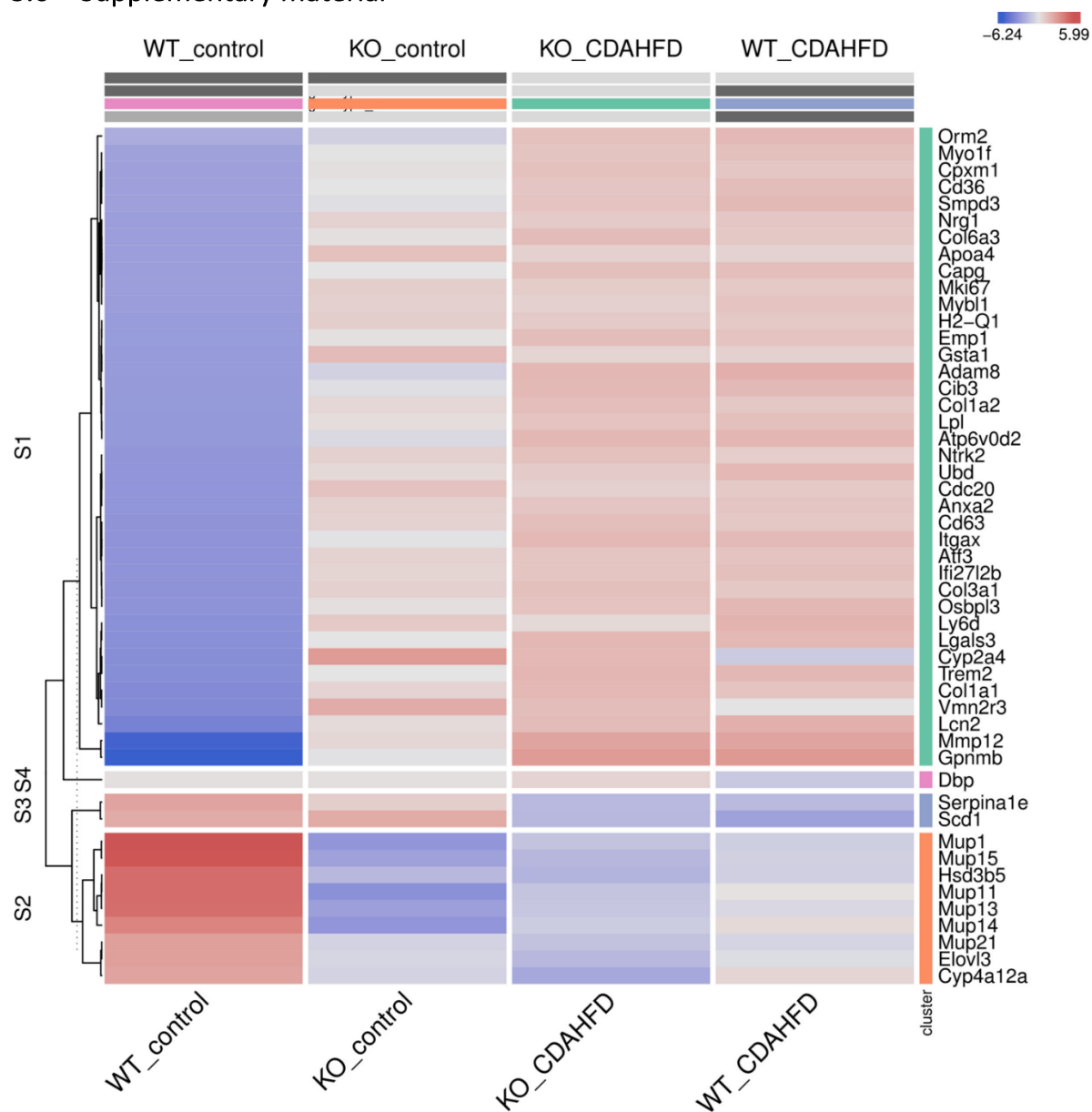
well as inflammatory ballooning and fibrosis properties in CDAHFD fed PPAR α KO/WT mice (stage 3, MASH). These results also confirm the data of Matsumoto *et al.* who has previously shown that a CDAHFD can induce MASH with fibrosis in mice in 6-week time, which is relatively fast compared to classical HFD used to induce MASLD in mice⁹⁰. By studying this mouse model, we were able to functionally characterize epigenetic driver and passenger functions of PPAR α in lipid metabolism in relation to MASLD/MASH, which has not been addressed before.

Remarkably, diet and genetic PPAR α knockout mice elicit similar transcriptional activation of multiple transcription factors, steroid hormone receptors and epigenetic factors involved in metabolic stress responses in the liver (Figure 3A-B). This is not completely unexpected, since loss of hepatocyte PPAR α function results in loss of lipid metabolism homeostasis due to impaired fatty acid, bile acid and amino acid catabolic processes (Figure 1D) which results in major changes in the lipidome composition⁹¹. Accordingly, multiple compensation mechanisms of lipid sensing transcription factors and nuclear hormone receptors (Myc, NR4A1, NR4A3, PPAR δ/γ , E2F1, PPARGC1B, Nrf2/NFE2L2, TCF21) are activated to mitigate lipidomic stress and to alleviate mitochondrial metabolic stress⁹²⁻¹⁰⁰. Similarly, expression of various epigenetic factors (DNMT, TET, SIRT, HDAC, Uhrf1) changes upon lipid metabolic inflammatory stress¹⁰¹⁻¹⁰⁸, some of which contain PPRE motifs in their gene promoters (Supplementary Table 5). Although the full mechanism has not been resolved, it appears that there is reciprocal regulation between PPAR α protein levels versus expression of DNMT, TET and other DNA-methyl binding proteins such as Uhrf1¹⁰⁹⁻¹¹¹. Moreover, besides transcriptional control mechanisms, PPAR α -dependent β -oxidation also promotes (mitochondrial) protein hyperacetylation via increased acetyl-coA production, which can change protein function, localisation, interaction and/or stability¹¹².

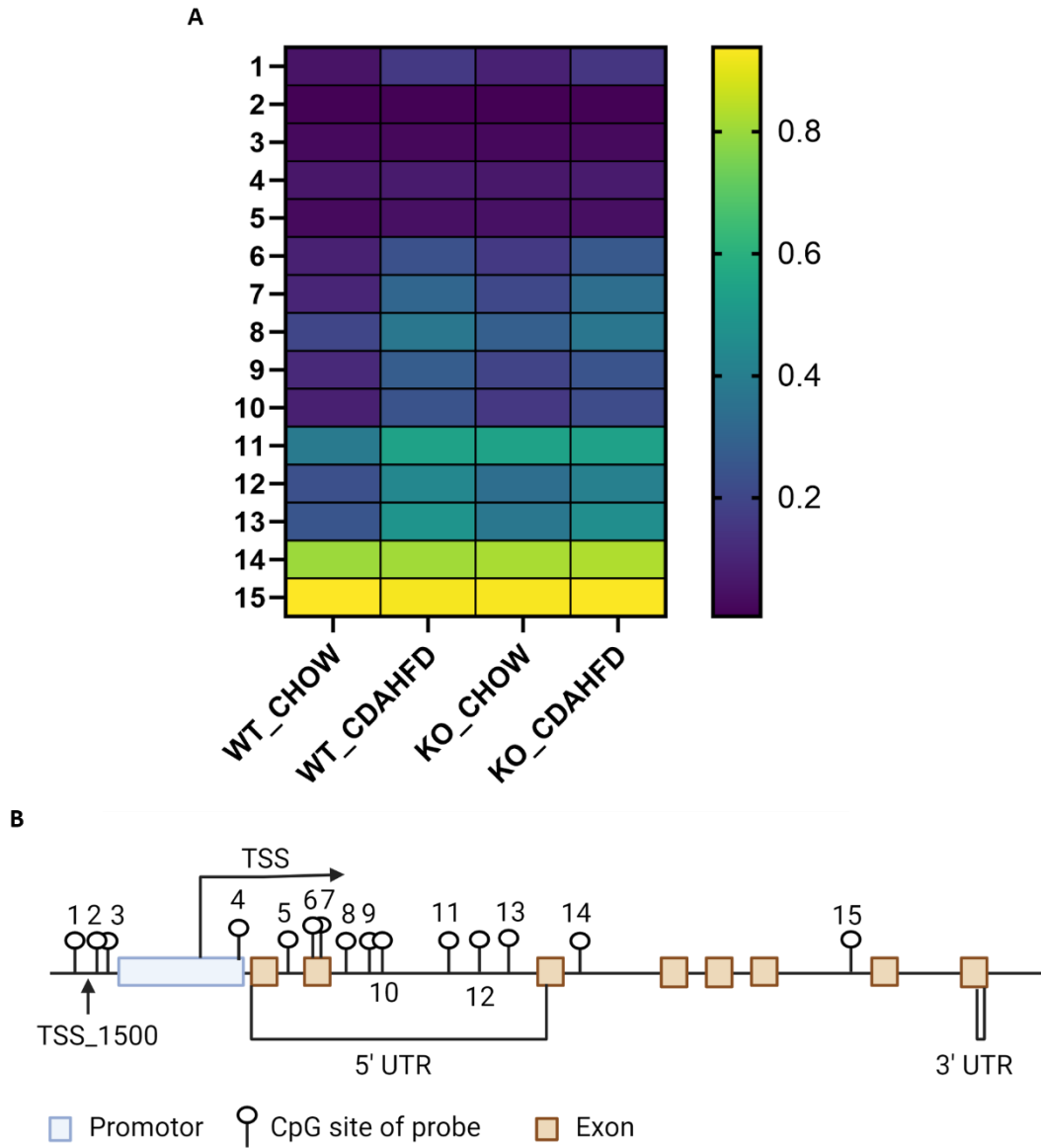
Not surprisingly, diet and genetic loss of PPAR α hepatocyte function trigger massive DNA methylation changes of multiple genes associated with fatty acid, bile acid and steroid hormone receptor pathways, including PPAR α , which changes the expression of multiple lipid metabolic genes (Figure 5). Since bisulfite sequencing does not discriminate between DNA methylation and hydroxymethylation changes, epigenetic changes trigger mixed metabolic gene silencing-activation effects involved in lipid metabolism and MASLD (RETSAT, FABP1, Eci1/2, Cyp7a1)¹¹³⁻¹¹⁸. Moreover, epigenetic changes following loss of PPAR α functions seem to fail to mitigate liver metabolic dysfunctions (autophagy, mitophagy, lipophagy), since downstream gene expression profiles and key regulatory proteins of ferroptosis and pyroptosis lipotoxicity pathways are highly enriched (Figure 7-8). Indeed, liver overload of fatty acid and bile acid metabolites promotes lipid peroxidation ferroptosis damage and sensitizes for inflammation-induced steatosis-pyroptosis (Figure 8), which can finally trigger liver fibrosis and cirrhosis or hepatocellular carcinoma^{68-71,74,119,120}. Accordingly, we identified various epigenetic changes in ferroptosis-pyroptosis target genes in liver biopsies of late-stage MASLD/MASH patients, which could hold promise as novel stochastic biomarkers of lipid-related inflammatory liver damage (Figure 9, Supplementary Table 6), besides fibrosis stage^{121,122} or epigenetic clock age^{123,124}. Interestingly, PPAR α was recently shown to protect against liver ferroptosis and might further suppress pathological progression into liver pyroptosis-fibrosis-cirrhosis¹²⁵⁻¹²⁸. Of special note, PPAR α DNA-binding was demonstrated to the Gpx4 promoter by ChIP experiments¹²⁹. These findings suggest that ferroptosis inhibitors and epigenetic drug combination therapies with PPAR ligands could hold promise to treat MASLD/MASH.

In conclusion, we demonstrate that loss of PPAR α function promotes epigenetic dysregulation of lipid homeostasis, driving ferroptosis and pyroptosis lipotoxicity in MASLD. Of special note, loss of function of a single lipid metabolic PPAR α hub seems to cause a lipidomic shockwave of gene expression changes of lipid sensing transcription factors and epigenetic enzymes, which fail to mitigate lipid metabolic stress and trigger epigenetic transition towards lipid hepatotoxicity driving fibrosis. This may explain why monotargeted therapeutic strategies in MASLD/MASH may not be effective to “cure” the multi-factorial nature of MASLD involving genetic predisposition, environmental factors (lifestyle, diet), insulin resistance, disordered lipid metabolism, mitochondrial dysfunction, lipotoxicity, hyperinflammation, oxidative stress, etc. This urges for applying integrative multi-omics systems biology approaches (incorporating data on genetic variants, epigenetic phenomena (*i.e.* DNA methylation, histone modifications and long non-coding RNA affecting gene expression), gut microbiota dysbiosis, and metabolomics/lipidomic fingerprints) to gain a deeper understanding of the molecular and physiological processes underlying MASLD pathogenesis and phenotype heterogeneity, as well as facilitating the further identification of lipidome-associated epigenetic biomarkers of disease progression and therapeutic targets for the implementation of tailored nutritional strategies^{130–134}. In this respect, besides pharmaceutical combination therapies, diet interventions and herbal phytomedicinal therapies may also have a role to play in the treatment of MASLD, due to their numerous bioactive constituents and the multiple pharmacological actions they exhibit^{134–136}. Finally, to capture a full understanding of adverse MASLD epigenome dysregulation, it will be mandatory to also integrate the complex epi-lipidomic post-translational modification landscape of transcription factors, histones and epigenetic modifiers which control the lipid metabolic network signalling activities in MASLD progression^{137–144}.

3.6 Supplementary material



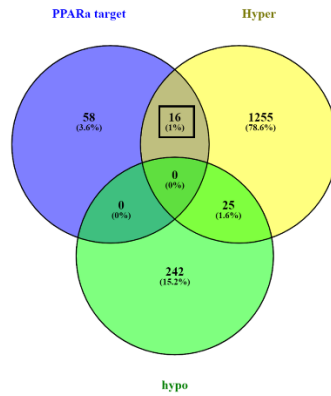
Supplementary figure 1: Heatmap representation of differentially expressed genes in WT or PPAR α KO mice on a 6-week chow or CDAHFD showing a similar expression in genes induced by a diet induced downregulation or KO of PPAR α .



Supplementary figure 2: **A)** Heatmap representing the different *b*-values of each probe (numbered 1-15) in the *PPARα* gene on the Infinium Mouse Methylation BeadChip array in the WT or *PPARα* KO mice on a 6-week chow or CDAHFD, showing a gradual methylation increase of several CpGs by the loss of *PPARα* and diet. **B)** Schematic overview of the *PPARα* gene with the location of each CpG on the different methylation probes.

Results: Chapter 3

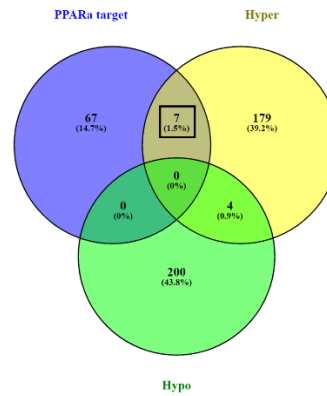
KO_CHW vs. WT_CHW



PPAR α target/ Hyper

CPT1A	CPT2	ECI1	PEX11A
FASN	ACACA	ME1	FGF21
CYP1A1	CPT1B	SLC25A20	CYP27A1
RETSAT	CYP7A1	FADS2	ACOX1

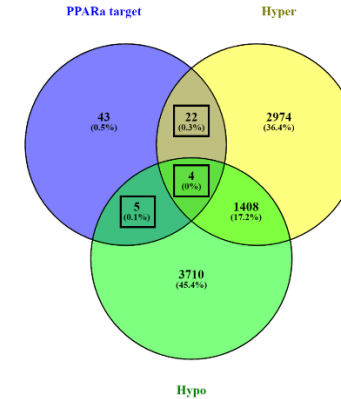
KO_CDAHFD vs. WT_CDAHFD



PPAR α target/ Hyper

CPT2	ECI1	PEX11A	CPT1B
CYP1A1	FADS2	RETSAT	

WT_CDAHFD vs. WT_CHW



PPAR α target/ Hyper

SLC10A2	AP2A2	SULT2A1	CPT2	ECI1
HMGCS2	LPIN2	ACACA	FASN	CYP8B1
APOA1	APOA2	APOA5	APOC3	SLC25A20
SLC29A1	UGDH	ACOX1	GPT	PDZK1
CYP7A1	RETSAT			

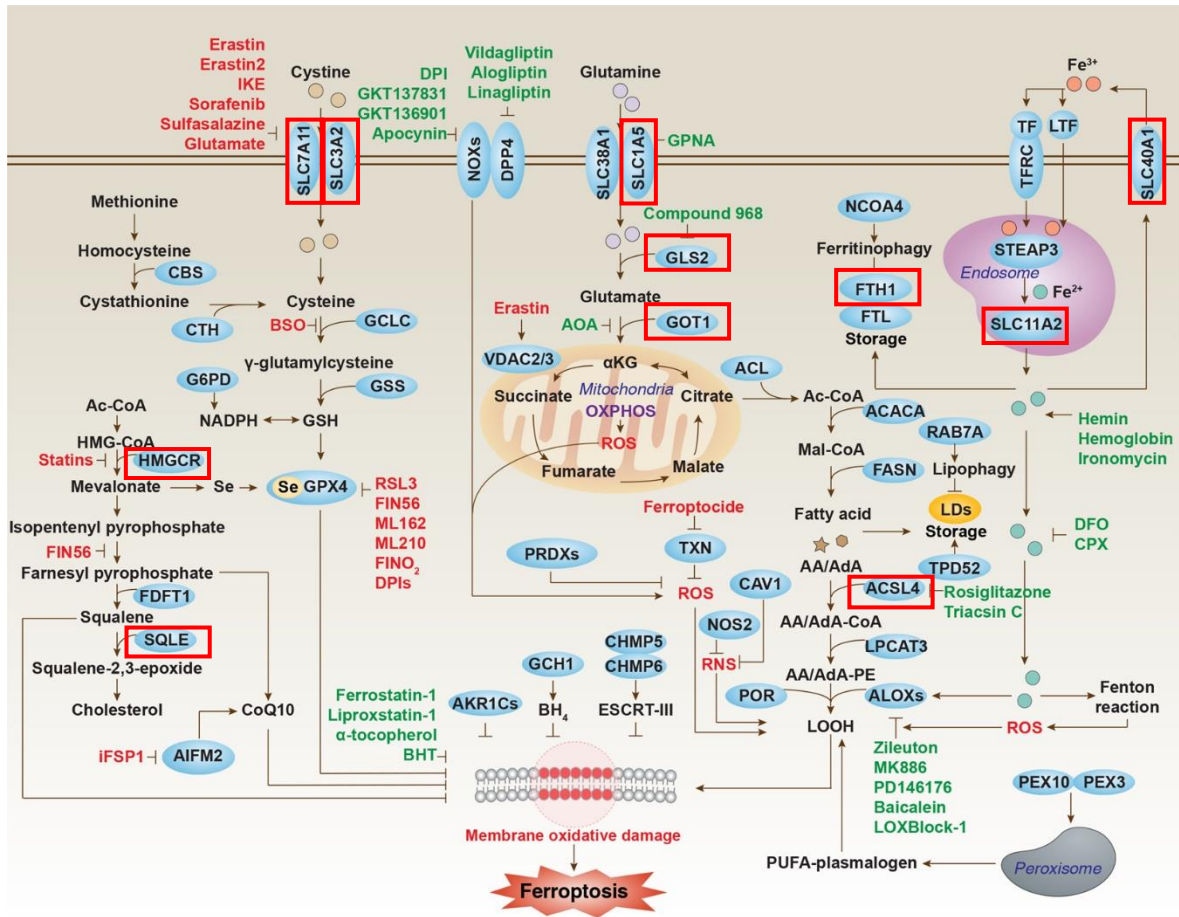
PPAR α target/ Hypo

FGF21	ME1	UCP3	KLF10	MAP3K8
-------	-----	------	-------	--------

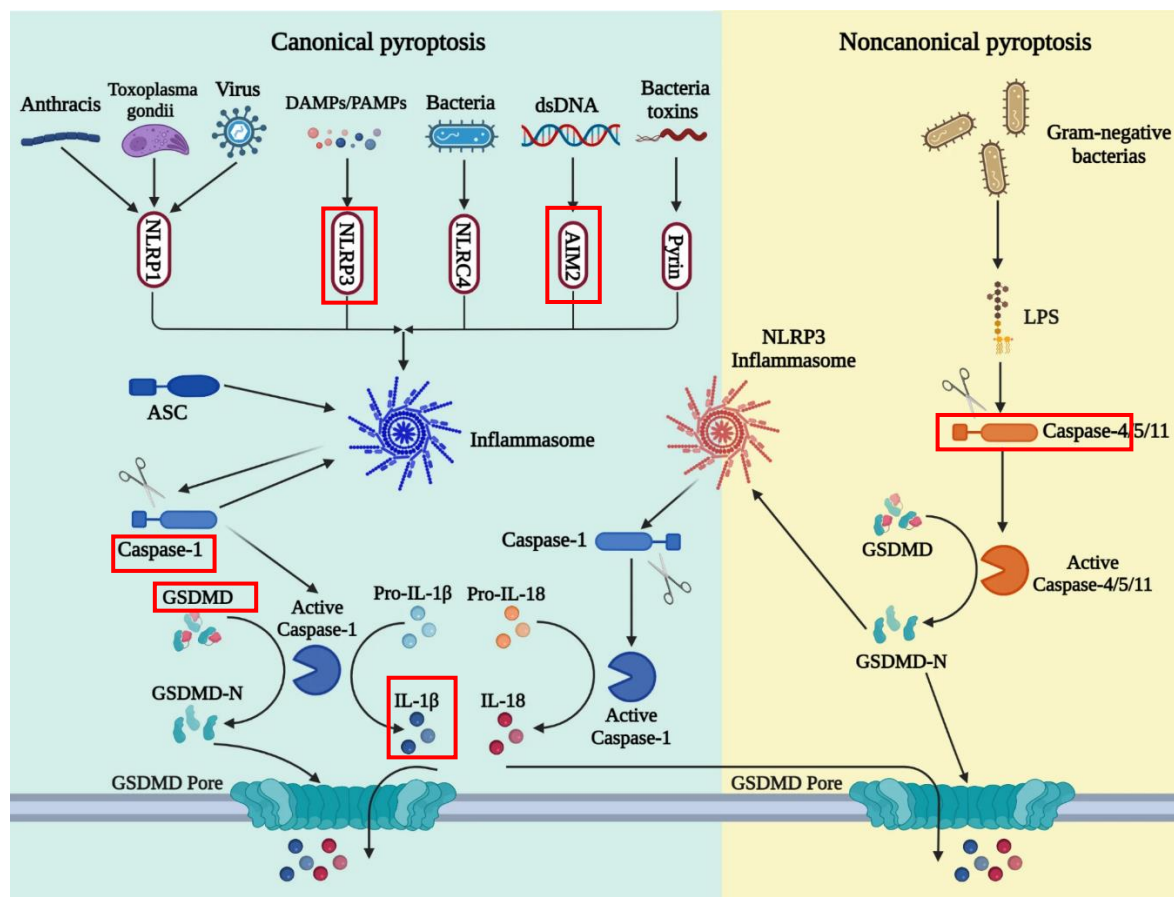
PPAR α target/ Hypo/Hyper

CD36	CPT1A	GYS2	C3
------	-------	------	----

Supplementary figure 3: Venn diagram showing the overlap between significantly hypermethylated (hyper), hypomethylated (hypo) probes and a list of PPAR α target genes (PPAR α target) in KO mice versus WT mice on a chow diet (left; FDR<0.05; DB>|0.15|), KO mice versus WT mice on a CDAHFD (middle; FDR<0.05; DB>|0.1|) and WT mice on a CDAHFD versus chow diet (right; FDR<0.05; DB>|0.15|).



Supplementary figure 4: The ferroptotic signalling pathway (Adapted from¹⁴⁵). Ferroptosis is a ROS-dependent cell death associated with iron accumulation and lipid peroxidation in the cell. When Fe²⁺ is not stored by ferritin (consisting of TFH1 and FTL), the cellular label iron pool will increase. This can directly increase ROS production by the fenton reaction or may increase the activity of lipoxygenases (ALOX) which are responsible for lipid peroxidation. In addition, activation of the mitochondria by the accumulation of glutamate or lipid degradation, will increase the amount ROS production that can further induce lipid peroxidation. In order to overcome this ROS production, the cell will activate several antioxidant systems including GPX4 activation by NRF2 (NFE2L2), CoQ10 and squalene production. The balance between the amount of lipid peroxidation and the prevention by the antioxidant system will decide if the cell undergoes ferroptotic cell death. Upregulated genes by the loss of PPARα function are indicated by a red square.



Supplementary figure 5: Canonical and non-canonical pyroptosis pathway (Figure adapted from¹⁴⁶). The canonical and non-canonical pathways driving pyroptosis development. The canonical pathway is activated by canonical inflammasomes in response to exogenous pathogens and endogenous agents (such as anthracis, toxoplasma gondii, the dsRNA of viruses, DAMPs (including ROS, mtDNA, ATP)/PAMPs, bacterial infection, and dsDNA). This process is driven by intracellular sensor proteins, including NLRP1, NLRP3, NLRC4, AIM2, and Pyrin. Once intracellular sensor proteins are activated, they recruit ASC and caspase-1 to form inflammasomes which induce self-cleavage and activation of caspase-1. Active caspase-1 cleaves pro-inflammatory cytokines (pro-IL-1 β and pro-IL-18) stimulating the release of IL-1 β and IL-18. Meanwhile, cleaved caspase-1 cleaves GSDMD proteins into GSDMD-N. The GSDMD-N forms a pore on the plasma membrane through which mature IL-1 β and IL-18 released. In the non-canonical pathway, LPS directly binds to caspase-4/5/11 to induce self-cleavage and activation of caspase 4/5/11. The cleaved caspase 4/5/11 cleaves GSDMD to produce GSDMD-N which subsequently forms a pore on the plasma membrane through which mature IL-1 β and IL-18 are secreted. Besides, the GSDMD-N activates NLRP3 inflammasomes to activate caspase-1-dependent canonical inflammasome-mediated pyroptosis. dsRNA, double-stranded RNA; DAMPs/PAMPs, damage-associated molecular patterns/pathogen-associated molecular patterns; dsDNA, double-stranded DNA; NLRP, NLR family pyrin domain-containing; AIM2, absent in melanoma 2; ASC, apoptosis-associated speck-like protein containing a CARD; GSDMD, gasdermin D; LPS, lipopolysaccharides; GSDMD-N, the N-terminus of GSDMD. Upregulated genes by the loss of PPAR α function are indicated by a red square.

Results: Chapter 3

Supplementary table 1: Overview of qPCR, PCR and pyrosequencing primers used in this study. (b= biotin tag)

Gene	Forward primer (5' → 3')	Reverse primer (5' → 3')	Sequencing primer (5' → 3')
qPCR primers			
PPAR α	CTGTAAGGGCTTCTTT CGGC	AGTACTGGCATTG TTCCGGT	
DNMT1	GGACAAGGAGAATGC CATGAAGC	TTACTCCGTCCAGTG CCACCAA	
GAPDH	AGGTCGGTGTGAACG GATTTG	GGGGTCGTTGATGG CAACA	
YWHAZ	TAAATGGTCTGTAC CGTCT	GGAAATACTCGGTAG GGTGT	
PCR after bisulphite conversion			
Line 1	GGTTGAGGTAGTATT TTGTGTG	TCCAAAACTATCAAA TTCTCTAAC	
Pyrosequencing			
RETSAT	GATTTGTTTTTATAG AAAGGGTGGGTAGT	CCAATTACCCTCAATA ATCTAATCC ^b	TTTGTATTTTTAATA GGAATTTAT
Eci1	GTGTAGTTTGAATTG GGTTATAGTTAT	TTCCACTACCCTTAA CTCCTTATACA ^b	GGGAGTTTTTTAGT AGTATTA

Supplementary table 2: Full CRN and SAF scoring of the mice used for RNA sequencing and Beadchip analysis.

Mice	Steatose CRN	Ballooning CRN	Lob infl CRN	Fibrosis CRN	NAS score CRN	Ballooning SAF	Lob infl SAF	Activity SAF	Diagnose
WT CTR1	0	0	0	0	0	0	0	0	normal
WT CTR2	0	0	0	0	0	0	0	0	normal
WT CTR3	0	0	0	0	0	0	0	0	normal
WT CTR4	0	0	0	0	0	0	0	0	normal
WT CDAHFD1	3	1	3	2	7	1	2	3	MASH
WT CDAHFD2	3	1	3	2	7	1	2	3	MASH
WT CDAHFD3	3	1	3	F1b	7	1	2	3	MASH
KO CTR1	1	0	1	F1b	2	0	1	1	Isolated steatosis
KO CTR2	0	0	0	0	0	0	0	0	normal
KO CTR3	1	0	1	F1b	2	0	1	1	Isolated steatosis
KO CDAHFD 1	3	2	3	F2	8	1	2	3	MASH
KO CDAHFD2	3	1	3	F1b	7	1	2	3	MASH

Results: Chapter 3

Supplementary table 3: MASLD signature gene list representing fold change (FC) between MASH/NASH patients and healthy controls (NORM) or MASLD/NAFLD patients and healthy controls in the dataset GSE126848.

GSE126848		
Gene	FC [NASH/MASH] vs [NORM]	FC [NAFLD/MASLD] vs [NORM]
BPI	-0,005	0,009
SLC43A3	0,127	0,010
ZNF738	0,046	0,017
ISCA2	0,030	0,032
RAB27A	0,095	0,036
NXN	-0,060	0,042
SDSL	0,293	0,046
NME2	0,236	0,049
GRIP2	0,158	0,052
CSRNP1	0,229	0,059
HYPK	0,522	0,064
TPM2	0,918	0,065
KDF1	-0,143	0,068
CACYBP	0,194	0,081
TIMP1	0,772	0,082
CXCL2	0,065	0,082
FLOT1	0,091	0,104
SLC5A6	0,132	0,104
PSMD8	0,121	0,111
ALAS1	0,027	0,115
RABAC1	0,403	0,116
UBA1	0,143	0,119
LMCD1	0,339	0,126
HSP90B1	0,280	0,131
DYNLL1	0,470	0,131
CRELD2	0,572	0,134
HSD17B2	0,204	0,135
HLA-DMB	0,517	0,139
CALCA	0,140	0,143
KLF6	0,745	0,145
SNRNP70	0,613	0,146
MRPL53	0,276	0,152
SYP	0,366	0,159
SNRPG	0,239	0,164
ADIPOR1	0,000	0,171
EIF4A1	0,462	0,176

EIF4EBP1	0,271	0,177
RPS25	0,176	0,188
EMC10	0,409	0,192
SRP72	0,323	0,194
PHACTR4	0,305	0,197
NOM1	0,400	0,198
ZFP36	0,190	0,199
CCR7	0,527	0,199
FKBP11	0,263	0,200
SCCPDH	0,164	0,207
CENPB	0,408	0,209
TSKU	0,156	0,213
EIF4G1	0,289	0,219
LDLR	0,865	0,220
TOMM40	0,469	0,251
PSMC4	0,491	0,253
CYB5B	0,417	0,259
IFITM3	0,102	0,261
TSEN54	0,591	0,263
ITGA3	0,919	0,269
UQCRHL	0,443	0,274
PKDCC	0,779	0,275
DAD1	0,227	0,276
CCT7	0,362	0,295
AGT	0,403	0,298
ARHGEF16	0,679	0,298
PSMD4	0,497	0,305
SARAF	0,276	0,306
PLOD3	0,402	0,309
EHD4	0,678	0,312
TM4SF5	0,374	0,331
RPL7A	0,378	0,333
RASD1	0,306	0,340
MTDH	0,640	0,341
CHI3L1	2,208	0,348
SPCS2	0,541	0,361
DNAJB11	0,704	0,362
NACA	0,444	0,366
PTRH2	0,650	0,367
LAMTOR5	0,533	0,391

Results: Chapter 3

CD63	0,617	0,396
CCT2	0,502	0,405
LDHA	0,223	0,409
SURF4	0,477	0,415
GLA	0,559	0,420
LRG1	0,050	0,429
PSMA4	0,717	0,436
DDX39B	0,758	0,443
ATP6V0E1	0,421	0,447
EEF1E1	0,858	0,453
ENO1	0,542	0,460
RPN2	0,523	0,461
ARL4D	0,574	0,463
LGALS2	0,484	0,467
FNDC4	0,488	0,471
RPL12	0,573	0,471
SF3B5	0,765	0,472
SLIRP	0,675	0,473
LRRC8E	0,736	0,478
SOD2	0,538	0,484
HTRA1	0,818	0,489
RPL37A	0,675	0,491
TSPAN6	0,429	0,491
CCL22	0,702	0,492
PRAF2	0,647	0,507
PPP1R14B	0,796	0,514
TMEM198	0,536	0,515
NAT9	0,686	0,520
TUBA1C	1,057	0,524
ZNF212	0,555	0,529
VSTM2L	0,820	0,537
MTCH2	0,575	0,540
ATG10	0,711	0,563
NNMT	-0,001	0,568
ZNF329	0,423	0,572
PSMB1	0,670	0,577
RPS27A	0,803	0,584
NDUFB9	0,674	0,586
RPL37	0,675	0,594
MRPS12	0,778	0,600
SYPL1	0,729	0,601
NME1	0,972	0,604

RPS19	0,923	0,640
PRDX4	0,751	0,644
AGPAT2	0,645	0,647
RPL23A	0,844	0,661
SNRPD2	0,911	0,663
EMC7	0,721	0,673
SNRPF	0,928	0,691
SPINK1	1,244	0,712
TMX2	0,889	0,713
PSMA6	0,990	0,733
CIB1	0,962	0,758
PABPN1	1,323	0,764
RPL7	0,807	0,773
NOP10	0,914	0,776
S100A6	1,216	0,778
C4BPB	0,744	0,789
TXNDC17	1,130	0,790
ADCK2	0,720	0,804
PLP2	1,133	0,817
TMEM258	0,861	0,840
ATP6V0B	1,204	0,866
MRPL51	1,021	0,882
LCN2	1,156	0,885
AURKAIP1	1,244	0,890
COX7B	1,211	0,892
COX6B1	1,106	0,898
ARF4	1,293	1,066
KRT18	1,671	1,365
SERPINE1	2,440	1,813
RPS7	1,221	1,063
CSTB	1,322	1,113
HSPE1	1,327	1,169
CDKN1A	2,063	1,197
GPX2	1,381	1,265
RPL21	1,416	1,345
MANF	1,837	1,345
CRP	1,787	2,102
SAA1	2,440	2,690
SRSF11	1,690	1,040
ARID4B	1,680	1,000
UPF3B	1,720	1,030
FAM133B	1,360	0,810

Results: Chapter 3

NKTR	1,270	0,811
LUC7L3	1,500	0,829
ZC3H13	1,570	0,925
RBM25	1,340	0,674
ZBTB20	1,420	0,391
ANKRD36C	2,130	1,370
ANKRD26	2,190	1,460
ANKRD12	2,300	1,520
ZMAT1	1,890	1,340
PNISR	1,920	1,230
AKR1B10	3,900	1,600
FABP4	3,010	1,840

IL32	2,250	1,740
CXCL10	3,150	2,810
ACSL4	1,810	0,775
CYP7A1	2,230	1,160
MLIP	1,700	0,198
ASCL1	1,210	1,270
TFF3	0,953	0,566
SMIM24	0,831	1,080
PZP	0,952	2,350
PEG10	3,250	2,240
HBB	2,100	2,270
HBA2	1,890	1,650

Supplementary table 4: List of PPAR α target genes, differentially expressed epigenetic enzymes and differentially expressed transcription factors used for HOMER analysis.

PPAR α target genes			Epigenetic enzymes	Transcription factors	
SLC27A1	CYP27A1	SULT2A1	DNMT1	Pparg	Prdm16
CD36	CYP8B1	AHR	DNMT3A	Ciita	Rarg
ACS	PKC1	CYP1A1	DNMT3B	Ap1s2	Lmo2
FABP	GDP	UGDH	MeCP2	Irf8	Tcf7
DBI	GK	ACOX1	MBD1	Ets2	Fli1
CPT1A	AQA3	GPT	MBD2	Egr1	Ikzf1
CPT2	AQA9	FADS2	MBD4	Runx1	Runx2
ACADM	PDK4	PDZK1	KAISO	Spi1	Lyl1
ACADL	GYS2	CYP1A1	ZBTB4	Jun	Tcf21
ACADVL	LPL	CREB3L3	ZBTB38	E2f1	Sox9
ECI1	ANGPTL4	KLF10	UHRF1	Ezh2	Atf3
ACOX	NR1D1	KLF11	UHRF2	Nfe2l2	Mybl1
EHHADH	APOA1	MAP3K8	TET1	Ets1	Myc
ACAA1	APOA2	TXN	TET2	Phc1	Foxm1
PEX11A	APOA5	ABCG2	TET3	Pbx1	Ccnd1
CYP4A	APOC3	TF		Klf5	Tbx3
HMGCS2	HMOX1	RETSAT		Tet1	Mycn
FGF21	SLC25A20	CPT1B		Klf4	Klf1
AP2A2	NPC1L1	UGT1A9		Ahr	Tead4
SCD	SLC29A1	UGT2B4		Ttf2	Rb1
ME1	UCP3	CYP3A4		Mitf	
LPIN2	FABP6	SLC10A2		Wt1	
ACACA	PLIN2	CYP2C8		Mef2a	
FASN	C3			Stat5a	
NR1H3	CYP7A1			Notch1	

Results: Chapter 3

Supplementary table 5: List of genes with a PPAR α motif based on a Homer analysis of the differentially expressed epigenetic enzymes, differentially expressed transcription factors and PPAR α target genes of supplementary table 4. The motif score shows the log odds score of the motif matrix, indicating whether a certain position in the DNA sequence is bound or unbound by the TF PPAR α . A higher scores Motif score indicates are better match.

Ensembl	Name	Offset	Sequence	Strand	MotifScore
ENSMUSG00000024817	Uhrf2	-205	CGAGGGCACAGGGCG	+	7,131544
ENSMUSG00000001228	Uhrf1	-284	AGAGGTCAAAGTTTG	+	7,934324
ENSMUSG00000005148	Klf5	-97	TACCCTCTGGCCCTG	-	8,839176
ENSMUSG00000034041	Lyl1	34	CCACCTTTCCCTTT	-	8,004002
ENSMUSG00000070348	Ccnd1	-155	TCCCCTTGCCCCGC	-	7,660048
ENSMUSG00000027490	E2f1	-195	GAGAGGCAGAGGGGA	+	7,194429
ENSMUSG00000002111	Spi1	-221	TAGCCTTTCTCCCTC	-	7,334501
ENSMUSG00000015839	Nfe2l2	21	TGCCTTGCCTAG	-	7,2952
ENSMUSG00000015839	Nfe2l2	14	TGGCCCTGCCTCTT	-	7,356834
ENSMUSG00000023942	Slc29a1	-27	TGGGGCCAAAGGCCA	+	9,681598
ENSMUSG00000022853	Ehhadh	-75	GAAGTGCAAGGGGCA	+	8,2632
ENSMUSG00000078937	Cpt1b	-233	TGACCTTTCCCTAC	-	11,544668
ENSMUSG00000020653	Klf11	-254	GGACCTTTCCCTAC	-	9,544712
ENSMUSG00000020777	Acox1	-284	TAACCTTTGTCCTGT	-	10,3533
ENSMUSG00000050445	Cyp8b1	-67	CAAAGTCCAAGGGCA	+	7,289098
ENSMUSG00000032418	Me1	-217	CTGGGTCAAAGTTGA	+	10,349941
ENSMUSG00000032079	Apoa5	-138	AAGGGGAAAAGGTGA	+	9,519173
ENSMUSG00000032081	Apoc3	-71	TGACCTTTGCCCAGC	-	10,790558
ENSMUSG00000032083	Apoa1	-273	CAGGCTCAGAGGGCA	+	7,563891
ENSMUSG00000015568	Lpl	-155	TGCCCTTTCCCTTC	-	10,64728
ENSMUSG00000030244	Gys2	-31	AAAGGCCAAAGGCCA	+	10,745558
ENSMUSG00000030244	Gys2	-24	AAAGGCCAAAGGACT	+	8,300462
ENSMUSG00000019577	Pdk4	-224	CACCCTTTGCCCTT	-	8,090005
ENSMUSG00000002944	Cd36	-49	TGGCCTCTGACTTAC	-	8,775952
ENSMUSG00000028494	Plin2	-211	GGACCCTGACCTAA	-	7,752807
ENSMUSG00000027875	Hmgcs2	-87	AGACCTTTGGCCAG	-	10,571529
ENSMUSG00000038298	Pdzk1	-59	GCAGGACAGAGGTCA	+	10,749131
ENSMUSG00000002108	Nr1h3	-107	GGACCTTTGCTCCGC	-	8,413102
ENSMUSG00000005681	Apoa2	-49	TGATCTCTGCCTTC	-	9,854075
ENSMUSG00000024665	Fads2	-220	GGAGGCCAAAAGTCCA	+	7,386384

Supplementary table 6: Log fold change (FC) and adjusted p-value of overlapping genes between differently methylated genes in MASH patients compared to healthy controls and ferroptosis or pyroptosis gene signature.

Ferroptosis			
Gene	logFC	P.Value	adj.P.Val
LPCAT2	0,86923	0,0003	0,04897
FASN	0,5943	0,00027	0,04824
ARNTL	0,92384	0,00026	0,04777
ACSL1	0,71671	0,00023	0,04707
NFE2L2	0,86928	0,00019	0,04567
AGPAT3	1,03175	0,00018	0,04467
NCOA4	0,79681	0,00016	0,04384
AIFM2	0,9055	9,4E-05	0,0408
FDFT1	0,89976	5,8E-05	0,03827
ANO6	1,38039	5,5E-07	0,02761
GPX4	-0,9915	0,00025	0,04734
CDKN1A	-0,8478	0,00031	0,04937
CPT1A	-0,7483	0,0001	0,04113

Pyroptosis			
Gene	logFC	P.Value	adj.P.Val
CHMP6	0,74019	0,0001	0,04113
GPX4	-0,9915	0,00025	0,04734
BAK1	-1,2019	0,00011	0,04161
CASP8	-1,043	8,1E-05	0,04015
HMGB1	-0,7299	0,00025	0,04769
IL1B	-0,7654	0,00017	0,04442
NLRP1	-0,6366	0,00017	0,04442
NLRP2	-0,7411	0,00014	0,04339
NOD1	-1,1957	1,2E-05	0,03318

3.7 References

1. Rinella, M. E. *et al.* A multi-society Delphi consensus statement on new fatty liver disease nomenclature. *J Hepatol* (2023) doi:10.1016/j.jhep.2023.06.003.
2. Younossi, Z. M. *et al.* Global epidemiology of nonalcoholic fatty liver disease-Meta-analytic assessment of prevalence, incidence, and outcomes. *Hepatology* **64**, 73–84 (2016).
3. Loomba, R. & Sanyal, A. J. The global NAFLD epidemic. *Nat Rev Gastroenterol Hepatol* **10**, 686–690 (2013).
4. Almeda-Valdés, P., Cuevas-Ramos, D. & Alberto Aguilar-Salinas, C. Metabolic syndrome and non-alcoholic fatty liver disease. *Ann Hepatol* **8**, S18–S24 (2009).
5. Chalasani, N. *et al.* The diagnosis and management of nonalcoholic fatty liver disease: Practice guidance from the American Association for the Study of Liver Diseases. *Hepatology* **67**, 328–357 (2018).
6. Stepanova, M. & Younossi, Z. M. Independent Association Between Nonalcoholic Fatty Liver Disease and Cardiovascular Disease in the US Population. *Clinical Gastroenterology and Hepatology* **10**, 646–650 (2012).
7. Romero-Gómez, M., Zelber-Sagi, S. & Trenell, M. Treatment of NAFLD with diet, physical activity and exercise. *J Hepatol* **67**, 829–846 (2017).
8. Vilar-Gomez, E. *et al.* Weight Loss Through Lifestyle Modification Significantly Reduces Features of Nonalcoholic Steatohepatitis. *Gastroenterology* **149**, 367–378.e5 (2015).
9. Tiffon, C. The Impact of Nutrition and Environmental Epigenetics on Human Health and Disease. *Int J Mol Sci* **19**, 3425 (2018).
10. Juanola, O., Martínez-López, S., Francés, R. & Gómez-Hurtado, I. Non-Alcoholic Fatty Liver Disease: Metabolic, Genetic, Epigenetic and Environmental Risk Factors. *Int J Environ Res Public Health* **18**, 5227 (2021).
11. Mwinyi, J. *et al.* NAFLD is associated with methylation shifts with relevance for the expression of genes involved in lipoprotein particle composition. *Biochim Biophys Acta Mol Cell Biol Lipids* **1862**, 314–323 (2017).
12. Lai, Z. *et al.* Association of Hepatic Global DNA Methylation and Serum One-Carbon Metabolites with Histological Severity in Patients with NAFLD. *Obesity (Silver Spring)* **28**, 197–205 (2020).
13. Ahrens, M. *et al.* DNA methylation analysis in nonalcoholic fatty liver disease suggests distinct disease-specific and remodeling signatures after bariatric surgery. *Cell Metab* **18**, 296–302 (2013).
14. Wegermann, K. *et al.* Branched chain amino acid transaminase 1 (BCAT1) is overexpressed and hypomethylated in patients with non-alcoholic fatty liver disease who experience adverse clinical events: A pilot study. *PLoS One* **13**, e0204308 (2018).
15. Hardy, T. *et al.* Plasma DNA methylation: a potential biomarker for stratification of liver fibrosis in non-alcoholic fatty liver disease. *Gut* **66**, 1321–1328 (2017).

16. Murphy, S. K. *et al.* Relationship between methylome and transcriptome in patients with nonalcoholic fatty liver disease. *Gastroenterology* **145**, 1076–87 (2013).
17. Kitamoto, T. *et al.* Targeted-bisulfite sequence analysis of the methylation of CpG islands in genes encoding PNPLA3, SAMM50, and PARVB of patients with non-alcoholic fatty liver disease. *J Hepatol* **63**, 494–502 (2015).
18. Zeybel, M. *et al.* Differential DNA methylation of genes involved in fibrosis progression in non-alcoholic fatty liver disease and alcoholic liver disease. *Clin Epigenetics* **7**, 25 (2015).
19. Alegría-Torres, J. A., Baccarelli, A. & Bollati, V. Epigenetics and lifestyle. *Epigenomics* **3**, 267–277 (2011).
20. Berger, S. L., Kouzarides, T., Shiekhhattar, R. & Shilatifard, A. An operational definition of epigenetics: Figure 1. *Genes Dev* **23**, 781–783 (2009).
21. Li, Y. Y. *et al.* Fatty liver mediated by peroxisome proliferator-activated receptor- α DNA methylation can be reversed by a methylation inhibitor and curcumin. *J Dig Dis* **19**, 421–430 (2018).
22. Lai, Z. *et al.* Association of Hepatic Global DNA Methylation and Serum One-Carbon Metabolites with Histological Severity in Patients with NAFLD. *Obesity* **28**, 197–205 (2020).
23. Francque, S. *et al.* PPAR α gene expression correlates with severity and histological treatment response in patients with non-alcoholic steatohepatitis. *J Hepatol* **63**, (2015).
24. Bugge, A. & Mandrup, S. Molecular Mechanisms and Genome-Wide Aspects of PPAR Subtype Specific Transactivation. *PPAR Res* **2010**, 1–12 (2010).
25. Francque, S. *et al.* Nonalcoholic steatohepatitis: the role of peroxisome proliferator-activated receptors. *Nat Rev Gastroenterol Hepatol* **18**, 24–39 (2021).
26. Fajas, L. *et al.* The Organization, Promoter Analysis, and Expression of the Human PPAR γ Gene. *Journal of Biological Chemistry* **272**, 18779–18789 (1997).
27. Escher, P. *et al.* Rat PPARs: Quantitative Analysis in Adult Rat Tissues and Regulation in Fasting and Refeeding. *Endocrinology* **142**, 4195–4202 (2001).
28. Francque, S. *et al.* PPAR α gene expression correlates with severity and histological treatment response in patients with non-alcoholic steatohepatitis. *J Hepatol* **63**, 164–173 (2015).
29. Kersten, S. & Stienstra, R. The role and regulation of the peroxisome proliferator activated receptor alpha in human liver. *Biochimie* **136**, 75–84 (2017).
30. Gawrieh, S. *et al.* Saroglitazar, a PPAR- α/γ Agonist, for Treatment of NAFLD: A Randomized Controlled Double-Blind Phase 2 Trial. *Hepatology* **74**, 1809–1824 (2021).
31. Staels, B. *et al.* Hepatoprotective effects of the dual peroxisome proliferator-activated receptor alpha/delta agonist, GFT505, in rodent models of nonalcoholic fatty liver disease/nonalcoholic steatohepatitis. *Hepatology* **58**, 1941–1952 (2013).

32. Yokote, K. *et al.* Effects of pemafibrate on glucose metabolism markers and liver function tests in patients with hypertriglyceridemia: a pooled analysis of six phase 2 and phase 3 randomized double-blind placebo-controlled clinical trials. *Cardiovasc Diabetol* **20**, 96 (2021).
33. Ratziu, V. *et al.* Elafibranor, an Agonist of the Peroxisome Proliferator-Activated Receptor- α and - δ , Induces Resolution of Nonalcoholic Steatohepatitis Without Fibrosis Worsening. *Gastroenterology* **150**, (2016).
34. Lange, N. F., Graf, V., Caussy, C. & Dufour, J.-F. PPAR-Targeted Therapies in the Treatment of Non-Alcoholic Fatty Liver Disease in Diabetic Patients. *Int J Mol Sci* **23**, 4305 (2022).
35. Nakajima, A. *et al.* Randomised clinical trial: Pemafibrate, a novel selective peroxisome proliferator-activated receptor α modulator (SPPAR α), versus placebo in patients with non-alcoholic fatty liver disease. *Aliment Pharmacol Ther* **54**, 1263–1277 (2021).
36. Remely, M. *et al.* Vitamin E Modifies High-Fat Diet-Induced Increase of DNA Strand Breaks, and Changes in Expression and DNA Methylation of Dnmt1 and MLH1 in C57BL/6J Male Mice. *Nutrients* **9**, 607 (2017).
37. Boubia, B. *et al.* Design, Synthesis, and Evaluation of a Novel Series of Indole Sulfonamide Peroxisome Proliferator Activated Receptor (PPAR) $\alpha/\gamma/\delta$ Triple Activators: Discovery of Lanifibranor, a New Antifibrotic Clinical Candidate. *J Med Chem* **61**, 2246–2265 (2018).
38. Sumida, Y. & Yoneda, M. Current and future pharmacological therapies for NAFLD/NASH. *J Gastroenterol* **53**, 362–376 (2018).
39. Moody, L., Xu, G. B., Chen, H. & Pan, Y.-X. Epigenetic regulation of carnitine palmitoyltransferase 1 (Cpt1a) by high fat diet. *Biochimica et Biophysica Acta (BBA) - Gene Regulatory Mechanisms* **1862**, 141–152 (2019).
40. Ehara, T. *et al.* Ligand-Activated PPAR α -Dependent DNA Demethylation Regulates the Fatty Acid β -Oxidation Genes in the Postnatal Liver. *Diabetes* **64**, 775–784 (2015).
41. Yuan, X. *et al.* Epigenetic modulation of Fgf21 in the perinatal mouse liver ameliorates diet-induced obesity in adulthood. *Nat Commun* **9**, 636 (2018).
42. Hashimoto, K. & Ogawa, Y. Epigenetic Switching and Neonatal Nutritional Environment. in 19–25 (2018). doi:10.1007/978-981-10-5526-3_3.
43. Hervouet, E., Vallette, F. M. & Cartron, P.-F. Dnmt1/Transcription Factor Interactions: An Alternative Mechanism of DNA Methylation Inheritance. *Genes Cancer* **1**, 434–443 (2010).
44. Aibara, D. *et al.* Gene repression through epigenetic modulation by PPARA enhances hepatocellular proliferation. *iScience* **25**, 104196 (2022).
45. Luo, Y. *et al.* Intestinal PPAR α Protects Against Colon Carcinogenesis via Regulation of Methyltransferases DNMT1 and PRMT6. *Gastroenterology* **157**, 744-759.e4 (2019).
46. Bedossa, P. *et al.* Histopathological algorithm and scoring system for evaluation of liver lesions in morbidly obese patients. *Hepatology* **56**, 1751–1759 (2012).

47. Kleiner, D. E. *et al.* Design and validation of a histological scoring system for nonalcoholic fatty liver disease. *Hepatology* **41**, 1313–1321 (2005).
48. Simon Andrews. Babraham Bioinformatics - FastQC A Quality Control tool for High Throughput Sequence Data. *Soil* vol. 5 Preprint at (2020).
49. Dobin, A. *et al.* STAR: Ultrafast universal RNA-seq aligner. *Bioinformatics* **29**, (2013).
50. Love, M. I., Huber, W. & Anders, S. Moderated estimation of fold change and dispersion for RNA-seq data with DESeq2. *Genome Biol* **15**, (2014).
51. Xu, Z., Niu, L., Li, L. & Taylor, J. A. ENmix: A novel background correction method for Illumina HumanMethylation450 BeadChip. *Nucleic Acids Res* **44**, (2016).
52. Niu, L., Xu, Z. & Taylor, J. A. RCP: A novel probe design bias correction method for Illumina Methylation BeadChip. in *Bioinformatics* vol. 32 (2016).
53. Zhou, Y. *et al.* Metascape provides a biologist-oriented resource for the analysis of systems-level datasets. *Nat Commun* **10**, (2019).
54. Gonzalez-Sanchez, E., Firrincieli, D., Housset, C. & Chignard, N. Expression patterns of nuclear receptors in parenchymal and non-parenchymal mouse liver cells and their modulation in cholestasis. *Biochimica et Biophysica Acta (BBA) - Molecular Basis of Disease* **1863**, 1699–1708 (2017).
55. Kleiner, D. E. *et al.* Design and validation of a histological scoring system for nonalcoholic fatty liver disease. *Hepatology* **41**, 1313–1321 (2005).
56. Suppli, M. P. *et al.* Hepatic transcriptome signatures in patients with varying degrees of nonalcoholic fatty liver disease compared with healthy normal-weight individuals. *American Journal of Physiology-Gastrointestinal and Liver Physiology* **316**, G462–G472 (2019).
57. Lai, Z. *et al.* Association of Hepatic Global DNA Methylation and Serum One-Carbon Metabolites with Histological Severity in Patients with NAFLD. *Obesity* **28**, 197–205 (2020).
58. Hyun, J. & Jung, Y. DNA Methylation in Nonalcoholic Fatty Liver Disease. *Int J Mol Sci* **21**, 8138 (2020).
59. Buzova, D. *et al.* Profiling of cell-free <sc>DNA</sc> methylation and histone signatures in pediatric NAFLD: A pilot study. *Hepatal Commun* **6**, 3311–3323 (2022).
60. Kuramoto, J. *et al.* Quantification of DNA methylation for carcinogenic risk estimation in patients with non-alcoholic steatohepatitis. *Clin Epigenetics* **14**, 168 (2022).
61. Melton, P. E. *et al.* Differential DNA methylation of steatosis and non-alcoholic fatty liver disease in adolescence. *Hepatal Int* **17**, 584–594 (2023).
62. Theys, C., Lauwers, D., Perez-Novo, C. & Vanden Berghe, W. PPAR α in the Epigenetic Driver Seat of NAFLD: New Therapeutic Opportunities for Epigenetic Drugs? *Biomedicines* **10**, (2022).

63. Bramhecha, Y. M. *et al.* Fatty acid oxidation enzyme $\Delta 3$, $\Delta 2$ -enoyl-CoA isomerase 1 (EC11) drives aggressive tumor phenotype and predicts poor clinical outcome in prostate cancer patients. *Oncogene* **41**, 2798–2810 (2022).
64. Pang, X.-Y., Wang, S., Jurczak, M. J., Shulman, G. I. & Moise, A. R. Retinol saturase modulates lipid metabolism and the production of reactive oxygen species. *Arch Biochem Biophys* **633**, 93–102 (2017).
65. Tayyeb, J. Z. *et al.* Short-Chain Fatty Acids (Except Hexanoic Acid) Lower NF- κ B Transactivation, Which Rescues Inflammation-Induced Decreased Apolipoprotein A-I Transcription in HepG2 Cells. *Int J Mol Sci* **21**, 5088 (2020).
66. Delerive, P. *et al.* Peroxisome Proliferator-activated Receptor α Negatively Regulates the Vascular Inflammatory Gene Response by Negative Cross-talk with Transcription Factors NF- κ B and AP-1. *Journal of Biological Chemistry* **274**, 32048–32054 (1999).
67. Zúñiga, J. *et al.* N-3 PUFA Supplementation Triggers PPAR- α Activation and PPAR- α /NF- κ B Interaction: Anti-Inflammatory Implications in Liver Ischemia-Reperfusion Injury. *PLoS One* **6**, e28502 (2011).
68. Gaul, S. *et al.* Hepatocyte pyroptosis and release of inflammasome particles induce stellate cell activation and liver fibrosis. *J Hepatol* **74**, 156–167 (2021).
69. Zhang, H., Zhang, E. & Hu, H. Role of Ferroptosis in Non-Alcoholic Fatty Liver Disease and Its Implications for Therapeutic Strategies. *Biomedicines* **9**, 1660 (2021).
70. Tsurusaki, S. *et al.* Hepatic ferroptosis plays an important role as the trigger for initiating inflammation in nonalcoholic steatohepatitis. *Cell Death Dis* **10**, 449 (2019).
71. Knorr, J., Wree, A. & Feldstein, A. E. Pyroptosis in Steatohepatitis and Liver Diseases. *J Mol Biol* **434**, 167271 (2022).
72. Dixon, S. J. *et al.* Ferroptosis: An Iron-Dependent Form of Nonapoptotic Cell Death. *Cell* **149**, 1060–1072 (2012).
73. Wree, A. *et al.* NLRP3 inflammasome activation results in hepatocyte pyroptosis, liver inflammation, and fibrosis in mice. *Hepatology* **59**, 898–910 (2014).
74. Wu, J., Lin, S., Wan, B., Velani, B. & Zhu, Y. Pyroptosis in Liver Disease: New Insights into Disease Mechanisms. *Aging Dis* **10**, 1094 (2019).
75. Beier, J. I. & Banales, J. M. Pyroptosis: An inflammatory link between NAFLD and NASH with potential therapeutic implications. *J Hepatol* **68**, 643–645 (2018).
76. Csak, T. *et al.* Fatty acid and endotoxin activate inflammasomes in mouse hepatocytes that release danger signals to stimulate immune cells. *Hepatology* **54**, 133–144 (2011).
77. Watanabe, A. *et al.* Inflammasome-mediated regulation of hepatic stellate cells. *American Journal of Physiology-Gastrointestinal and Liver Physiology* **296**, G1248–G1257 (2009).

78. Kisseleva, T. & Brenner, D. A. Role of hepatic stellate cells in fibrogenesis and the reversal of fibrosis. *J Gastroenterol Hepatol* **22**, S73–S78 (2007).
79. Wree, A. *et al.* NLRP3 inflammasome activation is required for fibrosis development in NAFLD. *J Mol Med* **92**, 1069–1082 (2014).
80. Zhou, N. *et al.* FerrDb V2: update of the manually curated database of ferroptosis regulators and ferroptosis-disease associations. *Nucleic Acids Res* **51**, D571–D582 (2023).
81. De Backer, J. *et al.* Cytoglobin Silencing Promotes Melanoma Malignancy but Sensitizes for Ferroptosis and Pyroptosis Therapy Response. *Antioxidants (Basel)* **11**, (2022).
82. Hassannia, B. *et al.* Nano-targeted induction of dual ferroptotic mechanisms eradicates high-risk neuroblastoma. *J Clin Invest* **128**, 3341–3355 (2018).
83. Ye, Y., Dai, Q. & Qi, H. A novel defined pyroptosis-related gene signature for predicting the prognosis of ovarian cancer. *Cell Death Discov* **7**, 71 (2021).
84. Zuo, J. *et al.* A novel refined pyroptosis and inflammasome-related genes signature for predicting prognosis and immune microenvironment in pancreatic ductal adenocarcinoma. *Sci Rep* **12**, 18384 (2022).
85. Deng, M. *et al.* The pyroptosis-related gene signature predicts prognosis and indicates immune activity in hepatocellular carcinoma. *Mol Med* **28**, 16 (2022).
86. Wang, Z. *et al.* A Pyroptosis-Related Gene Signature Predicts Prognosis and Immune Microenvironment for Breast Cancer Based on Computational Biology Techniques. *Front Genet* **13**, 801056 (2022).
87. Pan, Q., Luo, Y., Xia, Q. & He, K. Ferroptosis and Liver Fibrosis. *Int J Med Sci* **18**, 3361–3366 (2021).
88. Hassannia, B. *et al.* Nano-targeted induction of dual ferroptotic mechanisms eradicates high-risk neuroblastoma. *J Clin Invest* **128**, 3341–3355 (2018).
89. Hurtado-Navarro, L., Angosto-Bazarra, D., Pelegrín, P., Baroja-Mazo, A. & Cuevas, S. NLRP3 Inflammasome and Pyroptosis in Liver Pathophysiology: The Emerging Relevance of Nrf2 Inducers. *Antioxidants (Basel)* **11**, (2022).
90. Matsumoto, M. *et al.* An improved mouse model that rapidly develops fibrosis in non-alcoholic steatohepatitis. *Int J Exp Pathol* **94**, 93–103 (2013).
91. Régnier, M. *et al.* Hepatocyte-specific deletion of Ppara α promotes NAFLD in the context of obesity. *Sci Rep* **10**, 6489 (2020).
92. Cariello, M., Piccinin, E. & Moschetta, A. Transcriptional Regulation of Metabolic Pathways via Lipid-Sensing Nuclear Receptors PPARs, FXR, and LXR in NASH. *Cell Mol Gastroenterol Hepatol* **11**, 1519–1539 (2021).
93. Sharma, R. S. *et al.* Experimental Nonalcoholic Steatohepatitis and Liver Fibrosis Are Ameliorated by Pharmacologic Activation of Nrf2 (NF-E2 p45-Related Factor 2). *Cell Mol Gastroenterol Hepatol* **5**, 367–398 (2018).

94. Yan, C. *et al.* Curcumin regulates endogenous and exogenous metabolism via Nrf2-FXR-LXR pathway in NAFLD mice. *Biomedicine & Pharmacotherapy* **105**, 274–281 (2018).
95. Mohs, A. *et al.* Hepatocyte-specific NRF2 activation controls fibrogenesis and carcinogenesis in steatohepatitis. *J Hepatol* **74**, 638–648 (2021).
96. Li, L. *et al.* Hepatocyte-specific Nrf2 deficiency mitigates high-fat diet-induced hepatic steatosis: Involvement of reduced PPAR γ expression. *Redox Biol* **30**, 101412 (2020).
97. Ni, Y.-H. *et al.* Tcf21 Alleviates Pancreatic Fibrosis by Regulating the Epithelial-Mesenchymal Transformation of Pancreatic Stellate Cells. *Dig Dis Sci* (2023) doi:10.1007/s10620-023-07849-w.
98. Zirath, H. *et al.* MYC inhibition induces metabolic changes leading to accumulation of lipid droplets in tumor cells. *Proceedings of the National Academy of Sciences* **110**, 10258–10263 (2013).
99. Denechaud, P.-D. *et al.* E2F1 mediates sustained lipogenesis and contributes to hepatic steatosis. *Journal of Clinical Investigation* **126**, 137–150 (2015).
100. Walczak, R. & Tontonoz, P. PPARadigms and PPARadoxes: expanding roles for PPAR γ in the control of lipid metabolism. *J Lipid Res* **43**, 177–186 (2002).
101. Sukur, G., Uysal, F. & Cinar, O. High-fat diet induced obesity alters Dnmt1 and Dnmt3a levels and global DNA methylation in mouse ovary and testis. *Histochem Cell Biol* **159**, 339–352 (2023).
102. Keleher, M. R. *et al.* A high-fat diet alters genome-wide DNA methylation and gene expression in SM/J mice. *BMC Genomics* **19**, 888 (2018).
103. Byrnes, K. *et al.* Therapeutic regulation of autophagy in hepatic metabolism. *Acta Pharm Sin B* **12**, 33–49 (2022).
104. Hou, T. *et al.* Cytoplasmic SIRT6-mediated ACSL5 deacetylation impedes nonalcoholic fatty liver disease by facilitating hepatic fatty acid oxidation. *Mol Cell* **82**, 4099-4115.e9 (2022).
105. Kemper, J. K., Choi, S.-E. & Kim, D. H. Sirtuin 1 Deacetylase. in 385–404 (2013). doi:10.1016/B978-0-12-407766-9.00016-X.
106. Ding, R.-B., Bao, J. & Deng, C.-X. Emerging roles of SIRT1 in fatty liver diseases. *Int J Biol Sci* **13**, 852–867 (2017).
107. Dong, X. C. Sirtuin 6—A Key Regulator of Hepatic Lipid Metabolism and Liver Health. *Cells* **12**, 663 (2023).
108. Wang, J. *et al.* TET1 promotes fatty acid oxidation and inhibits NAFLD progression by hydroxymethylation of PPAR α promoter. *Nutr Metab (Lond)* **17**, 46 (2020).
109. Ashraf, W. *et al.* The epigenetic integrator UHRF1: on the road to become a universal biomarker for cancer. *Oncotarget* **8**, 51946–51962 (2017).
110. Unoki, M., Nishidate, T. & Nakamura, Y. ICBP90, an E2F-1 target, recruits HDAC1 and binds to methyl-CpG through its SRA domain. *Oncogene* **23**, 7601–7610 (2004).

111. Ren, Y. Regulatory mechanism and biological function of UHRF1–DNMT1-mediated DNA methylation. *Funct Integr Genomics* **22**, 1113–1126 (2022).
112. Pougovkina, O. *et al.* Mitochondrial protein acetylation is driven by acetyl-CoA from fatty acid oxidation. *Hum Mol Genet* **23**, 3513–3522 (2014).
113. Chiang, J. Y. L. Targeting bile acids and lipotoxicity for NASH treatment. *Hepatol Commun* **1**, 1002–1004 (2017).
114. Rom, O. *et al.* Glycine-based treatment ameliorates NAFLD by modulating fatty acid oxidation, glutathione synthesis, and the gut microbiome. *Sci Transl Med* **12**, (2020).
115. Heidenreich, S. *et al.* Retinol saturase coordinates liver metabolism by regulating ChREBP activity. *Nat Commun* **8**, 384 (2017).
116. Mukai, T., Egawa, M., Takeuchi, T., Yamashita, H. & Kusudo, T. Silencing of <sc>FABP</sc> 1 ameliorates hepatic steatosis, inflammation, and oxidative stress in mice with nonalcoholic fatty liver disease. *FEBS Open Bio* **7**, 1009–1016 (2017).
117. Lyall, M. J. *et al.* Non-alcoholic fatty liver disease (NAFLD) is associated with dynamic changes in DNA hydroxymethylation. *Epigenetics* **15**, 61–71 (2020).
118. Lyall, M. *et al.* The role of DNA hydroxymethylation in non-alcoholic fatty liver disease. *Endocrine Abstracts* (2016) doi:10.1530/endoabs.45.OC8.2.
119. Wu, H., Wang, F., Ta, N., Zhang, T. & Gao, W. The Multifaceted Regulation of Mitochondria in Ferroptosis. *Life* **11**, 222 (2021).
120. Chen, J., Li, X., Ge, C., Min, J. & Wang, F. The multifaceted role of ferroptosis in liver disease. *Cell Death Differ* **29**, 467–480 (2022).
121. Sokolowska, K. E. *et al.* Identified in blood diet-related methylation changes stratify liver biopsies of NAFLD patients according to fibrosis grade. *Clin Epigenetics* **14**, 157 (2022).
122. Sun, Q.-F. *et al.* Potential Blood DNA Methylation Biomarker Genes for Diagnosis of Liver Fibrosis in Patients With Biopsy-Proven Non-alcoholic Fatty Liver Disease. *Front Med (Lausanne)* **9**, 864570 (2022).
123. Loomba, R. *et al.* DNA methylation signatures reflect aging in patients with nonalcoholic steatohepatitis. *JCI Insight* **3**, (2018).
124. Li, X. *et al.* Lipid metabolism dysfunction induced by age-dependent DNA methylation accelerates aging. *Signal Transduct Target Ther* **7**, 162 (2022).
125. Qiu, Y. *et al.* A Lipid Perspective on Regulated Pyroptosis. *Int J Biol Sci* **19**, 2333–2348 (2023).
126. Grabacka, M., Pierzchalska, M., Płonka, P. M. & Pierzchalski, P. The Role of PPAR Alpha in the Modulation of Innate Immunity. *Int J Mol Sci* **22**, (2021).
127. Xing, G. *et al.* PPAR α alleviates iron overload-induced ferroptosis in mouse liver. *EMBO Rep* **23**, e52280 (2022).

128. Xiao, Z. *et al.* Programmed cell death and lipid metabolism of macrophages in NAFLD. *Front Immunol* **14**, 1118449 (2023).
129. Xing, G. *et al.* PPAR α alleviates iron overload-induced ferroptosis in mouse liver. *EMBO Rep* **23**, e52280 (2022).
130. Soltis, A. R. *et al.* Hepatic Dysfunction Caused by Consumption of a High-Fat Diet. *Cell Rep* **21**, 3317–3328 (2017).
131. Minami, J. K. *et al.* CDKN2A deletion remodels lipid metabolism to prime glioblastoma for ferroptosis. *Cancer Cell* (2023) doi:10.1016/j.ccell.2023.05.001.
132. Fang, Y.-L., Chen, H., Wang, C.-L. & Liang, L. Pathogenesis of non-alcoholic fatty liver disease in children and adolescence: From ‘two hit theory’ to ‘multiple hit model’. *World J Gastroenterol* **24**, 2974–2983 (2018).
133. Buzzetti, E., Pinzani, M. & Tsochatzis, E. A. The multiple-hit pathogenesis of non-alcoholic fatty liver disease (NAFLD). *Metabolism* **65**, 1038–48 (2016).
134. Ore, A. & Akinloye, O. A. Phytotherapy as Multi-Hit Therapy to Confront the Multiple Pathophysiology in Non-Alcoholic Fatty Liver Disease: A Systematic Review of Experimental Interventions. *Medicina (Kaunas)* **57**, (2021).
135. Cheng, R. *et al.* A randomized controlled trial for response of microbiome network to exercise and diet intervention in patients with nonalcoholic fatty liver disease. *Nat Commun* **13**, 2555 (2022).
136. Gao, Y. *et al.* Exercise and dietary intervention ameliorate high-fat diet-induced NAFLD and liver aging by inducing lipophagy. *Redox Biol* **36**, 101635 (2020).
137. Dai, Z., Ramesh, V. & Locasale, J. W. The evolving metabolic landscape of chromatin biology and epigenetics. *Nat Rev Genet* **21**, 737–753 (2020).
138. Sabari, B. R., Zhang, D., Allis, C. D. & Zhao, Y. Metabolic regulation of gene expression through histone acylations. *Nat Rev Mol Cell Biol* **18**, 90–101 (2017).
139. Bartke, T. & Schneider, R. You are what you eat - How nutrition and metabolism shape the genome through epigenetics. *Mol Metab* **38**, 100987 (2020).
140. Nieborak, A. & Schneider, R. Metabolic intermediates - Cellular messengers talking to chromatin modifiers. *Mol Metab* **14**, 39–52 (2018).
141. Kebede, A. F. *et al.* Histone propionylation is a mark of active chromatin. *Nat Struct Mol Biol* **24**, 1048–1056 (2017).
142. Arima, Y. *et al.* Murine neonatal ketogenesis preserves mitochondrial energetics by preventing protein hyperacetylation. *Nat Metab* **3**, 196–210 (2021).
143. Guerra, I. M. S. *et al.* Mitochondrial Fatty Acid β -Oxidation Disorders: From Disease to Lipidomic Studies-A Critical Review. *Int J Mol Sci* **23**, (2022).
144. Amado, F. M., Barros, A., Azevedo, A. L., Vitorino, R. & Ferreira, R. An integrated perspective and functional impact of the mitochondrial acetylome. *Expert Rev Proteomics* **11**, 383–94 (2014).

145. Tang, D., Chen, X., Kang, R. & Kroemer, G. Ferroptosis: molecular mechanisms and health implications. *Cell Res* **31**, 107–125 (2021).
146. Zou, Z. *et al.* The role of pyroptosis in hepatocellular carcinoma. *Cellular Oncology* **46**, 811–823 (2023).

CHAPTER IV

*Optimisation of mitochondrial DNA methylation
detection in an in vitro MASLD model*

Results: Chapter 4

Chapter 4

Optimisation of mitochondrial DNA methylation detection in an in vitro MASLD model

Claudia Theys¹, Tim de Pooter², Peter De Rijk², Mojca Strazisar², İkbal Agah İnce^{3,4}, Marianne Rots³, Wim Vanden Berghe¹

¹ Lab Protein Chemistry, Proteomics & Epigenetic Signaling (PPES), Department Biomedical Sciences, University of Antwerp, 2610 Wilrijk, Belgium.; claudia.theys@uantwerpen.be; wim.vandenbergh@uantwerpen.be

² Neuromics Support Facility, VIB Center for Molecular Neurology, VIB, Antwerp, Belgium

³ Division of Medical Biology, Department of Pathology and Medical Biology, University Medical Center Groningen, Netherlands.

⁴ Department of Medical microbiology, School of Medicine, Acibadem Mehmet, Ali Aydınlar University, Ataşehir, İstanbul, Turkey, Türkiye

*Corresponding author: wim.vandenbergh@uantwerpen.be

Conflict of Interest: The authors declare no conflict of interest

4.1 Abstract

Mitochondria are important organelles for the maintenance of the cellular homeostasis, because they produce almost all the energy in the form of ATP by the use of cellular nutrients including glucose and free fatty acids (FFA). However imbalance between cellular fatty acid influx and catabolism can promote mitochondrial dysfunction, which is a typical hallmark of metabolic dysfunction associated steatotic liver disease (MASLD). Whether mitochondrial dysfunction translates into changes in mtDNA methylation or vice versa remains unclear and was studied in more detail in this chapter. Interestingly, recent advances in epigenetic sequencing including Nanopore episequencing now allow to study mitochondrial DNA (mtDNA) specific methylation in absence of bisulfite conversion steps. Methylation specific bisulfite PCR of a few mitochondrial genes previously showed hypermethylation of the mitochondrial ND6 region in metabolic dysfunction associated steatohepatitis (MASH) patients. Here, we applied Nanopore episequencing, to map the full mtDNA methylation signature in an *in vitro* MASLD model. This pilot study revealed small differences in CpG and GpC methylation in different mitochondrially encoded oxidative phosphorylation (OXPHOS) genes with concomitant accumulation of lipids and activation of mitochondrial respiration metabolism. Altogether, these results support a functional association between mitochondrial mtDNA methylation and metabolic respiration. Further confirmation studies with more biological replicates and patient samples are needed to validate mtDNA signatures as a useful clinical biomarker for mitochondrial (dys)function and/or MASLD patient stratification.

Keywords: Mitochondria, MASLD, mtDNA methylation, Nanopore, mitochondrial function

4.2 Introduction

Mitochondria are the powerhouses of the cell, generating most of the ATP that is necessary to maintain the processes involved in cellular homeostasis. In order to generate this energy, mitochondria metabolize nutrients including lipids and glucose that are processed into acetyl-CoA that can be used in the tricarboxylic acid (TCA) cycle to produce electron donors for the electron transport chain (ETC) in the inner mitochondrial membrane (IMM) that will generate ATP, a process known as the oxidative phosphorylation (OXPHOS) pathway¹. Since metabolic dysfunction associated steatotic liver disease (MASLD) is characterised by an accumulation of lipids, β -oxidation that is known as the first step of lipid catabolism will be upregulated in the mitochondria. This process will further trigger activation of the OXPHOS pathway and thus mitochondrial metabolism, due to the accumulation of acetyl-CoA. However the constant influx of lipids induces oxidative mitochondrial damage which will eventually lead to mitochondrial dysfunction, a known hallmark of MASLD²⁻⁴.

Mitochondria contain their own DNA, coding for different proteins of the OXPHOS cycle, two ribosomal proteins and several tRNAs. These proteins are transcribed by the mitochondrial transcription machinery and translated in the mitochondria, depending on the cellular needs^{5,6}. This flexibility of the mitochondrial metabolism is established by a close communication between the nucleus and mitochondria to adapt their metabolism to the cellular needs. However, the regulatory pathways leading to these changes in mitochondrial function are not fully understood yet^{7,8}.

Interestingly, recent developments in epigenetic sequencing technologies allow to specifically epi-sequence mtDNA methylation⁹⁻¹¹. Although it was questioned for a long time whether mtDNA can be epigenetically modified, both Shock et al. and Rebelo et al. demonstrated a clear role for mtDNA methylation in mitochondrial gene expression and copy number^{12,13}. Their research sparked renewed interest in mtDNA methylation research in different diseases, especially cancer. Cancer research studies mainly focused on methylation of the D-loop region of the mtDNA, containing both the promoter for the light and heavy strand of the mtDNA, which translated into differences in mitochondrial gene expression and allowed to distinguish cancerous from non-cancerous tissue^{10,14-16}. Besides, mtDNA methylation has also been studied in neurodegenerative diseases, aging-senescence and cardiovascular diseases showing changes in mtDNA methylation related to differences in gene expression and copy number¹⁶⁻¹⁹. Remarkably, the changes in mtDNA methylation related to MASLD have not been widely studied. Pirola et al. showed that MASH patients show a hypermethylation of the mitochondrial ND6 region, related to a downregulation of this gene. However this research was based on methylation specific PCR checking only a few genes of the mtDNA²⁰. Since mitochondrial dysfunction is a main hallmark of MASLD and currently more advanced techniques allow to study methylation changes of the whole mtDNA without prior bisulfite conversion, including Nanopore sequencing, we were interested whether MASLD can be associated with a mtDNA methylation signature. Therefore we developed and characterised an *in vitro* MASLD model in the liver HepG2 cell line and optimised mtDNA extraction-enrichment methods for downstream Nanopore epi-sequencing to define mtDNA methylation signatures of MASLD associated with mitochondrial dysfunction.

4.3 Material and methods

4.3.1 Cell culture

The Human hepatoma cells (HepG2) cell lines were cultured in Dulbecco's modified Eagle medium (DMEM, Gibco, Thermo Fisher Scientific, 41965039) supplemented with 10% foetal bovine serum (Gibco, Thermo Fisher Scientific, 10270106), 1% penicillin-streptomycin solution (Gibco, Thermo Fisher Scientific, 15140122) and 1mM pyruvate in T75 or T25 flasks in a humidified atmosphere (37°C and 5% CO₂).

4.3.2 FFA medium

The FFAs medium to obtain MASLD-like conditions consisted of oleic (OA) and palmitic (PA) acid in a 2:1 ratio. Stock solutions of 0.66M oleic acid and (1.32M) palmitic acid (Sigma- Aldrich, Germany) were prepared in isopropanol. Equal amounts of oleic and palmitic acid were mixed to prepare a FFA stock of 1 mM FFA. FFA-free bovine serum albumin (BSA) was dissolved in serum-free DMEM medium without antibiotics at the final concentration of 1% and then sterilized using syringe-driven 0.22 µm filters. Afterwards, the medium was supplemented with the mixture of FFA at the final concentration of 1 mM and sonicated for 6- 8 hours until FFA was completely dissolved using a Branson 3200 sonication bath. FFAs medium was protected from light and stored at 4 °C

4.3.3 Lipid quantification with Adipored

AdipoRed Adipogenesis Assay (Lonza, Walkersville, MD, USA) was used to quantify intracellular lipid accumulation in HepG2 cells, both untreated or treated with 1mM FFA for 24h according to the manufacturer's protocol (n=3 biologically independent samples per treatment). Briefly, medium of treated cells was replaced by phosphate buffered saline (PBS) and incubated with the AdipoRed Reagent. Afterwards, fluorescence was measured at 485 nm excitation and 572 nm emission, using a microplate reader (FLUOstar Omega, BMG Labtech). Statistical analysis was carried out using a Two-Way ANOVA test with Tukey's correction for multiple comparisons. P-value < 0.05 was considered statistically significant.

4.3.4 Oil red O staining

Lipid accumulation was visualised with Oil red O staining according to the manufacturers protocol (n=3 biologically independent samples per treatment). Briefly, 1×10^4 HepG2 cells were seeded in 24 well plate and left untreated or treated with 1mM FFA for 24h. After medium removal, cells were washed 2 times with PBS and fixed in 10% formalin for 30min. Next cells were washed 2 times in H₂O and 60% isopropanol was added for 15 min before adding the Oil red O working solution to the cells (3:2 ratio Oil red O stock (120mg Oil red O in 40mL 100% isopropanol) and H₂O). Finally cells were washed 2-5 times in H₂O until no excess stain was seen and viewed under the Motic AE 2000 light microscope.

4.3.5 RNA extraction

Total RNA was extracted from both untreated and treated with 1mM FFA HepG2 cells with the RNeasy kit (Qiagen, 75162), according to the manufacturer's protocol. Afterwards RNA quantity was determined using Qubit™ RNA Broad Range Assay kit with the aid of the Invitrogen Qubit™ Fluorometer (Thermo Fisher Scientific, USA). The extracted RNA was stored at -80°C until further analysis.

4.3.6 Quantitative polymerase chain reaction (qPCR)

After RNA extraction, total RNA was converted into cDNA with the iScript™ cDNA Synthesis Kit (BioRad, 1708890) according to the manufacturer's protocol. Next, qPCR analysis was performed using the PowerUp SYBR™ green PCR master mix (Thermo Fisher Scientific, USA) according to the manufacturer's instructions. In brief, a 20 µl reaction volume mix per sample was prepared containing 10 µl PowerUp SYBR Green Master Mix, 0.4 µM forward and reverse primer, and nuclease-free water. The following PCR program was applied on the Rotor-Gene Q qPCR machine of Qiagen: 95°C for 10 min, 40 cycles denaturation (95°C, 15 s) and annealing/extension (60°C, 1 min), and dissociation (60-95°C). Each sample was run in triplicate. The median value of the triplicates was taken to calculate the $\Delta\Delta C_t$ -values using GAPDH as the normalization gene. GAPDH, APOA5, SCD1, CPT1A, PLIN2, HADH and PPAR α primer sequences (supplementary table 1) were designed by Primer3 and synthesized by Integrated DNA Technologies (IDT, USA). Statistical analysis was carried out using a Two-way ANOVA with Šidák's correction for multiple comparisons. P-value < 0.05 was considered statistically significant.

4.3.7 Mitochondrial DNA extraction

Since the mtDNA is circular, the Qiaprep spin miniprep kit (Qiagen, #27104) was used to directly extract mtDNA from 1×10^6 HepG2 cells according to the manufacturer's instructions. Besides, different mitochondrial DNA isolation kits following differential centrifugation were tested in combination with the Qiagen Blood Tissue DNA isolation kit (Qiagen, 69504) according to manufacturer protocols, i.e. the Mitochondria Isolation Kit (ThermoFisher #89874) and MitoISO2 kit (Sigma) using a 1:200 dilution for the lysis buffer. Besides the Mitochondrial DNA purification kit (Biovision, #K389-25) was also tested to directly extract mtDNA from 5×10^7 HepG2 cells as starting material according to the manufacturer's protocol. The protocol described before by Wieckowski et al. was also tested with some modifications based on the protocol of Sareen et al.^{21,22} After collecting the cells, they were resuspend in ice cold mitochondrial extraction buffer consisting of 10mM HEPES, 200mM mannitol, 70mM sucrose and 1mM EGTA. Besides the final step to pellet the mitochondria was done by a centrifugation at 11.000g for 10min at 4°C followed by a DNA extraction with the Qiagen Blood Tissue DNA isolation kit (Qiagen, 69504) according to the manufacturer's protocol starting from adding proteinase K. After mtDNA extraction, DNA was quantified using the Qubit™ DNA High Sensitivity Assay kit and read with the Invitrogen Qubit™ Fluorometer (Thermo Fisher Scientific, USA). Purity of the mtDNA was determined with qPCR based on the ratio of the nuclear B2M gene and the mitochondrial tRNA_{LEU} as described before by Weerts, M. taking into account the size of the mitochondrial and nuclear genome²³ (supplementary table 1).

4.3.8 Protein extraction and western immunoblot analysis

For western blot analysis, both untreated and 1mM FFA treated HepG2 cells were lysed in 0.5 mL 1xRIPA lysis buffer (150 mM NaCl, 0.1% Triton x-100, 0.1% SDS, 50 mM Tris-HCl pH 8 supplemented with protease inhibitor cocktail (Sigma-Aldrich, Germany)) on ice for 15 min. Afterwards cells were briefly sonicated and centrifugated at 13,000 rpm for 15 min at 4°C. Next, supernatant with soluble protein extract was transferred to new Eppendorf tubes and used for protein quantification with Pierce™ BCA Protein Assay Kit (Thermo Fisher Scientific, USA). After protein extraction, SDS-PAGE was performed to separate proteins on a 6-12% gradient Bis-Tris gel. First, samples were mixed with Laemmli buffer (Biorad, USA) and 50 mM 1,4- dithiothreitol (DTT) and then heated at 70 °C for

10 min to denature the protein. Afterwards, both the samples and protein ladder (BenchMark™ Protein Ladder, Thermo Fisher Scientific, USA) were loaded on the Bis-Tris gel at a protein concentration of 10 µg/well. Electrophoresis was performed in a Mini-PROTEAN Tetra Cell System (Biorad, USA) using a high molecular weight buffer (100 mM MOPS, 100 mM Tris, 0.2% SDS, 2 mM EDTA, 5 mM sodium bisulphite). Afterwards, the proteins were transferred to pre-wet nitrocellulose membranes (Cytiva, USA) for 1 hour at 4°C on 250 mA. After blocking the membranes in 5% BSA /TBST blocking buffer for 1 hour at room temperature, the primary antibody anti-PPAR α (Abcam, #ab24509) was diluted (1:1000) in blocking buffer and incubated overnight at 4°C. The next day, membranes were washed three times with TBST and incubated with HRP-conjugated anti-rabbit secondary antibody diluted in blocking buffer (1:2000) for 1 hour at room temperature. Anti-GAPDH antibody (Bioké #5174S, diluted 1:1000) in blocking buffer was used as loading control. Protein detection was performed on the Amersham imager 680 (Cytiva, USA) using SuperSignal™ West Pico PLUS Chemiluminescent Substrate (Thermo Fisher Scientific, 34577) and quantified using Image-J software. Statistical analysis was carried out using an Unpaired student t-test. P-value < 0.05 was considered statistically significant.

4.3.9 Seahorse

Mitochondrial respiratory function was examined using the Seahorse XFp Cell Mito Stress Test Kit (Agilent Technologies,103010-100) according to the manufacturer's instructions. Briefly, 8×10^3 cells/well resuspended in 80 µL complete DMEM were seeded in an 8 well XFp cell culture miniplate (Agilent Technologies,103025-100; 3 wells with untreated cells and 3 wells with cells treated for 24h with 1mM FFA). After the 24h treatment, XF DMEM pH 7.4 (assay medium), supplemented with Seahorse XF Glucose (10 mM), Seahorse XF Pyruvate (1 mM) and Seahorse XF L-Glutamine (2 mM) was used to rinse the cells (60 µL of growth medium is removed, 200 µL of assay medium is added, 200 µL medium is removed and 160 µL of assay medium is added) and the cell culture miniplate was placed into a 37 °C non-CO₂ incubator for 45 minutes to 1 hour prior to the assay. Next, the Seahorse was calibrated and loaded with the XFp sensor cartridge filled with 1.5 µM oligomycin (Port A), 3µM FCCP (Port B) and 0.5µM Rotenone/Antimycin A (Port C) . Afterwards the cell culture XFp miniplate was loaded into the Seahorse XFp analyzer (Seahorse Biosciences, Agilent Technologies) and real-time oxygen consumption rate was measured for 1.5 h. First baseline respiration was measured (Basal OCR) prior to mitochondrial perturbation by sequential injection of 1.5 µM oligomycin (a complex V inhibitor to decrease the electron flow through ETC); 3 µM FCCP (the uncoupling agent to promote maximum electron flow through ETC); and a mixture of 0.5 µM Rotenone/Antimycin A (complex I and complex II inhibitors, respectively, to shut down the mitochondria-related respiration). Data was analysed using Agilent Seahorse analytics. Statistical analysis was carried out using a Two-way ANOVA with Šidák's correction for multiple comparisons. P-value < 0.05 was considered statistically significant.

4.3.10 Nanopore sequencing

DNA was extracted using the Qiagen Blood Tissue DNA isolation kit (Qiagen, 69504) according to the manufacturer's protocol. The quality of the extracted DNA was measured using the Qubit 4 Fluorometer (Thermo Fisher Scientific, Q33238) and Qubit™ dsDNA BR kit (Thermofisher, Q32850) for concentration, Little Lunatic (Unchained Labs) for purity and Fragment 267 Analyzer for integrity using either the Agilent DNF-464 HS Large Fragment Kit (integrity of extracted hmw-DNA) or the Agilent DNF-492 Large Fragment Kit (fragmentation and size selection). After the QC, 5µg of DNA

was fragmented using Megaruptor 3 (Diagenode) to final fragment sizing 20-30kb, which resulted also in linearization of mtDNA and exposing fragments' ends for end repair and adapter ligation. After Fragmentation, small molecules were depleted using Short Read Eliminator kit (SRE XS, PacBio), depleting short DNA fragments <10 kb progressively and DNA <4 kb almost completely. Library preparation was started with 250fmol size selected DNA per sample ($\pm 3,4\mu\text{g}$ of fragmented, size selected DNA) and consisted of FFE DNA end repair in combination with a preparation of the ends for adapter attachment, native barcode ligation and sequencing adapter ligation with the use of the Native barcoding expansion 13-24 kit (Oxford Nanopore Technologies, EXP-NBD114) in conjunction with the Ligation sequencing kit (Oxford Nanopore Technologies, SQK-LSK109). Prior to the final sequencing adapter ligation, samples were pooled equimolar for optimal read distribution and afterwards sequenced on the MinION (Oxford Nanopore Technologies). In total 50fmol of final library was loaded on the Flow cell ($\sim 678\text{ng}$). Total sequencing time was 80h on MinION 12 (Oxford Nanopore Technologies), with a flush using DNase I before loading of fresh library at 24 and 48h of sequencing. The sequencing run per sample (WT-MASLD) produced 610×10^3 - 255×10^3 reads with a read length N50 of 27-33kb, resulting in a total base output of 11,7-5,9Gb. MtDNA is well covered performing shallow gDNA sequencing (102-270x vs 2-4x for gDNA). Reads were basecalled using GUPPY (version 6.0.6). Further analysis was performed using a pipeline integrated in genomecomb²⁴. Reads were aligned to the hg38 genome reference²⁵ using minimap²⁶ and the resulting sam file was sorted and converted to bam using samtools²⁷. Structural variants were called using sniffles²⁸, cuteSV²⁹ and npinv³⁰. For methylation calls nanopolish³¹ was used. The resulting variant sets of different cell lines were combined and annotated using genomecomb²⁴. Nanopolish analysis (version 0.13.2)³¹ was performed for CpG and GpC methylation analyses on the mitochondrial genome without applying NUMT filtering, as NUMTs were shown to only have a marginal impact on methylation assessment^{31,32}.

4.4 Results and discussion

4.4.1 Characterisation of an *in vitro* MASLD model

In order to study the mtDNA methylation signature in MASLD, we first developed and characterised an *in vitro* MASLD model in HepG2 cells. Several studies based on *in vitro* MASLD models used a treatment combination of the most common lipids in liver triglycerides, oleic acid and palmitic acid³³⁻³⁵. Based on these studies, we treated HepG2 cells for 24h with 1mM FFA consisting of a mixture of oleic acid and palmitic acid in a 2:1 ratio. Indeed, both fluorescence quantification and Oil red O staining showed a clear accumulation of lipid droplets in the HepG2 cells after a 24h treatment with 1mM FFA, similar to liver lipid accumulation in MASLD patients (Figure 1A-B)^{36,37}. Whereas PPAR α expression levels do not change upon FFA treatment (Figure 1C), downstream PPAR α target gene expression involved in lipid transport over the mitochondrial membrane and lipid droplet coating (CPT1A and PLIN2) is significantly increased (Figure 1D). This suggests that the activity of PPAR α is increased to metabolize the constant influx of lipids. Along the same line, mitochondrial seahorse experiments further confirm the increase in lipid metabolism by a consistent small increase in basal respiration and ATP production and especially a significant increase in maximum respiration compared to the untreated WT HepG2 cells (Figure 1D).

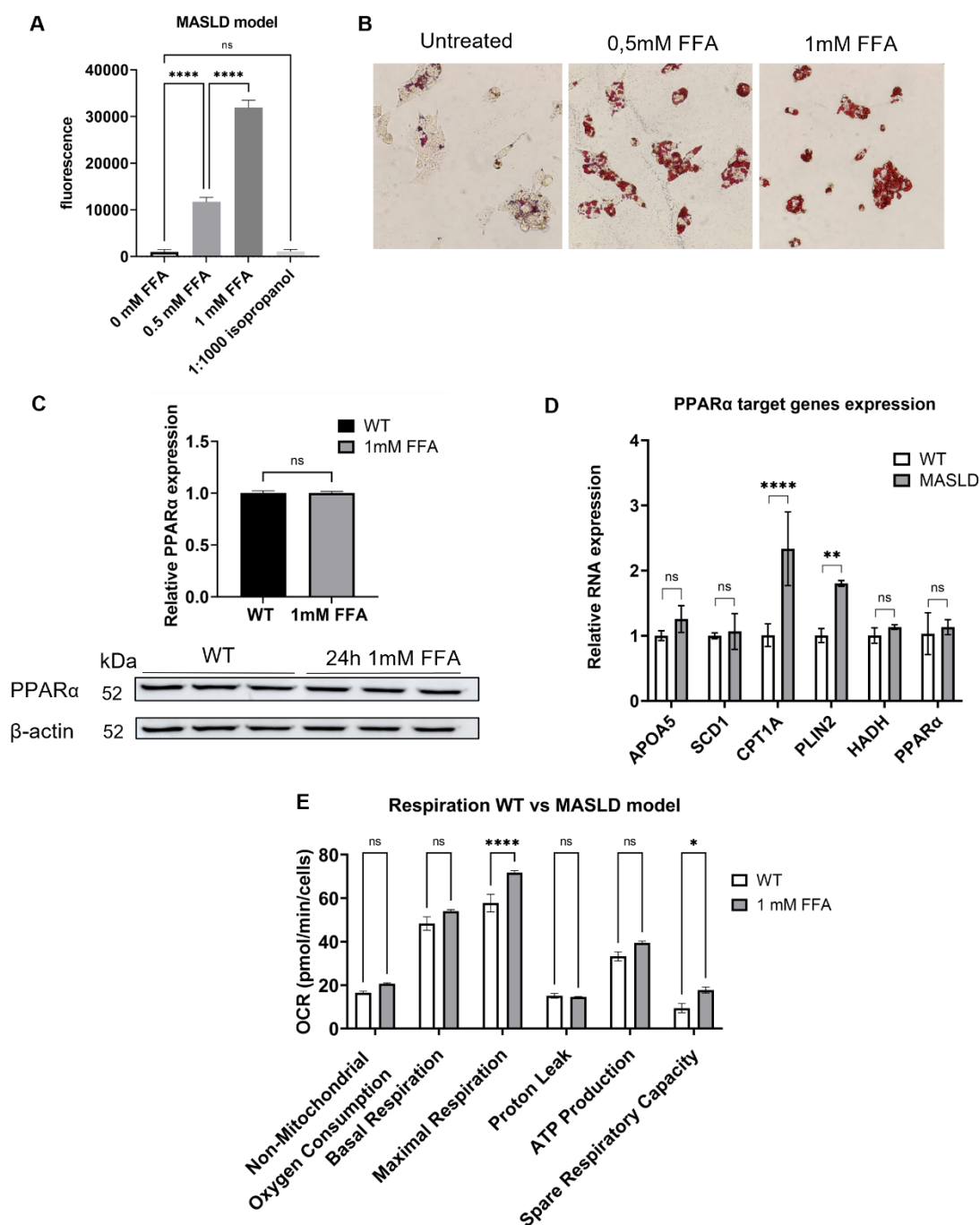


Figure 1: A) Adipored quantification ($n=3$ biological independent samples) and **B)** Representative images of Oil red O staining showing the accumulation of lipid droplets in HepG2 cells after treatment with 1mM FFA for 24h. ($ns=$ not significant; $*p < 0.05$, $**p < 0.01$, $***p < 0.001$, $****p < 0.0001$, One-way ANOVA with Tukey's correction for multiple comparisons) **C)** Western blot detection and quantification of the nuclear receptor PPARα in both WT and 24h treated samples. ($n=3$ biological independent samples; $ns=$ not significant, Unpaired student t-test) **D)** qPCR quantification of PPARα and its target genes in WT and 24h FFA treated MASLD mimetic samples ($n=3$ biological independent samples). **E)** The Seahorse XF Cell Mito Stress assay was used to measure changes in oxygen consumption rate after different triggers that inhibit or activate mitochondrial respiration (Oligo= oligomycin; FFCP; Rot/AA = rotenone and antimycin A) in both untreated and treated with 1mM FFA for 24h cells. Based on the changes in oxygen consumption several aspects of the mitochondrial respiration could be quantified. ($n=3$ biological independent samples; ($ns=$ not significant; $*p < 0.05$, $**p < 0.01$, $***p < 0.001$, $****p < 0.0001$, Two-way ANOVA with Šidák's correction for multiple comparisons).

These results indicate that the lipids of the treatment are metabolized by the cells and can be used to increase mitochondrial respiration. However it seems that the cells did not yet reach maximum respiration and can still process the lipid influx, which resembles mostly the steatosis stage in MASLD patients. Indeed, these results are similar to the study of Gómez-Lechón et al. showing that this combination of oleic acid with palmitic acid induces similar conditions as benign steatosis in liver tissue of MASLD patients. Higher concentrations of palmitic acid may promote lipotoxicity towards apoptosis and thus show a more acute harmful effect of fat accumulation in the liver³⁴.

4.4.2 Optimisation of pure mitochondrial DNA extraction

To reduce the total episequencing cost of mtDNA methylation, the challenge is to enrich for mtDNA without contamination of the nuclear DNA, to avoid aspecific nuclear DNA competing with mtDNA for nanopore episequencing. Therefore we tested different mtDNA extraction kits and strategies and quantified the amount of mtDNA based on the ratio of the mitochondrial gene $tRNA_{Leu}$ to the nuclear gene B2M determined by qPCR (Table 1).

Table 2: Overview of mtDNA yield using different kits and protocols to extract pure mitochondrial DNA. Mitochondrial percentage is calculated based on the amount of mitochondrial $tRNA_{Leu}$ gene to nuclear B2M gene and used to calculate concentration of mtDNA based on the total amount of extracted DNA. The total number of cells used for the extraction is and end volume of DNA are also shown.

Mitochondrial DNA isolation kit	Mitochondrial DNA percentage	Concentration of mitochondrial DNA (ng/ μ L)	Starting number of cells	Total volume/sample
QIAprep Spin Miniprep kit (Qiagen)	4,28%	0,264	$1 \cdot 10^6$	50 μ L
	1,90%	0,522	$20 \cdot 10^6$	50 μ L
Differential centrifugation + DNeasy kit (Qiagen)	0,27%	0,020	$3 \cdot 10^6$	50 μ L
Mitochondrial Isolation kit (Thermofisher) + DNeasy kit (Qiagen)	1,84%	0,002	$5 \cdot 10^6$	50 μ L
MitoISO2 (Sigma Aldrich) + DNeasy kit (Qiagen)	3,84%	2,341	$20 \cdot 10^6$	200 μ L
Mitochondrial DNA purification kit (Biovision)	14,02%	0,359	$50 \cdot 10^6$	50 μ L

The technique that generated the highest percentage of mitochondrial DNA based on the total amount of extracted DNA, is the Mitochondrial DNA purification kit (Biovision, #389) with a percentage of 14,02% of mtDNA. However this indicates that almost 85% of the total DNA sample still consists of nuclear gDNA. Moreover, the concentration of mtDNA with this kit only reaches 0,359 ng/ μ L, which is too low for further nanopore sequencing analysis.

To circumvent low yield mtDNA enrichment strategies, we alternatively applied preprocessing of Nanopore samples via size selection of the extracted DNA. Briefly, regular DNA extraction with the DNeasy kit (Qiagen) is followed by DNA fragmentation and size selection to a final fragment size range of 20-30 kb allowing to enrich full length mtDNA with a size of 16.569kb. This approach generated a high coverage of pure mtDNA in downstream Nanopore epi-sequencing applications, allowing to further study the methylation signature of the mtDNA.

4.4.3 *Characterising the mtDNA methylation signature in an in vitro MASLD model with Nanopore sequencing*

A pilot Nanopore epi-sequencing experiment on one MASLD and one WT sample consisting of a pool of 3 biologically independent samples generated a median coverage of 102x and 270x of the mtDNA respectively. Since mtDNA methylation percentages are low compared to the nuclear DNA, this high coverage allowed us to reliably estimate methylation frequencies of all cytosines in the mtDNA¹¹. Moreover the median total/nuclear genome coverage is 2x and 4x respectively, which indicates that the DNA size selection allowed us to generate a high percentage of pure mtDNA. Together this shows that the method used in this study is appropriate to correctly estimate mtDNA methylation. Figure 2 shows that in both samples, the overall percentage of CpG methylation ($\pm 6\%$) is higher compared to the overall percentage of GpC methylation ($\pm 4\%$). Since these overall percentages are relatively low compared to the nuclear DNA, the differences in methylation between the WT and MASLD sample are also relatively small. However, Goldsmith et al. observed similar percentages of CpG methylation in HepaRG cells³⁸ and Corsi et al. demonstrated that only small differences in methylation (0,6-1.7%) in the Mt-CO₁, Mt-CO₃ and Mt-TL₁ genes are sufficient to predict future cardiovascular disease risk in overweight and obese patients³⁹. Therefore we further explored mitochondrial gene specific methylation patterns (Figure 3).

As shown in figure 3 some regions of the mtDNA show a clear higher methylation percentage in both CpG and GpC methylation in the MASLD sample compared to the untreated WT sample. Remarkably, those regions span the same genes, which suggests that only parts of the mtDNA are available for methylation. In line, Goldsmith et al. showed that also in liver tissue consistent CpG sites are methylated in liver cancer and normal liver tissue. Although only small differences in methylation percentages were found between the two samples, some CpG sites with the smallest p-value could partially discriminate tumors from non-tumors tissue³⁸. Moreover, Rebelo et al. showed that the expression and thus occupancy of TFAM on the mitochondrial DNA influences mtDNA accessibility for DNA methylation¹². Interestingly, the genes that are mostly affected in our results are proteins that are part of the cytochrome C oxidase and NADH dehydrogenase which translate into complex IV and I, respectively of the ETC cycle that is known to be important for lipid metabolism and energy production. This generates the question whether accessibility and methylation is regulating the expression of mitochondrial genes to overcome metabolic challenges according to the environmental stressor.

Although more samples need to be analysed before final conclusions can be made about mitochondrial gene-specific methylation related to MASLD, it is interesting to note that some similarities could be detected with previously published data. One of the differently methylated genes in our data is the Mt-ND6 region that shows an average 2% higher CpG and GpC methylation compared to the WT sample. Interestingly Pirola et al. showed that this region is significantly hypermethylated in MASH patients, correlating with MAS scoring and fibrosis. Although in the study of Pirola et al. no correlation was found between Mt-CO₁ methylation and MASH, there was an inverse correlation found between methylation and high-density lipoprotein (HDL) cholesterol levels and a positive correlation with BMI²⁰. Since our previous results showed an increase in lipid droplets after treatment with 1mM FFA, the positive correlation with BMI could explain the hypermethylation of some parts of the Mt-CO₁ gene in our results. Moreover, hypermethylation of this gene has been associated with cardiovascular diseases and could therefore be a predictive mark for patients with obesity and MASLD^{17,39}. New observations in our pilot experiment include a whole region spanning genes of the NADH dehydrogenase (ND3-6), that have an average 2% increase in GpC methylation in the MASLD sample compared to the WT sample. Besides, there are a lot of Mt-tRNAs that are hypermethylated in the MASLD sample, which could affect mitochondrial gene transcription and/or ETC functions. However, according to our knowledge, these observations have not been previously reported in the context of MASLD and therefore need further investigation.

4.5 Conclusion

Today, most evidence for mtDNA methylation has been obtained in cancer, besides cardiovascular diseases, neurodegenerative diseases, aging and senescence. For example, methylation differences in the D-loop allow to discriminate between non-cancerous and cancerous tissue¹⁶. Surprisingly, the role of mtDNA methylation in MASLD remains poorly characterized, despite clear evidence of mitochondrial dysfunctions in MASLD. According to our knowledge only Pirola et al. showed an association between MASH and hypermethylation of the Mt-ND6 region²⁰. However research studies on the functional role of these methylation changes in mitochondrial function are lacking. Our pilot study showed some similarities with previously published data, including a hypermethylation of the Mt-ND6 region in FFA treated HepG2 cells mimicking steatosis in MASLD patients. Moreover, it revealed that mostly genes related to the ETC cycle are differentially methylated in the FFA treated HepG2 cells compared to the untreated WT HepG2 cells. Although this observation needs further validation, we wanted to investigate whether these methylation changes can be related to changes in mitochondrial function and may contribute to MASLD progression. Therefore in the next chapter we analysed different aspects of mitochondrial function mtDNA methylation and gene expression regulation in HepG2 cells upon mitochondrial overexpression of CpG and GpC specific methyltransferases to estimate the contribution of mtDNA methylation in MASLD disease aetiology.

Results: Chapter 4

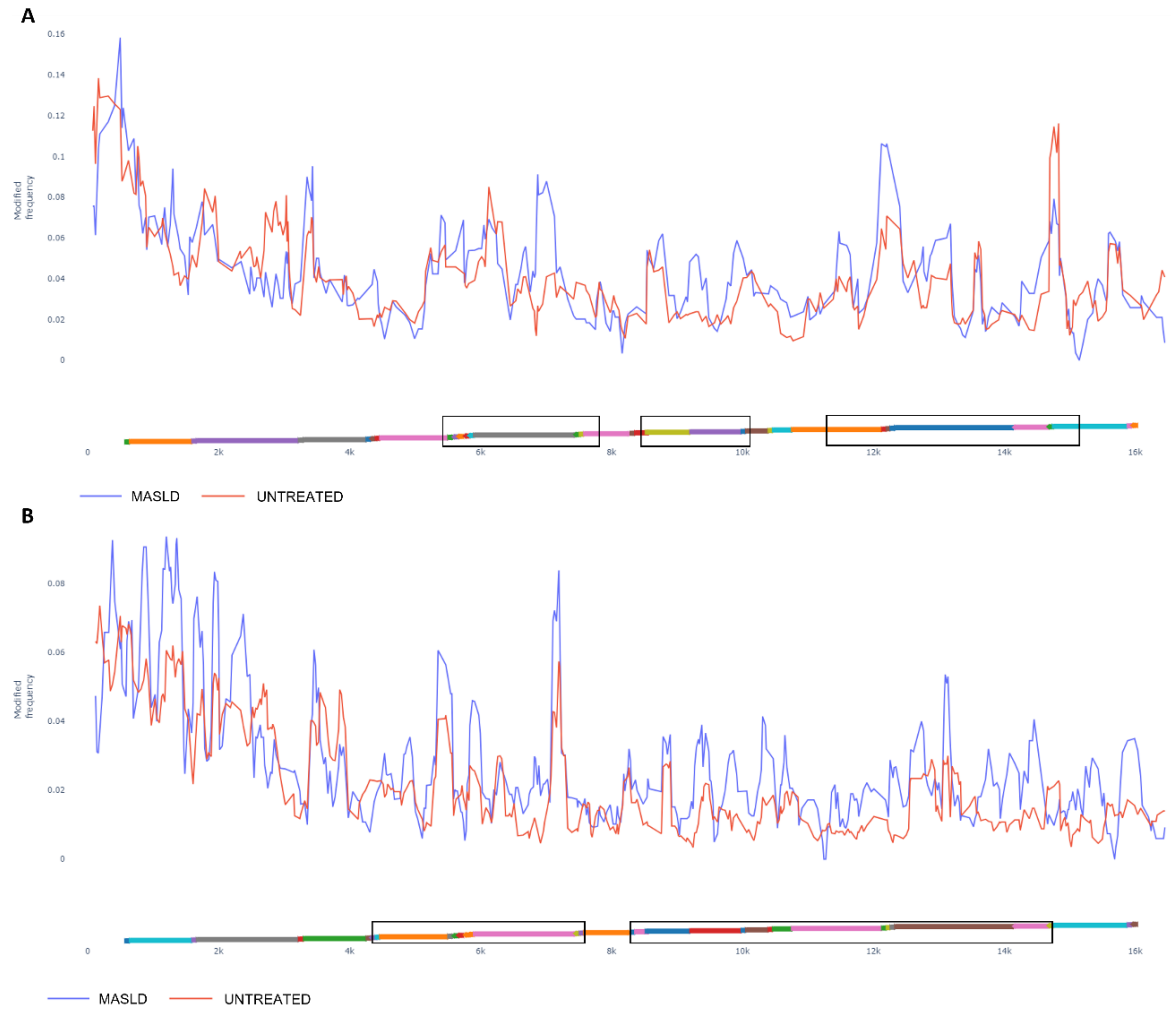


Figure 2: Modified frequency (Y-axis) showing the per position frequency of CpG (A) or GpC (B) methylation in the mitochondrial genome (x-axis) of an untreated WT and a MASLD sample treated for 24h with 1mM FFA (n=1). Mitochondrial genes are represented as different colours in the x-axis with boxes to show the enlarged regions in figure 3.

Results: Chapter 4

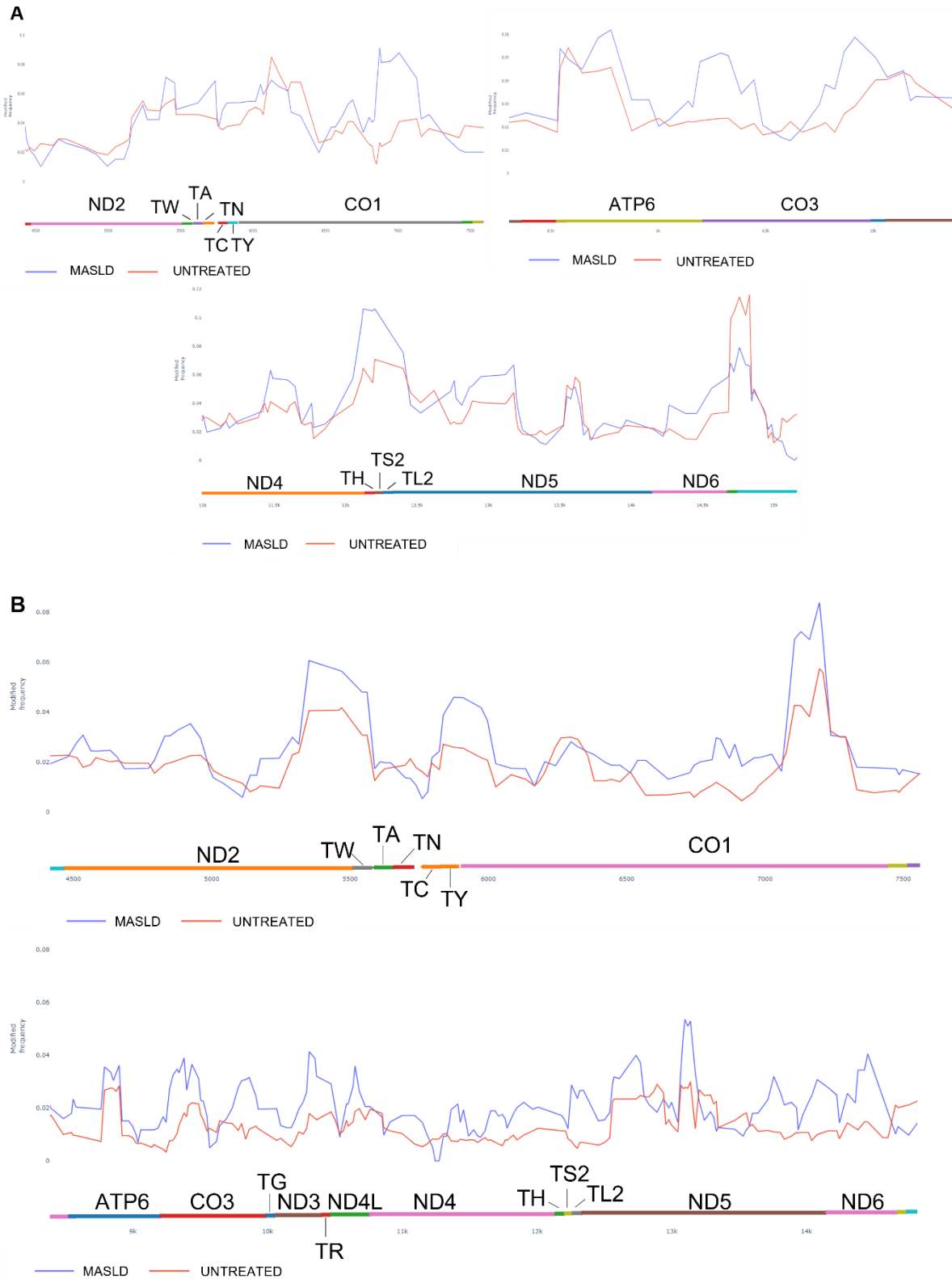


Figure 3: Modified frequency showing the per position frequency of CpG (A) or GpC (B) methylation of enlarged regions of the mitochondrial DNA of an untreated WT and a MASLD sample treated for 24h with 1mM FFA (n=1). Mitochondrial genes are represented as different colours in the x-axis and the representative gene is written above this colour.

4.6 Supplementary material

Supplementary table 1: Overview of qPCR primers used in this study.

Gene	Forward primer (5' → 3')	Reverse primer (5' → 3')
PPAR α	ACGATTCGACTCAAGCTGGT	GTTGTGTGACATCCCGACAG
APOA5	AATGTCTGCTCTCTGTGCC	AGCCATGCTTGCCATTACCT
SCD1	GGGCTTTGAAGTGTGCTGTG	GAGGGATGGGTAGGACTGGT
CPT1A	CCTACCACGGGTGGATGTTT	CAACATGGGTTTTCGGCCTG
PLIN2	GCTGAGCACATTGAGTCACG	TGGTACACCTTGGATGTTGG
HADH	TGTCGGACTGGATACTACGA	GATGGGCTGGGCTGATGTAA
tRNA _{LEU}	CACCCAAGAACAGGGTTTGT	TGGCCATGGGTATGTTGTTA
B2M	TGCTGTCTCCATGTTTGATGTATCT	TCTCTGCTCCCCACCTCTAGGT
GAPDH	GCTCTCTGCTCCTCCTGTTC	ACGACCAAATCCGTTGACTC

4.7 References

1. Spinelli, J. B. & Haigis, M. C. The multifaceted contributions of mitochondria to cellular metabolism. *Nat Cell Biol* **20**, 745–754 (2018).
2. Ramanathan, R., Ali, A. H. & Ibdah, J. A. Mitochondrial Dysfunction Plays Central Role in Nonalcoholic Fatty Liver Disease. *Int J Mol Sci* **23**, 7280 (2022).
3. Moore, M. P. *et al.* Compromised hepatic mitochondrial fatty acid oxidation and reduced markers of mitochondrial turnover in human NAFLD. *Hepatology* **76**, 1452–1465 (2022).
4. Koliaki, C. *et al.* Adaptation of Hepatic Mitochondrial Function in Humans with Non-Alcoholic Fatty Liver Is Lost in Steatohepatitis. *Cell Metab* **21**, 739–746 (2015).
5. Couvillion, M. T., Soto, I. C., Shipkovenska, G. & Churchman, L. S. Synchronized mitochondrial and cytosolic translation programs. *Nature* **533**, 499–503 (2016).
6. Criscuolo, D., Avolio, R., Matassa, D. S. & Esposito, F. Targeting Mitochondrial Protein Expression as a Future Approach for Cancer Therapy. *Front Oncol* **11**, (2021).
7. Quirós, P. M., Mottis, A. & Auwerx, J. Mitonuclear communication in homeostasis and stress. *Nat Rev Mol Cell Biol* **17**, 213–226 (2016).
8. Janssen, J. J. E., Grefte, S., Keijer, J. & de Boer, V. C. J. Mito-Nuclear Communication by Mitochondrial Metabolites and Its Regulation by B-Vitamins. *Front Physiol* **10**, (2019).
9. Liu, Y. *et al.* DNA methylation-calling tools for Oxford Nanopore sequencing: a survey and human epigenome-wide evaluation. *Genome Biol* **22**, 295 (2021).
10. Goldsmith, C. *et al.* Low biological fluctuation of mitochondrial CpG and non-CpG methylation at the single-molecule level. *Sci Rep* **11**, 8032 (2021).
11. Lüth, T. *et al.* Nanopore Single-Molecule Sequencing for Mitochondrial DNA Methylation Analysis: Investigating Parkin-Associated Parkinsonism as a Proof of Concept. *Front Aging Neurosci* **13**, (2021).
12. Rebelo, A. P., Williams, S. L. & Moraes, C. T. In vivo methylation of mtDNA reveals the dynamics of protein–mtDNA interactions. *Nucleic Acids Res* **37**, 6701–6715 (2009).
13. Shock, L. S., Thakkar, P. V., Peterson, E. J., Moran, R. G. & Taylor, S. M. DNA methyltransferase 1, cytosine methylation, and cytosine hydroxymethylation in mammalian mitochondria. *Proceedings of the National Academy of Sciences* **108**, 3630–3635 (2011).
14. Han, X. *et al.* Maternal trans-general analysis of the human mitochondrial DNA pattern. *Biochem Biophys Res Commun* **493**, 643–649 (2017).
15. Yang, H. Correlation between increased ND2 expression and demethylated displacement loop of mtDNA in colorectal cancer. *Mol Med Rep* (2012) doi:10.3892/mmr.2012.870.

16. Stoccoro, A. & Coppedè, F. Mitochondrial DNA Methylation and Human Diseases. *Int J Mol Sci* **22**, 4594 (2021).
17. Baccarelli, A. A. & Byun, H.-M. Platelet mitochondrial DNA methylation: a potential new marker of cardiovascular disease. *Clin Epigenetics* **7**, 44 (2015).
18. Bianchessi, V. *et al.* Methylation profiling by bisulfite sequencing analysis of the mtDNA Non-Coding Region in replicative and senescent Endothelial Cells. *Mitochondrion* **27**, 40–47 (2016).
19. Xu, Y. *et al.* Hypermethylation of Mitochondrial Cytochrome b and Cytochrome c Oxidase II Genes with Decreased Mitochondrial DNA Copy Numbers in the APP/PS1 Transgenic Mouse Model of Alzheimer's Disease. *Neurochem Res* **46**, 564–572 (2021).
20. Pirola, C. J. *et al.* Epigenetic modification of liver mitochondrial DNA is associated with histological severity of nonalcoholic fatty liver disease. *Gut* **62**, 1356–1363 (2013).
21. Wieckowski, M. R., Giorgi, C., Lebiezinska, M., Duszynski, J. & Pinton, P. Isolation of mitochondria-associated membranes and mitochondria from animal tissues and cells. *Nat Protoc* **4**, 1582–1590 (2009).
22. Sareen, D. *et al.* Mitochondria as the Primary Target of Resveratrol-Induced Apoptosis in Human Retinoblastoma Cells. *Investigative Ophthalmology & Visual Science* **47**, 3708 (2006).
23. Weerts, M. J. A. *et al.* Sensitive detection of mitochondrial DNA variants for analysis of mitochondrial DNA-enriched extracts from frozen tumor tissue. *Sci Rep* **8**, 2261 (2018).
24. Reumers, J. *et al.* Optimized filtering reduces the error rate in detecting genomic variants by short-read sequencing. *Nat Biotechnol* **30**, 61–68 (2012).
25. Schneider, V. A. *et al.* Evaluation of GRCh38 and de novo haploid genome assemblies demonstrates the enduring quality of the reference assembly. *Genome Res* **27**, 849–864 (2017).
26. Li, H. Minimap2: pairwise alignment for nucleotide sequences. *Bioinformatics* **34**, 3094–3100 (2018).
27. Li, H. *et al.* The Sequence Alignment/Map format and SAMtools. *Bioinformatics* **25**, 2078–2079 (2009).
28. Sedlazeck, F. J. *et al.* Accurate detection of complex structural variations using single-molecule sequencing. *Nat Methods* **15**, 461–468 (2018).
29. Jiang, T. *et al.* Long-read-based human genomic structural variation detection with cuteSV. *Genome Biol* **21**, 189 (2020).
30. Shao, H. *et al.* nplnv: accurate detection and genotyping of inversions using long read sub-alignment. *BMC Bioinformatics* **19**, 261 (2018).
31. Edge, P. & Bansal, V. Longshot enables accurate variant calling in diploid genomes from single-molecule long read sequencing. *Nat Commun* **10**, 4660 (2019).
32. Loman, N. J., Quick, J. & Simpson, J. T. A complete bacterial genome assembled de novo using only nanopore sequencing data. *Nat Methods* **12**, 733–735 (2015).

33. Hodson, L., Skeaff, C. M. & Fielding, B. A. Fatty acid composition of adipose tissue and blood in humans and its use as a biomarker of dietary intake. *Prog Lipid Res* **47**, 348–380 (2008).
34. Gómez-Lechón, M. J. *et al.* A human hepatocellular in vitro model to investigate steatosis. *Chem Biol Interact* **165**, 106–116 (2007).
35. Ramos, M. J., Bandiera, L., Menolascina, F. & Fallowfield, J. A. In vitro models for non-alcoholic fatty liver disease: Emerging platforms and their applications. *iScience* **25**, 103549 (2022).
36. Brunt, E. M., Neuschwander-Tetri, B. A., Oliver, D., Wehmeier, K. R. & Bacon, B. R. Nonalcoholic steatohepatitis: Histologic features and clinical correlations with 30 blinded biopsy specimens. *Hum Pathol* **35**, 1070–1082 (2004).
37. Brunt, E. M. Histopathology of nonalcoholic fatty liver disease. *World J Gastroenterol* **16**, 5286 (2010).
38. Goldsmith, C. *et al.* Low biological fluctuation of mitochondrial CpG and non-CpG methylation at the single-molecule level. *Sci Rep* **11**, 8032 (2021).
39. Corsi, S. *et al.* Platelet mitochondrial DNA methylation predicts future cardiovascular outcome in adults with overweight and obesity. *Clin Epigenetics* **12**, 29 (2020).

CHAPTER V

Mitochondrial GpC and CpG DNA hypermethylation cause metabolic stress-induced mitophagy and cholestophagy

Chapter 5

Mitochondrial GpC and CpG DNA hypermethylation cause metabolic stress-induced mitophagy and cholestophagy

Claudia Theys¹, Joe Ibrahim^{2,3}, Ligia Mateiu², Archibold Mposhi⁴, Laura García-Pupo¹, Tim de Pooter^{5,6}, Peter De Rijk^{5,6}, Mojca Strazisar^{5,6}, İkbal Agah İnce^{4,7}, Iuliana Vintea⁸ Marianne Rots⁴, Wim Vanden Berghe^{1*}

¹ Lab Protein Chemistry, Proteomics & Epigenetic Signaling (PPES), Department Biomedical Sciences, University of Antwerp, 2610 Wilrijk, Belgium.; claudia.theys@uantwerpen.be; wim.vandenbergh@uantwerpen.be

² Center of Medical Genetics, University of Antwerp and Antwerp University Hospital, 2650 Edegem, Belgium.

³ Center for Oncological Research, University of Antwerp and Antwerp University Hospital, 2650 Edegem, Belgium

⁴ Department of Pathology and Medical Biology, University of Groningen, University Medical Center Groningen, 9713 GZ Groningen, The Netherlands

⁵ Neuromics Support Facility, VIB Center for Molecular Neurology, VIB, Wilrijk, 2610 Antwerp, Belgium

⁶ Department of Biomedical Sciences, University of Antwerp, Wilrijk, 2610 Antwerp, Belgium.

⁷ Department of Medical Microbiology, School of Medicine, Acıbadem Mehmet, Ali Aydınlar University, 34752 Ataşehir, İstanbul, Türkiye

⁸ Pathophysiology lab, Infla-Med Centre of Excellence, Department of Biomedical Sciences, University of Antwerp, Antwerp, Belgium

*Corresponding author: wim.vandenbergh@uantwerpen.be

Conflict of Interest: The authors declare no conflict of interest

Published as: Theys, C.; Ibrahim, J.; Mateiu, L.; Mposhi, A.; García-Pupo, L.; De Pooter, T.; De Rijk, P.; Strazisar, M.; İnce, İ.A.; Vintea, I.; et al. Mitochondrial GpC and CpG DNA Hypermethylation Cause Metabolic Stress-Induced Mitophagy and Cholestophagy. Int. J. Mol. Sci. 2023, 24, 16412. <https://doi.org/10.3390/ijms242216412>

5.1 Abstract

Metabolic dysfunction associated steatotic liver disease (MASLD) is characterized by a constant accumulation of lipids in the liver. This hepatic lipotoxicity is associated with a dysregulation of the first step in lipid catabolism, known as beta oxidation, which occurs in the mitochondrial matrix. Eventually, this dysregulation will lead to mitochondrial dysfunction. To evaluate possible involvement of mitochondrial DNA methylation in this lipid metabolic dysfunction, we investigated the functional metabolic effects of mitochondrial overexpression of CpG (MSssl) and GpC (MCviPI) DNA methyltransferases in relation to gene expression and (mito)epigenetic signatures. Overall, the results show that mitochondrial GpC and to a lesser extent CpG methylation increase bile acid metabolic gene expression, inducing the onset of cholestasis through mito-nuclear epigenetic reprogramming. Moreover, both increase expression of metabolic nuclear receptors and thereby induce basal overactivation of mitochondrial respiration. The latter promotes mitochondrial swelling favoring lipid accumulation and metabolic-stress induced mitophagy and autophagy stress responses. In conclusion, both mitochondrial GpC and CpG methylation create a metabolic challenging environment that induces mitochondrial dysfunction, which may contribute to the progression of MASLD.

Keywords: Mitochondria, MASLD, Epigenetics, Lipid metabolism, Bile acid metabolism, Cholestasis, Autophagy

5.2 Introduction

Metabolic dysfunction associated steatotic liver disease (MASLD) is a growing epidemic, which mirrors the increased trend of obesity in Western diet consuming countries. It has an estimated prevalence of 20–30% in Europe and is the most common cause of chronic liver disease worldwide^{1,2}. MASLD consists of a spectrum of liver disorders ranging from simple steatosis to metabolic dysfunction associated steatohepatitis (MASH) which predisposes patients to further fibrosis, cirrhosis and hepatocarcinoma but also extrahepatic diseases, especially cardiovascular diseases^{3,4}. Despite the increasing prevalence, there is still no FDA approved treatment for MASLD. A change in lifestyle including a restricted diet and an increase in exercise is currently the only approved therapy. However this treatment is difficult to maintain, which causes relapse in a lot of patients^{5,6}. Therefore a lot of research has been focusing on the identification of new therapeutic targets.

There are several risk factors for the development of MASLD including environment, genetics and epigenetics. It is known that environmental factors including diet and pollutants are related to an increased risk for the development of MASLD⁷. Besides, different mutants have been associated with an increased risk for MASLD development, with mutations in the PNPLA3 gene as one of the main genetic risk factors^{7,8}. However, neither environmental factors nor genetic factors alone can give a satisfactory explanation for the high prevalence of MASLD. Therefore, researchers are now also searching for epigenetic factors contributing to the development and progression of MASLD. Interestingly, epigenetic modifications are both related to environmental exposures and genetic predisposition. These modifications include DNA methylation, histone modifications and miRNAs⁹, although most of the epigenetic studies in MASLD patients have mainly focused on DNA methylation, revealing MASLD stage dependent signatures^{10–17}. Besides nuclear DNA methylation patterns, MASLD specific methylation changes have recently also been reported in mitochondrial DNA^{18–21}.

Mitochondria are critically involved in MASLD progression, because fatty acid beta oxidation takes place in the mitochondrial matrix which is part of lipid catabolism²². Hence, in the steatosis stage hepatocytes try to overcome excess lipid accumulation by increasing the beta oxidation in the mitochondria. This mitochondrial hyperactivation can result in oxidative mitochondrial damage and eventually a complete metabolic shutdown due to mitochondrial dysfunction. The latter is closely linked to MASH, showing less active mitochondria and more mitochondrial stress which is a contributing factor to other complications including inflammation and fibrosis^{23,24}. Whether epigenetic modifications are able to finetune mitochondrial metabolic respiratory functions following lipid-induced stress has not yet been functionally addressed. Interestingly, DNA methyltransferase 1 (DNMT1) can translocate into the mitochondria and thereby contribute to the hypermethylation of the mtDNA during MASLD progression because MASH patients show an increased expression of DNMT1^{25,26}. Indeed, Pirola et al. and Mposhi et al. showed that MASH patients have an increased methylation of the *ND6* region of the mitochondrial DNA, which resulted in a downregulation of ND6 expression^{21,26}. Mposhi et al. further functionally confirmed these findings by bisulfite pyrosequencing, qPCR and nanopore-episequencing approaches in a mouse model and in transgenic steatosis HepG2 cell models with mitochondrial overexpression of CpG (MSssl) or GpC (MCviPI) specific DNA methyltransferases, which similarly revealed evidence for MASH-specific lipid metabolic changes in gene expression²¹. Following up on these observations,

we here applied a systems biology approach to further address the functional contribution of mitochondrial DNA methylation in metabolic dysfunctions during MASLD associated lipid accumulation stress. More particularly, to resolve mito-nuclear epigenetic crosstalk associated with mitochondrial DNA methylation and functional mitochondrial changes in morphology, respiratory activity and metabolic competence we performed an in depth integrative genome-wide transcriptome-epigenome analysis.

5.3 Material and methods

5.3.1 Cell culture

The Human hepatoma cells (HepG2) cell lines overexpressing mitochondria-targeted DNMTs MCviPI, MSsI or inactivated MCviPI (MCviPI mutant) and the un-transfected control (WT) HepG2 cells were a kind gift of prof. dr. Marianne Rots (UMCG, Groningen)²¹. The overexpressing cell lines were constructed as described by Van der Wijst et al.²⁷. Briefly, the sequence of the MCviPI, MCviPI mutant (catalytically inactive) and MSsI was cloned in a pCDH-CMV-MCS-SV40-puro plasmid, resulting in a pCDH-CMV-master synthetic construct-conII-SV40-puro containing a mitochondrial localisation signal (MLS) followed by [MCviPI/ MCviPI mutant/ MSsI] and two nuclear export signals (NES). This construct was subsequently lentiviral transduced in HepG2 cells followed by antibiotic selection with puromycin for positive clones.

Cells were cultured in Dulbecco's modified Eagle medium (DMEM, Gibco, Thermo Fisher Scientific, 41965039) supplemented with 10% foetal bovine serum (Gibco, Thermo Fisher Scientific, 10270106), 1% penicillin-streptomycin solution (Gibco, Thermo Fisher Scientific, 15140122) and 1mM pyruvate. Both cell lines were cultured in T75 or T25 flasks in a humidified atmosphere (37°C and 5% CO₂).

5.3.2 FFA medium

The FFAs medium to obtain MASLD-like conditions is composed of oleic (OA) and palmitic (PA) acid in a 2:1 ratio. Stock solutions of 0.66M oleic acid and (1.32M) palmitic acid (Sigma- Aldrich, Germany) were prepared in isopropanol. Equal amounts of oleic and palmitic acid were mixed to prepare a FFA stock of 1 mM FFA. FFA-free bovine serum albumin (BSA) was dissolved in serum-free DMEM medium without antibiotics at the final concentration of 1% and then sterilized using syringe-driven 0.22 µm filters. Afterwards, the medium was supplemented with the mixture of FFA at the final concentration of 1 mM and sonicated for 6- 8 hours until FFA was completely dissolved using a Branson 3200 sonication bath. FFAs medium was protected from light and stored at 4 °C.

5.3.3 Nanopore sequencing

DNA was extracted using the Qiagen Blood Tissue DNA isolation kit (Qiagen, 69504) according to the manufacturer's protocol. The quality of the extracted DNA was measured using the Qubit 4 Fluorometer (Thermo Fisher Scientific, Q33238) and Qubit™ dsDNA BR kit (Thermofisher, Q32850) for concentration, Little Lunatic (Unchained Labs) for purity and Fragment Analyzer (DNF-492 Large Fragment kit, Agilent) for integrity using either the "Agilent DNF-464 HS Large Fragment Kit" (integrity of extracted hmw-DNA) or the "Agilent DNF-492 Large Fragment Kit" (fragmentation and size selection). After quality control, 5µg of DNA was fragmented using Megaruptor 3 (Diagenode) to final fragment sizing 15-20kb, which resulted also in linearization of mtDNA and exposing fragments' ends for end repair and adapter ligation. After Fragmentation, small molecules were depleted using Short Read Eliminator kit (SRE XS, PacBio), depleting short DNA fragments <10 kb

progressively and DNA <4 kb almost completely. Library preparation was started with 175fmol size selected DNA per sample (+/-2µg of fragmented, size-selected DNA) and consisted of FFPE DNA end repair in combination with a preparation of the ends for adapter attachment, native barcode ligation and sequencing adapter ligation with the use of the Native barcoding expansion 13-24 kit (Oxford Nanopore Technologies, EXP-NBD114) in conjunction with the Ligation sequencing kit (Oxford Nanopore Technologies, SQK-LSK109). Prior to the final sequencing adapter ligation, samples were pooled equimolar for optimal read distribution. Sequencing was performed on the R9.4.1 PromethION Flow Cell that had 8750 pores available for sequencing. In total 50fmol of final library was loaded on the Flow cell (~550ng). Total sequencing time was 80h on PromethION 24 (Oxford Nanopore Technologies), with a flush using DNase I before loading of fresh library at 24 and 48h of sequencing. The sequencing run produced 12.49 M reads with an N50 of 17.39 kb, resulting in a total base output of 153.16 Gb and a total amount of data of 1.2TB. MtDNA is well covered performing shallow gDNA sequencing (60-80x vs 1x for gDNA). Reads were basecalled using GUPPY (version 6.0.6). Further analysis was performed using a pipeline integrated in genomecomb²⁸. Reads were aligned to the hg38 genome reference²⁹ using minimap2³⁰ and the resulting sam file was sorted and converted to bam using samtools³¹. Structural variants were called using sniffles³², cuteSV³³ and npinv³⁴. The resulting variant sets of different cell lines were combined and annotated using genomecomb²⁸. Nanopolish analysis (version 0.13.2)³⁵ was used for CpG and GpC methylation analyses on the mitochondrial genome without applying NUMT filtering, as NUMTs were shown to only have a marginal impact on methylation assessment^{35,36}. Raw nanopore epi-sequencing data of transgenic HepG2 cell models with mitochondrial overexpression of CpG (MSSSI) or GpC (MCviPI) specific DNA methyltransferases²¹, have been deposited in the NCBI GEO database with accession number PRJNA95689.

5.3.4 RNA extraction and RNA sequencing

Total RNA was extracted with the RNeasy kit (Qiagen, 75162) from the 3 cell lines (MCviPI mutant, MSssl, MCviPI) both untreated or treated with 1mM FFA for 24h, according to the manufacturer's protocol (n=4 biological replicates per cell line per treatment, except untreated MCviPI mutant n=3). Afterwards RNA quantity was determined using Qubit™ RNA Broad Range Assay kit (Thermo Fisher Scientific, Q10210) with the aid of the Invitrogen Qubit™ Fluorometer (Thermo Fisher Scientific, Q33238). The extracted RNA was stored at -80°C and subsequently sent to Novogene Leading Edge Genomic Services & Solutions where RNA integrity was determined using the 2100 Bioanalyzer system (Agilent Technologies, USA). All 40 samples with acceptable quality level (RNA content ≥20ng/µL, OD260/280 ≥ 2.0 and RIN ≥ 4.0) were included for sequencing library preparation and RNA sequencing analysis. In brief messenger RNA was purified from total RNA using poly-T oligo-attached magnetic beads. After fragmentation, the first strand cDNA was synthesized using random hexamer primers, followed by the second strand cDNA synthesis and library construction. The library was checked with Qubit and real-time PCR for quantification and bioanalyzer for size distribution detection. Quantified libraries were pooled and 150 bp paired-end sequenced on the Illumina Novaseq6000 platform.

The quality of the raw sequencing reads was evaluated using FastQC (v0.11.5)³⁷ and subsequent alignment to genome reference consortium human build 38 (GRCh38/hg38) was performed with the STAR (v.2.7.3a) tool³⁸. Differential gene expression and pathway analysis was performed using DESeq2 R package software³⁹ and the Omics Playground tool (v2.8.12) platform which was also used for further visualisation. Protein interaction networks were generated using the STRING database

(v11)⁴⁰. RNA sequencing was validated by qPCR and deposited in the NCBI GEO database with accession number GSE241526.

5.3.5 Quantitative polymerase chain reaction (qPCR)

After RNA extraction, total RNA was converted into cDNA with the iScript™ cDNA Synthesis Kit (BioRad, 1708890) according to the manufacturer's protocol. Next, qPCR analysis was performed using the PowerUp SYBR™ green PCR master mix (Thermo Fisher Scientific, USA) according to the manufacturer's instructions. In brief, a 20 µl reaction volume mix per sample was prepared containing 10 µl PowerUp SYBR Green Master Mix, 0.4 µM forward and reverse primer, and nuclease-free water. The following PCR program was applied on the Rotor-Gene Q qPCR machine of Qiagen: 95°C for 10 min, 40 cycles denaturation (95°C, 15 s) and annealing/extension (60°C, 1 min), and dissociation (60–95°C). Each sample was run in triplicate. The median value of the triplicates was taken to calculate the $\Delta\Delta C_t$ -values using B2M as the normalization gene. B2M, GSTA1, GSTA2, NR5a2, SLC22a7, mtND1, mtCOX1 and mtCYB primer sequences (supplementary table 1) were designed by Primer3 and synthesized by Integrated DNA Technologies (IDT, USA). Statistical analysis was carried out using a One-Way ANOVA test with Tukey's correction for multiple comparisons. P-value < 0.05 was considered statistically significant.

5.3.6 Methylation analysis

Whole-genome methylation profiling targeting over 935,000 CpG sites was performed on total DNA of the MCviPI mutant and MCviPI using the Infinium MethylationEPIC array (Illumina, San Diego, CA, USA) at the Centre for Medical Genetics (UZA, University of Antwerp), both untreated or treated with 1mM FFA for 24h. Genomic DNA (gDNA) was extracted from the cells using the Dneasy Blood & Tissue Kit (Qiagen, 69504) according to the manufacturer's protocol. DNA concentration and purity was determined by the Qubit 4 Fluorometer (Thermo Fisher Scientific, Q33238). Next, 750 ng DNA was bisulphite converted with the EZ DNA Methylation Kit (Zymo Research, D5001/D5002, Irvine, CA, USA) according to the manufacturer's instructions. Successful bisulphite conversion was confirmed by PCR with the PyroMark PCR kit (Qiagen) in a region of the Sall3 gene (supplementary table 1). The resulting PCR products were run on a 2% agarose gel. This converted DNA was then further hybridized with Infinium MethylationEPIC array (Illumina, San Diego, CA, USA) according to the manufacturer's instructions. In brief, converted DNA was amplified overnight and fragmented enzymatically. Subsequently, DNA was precipitated and resuspended in hybridization buffer and afterwards dispensed onto the BeadChips. The hybridization procedure was performed at 48°C overnight using an Illumina Hybridization oven. After hybridization, free DNA was washed away, and single nucleotide extension followed by fluorescent readout was performed. The BeadChips were imaged using an Illumina HiScan (Illumina, San Diego, CA, USA). The platform interrogates more than 935,000 methylation sites per sample at single-nucleotide resolution. Annotations for the interrogated sites were taken from Illumina's BeadChip array manifest based on genome reference consortium human build 37 (GRCh37/hg19). Raw intensity data from IDAT files was read and processed in R (v. 4.2.0) via the minfi⁴¹ R package. Data pre-processing consisted of masking probes with poor design, control probes, X-/Y chromosome probes and non-cg and non-ch probes. Probes with detection p-values > 0.01 in more than 50% of the samples were filtered out. No samples had more than 10% missing values thus, all were considered for further analysis. For quality control, the ratio of log₂ median intensities (methylated and unmethylated) along with β -value densities were calculated. β -values were then further processed using ChAMP (v 2.21.1)⁴². The

difference in signal intensity between the two-colour channels (dye bias correction) was corrected for using the beta mixture interquartile matrix (BMIQ) method⁴³. Methylation levels were reported as β -values ranging from 0 for unmethylated probes to 1 for fully methylated probes. To identify significantly differentially methylated CpGs between the different groups, parametric linear mixed models were used via ChAMP⁴². P-values were adjusted for multiple testing using the Benjamini–Hochberg correction ($p < 0.01$). Further Metascape pathway analysis of genes with a delta beta (DB) $> |0.1|$ and FDR < 0.05 was performed with the online Metascape Web tool⁴⁴. Methylation data was deposited in the NCBI GEO database with accession number GSE240988.

5.3.7 Lipid quantification with Adipored

AdipoRed Adipogenesis Assay (Lonza, Walkersville, MD, USA) was used to quantify intracellular lipid accumulation in all 3 cell lines (MCviPI mutant, MSssl, MCviPI), both untreated or treated with 1mM FFA for 24h according to the manufacturer's protocol (n=3 biologically independent samples per cell line per treatment). Briefly, medium of treated cells was replaced by phosphate buffered saline (PBS) and incubated with the AdipoRed Reagent. Afterwards, fluorescence was measured at 485 nm excitation and 572 nm emission, using a microplate reader (FLUOstar Omega, BMG Labtech). Statistical analysis was carried out using a Two-Way ANOVA test with Tukey's correction for multiple comparisons. P-value < 0.05 was considered statistically significant.

5.3.8 Lipid peroxidation

Cellular lipid reactive oxygen species were measured in live cells through oxidation of the BODIPYTM 581/591 C11 reagent using the Image-iT™ Lipid Peroxidation Kit (C10445, ThermoFisher Scientific, Waltham, MA, USA) according to the manufacturer's protocol. In short, cells were seeded in 6 well plates at a density of 5×10^4 cells/well and treated the next day for 24h with 1mM FFA (2:1 ratio oleic acid and palmitic acid respectively) or 2h with 100 μ M cumene hydroperoxide (positive control). Cells were subsequently incubated for 30 min with 10 μ M Image-iT™ Lipid Peroxidation Sensor at 37 °C. After incubation, cells were collected by trypsinization with TrypLE Express Enzyme (ThermoFisher Scientific, Waltham, MA, USA). Cells were washed three times with pre-warmed PBS and the fluorescence shift from 590 nm to 510 nm representing oxidation of the reagent by lipid hydroperoxides was measured with the CytoFlex flow cytometer (Beckman Coulter Life Sciences, Indianapolis, IN, USA). Finally, the 510/590 ratio was calculated and visualized as a ratio showing red to green shift. Hence the more lipid peroxidation, the lower the red to green shift will be.

5.3.9 Mitochondrial visualisation

MitoTracker™ Red CMH2Xros (Thermofisher, M7513) was used to visualise and quantify mitochondria in all 3 cell lines (MCviPI mutant, MSssl, MCviPI), both untreated or treated with 1mM FFA for 24h according to the manufacturer's protocol (n=3 biologically independent samples per cell line per treatment). Briefly, cell were seeded at a density of 4×10^4 cells/well in a 96 well plate and treated with 1mM FFA for 24h the next day. Subsequently, medium was replaced with staining medium consisting of DMEM medium (DMEM, Gibco, Thermo Fisher Scientific, 41965039) without FBS with a final concentration of 250nM Mitotracker and incubated for 30 min. Afterwards medium was replaced by complete medium and cells were observed with the Olympus CKX53 fluorescence microscope (Olympus, Antwerp, Belgium) or red fluorescence was measured at 579 nm excitation and 599 nm emission, using the Tecan Spark Cyto (Tecan, Switzerland). Statistical analysis was

carried out using a Two-Way ANOVA test with Šidák's correction for multiple comparisons. P-value < 0.05 was considered statistically significant.

5.3.10 Cell death assay – Ferroptosis screening

Sytoxgreen (Invitrogen, S7020) was used to quantify cell death in all 3 cell lines (MCviPI mutant, MSssl, MCviPI), after treatment with varying concentrations of ferroptosis inducer RSL3 (0-20 μ M, 1:2 dilution steps) according to the manufacturer's protocol (n=3 biologically independent samples per cell line). Briefly, cell were seeded at a density of 5×10^5 cells/well in a 96 well plate and treated with RSL3 for 24h. Afterwards, SYTOX green was added and fluorescence was measured at 485 nm excitation and 520 nm emission, using a microplate reader (FLUOstar Omega, BMG Labtech). Statistical analysis was carried out using a Two-Way ANOVA test with Tukey's correction for multiple comparisons. P-value < 0.05 was considered statistically significant.

5.3.11 Immunofluorescence staining

The three overexpressing HepG2 cell lines (MCviPI mutant, MSssl and MCviPI) were seeded at a density of 0.3×10^6 cells/well in a 6 well plate and incubated with 250nm μ M MitoTracker Red CMXRos (Invitrogen) for 30 min at 37°C, 5% CO₂. Cells were washed in PBS and fixed with 4% paraformaldehyde for 15 min and then permeabilized and blocked with 0.1% Triton X-100 and 1% BSA in PBS for 1h. Subsequently, cells were incubated with a primary antibody directed against HA-tag (Sigma-Aldrich, H3663) diluted 1:250 in PBS containing 2.5% BSA overnight at 4°C. After washing, they were incubated for 1 h at room temperature with goat anti-mouse Alexa Fluor™ 488 (Invitrogen; A-11001), diluted in 1:500 in PBS containing 2.5% BSA and *washed* again. After immunolabeling, cells were incubated with NucBlue™ Fixed Cell ReadyProbes™ Reagent (DAPI) (Invitrogen; R37606) according to the manufacturer's protocol and imaged with the Leica DMI8 microscope (Leica Microsystems, Wetzlar, Germany) in the Leica Application Suite X 3.7.4.23463.

5.3.12 Seahorse XFp analyzer

Mitochondrial respiratory function was examined using the Seahorse XFp Cell Mito Stress Test Kit (Agilent Technologies,103010-100) according to the manufacturer's instructions. Briefly, 8×10^3 cells/well resuspended in 80 μ L complete DMEM were seeded in an 8 well XFp cell culture miniplate (Agilent Technologies,103025-100; 3 wells with untreated cells and 3 wells with cells treated for 24h with 1mM FFA of the same cell line). The day after the 24h treatment, XF DMEM pH 7.4 (assay medium), supplemented with Seahorse XF Glucose (10 mM), Seahorse XF Pyruvate (1 mM) and Seahorse XF L-Glutamine (2 mM) was used to rinse the cells (60 μ L of growth medium is removed, 200 μ L of assay medium is added, 200 μ L medium is removed and 160 μ L of assay medium is added) and the cell culture miniplate was placed into a 37 °C non-CO₂ incubator for 45 minutes to 1 hour prior to the assay. Next, the Seahorse was calibrated and loaded with the XFp sensor cartridge filled with 1.5 μ M oligomycin (Port A), 3 μ M FCCP (Port B) and 0.5 μ M Rotenone/Antimycin A (Port C) . Afterwards the cell culture XFp miniplate was loaded into the Seahorse XFp analyzer (Seahorse Biosciences, Agilent Technologies) and real-time oxygen consumption rate was measured for 1.5 h. First baseline respiration was measured (Basal OCR) prior to mitochondrial perturbation by sequential injection of 1.5 μ M oligomycin (a complex V inhibitor to decrease the electron flow through ETC); 3 μ M FCCP (the uncoupling agent to promote maximum electron flow through ETC); and a mixture of 0.5 μ M Rotenone/Antimycin A (complex I and complex II inhibitors, respectively, to shut down the mitochondria-related respiration). Data was analysed using with Agilent Seahorse

analytics. Statistical analysis was carried out using a Two-Way ANOVA test with Tukey's correction for multiple comparisons. P-value < 0.05 was considered statistically significant.

5.3.13 Electron microscopy

Cells were seeded in a T25 culture flask in a humidified atmosphere (37°C and 5% CO₂). Reaching approximately 70% confluency, cells were trypsinized (Thermo Fisher Scientific, 25300062) and 1×10^6 were pelleted and fixed in 0.1 M sodium cacodylate-buffered (pH 7.4) 2.5% glutaraldehyde and 0.05% CaCl₂·2H₂O solution at 4°C overnight. Fixative was removed and the sample was rinsed three times with 0.1 M sodium cacodylate, pH 7.4 (Sigma-Aldrich, 6131-99-3) containing 7.5% saccharose (Sigma-Aldrich, 57-50-1) at room temperature. Next, cells were incubated for 1 h in 1% osmium tetroxide (OsO₄) (Sigma-Aldrich, 20816-12-0). After dehydration in an ethanol gradient, cells were embedded in EM-bed 812 resin mixture (Electron Microscopy Sciences, EMS14120). Ultrathin sections were stained with lead citrate and samples were examined in a Tecnai G2 Spirit Bio Twin Microscope (ThermoFisher Scientific, FEI, Eindhoven, The Netherlands) at 120 kV. Quantification of the mitochondrial morphology was performed manually by delineating mitochondria and measuring circularity, aspect ratio ($[(\text{major axis})/(\text{minor axis})]$), reflects the 'length-to-width ratio) and surface area in Fiji⁴⁵ as described by Lam et al.⁴⁶ Statistical analysis was carried out using a One-Way ANOVA test with Dunnett's correction for multiple comparisons. P-value < 0.05 was considered statistically significant.

5.4 Results

5.4.1 Overexpression of mitochondrial targeted DNMTs promote GpC and CpG mtDNA hypermethylation

Mitochondria play a crucial role in lipid catabolism, because the beta oxidation is regulated in the mitochondrial matrix²². Thus, it is not surprising that mitochondrial dysfunctions are involved in lipid metabolic disorders such as MASLD. Mposhi et al. and Pirola et al. reported that the mitochondrial ND6 region, an essential component of Complex I of the OXPHOS cycle, is hypermethylated and downregulated in cell lines overexpressing a mitochondrial targeted CpG-specific DNMT (MSssl) or a GpC-specific DNMT (MCviPI) and MASH patients compared to patients with steatosis^{21,26}. To further dissect how mitochondrial DNA methylation promotes onset-progression of MASLD in the latter *in vitro* steatosis model with mitochondrial CpG and GpC DNA methyltransferases, we combined genome-wide transcriptomic-epigenomic systems biology approaches with functional mitochondrial assays to compare morphology, respiratory activity and metabolic competence in the different setups. First, changes in mitochondrial CpG and GpC DNA methylation levels were confirmed by Nanopore episequencing in the MCviPI and MSssl DNMT overexpressing HepG2 cell lines showing specifically increased CpG and GpC mtDNA methylation, versus low baseline mtDNA methylation levels in the mock transfected MCviPI DNMT mutant and un-transfected (WT) HepG2 cell lines, as observed earlier by Mposhi et al²¹ (Figure 1). Generally, there was a coverage of 60-80x of the mitochondrial DNA which is sufficient for qualitative and quantitative mapping of mitochondrial methylation changes. The un-transfected naive HepG2 cell line (WT) which lacks DNMT overexpression and the HepG2 cell line which overexpresses a MCviPI-deficient DNMT (MCviPI mutant), were both used as baseline reference mtDNA methylation control cell lines (mean methylation frequency \pm SD: WT- CpG Me 0.040 \pm 0.04 or 4.0 \pm 0.4%, MCviPI mutant CpG Me 0.041 \pm 0.04 or 4.1 \pm 0.4%; WT GpC Me 0.019 \pm 0.02 or 1.9 \pm 0.2%, MCviPI mutant GpC

0.021±0.02 or 2.1±0.2%). This reveals that baseline CpG methylation is slightly more abundant than GpC mtDNA methylation in both cell lines.

The MSssl cell line which overexpresses a CpG-specific bacterial DNMT MSssl shows an increased overall CpG methylation of 20%, which is a clear increase compared to the untransfected (WT) and MCviPI mutant cell line (Figure 1A). Moreover, the MSssl cell line shows almost no GpC methylation, indicating that the MSssl DNMT induces predominantly CpG methylation (Figure 1B). The MCviPI cell line overexpressing the viral GpC DNMT MCviPI shows an increased global GpC methylation of 20%, which is a clear increase compared to the control WT and MCviPI mutant cell lines (Figure 1B). Interestingly, the MCviPI cell line also reveals a global 10% increase in CpG methylation, which not present in the MCviPI mutant cell line (Figure 1A). This suggests that the MCviPI GpC-inducing DNMT also elicits partial CpG methylation in the mitochondrial genome. As such, the MCviPI mutant overexpressing cell line acts as a robust negative control for both CpG and GpC mtDNA methylation. Since the amount of CpG methylation in the MCviPI cell line is only half the methylation increase in the MSssl cell line, there is a clear difference in mitochondrial methylation patterns between MSssl and MCviPI cell lines, allowing to compare the relative contribution of CpG and GpC methylation in mitochondrial regulatory functions.

5.4.2 MtDNA GpC hypermethylation promotes specific changes in bile acid metabolic gene expression

Since there is a clear increase of mitochondrial CpG and GpC mtDNA methylation in both overexpressing cell lines (MSssl, MCviPI) as compared to the MCviPI mutant cell line, we next evaluated whether this differential mtDNA methylation also affects cellular (metabolic) gene expression. Since MCviPI mutant overexpressing and WT cells showed similar background CpG and GpC methylation levels (See Figure 1), in further experiments, we only included the MCviPI mutant overexpressing cell line as a reference (negative control) cell line. As such, all 3 cell lines received similar transfection-selection conditions. Mitochondrial localization of the overexpressed MSssl and MCviPI DNMTs in the HepG2 cells was confirmed by immunofluorescence microscopy, as previously shown in HCT116 and C33A cells²⁷ (Supplementary Figure 1). Moreover, in line with earlier observations of Van Der Wijst et al.²⁷, we did not detect major gene expression changes of selective mitochondrially encoded genes (Supplementary Figure 2). However RNA sequencing identified 43 and 650 uniquely differentially expressed nuclear genes (DEG) upon mitochondrial CpG or GpC methylation, respectively without further treatment with FFAs (Supplementary Figure 3). The Venn diagram identifies 58 common genes, primarily involved in metabolic processes, which are differentially expressed in both the MSssl (CpG) or MCviPI (GpC) DNMT overexpressing cell lines (Supplementary Figure 3, Supplementary Table 2).

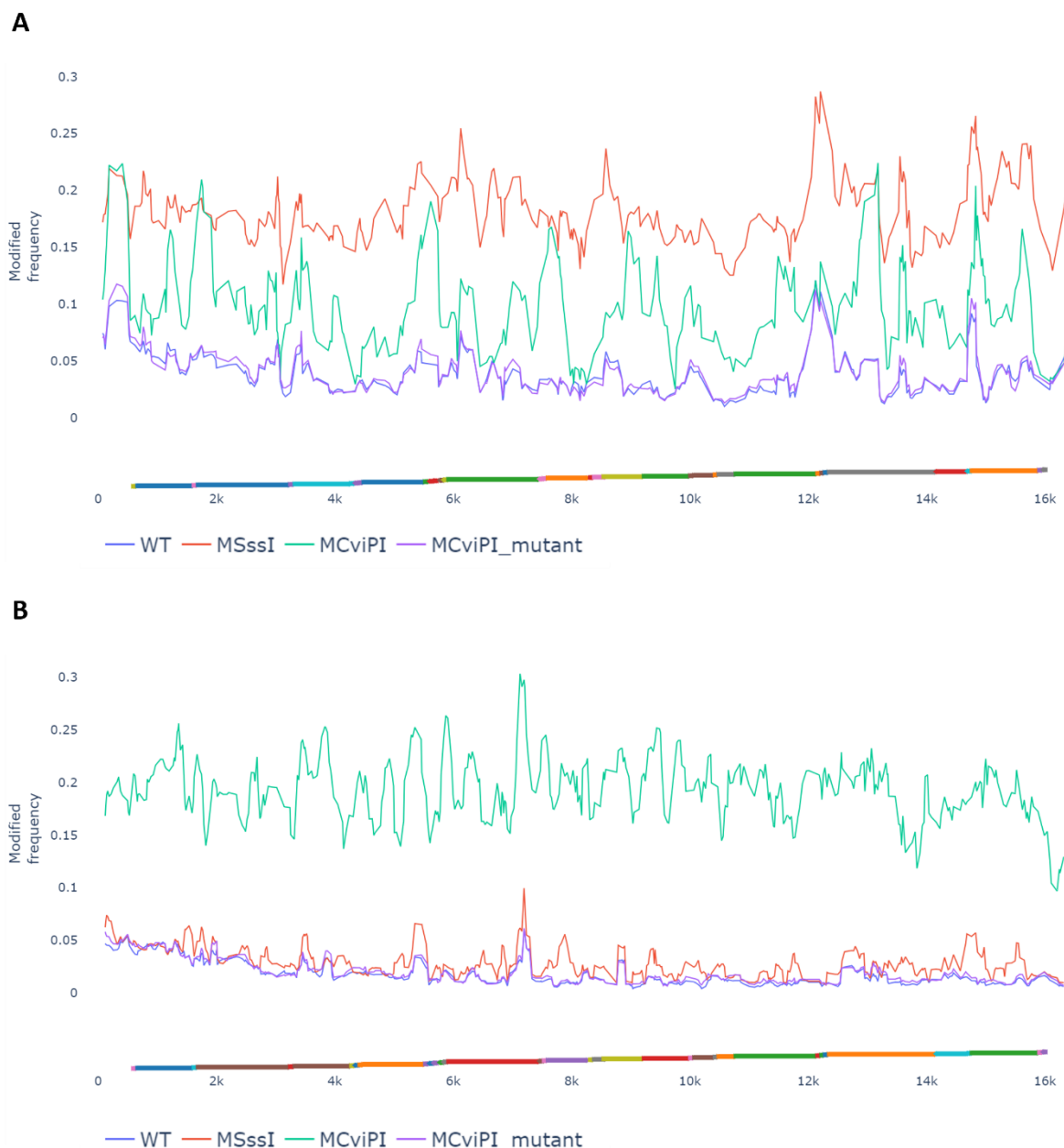


Figure 1: Modified frequency showing the per read per position frequency of CpG (**A**) or GpC (**B**) methylation in the mitochondrial genome of the different cell lines. WT and MCviPI mutant are both control cell lines with no expression (un-transfected) or overexpression of an inactive DNMT (mock transfected), respectively. MCviPI overexpresses a GpC DNMT targeted to the mitochondrial genome; MSssI overexpresses a CpG DNMT targeted to the mitochondrial genome. Mitochondrial genes are represented as different colours on the x-axis.

Next, integrated Bigomics™ based pathway enrichment analysis of the DEG revealed that FFA treatment induces a similar upregulation of fatty acid metabolism (gene cluster S1) and downregulation of genes involved in TNF/mTORC signalling and cholesterol homeostasis (gene cluster S2) in all three cell lines, irrespective of the mtDNA methylation status (Figure 2A–B). Interestingly, MCviPI overexpressing cells and to a much lesser extent MSssI overexpressing cells promote specific upregulation of genes involved in bile acid metabolism (gene cluster 3) (Figure 2A–B). The latter, suggests that GpC rather than CpG mtDNA methylation elicits changes in bile acid

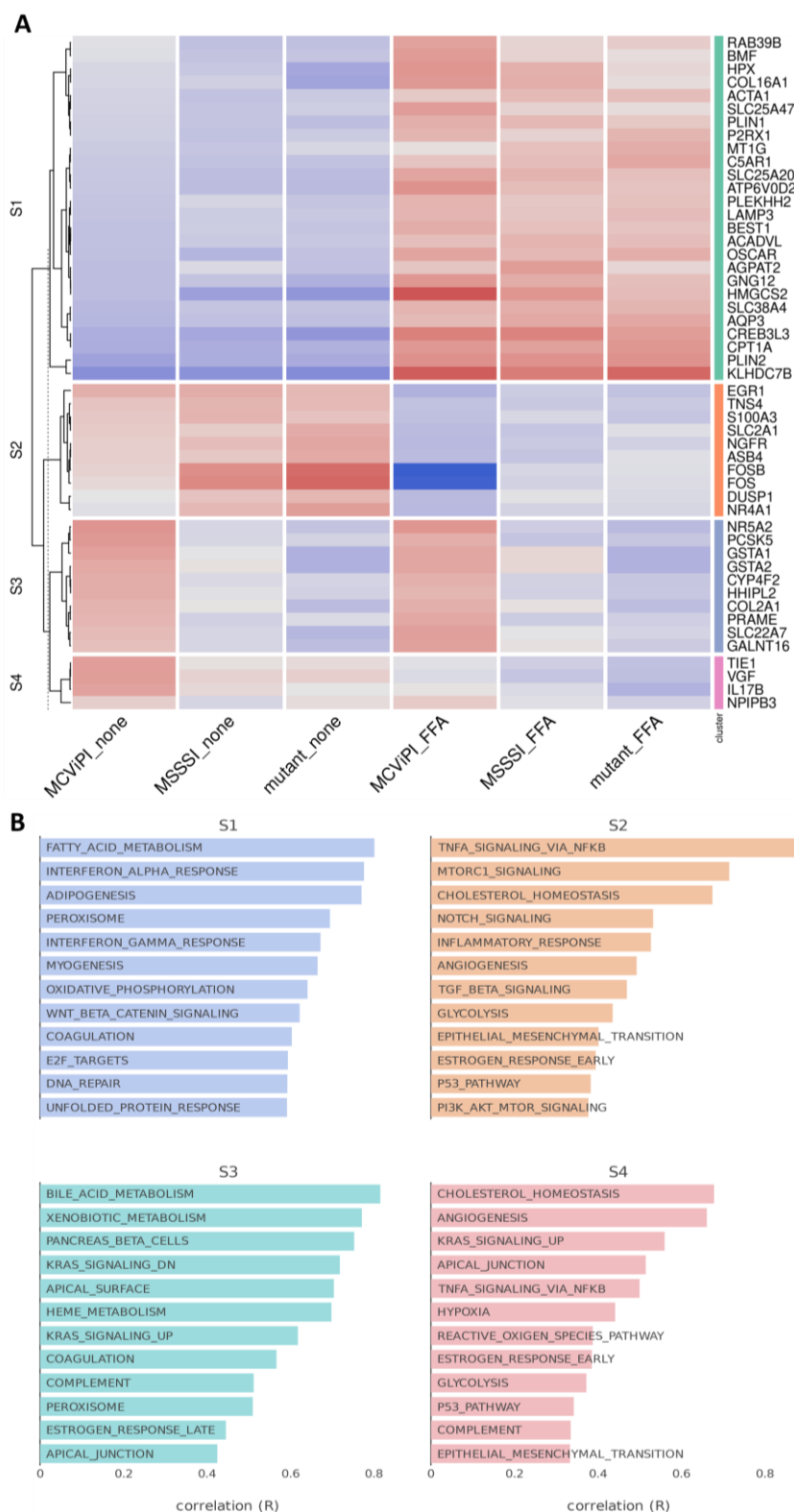


Figure 2: **A**) Heatmap representation of differentially expressed genes in three different HepG2 cell lines overexpressing a GpC DNMT MCviPI (MCviPI), a CpG DNMT (MSSSI) or overexpressing a GpC/CpG DNMT deficient MCviPI mutant. Cells were left untreated (none) or treated with 1mM FFA for 24h (FFA) to induce a MASLD phenotype in vitro. **B**) Pathway enrichment analysis of four main differentially expressed gene clusters.

metabolic gene expression. This differential gene expression by mtDNA methylation was further validated with qPCR of four genes related to bile acid metabolism or stress pathways: GSTA1, GSTA2, SLC22A7 and NR5A2, showing results in line with the RNAseq data (Supplementary Figure 4)

Of special interest, upon further searching for corresponding changes in nuclear hormone receptors involved in metabolic gene expression (Figure 3A), we identified increased expression of various key nuclear receptors involved in bile acid/fatty acid metabolism (i.e. NR5A2, NROB2, NR1H3, NR1I2, NR1H4, PPAR α , HNF4⁴⁷), as well as elevated expression of multiple PPAR α target genes (CYP8B1, UGT2B4, SULT2A1) involved in bile acid metabolism⁴⁸ in the MCviPI cell line (Figure 3B). Furthermore, protein-protein interaction analysis (<https://string-db.org/>) shows a strong interaction of the GpC mtDNA methylation specific gene expression changes with key regulatory proteins for bile acid metabolism (Supplementary Figure 5). Interestingly, MCviPI mtDNA methylation specific gene expression changes also directly reveal an enrichment of a human MASLD/MASH gene signature (Figure 4A–B).

5.4.3 MtDNA GpC/CpG hypermethylation modulates mito-nuclear epigenetic crosstalk.

The concept “mito-nuclear communication” refers to the interplay of mitochondrial dynamics with nuclear epigenetic regulation to adapt to environmental metabolic (energetic) challenges. Since the mitochondria regulate the production of the universal methyl donor s-adenosyl methionine (SAM) by the production of ATP and folate, this may also affect both mitochondrial as well as nuclear epigenetics^{49,50}. Since our RNA sequencing results revealed predominant mitochondrial GpC hypermethylation-induced changes in bile acid metabolic gene expression, we next characterized whether this may also translate into crosstalk with nuclear epigenetic DNA methylation changes in the MCviPI overexpressing cell line. Upon analysis of the Illumina Epic 850K bead array β -value DNA methylation signal intensities in MCviPI and MCviPI mutant overexpressing HepG2 cell lines left untreated or treated for 24h with FFA, we could identify 1754 differentially methylated probes (DMPs) in the untreated or 7565 DMPs in the FFA treated MCviPI cell line as compared to the mutant counterpart cell line ($DB > |0.1|$).

Upon cross comparing differentially methylated genes ($DB > |0.1|$) with lists of differentially expressed genes derived from the RNAseq data, via the integrative BigOmics platform, we identified various nuclear epigenetic controlled gene clusters that are enriched in processes related to fatty acid metabolism, cholesterol metabolism, bile acid metabolism, unfolded protein response or TNF signalling (Figure 5). Of special note, differential methylation of various genes involved in bile acid metabolism can only exclusively be detected in MCviPI GpC mtDNA cells but not the MCviPI mutant cell line, irrespective of the treatment. Altogether, these results strongly support the concept of mito-nuclear epigenetic communication between both compartments to regulate bile acid metabolism.

Results: Chapter 5

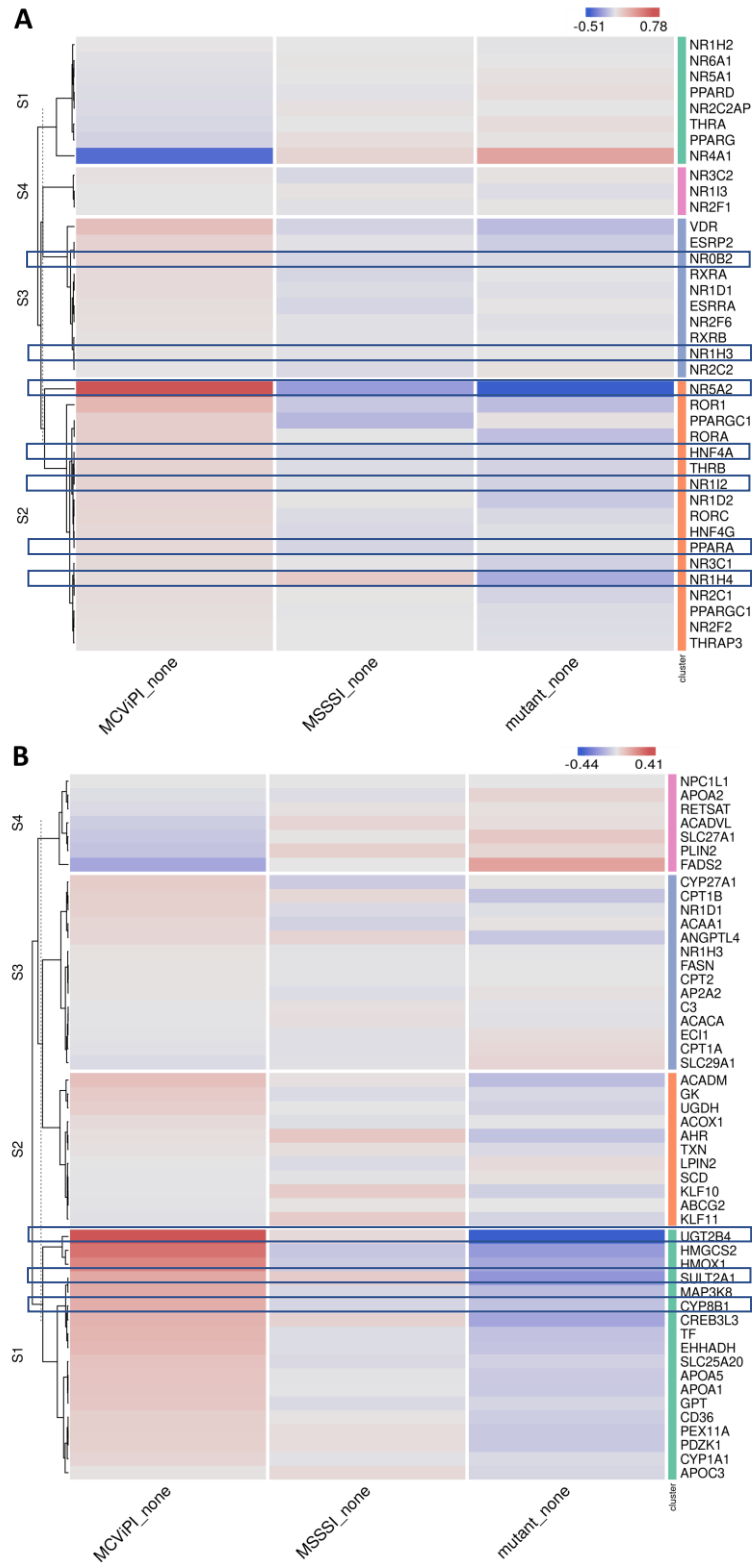


Figure 3: Heatmap representation of differentially expressed nuclear receptors (C) or PPARα target genes (D) in three different untreated (none) HepG2 cell lines overexpressing a GpC DNMT MCvPII (MCvPII), a CpG DNMT (MSSSI) or overexpressing a GpC/CpG DNMT deficient MCvPII mutant.

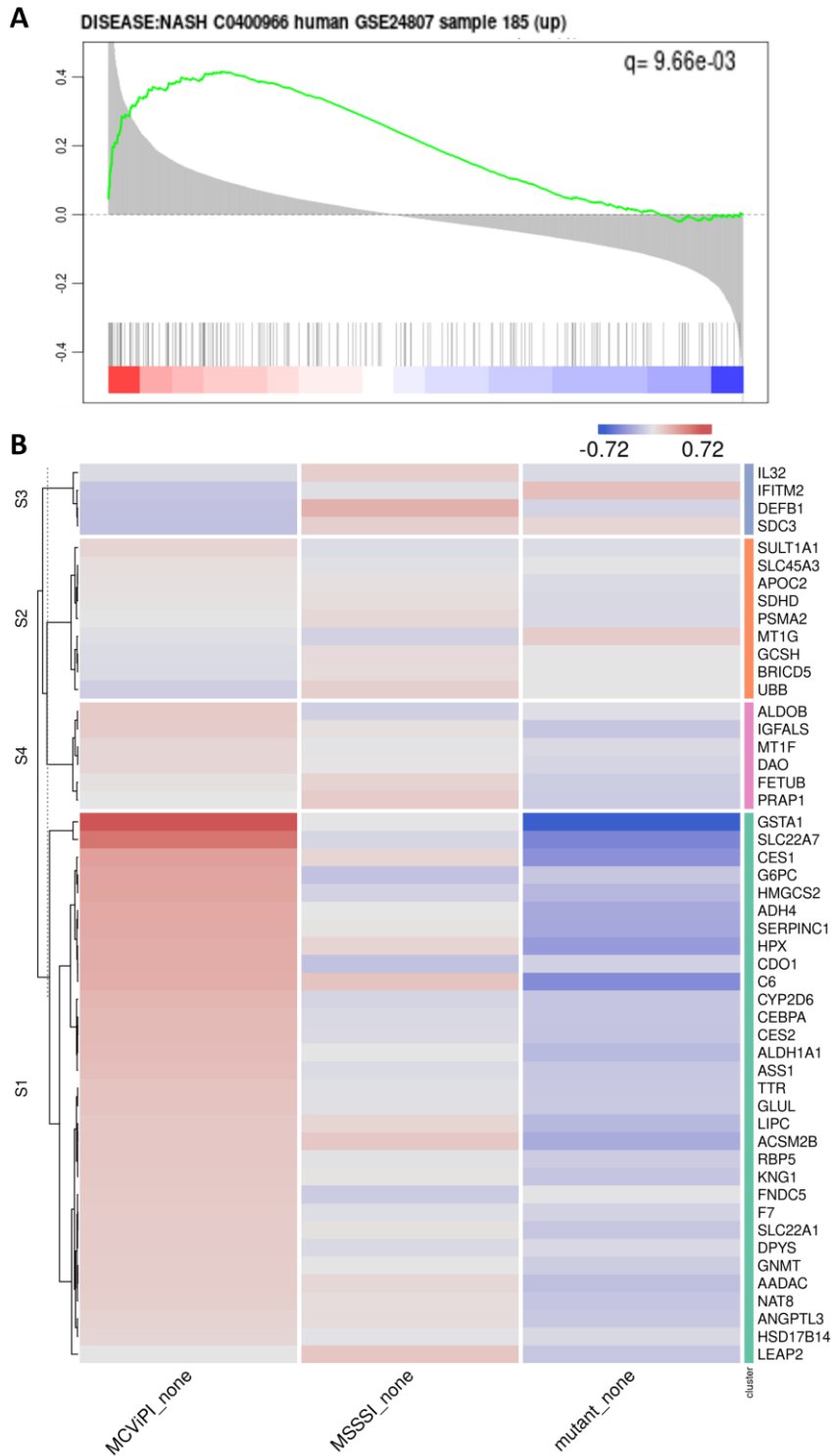


Figure 4: **A)** Functional GSEA enrichment of MASLD-associated genes correlating with mitochondrial GpC methylation MCviPI_none vs Mutant_none. The green curve corresponds to the 'running statistics' of the enrichment score (ES). The more the green ES curve is shifted to the upper left of the graph, the more the gene set is enriched in the first group. Black vertical bars indicate the rank of genes in the gene set in the sorted correlation metric. FDR is represented by the q-value in the figure. Figure was generated using the Omics Playground tool (v3). **B)** Heatmap representation of MASH-related gene signature (GSE24807) in 3 different HepG2 cell overexpressing a GpC DNMT MCviPI (MCviPI), a CpG DNMT (MSSSI) or overexpressing a GpC/CpG DNMT deficient MCviPI mutant. Cells were left untreated (none).

5.4.4 *MtDNA GpC/CpG hypermethylation promotes functional mitochondrial changes in respiration and morphological features associated with mitophagy stress response*

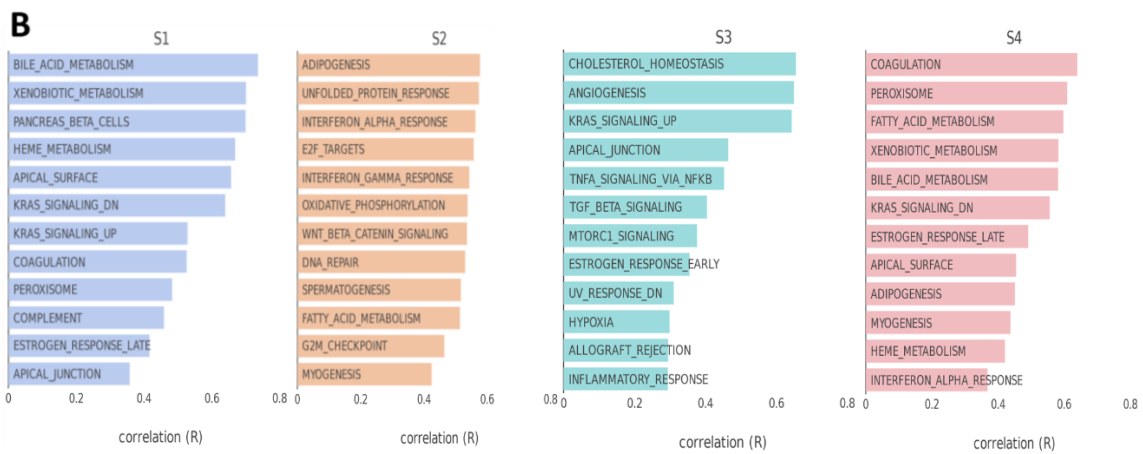
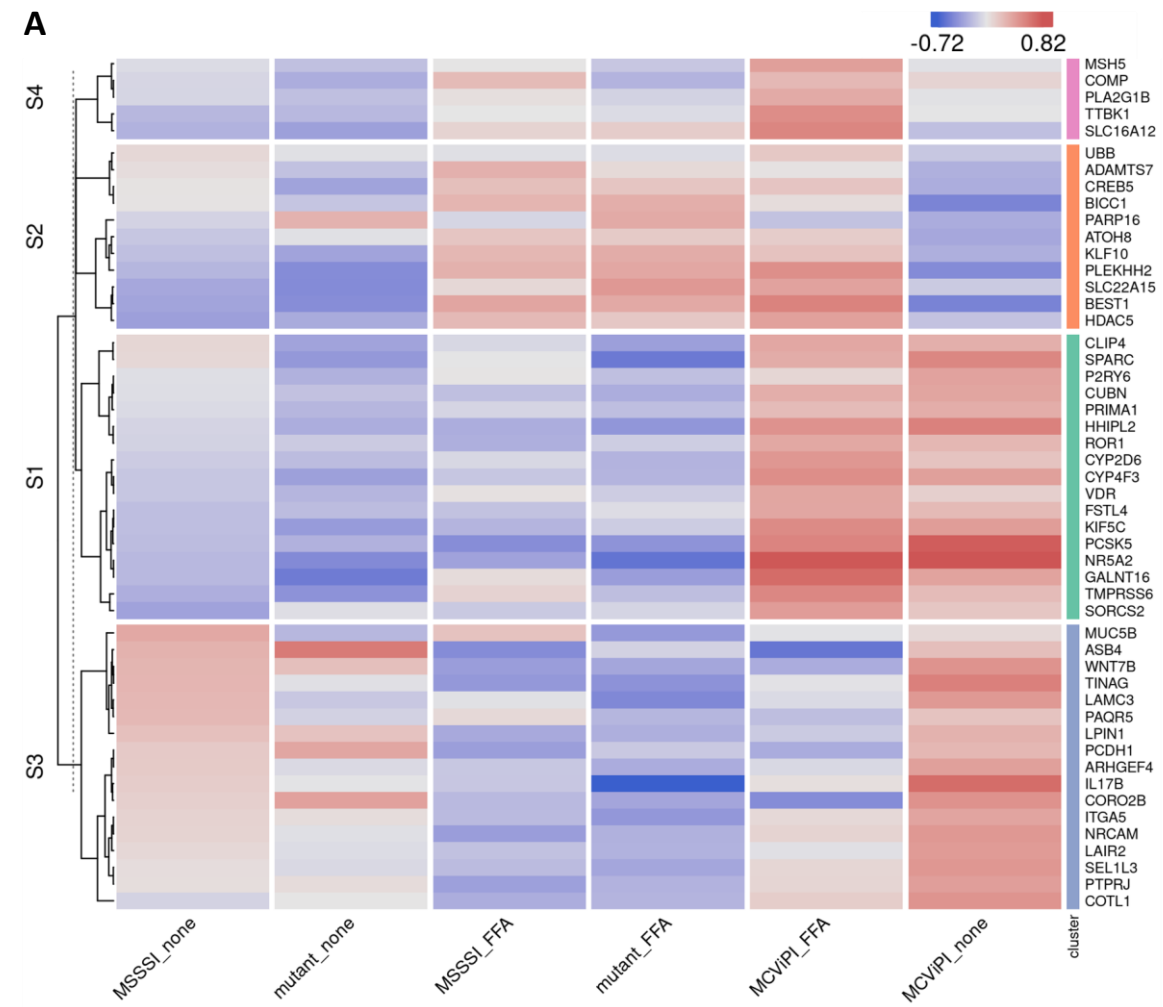
The preceding findings indicated significant alterations in gene expression patterns within metabolic pathways, closely linked to mitochondrial functioning. Therefore in the subsequent experiments, we integrated various experimental approaches to assess potential functional changes in mitochondrial morphology, respiration and ROS-lipid peroxidation damage associated with mtDNA GpC/CpG hypermethylation in MCviPI and MSssl cell lines versus deficient DNMT MCviPI mutant cells.

First, we applied electron microscopy to compare mitochondrial morphology in the MSssl and MCviPI overexpressing cell lines compared to the MCviPI mutant reference cell line. Therefore, we quantified three aspects of the mitochondrial shape including the area, aspect ratio and perimeter indicating the size (area and perimeter) and shape (aspect ratio) of the mitochondria. Both the area and perimeter, representing the size, are significantly increased in the MSssl and MCviPI overexpressing cell lines as compared to the MCviPI mutant reference cell line, indicating that GpC/CpG mtDNA hypermethylation is associated with mitochondrial swelling (Figure 6B). However the aspect ratio is not increased compared to the MCviPI mutant cell line, because the overall shape of the mitochondria is not changed. These morphological changes are also clear from the images of the mitochondria showing overall mitochondrial swelling and disruption of the cristae structure in the MSssl and MCviPI cell lines, which is less prominent in the MCviPI mutant cell line (Figure 6A). Furthermore, autophagosomes could be detected in the MSssl and MCviPI cell lines which were less frequently observed in the MCviPI mutant cell line, suggesting possible involvement of mitophagy-autophagy mitochondrial stress responses following GpC/CpG mtDNA hypermethylation (Figure 6C).

Since the results of the TEM show morphological abnormalities caused by mtDNA GpC/CpG hypermethylation, we next compared possible effects on cellular distribution-localisation of mitochondria. Therefore, mitochondria were stained with Mitotracker Red CMXRos dye which accumulates in active mitochondria in a potential-dependent manner, allowing us to visualise and study their distribution (Figure 7A). Our results show that, GpC/CpG mtDNA hypermethylation in both MCviPI and MSssl cells does not influence the localisation of the mitochondria. Mitochondria could be observed equally distributed all over the cytoplasm around the nucleus in all cell lines. Furthermore, when examining fluorescence intensity, both the MCviPI and MSssl cell lines display a slight decrease compared to the mutant MCviPI cell line, whether they were left untreated (0.061 ± 0.020 and 0.080 ± 0.006 vs 0.090 ± 0.016) or treated with 1mM FFA (0.046 ± 0.002 and 0.059 ± 0.019 vs 0.076 ± 0.009). However, this decrease reached only statistical significance in the MCviPI cell line (Figure 7B).

Taking into account the observed morphological phenotypic mitochondrial alterations, we next performed a mitochondrial stress test using Agilent Seahorse XF Technology. This assay allows us to assess different aspects of the mitochondrial respiration, such as basal respiration, ATP-coupled respiration and maximal respiration based on differences in oxygen consumption rate (OCR) upon

Results: Chapter 5



Results: Chapter 5

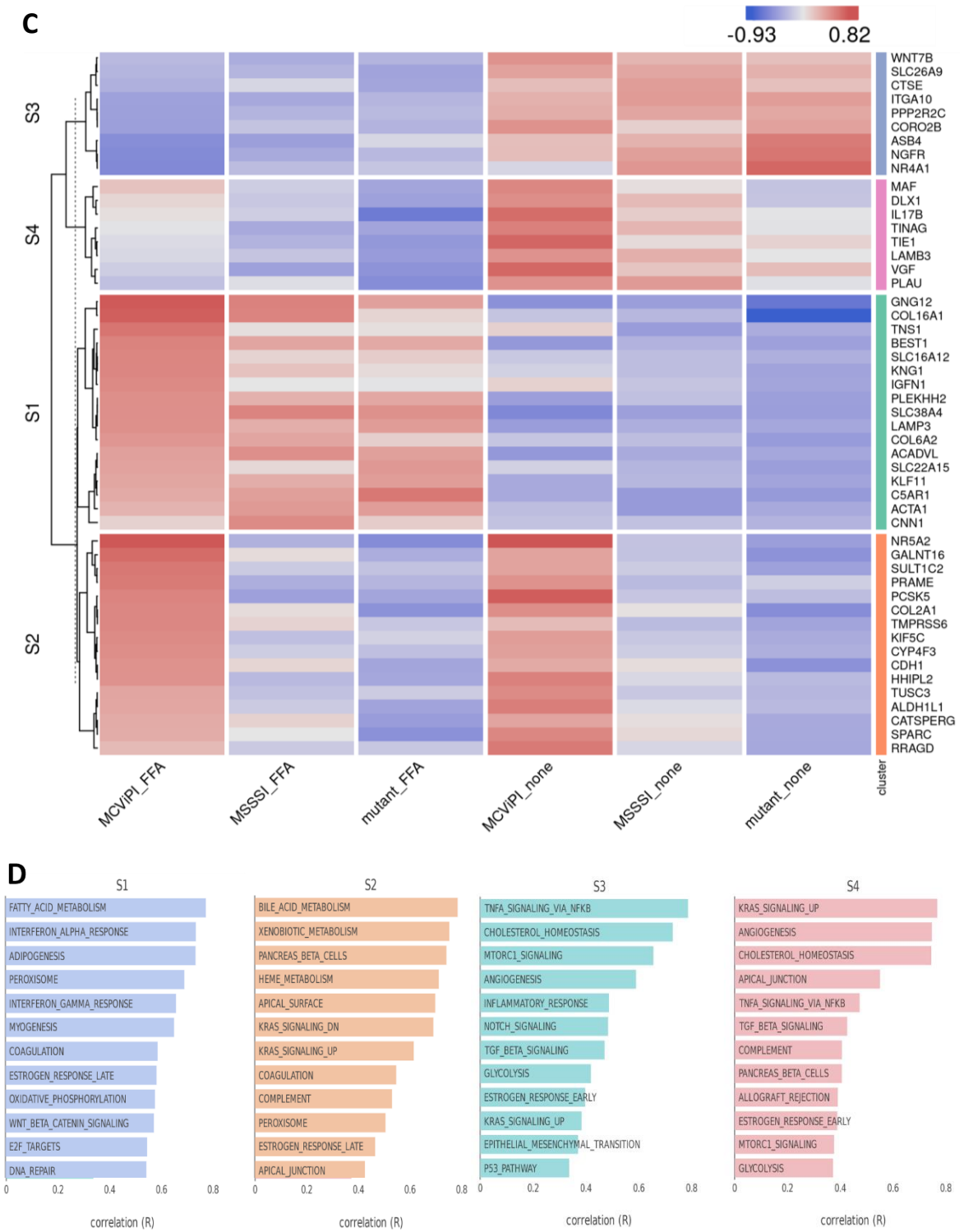


Figure 5: Heatmap representation of four differentially expressed gene clusters which are also differentially methylated ($DB > |0.1|$) in MCviPI versus MCviPI mutant cells left untreated (A-B) or treated with 1mM FFA (C-D).

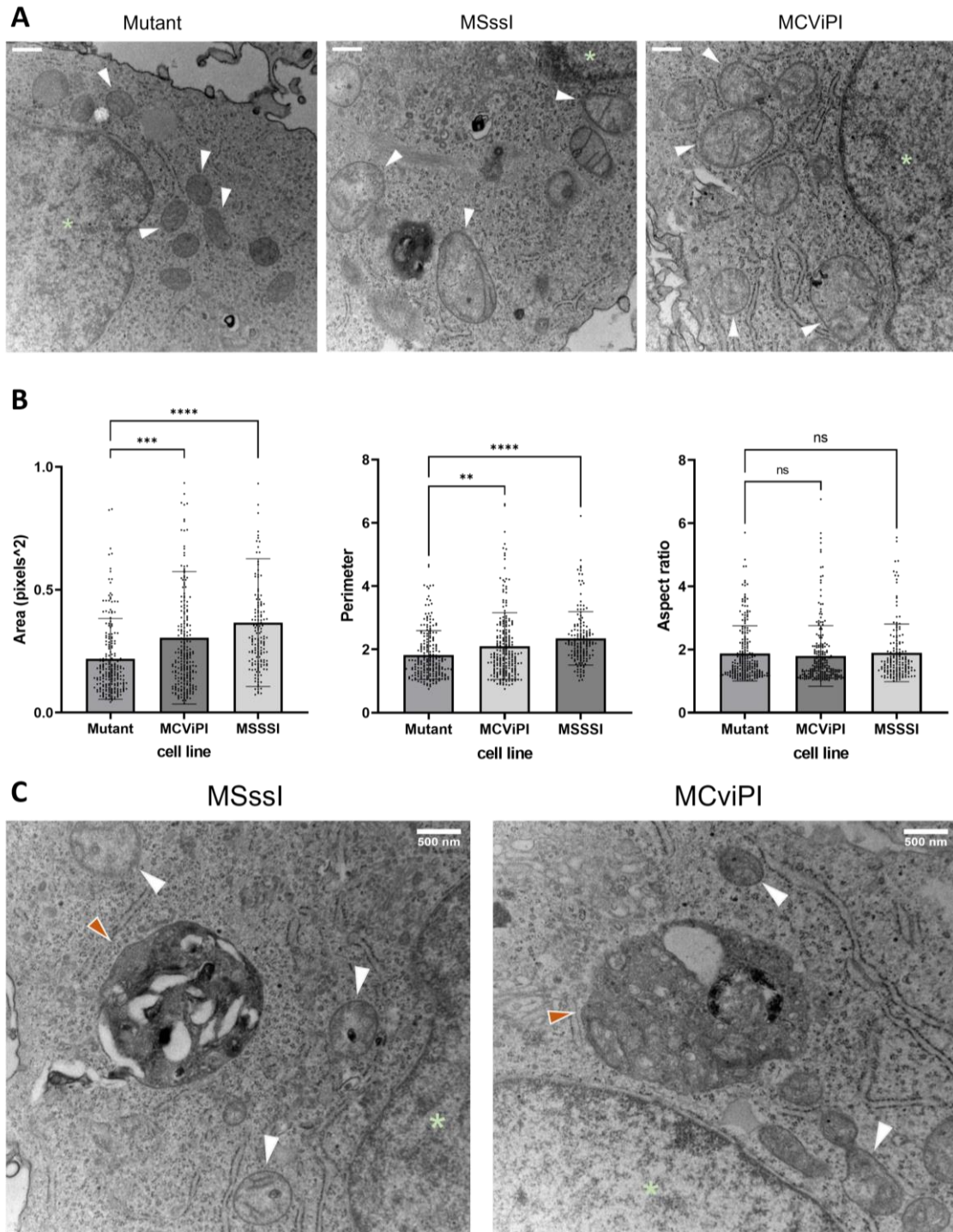


Figure 6: A) Representative images of TEM of the reference MCviPI mutant cell line and the mitochondrially CpG or GpC methylated cell lines MSssl and MCviPI, respectively. White arrowheads indicate mitochondria and green asterisks indicate the nucleus. **B)** quantification of surface area, perimeter and aspect ratio of the mitochondria in the three cell lines ($n=2$ biologically independent samples, scale bar (upper left) represents 500 nm). Each data point represents a different mitochondrion ($n=158-234$ mitochondria). Data is shown as mean \pm s.d.; (ns= not significant; * $p < 0.05$, ** $p < 0.01$, *** $p < 0.001$, **** $p < 0.0001$, One-way ANOVA with Dunnett's correction for multiple comparisons) **C)** Representative images of TEM imaging of the mitochondrially CpG or GpC methylated cell lines MSssl and MCviPI respectively. White arrowheads indicate mitochondria, green asterisk indicates the nucleus and orange arrowheads indicate autophagosomes.

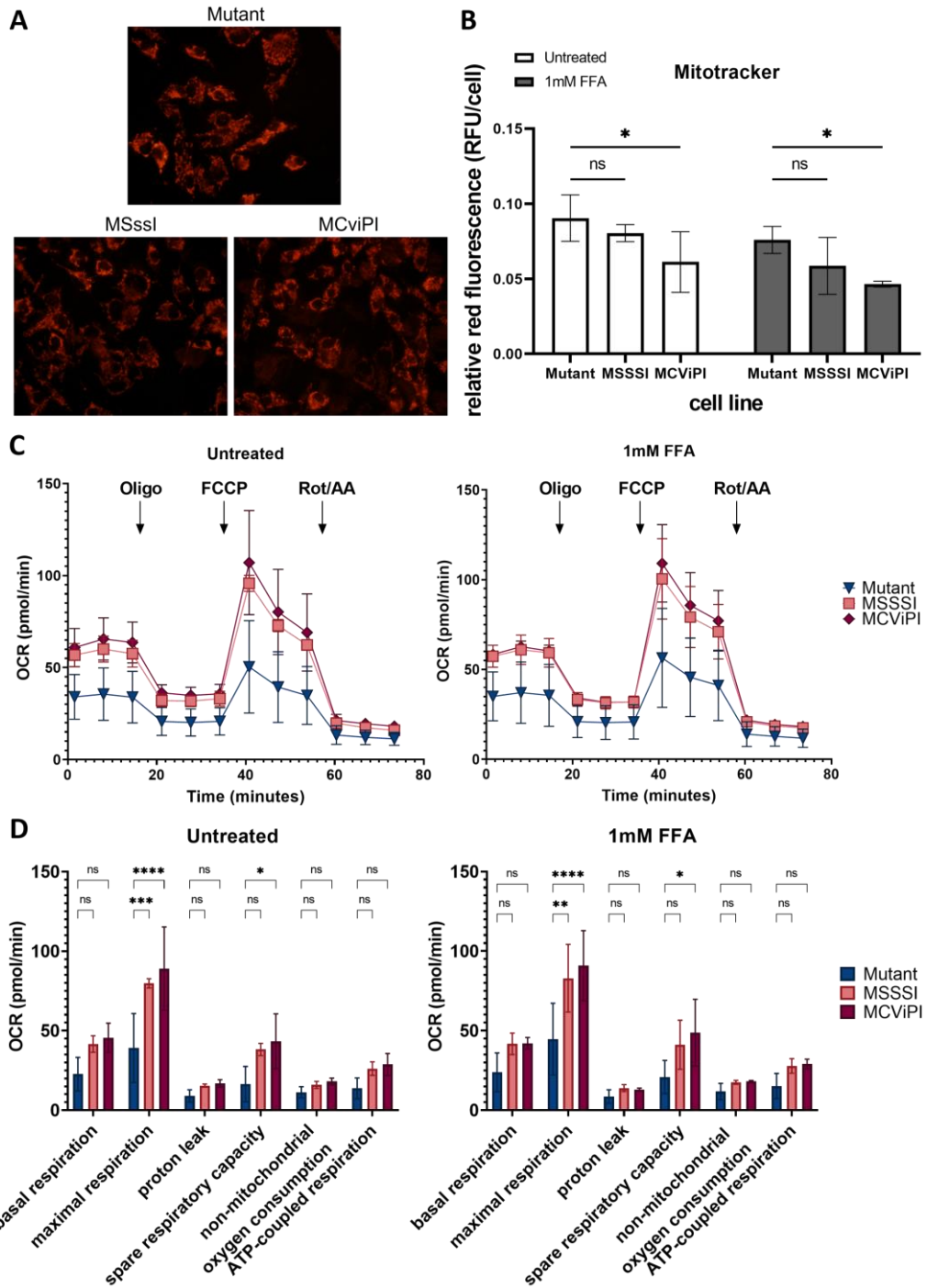


Figure 7: **A**) Mitochondria stained with Mitotracker Red CMXRos dye in untreated cells and **B**) Quantification showing relative fluorescence per cell based on the overall fluorescence to the total amount of cells in all cell lines (MCViPI mutant (mutant), MSSSI (MSSSI), MCViPI and WT) ($n=3$ independent biological replicates, Two-Way ANOVA test with Šidák's correction for multiple comparisons). **C**) The Seahorse XF Cell Mito Stress assay was used to measure changes in oxygen consumption rate after different triggers that inhibit or activate mitochondrial respiration (Oligo= oligomycin; FCCP; Rot/AA = rotenone and antimycin both untreated (left) and treated with 1mM FFA for 24h cells (right)). **D**) Based on the changes in oxygen consumption several aspects of the mitochondrial respiration could be quantified, showing an increased respiration in cell lines with mitochondrial methylation (MSSSI and MCViPI). Data is shown as mean \pm s.d.; $n=3$ independent biological replicates (ns= not significant; * $p < 0.05$, ** $p < 0.01$, *** $p < 0.001$, **** $p < 0.0001$, Two-way ANOVA with Tukey's correction for multiple comparisons)

GpC/CpG mtDNA hypermethylation. MSssl, MCviPI and MCviPI mutant overexpressing cell lines were either left untreated or treated 24h with 1mM FFA to simulate a steatosis phenotype *in vitro*, allowing us to assess the corresponding mitochondrial respiration. Figure 7C-D shows that MSssl and MCviPI DNMT overexpressing cell lines have an increased overall respiration, both treated and untreated compared to the GpC/CpG deficient MCviPI mutant cell line. This is reflected by a significant increase in maximal respiration for both cell lines. Besides, the spare respiratory capacity is also increased in both cell lines, although not statistically significant in the MSssl cell line (Figure 7D). These results suggest that GpC and CpG mtDNA hypermethylation promote increased metabolic activity of the mitochondria. However, this increased respiratory capacity cannot be further enhanced in the presence of 1mM FFA for 24h.

Since byproducts of aerobic respiration in the mitochondria are free radicals (ROS) which frequently trigger lipid peroxidation damage, we next compared levels of lipid peroxidation ROS damage in the different cell lines left untreated or upon lipid accumulation following treatment with 1mM FFA. First, lipid accumulation was quantified with an Adipored staining of lipid droplets, showing a clear accumulation of lipid droplets by treatment with 1mM FFA in all cell lines, irrespective of the mtDNA methylation status. Moreover, a significant increase of lipid droplets was found in the MSssl/MCviPI DNMT overexpressing cell lines compared to the reference MCviPI mutant cell line (Figure 8A). Next, ROS lipid peroxidation damage was quantified via flow cytometry using a fluorescent BODIPY™ 581/591 C11 reagent. This reagent localizes to membranes throughout live cells and upon oxidation by lipid hydroperoxides, displays a shift in peak fluorescence emission from ~590 nm to ~510 nm, providing a ratiometric indication of lipid peroxidation levels. However, no significant difference in lipid peroxidation levels could be observed between MCviPI or MCviPI mutant cell lines left untreated or FFA-treated conditions (Figure 8B). Along the same line, a lipid peroxidation-dependent cell death assay revealed no significant changes in sensitivity to ferroptosis upon treatment with the ferroptosis inducer compound RSL3 (Supplementary Figure 6).

5.4.5 MtDNA GpC-CpG hypermethylation promotes cholestasis associated autophagy-mitophagy stress response

Based on the MCviPI GpC mtDNA hypermethylation associated gene expression changes in bile acid metabolism (Figure 2A), as well as mitochondrial morphology changes (Figure 6A) and increased respiratory functions (Figure 7C), we next performed a more specialized GSEA enrichment analysis of cellular and mitochondrial stress gene signatures⁵¹⁻⁵³.

First we checked a cholestasis signature, which is typically related to increased bile acid metabolism. Interestingly, the MCviPI overexpressing cell line (MCviPI) shows a significant enrichment of cholestasis disease signature compared to the MSssl and MCviPI mutant overexpressing cell lines. The mechanisms by which cholestasis induces liver damage due to the accumulation of bile acids include mitochondrial dysfunction, oxidative stress, and ER stress. These cellular stressors typically further induce cell death and stimulate an integrated autophagy-mitophagy (also known as “cholestophagy”) stress response as a compensatory mechanism aiming to reduce (liver cell) damage⁵⁴. Accordingly, besides cholestasis, we also identified most prominent upregulation of autophagy and mitophagy pathways in the MCviPI and MSssl overexpressing cell lines as compared to the MCviPI mutant cell line (Figure 9).

Together, these results suggest that hypermethylated mitochondria are sensed as functionally overactivated damaged mitochondria, which need to be cleared from the cell to limit liver toxicity, aiming to restore metabolic homeostasis. Interestingly, this is highly similar to the mitochondrial dysfunction in the progression from steatosis to steatohepatitis and fibrosis in MASLD^{54,55}.

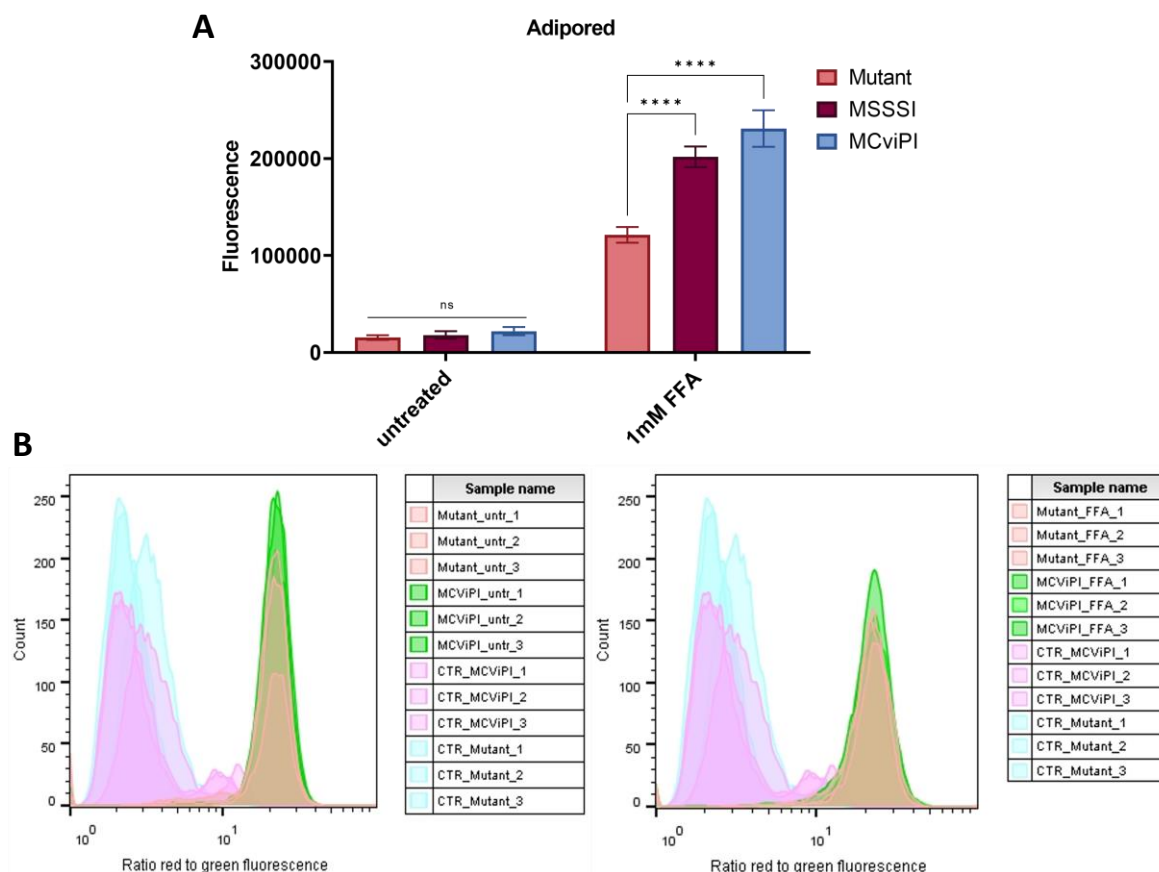
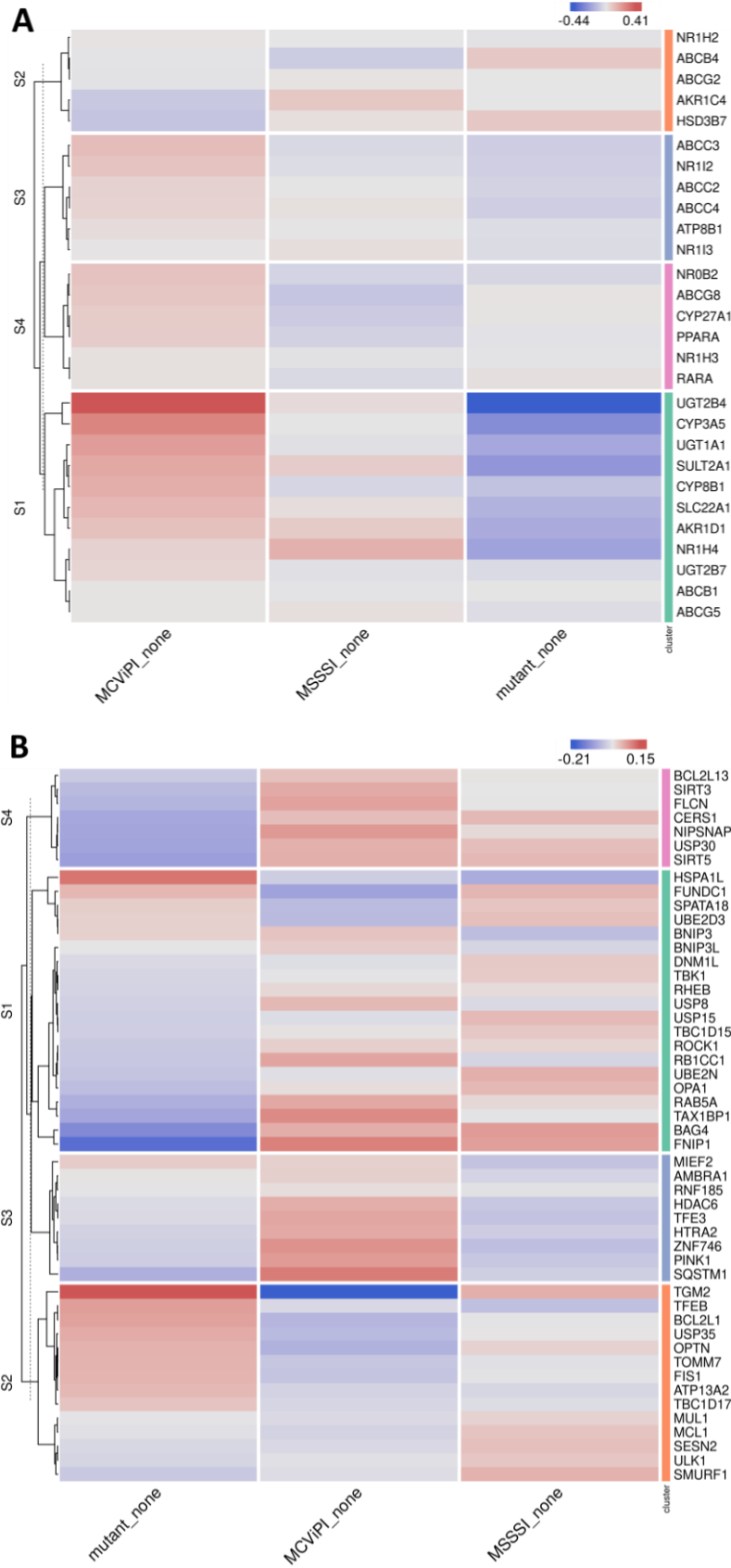


Figure 8: A) Quantification of lipid droplets in both untreated and 24h treated with 1mM FFA cell lines (MCviPI mutant (mutant), MSSSI (MSSSI) and MCviPI) with Adipored fluorescent staining. Data is shown as mean \pm s.d.; $n=3$ independent biological replicates (ns= not significant; $*p < 0.05$, $**p < 0.01$, $***p < 0.001$, $****p < 0.0001$, Two-way ANOVA with Tukey's correction for multiple comparisons). **B)** Lipid peroxidation quantification with the Image-iT Lipid Peroxidation kit using flow cytometry. The lipid peroxidation reagent is a ratiometric probe and the signal is detected on a flow cytometer with 488 nm laser excitation and fluorescence emission measured at 530/30 nm and 532 nm laser excitation and fluorescence emission measured at 585/42 nm. The data are represented as the ratio of red/green fluorescence intensities. Ratios are lower (indicating more green signal) in cells treated with cumene hydroperoxide (positive control; CTR), but there is no difference between ratios of the MCviPI mutant (Mutant) and MCviPI cell line both untreated and treated with 1mM FFA for 24h ($n= 3$ independent technical replicates).

Results: Chapter 5



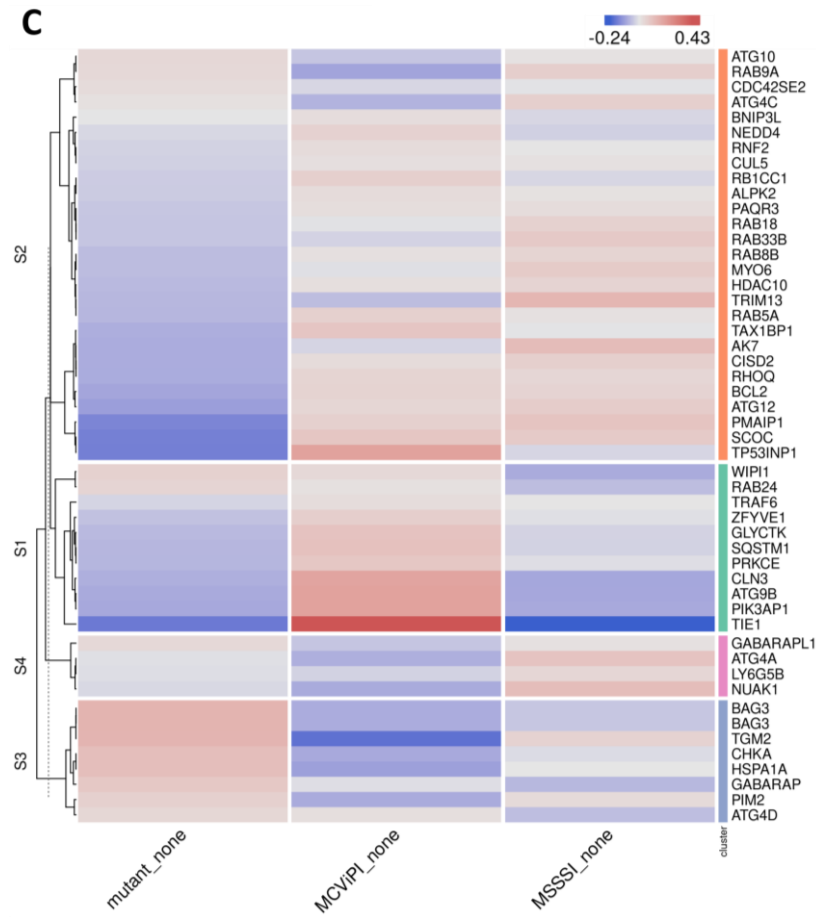


Figure 9: Heatmap representation of differentially expressed genes related to **A)** cholestasis, **B)** mitophagy and **C)** autophagy in 3 different untreated cell lines including a cell line overexpressing an inactive MCviPI DNMT named MCviPI mutant (Mutant) and the MCviPI cell line or MSSsl cell line overexpressing the GpC DNMT MCviPI and CpG DNMT MSSsl, respectively. ($n=3$ biological independent replicates)

5.5 Discussion

In follow up of a pilot study by Mposhi et al.²¹ showing first evidence for impact of targeted mitochondrial CpG (MSssl) and GpC (MCviPI) DNA methylation on MASH associated gene expression, we here further characterized mito-nuclear epigenetic crosstalk by functional mitochondrial changes in morphology, respiratory activity and metabolic competence during MASLD lipid stress in relation to gene expression and (mito)epigenetic signatures.

First, nanopore episequencing of the mtDNA of the different cell lines overexpressing a MCviPI (GpC), MSssl (CpG) or a MCviPI mutant deficient DNMT targeted to the mitochondria, confirmed increased mitochondrial GpC and CpG methylation in the MCviPI and MSssl cell lines, respectively. Importantly, the observed augmentation in CpG and GpC methylation was absent in the MCviPI mutant cell line, showing a similar methylation pattern to the un-transfected HepG2 cells. Remarkably, besides GpC methylation, MCviPI overexpressing cells also showed increased CpG methylation levels, although weaker than CpG methylation levels achieved in the MSssl overexpressing cell line. This suggests the possibility of dual GpC/CpG mtDNA methylation properties of the MCviPI DNMT. Overall low mtDNA methylation levels were observed in the MCviPI mutant cell line, similar to un-transfected HepG2 cells. The average 4% CpG methylation found in

both cell lines is similar to the 3.4% methylation found by Lüth et al. in healthy controls upon Nanopolish analysis of the Nanopore data⁵⁶. Besides, similar methylation levels were reported by Goldsmith et al. in HepaRG cells⁵⁷. Of special note, the research of Goldsmith et al. also showed that higher percentages of mtDNA methylation can be found in tissue as compared to cell lines. Interestingly, the un-transfected and MCviPI mutant HepG2 cell line show higher baseline CpG than GpC methylation levels, which suggests that mitochondrial DNA is more susceptible to CpG methylation than GpC methylation. Similarly, Goldsmith et al. observed more CpG methylation than non-CpG methylation in liver tissue⁵⁷. Nevertheless, strand-specific GpC methylation in the D-loop of human mtDNA samples has previously showed associations with mitochondrial transcription changes and therefore remains important to study^{58,59}. In our DNMT overexpressing cell lines, an average CpG/GpC mtDNA methylation of 20% could be detected. While this approach gives the opportunity to directly investigate the functional effects of mitochondrial CpG/GpC DNA hypermethylation, it is important to acknowledge that the artificially achieved percentages resulting from mitochondrial DNMT overexpression surpass the physiologically observed DNA methylation levels. In control and patient tissue, CpG methylation levels ranged from 5.12 to 5.96%, while non-CpG methylation levels were observed in the range of 0.12 to 0.15%⁵⁷.

Hypermethylation of nuclear genes is generally associated with gene repression. Interestingly, in line with Van Der Wijst et al. we found that essentially only mitochondrial GpC methylation induces a minor downregulation of selective mitochondrial genes (Supplementary Figure 2)²⁷. Besides, recent papers show that besides correct transcription, mitochondrial protein translation and therefore mitochondrial function is also depending on correct post transcriptional RNA modifications^{60,61}. Furthermore, we found that mitochondrial GpC and to a lesser extent CpG methylation specifically increases nuclear bile acid metabolic gene expression. Accordingly, expression of multiple key nuclear receptors involved in regulation of bile acid/fatty acid/cholesterol/lipid metabolism (i.e. NR5A2 (LRH1), NROB2 (SHP), NR1H3 (LXR α), NR1I2 (PXR/SXR), NR1H4 (FXR), PPAR α , HNF4)^{47,62} were increased, which resulted in elevated expression of various PPAR α target genes (CYP8B1, UGT2B4, SULT2A1) involved in bile acid metabolism. Moreover, similar to Schiöth et al., we observed multiple nuclear DNA methylation changes of various bile acid metabolic genes upon MASLD related lipid stress⁶³. Interestingly, the methylation changes of bile acid metabolic genes in our data were specifically associated with GpC mtDNA hypermethylation, irrespective of FFA treatment, which confirms important mito-nuclear metabolic crosstalk in epigenetic regulation and gene expression⁶⁴.

Hepatic bile acid synthesis is the major catabolic mechanism for cholesterol elimination from the body and is strictly regulated. Interestingly, recent studies identified bile acid metabolic dysregulation induced cholestasis as a key factor in steatohepatitis disease aetiology in MASLD⁶⁵⁻⁷⁰. In line, we also found enrichment of MASH (Figure 4) and cholestasis disease signatures (Figure 9A) associated with the epigenetic remodelled increased bile acid metabolic gene expression network in MCviPI overexpressing cells with GpC mtDNA hypermethylation.

Furthermore, new evidence links disturbed bile acid metabolism to mitochondrial dysfunctions, including changes in respiration, mitochondrial swelling and a decrease in mitochondrial transmembrane potential⁷¹⁻⁷³. Interestingly, similar mitochondrial malfunctions also contribute to MASLD/MASH disease aetiology⁷⁴, implicating a contribution of bile acid dysfunction in the mitochondrial dysfunction of MASLD/MASH patients. As a compensation mechanism to cope with

bile acid metabolic stress and avoid liver injury, bile acids promote selective hepatic “cholestophagy” to get rid of cholestasis-induced damage and thereby maintain cellular integrity and energy homeostasis. This process involves a complex interplay of autophagy-mitophagy-lipophagy pathways, regulated by bile acids and the bile acid receptor NR1H4 (FXR)^{75–77}. In line, electron microscopy experiments showed a mix of regular and aberrant shaped mitochondria revealing more mitochondrial swelling and autophagosome formation in MCviPI, as well as MSssl overexpressing cells with GpC/CpG mtDNA hypermethylation, but absent in MCviPI mutant deficient cells (Figure 6A-B). This may reflect a higher mitochondrial turnover rate in cells with GpC/CpG mtDNA hypermethylation to remove “dysfunctional” mitochondria by mitophagy-autophagy⁷⁸. In line with this hypothesis, our RNA sequencing also revealed increased expression of multiple genes related to mitophagy-autophagy pathways in the MCviPI and MSssl overexpressing cell lines. Interestingly, the MCviPI and MSssl cell lines do not always upregulate the same genes, suggesting different degrees or types of metabolic stress, induced by mitochondrial GpC or CpG methylation, activate different mitophagy and autophagy regulation.

Altogether these findings suggest that mitochondrial GpC/CpG methylation elicits metabolic stress-damage, which needs to be overcome by a fast turnover of dysfunctional mitochondria through the process of mitophagy. Consequently, mitochondrial methylation could represent another risk factor in MASLD, giving the mounting body of evidence demonstrating a robust correlation between impaired mitophagy-autophagy and the progression of MASLD^{79–82}.

Further characterisation of the metabolic changes induced by mtDNA CpG/GpC methylation showed that, under *in vitro* steatotic conditions following FFA treatment, MCviPI and MSssl overexpressing cells with GpC/CpG mtDNA hypermethylation show a similar increase in free fatty acid metabolic gene expression as MCviPI mutant mtDNA methylation deficient cells (Gene cluster S1 Figure 2). However, in contrast mitochondrial respiration is only significantly increased in MCviPI and MSssl overexpressing cells with GpC/CpG mtDNA hypermethylation as compared to MCviPI mutant cells (Figure 7C–D). This divergence in respiratory activity might be attributed to the upregulation of additional nuclear receptors (i.e. NR5a2 (LRH1)), known to be involved in upregulation of mitochondrial respiration, as a direct consequence of GpC/CpG mtDNA hypermethylation⁸³ (Figure 3A). Although the comprehensive mechanism has not been resolved, it is noteworthy that the overactivated mitochondrial respiration observed in the methylated cell lines (MSssl and MCviPI) could not be further elevated following treatment with FFA. Intriguingly, this lack of response to FFA treatment coincided with the induction of lipid accumulation, as depicted in Figure 8A. Moreover, this maximal hyperactivation of the mitochondria may slowly promote the decline (exhaustion) of mitochondrial activity, as was already slightly observed by the decreasing fluorescent intensities by Mitotracker staining (Figure 7A–B). Interestingly, increased basal mitochondrial respiration and maximum respiration have been observed as an adaptive mitochondrial response in early steatosis. However this will eventually induce structural mitochondrial deformations and metabolic shutdown of mitochondrial metabolism in the MASH stage, which is similar to the mitochondrial methylation-induced metabolic changes in our results^{84–86}. Surprisingly, despite increased levels of lipid accumulation and mitochondrial respiration activity in MCviPI and MSssl overexpressing cells as compared to MCviPI mutant cells we could not detect increased levels of lipid peroxidation damage or ferroptosis sensitivity. Remarkably, disturbed

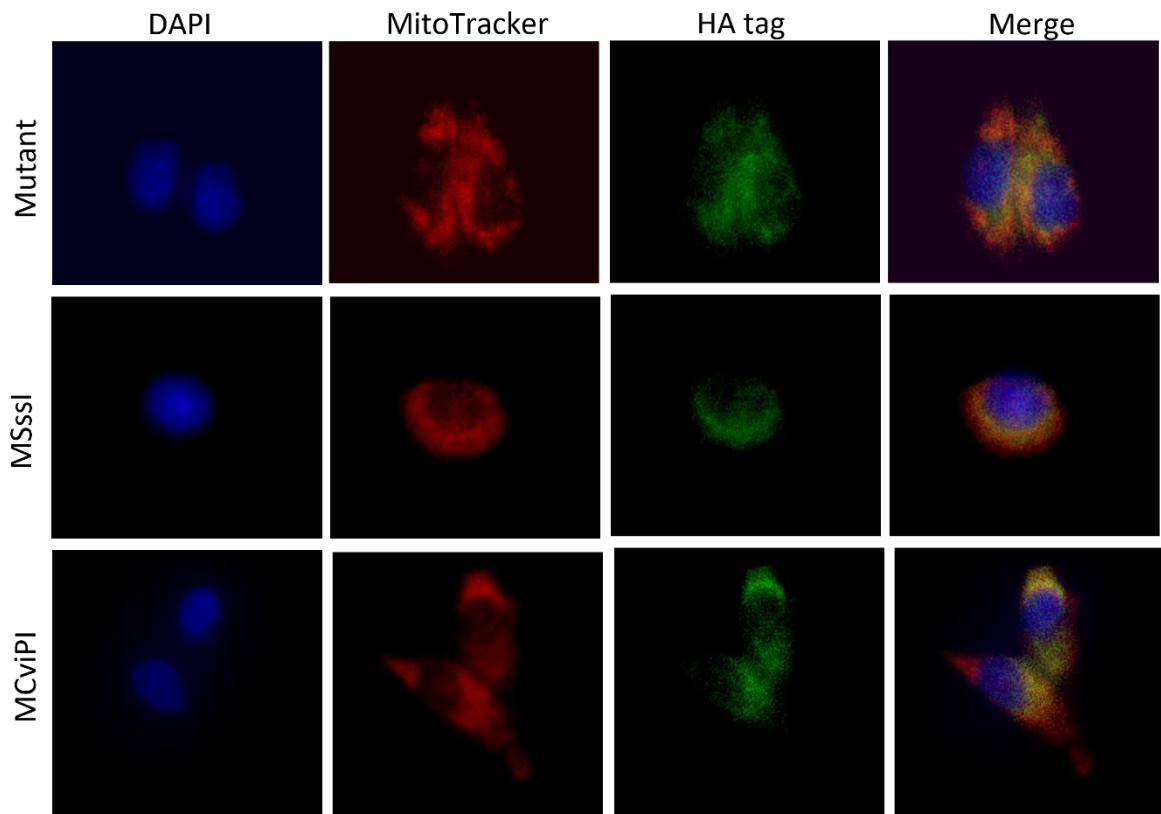
cholesterol homeostasis has recently been found to trigger ferroptosis resistance⁸⁷. However, how bile acids and cholestasis specifically promote ferroptosis resistance needs further investigation.

In summary, our study represents the first evidence of mitochondrial GpC methylation initiating a novel phenomenon termed "cholestasis-induced mitophagy" or "cholestophagy" through the alteration of mito-nuclear epigenetic alterations within the bile acid metabolism. Furthermore, both mitochondrial CpG and GpC methylation induce a basal state of mitochondrial overactivity, leading to lipid accumulation in response to lipid stress, accompanied by morphological changes that promote mitophagy. Consequently, future therapeutic investigations targeting mitochondrial DNA methylation present a promising avenue for mitigating the progression by reverting the epigenomic conditions that cause MASLD.

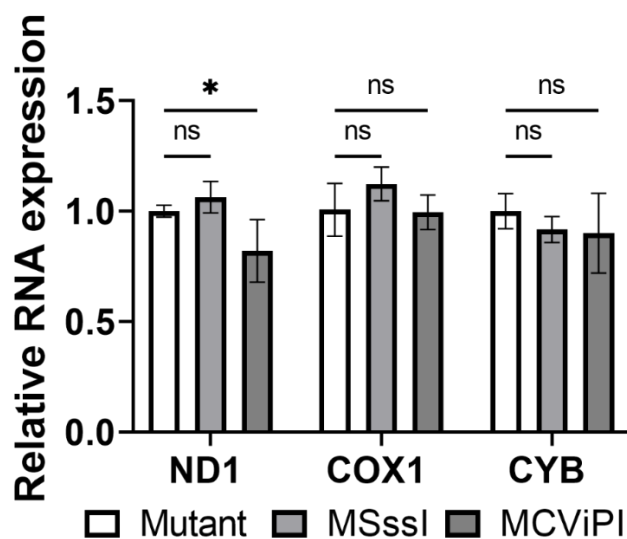
5.6 Supplementary material

Supplementary table 1: Overview of qPCR and PCR primers used in this study.

Gene	Forward primer (5' → 3')	Reverse primer (5' → 3')
B2M	TGCTGTCTCCATGTTTGATGTATCT	TCTCTGCTCCCCACCTCTAAGT
GSTA1	GCAGACCAGAGCCATTCTCAAC	ACATACGGGCAGAAGGAGGATC
GSTA2	CTGCCCTTTAGTCAACCTGAGG	ACAAGGTAGTCTTGTCCGTGGC
NR5a2	GGCTTATGTGCAAAATGGCAGATC	GCTCACTCCAGCAGTTCTGAAG
SLC22a7	CCTTCACCACTGCCTACCTGTT	ACAGCCACACTCCATCCAGCAA
mtND1	ATACCCCCGATTCCGCTACGAC	GTTTGAGGGGGAATGCTGGAGA
mtCOX1	CGATGCATACACCACATGAA	AGCGAAGGCTTCTCAAATCA
mtCYB	AATTCTCCGATCCGTCCTA	GGAGGATGGGGATTATTGCT
Sall3	GTTTGGGTTTGGTTTTTGT	ACCCTTTACCAATCTCTTAACTTTC



Supplementary figure 1: Colocalisation of overexpressed deficient MCviPI (Mutant), MSssl or MCviPI DNMT and mitochondria in HepG2 cells. Images showing immunofluorescence staining with anti-HA-tag targetting the overexpressed MSssl, MCviPI or MCviPI Mutant DNMT (green), the nucleus stained with dapi, the mitochondria stained with Mitotracker (red) and an overlay of these images in all three overexpressing cell lines.



Supplementary figure 2: Mitochondrial gene expression. Relative mRNA expression in three different HepG2 cell lines overexpressing a GpC DNMT MCViPI (MCViPI), a CpG DNMT (MSssI) or overexpressing a GpC/CpG DNMT deficient MCViPI mutant (Mutant). Cells were left untreated (none) (n=3 independent biological replicates). Data is shown as mean \pm s.d.; (ns= not significant; *p < 0.05, Two-way ANOVA).

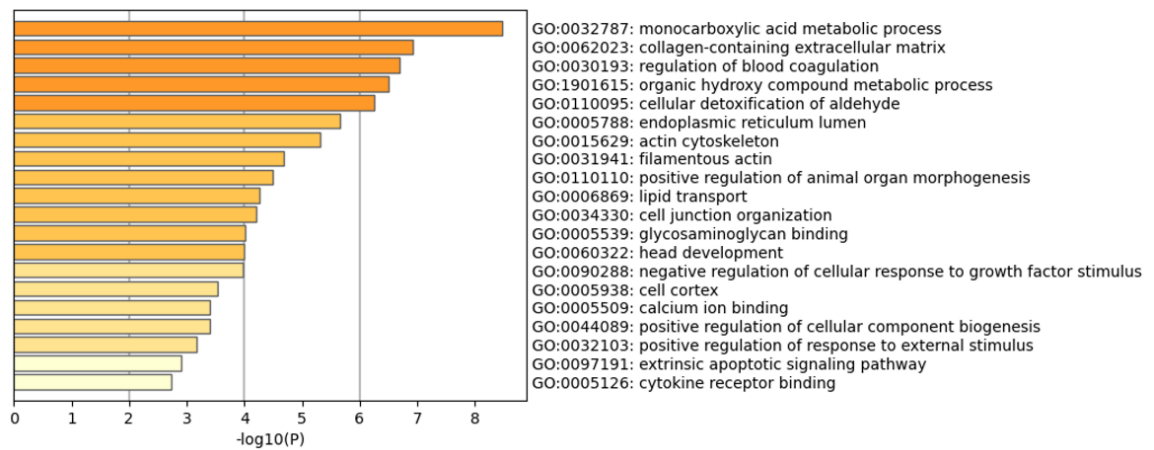
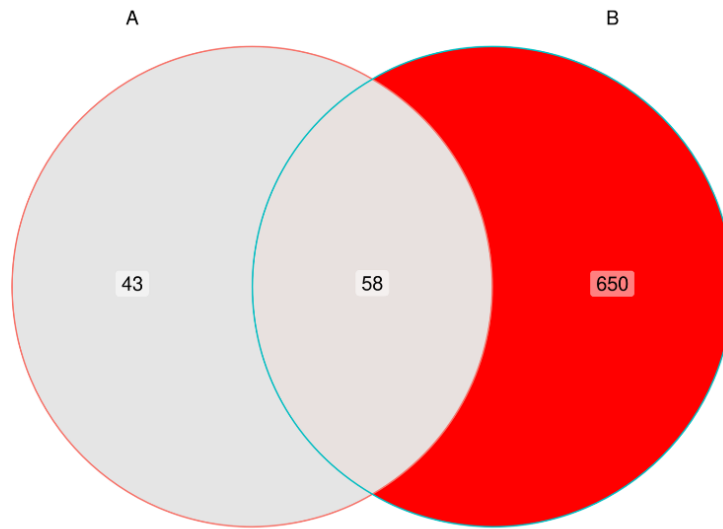
Supplementary table 2: Gene names of overlapping differentially expressed genes (FDR<0.05; logFC > |0.2|) in the different comparisons between untreated (none) GpC MCViPI and CpG MSssI overexpressing cell lines compared to untreated control cell line MCViPI mutant.

GSTA1	PLAU	ZNF678	VLDLR	HPX
GSTA2	AKR1B10	ALDH1A1	ATP10A	SMTNL2
COL2A1	SERPINC1	IL1RAP	SERPINE2	UGT2B11
CDH1	ADH4	NR1H4	MYL9	NPNT
SPARC	SSC4D	VAV3	SLC2A1	LIPC
C6	CLDN6	SAT2	CEBPD	PTGR1
COL16A1	SYNPO	CLK1	ASB4	DKK1
UGT2B4	MYO1A	DMKN	BEX3	BAG3
CES1	SULT2A1	BTG2	ABCA3	EMILIN1
MAGED4	SULF2	CARMIL1	MATN3	ISM2
CXCL8	PARD6B	FRS2	PARP16	
DLX1	CCDC69	IGSF1	EDN1	

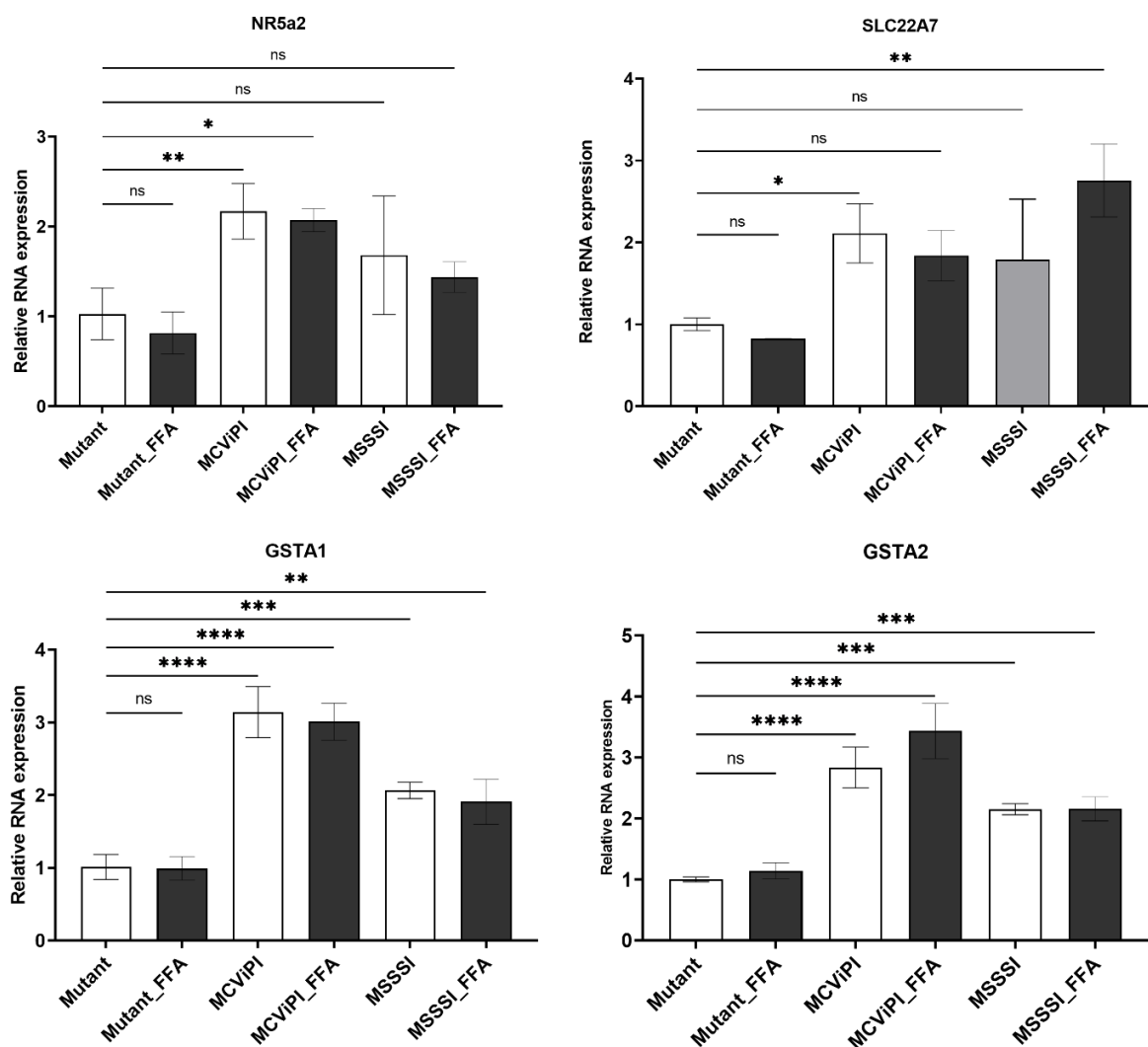
Results: Chapter 5

A = MSSSI.none_vs_mutant.none

B = MCViPI.none_vs_mutant.none

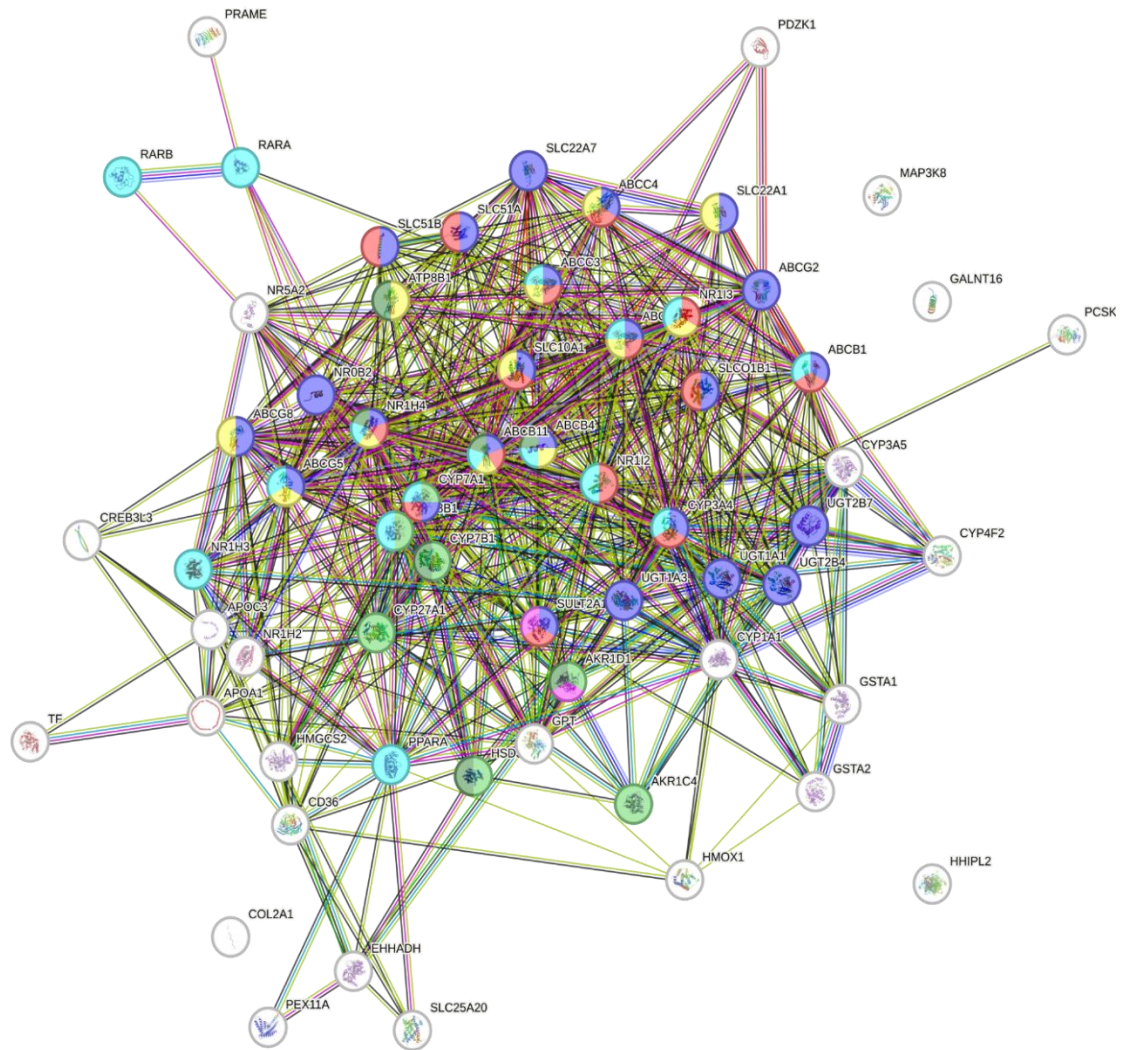


Supplementary figure 3: Venn diagram showing overlapping differentially expressed genes ($FDR < 0.05$; $\log_2FC > |0.2|$) in the different comparisons between untreated (none) GpC MCviPI and CpG MSsSI overexpressing cell lines compared to untreated control cell line MCviPI mutant (top). Metascape GO pathway analysis of the 58 overlapping genes (bottom).



Supplementary figure 4: qPCR validation of 4 differentially expressed genes in the 3 different cell lines (MCViPI Mutant (mutant), MSSSI and MCViPI) that are untreated (none) or treated with 1mM FFA for 24h. Data is shown as mean \pm s.d.; $n=3$ independent biological replicates (ns= not significant; * $p < 0.05$, ** $p < 0.01$, *** $p < 0.001$, **** $p < 0.0001$, One-way ANOVA with Tukey's correction for multiple comparisons).

Results: Chapter 5

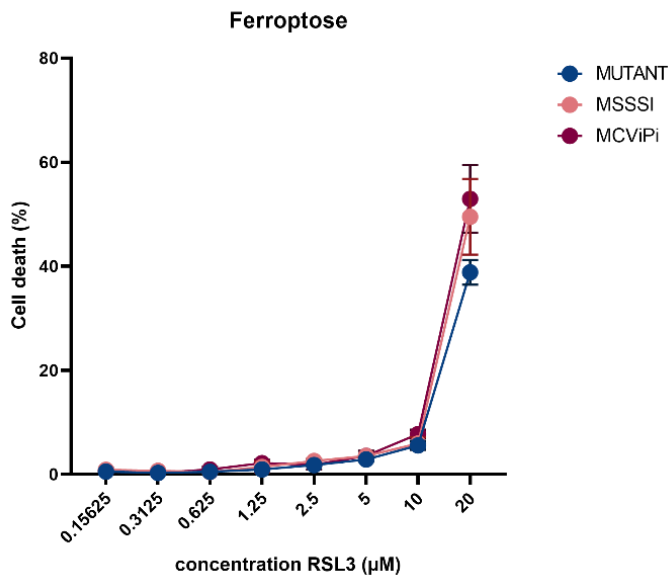


KEGG Pathways				
pathway	description	count in network	strength	false discovery rate
hsa00120	Primary bile acid biosynthesis	7 of 17	2.12	3.36e-11
hsa04976	Bile secretion	24 of 88	1.94	2.38e-36
hsa02010	ABC transporters	9 of 45	1.8	6.43e-12
hsa00140	Steroid hormone biosynthesis	11 of 60	1.77	4.23e-14
hsa04979	Cholesterol metabolism	8 of 48	1.72	3.12e-10

WikiPathways				
pathway	description	count in network	strength	false discovery rate
WP2289	Drug induction of bile acid pathway	15 of 16	2.47	5.06e-28
WP5238	Cholestasis	12 of 19	2.3	7.72e-21
WP5176	Disorders of bile acid synthesis and biliary transport	12 of 20	2.28	9.85e-21
WP1604	Codeine and morphine metabolism	8 of 14	2.26	1.29e-13
WP2879	Farnesoid X receptor pathway	10 of 19	2.22	8.05e-17
WP299	Nuclear receptors in lipid metabolism and toxicity	16 of 32	2.2	5.82e-27

Annotated Keywords (UniProt)				
keyword	description	count in network	strength	false discovery rate
KW-0088	Bile acid catabolism	2 of 2	2.5	0.0020
KW-0988	Intrahepatic cholestasis	7 of 10	2.35	1.50e-11
KW-1278	Translocase	8 of 69	1.57	1.75e-08
KW-0752	Steroid biosynthesis	5 of 43	1.57	2.43e-05
KW-0753	Steroid metabolism	10 of 98	1.51	2.95e-10

Supplementary figure 5: Protein-protein interaction network of differentially expressed genes in HepG2 cells overexpressing a GpC DNMT MCvPI (MCvPI) compared to HepG2 cells overexpressing a GpC/CpG DNMT deficient MCvPI mutant.



Supplementary figure 6: Cell death assay with SYBR green after treatment with different concentrations of the ferroptosis inducer RSL3 in all different untreated cell lines. (n=3 independent biological replicates)

5.7 References

1. Younossi, Z. M. *et al.* Global epidemiology of nonalcoholic fatty liver disease-Meta-analytic assessment of prevalence, incidence, and outcomes. *Hepatology* **64**, 73–84 (2016).
2. Loomba, R. & Sanyal, A. J. The global NAFLD epidemic. *Nat Rev Gastroenterol Hepatol* **10**, 686–690 (2013).
3. Chalasani, N. *et al.* The diagnosis and management of nonalcoholic fatty liver disease: Practice guidance from the American Association for the Study of Liver Diseases. *Hepatology* **67**, 328–357 (2018).
4. Stepanova, M. & Younossi, Z. M. Independent Association Between Nonalcoholic Fatty Liver Disease and Cardiovascular Disease in the US Population. *Clinical Gastroenterology and Hepatology* **10**, 646–650 (2012).
5. Romero-Gómez, M., Zelber-Sagi, S. & Trenell, M. Treatment of NAFLD with diet, physical activity and exercise. *J Hepatol* **67**, 829–846 (2017).
6. Vilar-Gomez, E. *et al.* Weight Loss Through Lifestyle Modification Significantly Reduces Features of Nonalcoholic Steatohepatitis. *Gastroenterology* **149**, 367-378.e5 (2015).
7. Juanola, O., Martínez-López, S., Francés, R. & Gómez-Hurtado, I. Non-Alcoholic Fatty Liver Disease: Metabolic, Genetic, Epigenetic and Environmental Risk Factors. *Int J Environ Res Public Health* **18**, 5227 (2021).
8. Speliotes, E. K., Butler, J. L., Palmer, C. D., Voight, B. F. & Hirschhorn, J. N. *PNPLA3* variants specifically confer increased risk for histologic nonalcoholic fatty liver disease but not metabolic disease. *Hepatology* **52**, 904–912 (2010).
9. Berger, S. L., Kouzarides, T., Shiekhattar, R. & Shilatifard, A. An operational definition of epigenetics: Figure 1. *Genes Dev* **23**, 781–783 (2009).
10. Tiffon, C. The Impact of Nutrition and Environmental Epigenetics on Human Health and Disease. *Int J Mol Sci* **19**, 3425 (2018).
11. Lai, Z. *et al.* Association of Hepatic Global DNA Methylation and Serum One-Carbon Metabolites with Histological Severity in Patients with NAFLD. *Obesity* **28**, 197–205 (2020).
12. Vachher, M., Bansal, S., Kumar, B., Yadav, S. & Burman, A. Deciphering the role of aberrant DNA methylation in NAFLD and NASH. *Heliyon* **8**, e11119 (2022).
13. Sun, Q.-F. *et al.* Potential Blood DNA Methylation Biomarker Genes for Diagnosis of Liver Fibrosis in Patients With Biopsy-Proven Non-alcoholic Fatty Liver Disease. *Front Med (Lausanne)* **9**, 864570 (2022).
14. Sokolowska, K. E. *et al.* Identified in blood diet-related methylation changes stratify liver biopsies of NAFLD patients according to fibrosis grade. *Clin Epigenetics* **14**, 157 (2022).
15. Buzova, D. *et al.* Profiling of cell-free DNA methylation and histone signatures in pediatric NAFLD: A pilot study. *Hepatol Commun* **6**, 3311–3323 (2022).

16. Ma, J. *et al.* A Peripheral Blood DNA Methylation Signature of Hepatic Fat Reveals a Potential Causal Pathway for Nonalcoholic Fatty Liver Disease. *Diabetes* **68**, 1073–1083 (2019).
17. Hardy, T. *et al.* Plasma DNA methylation: a potential biomarker for stratification of liver fibrosis in non-alcoholic fatty liver disease. *Gut* **66**, 1321–1328 (2017).
18. Loomba, R. *et al.* DNA methylation signatures reflect aging in patients with nonalcoholic steatohepatitis. *JCI Insight* **3**, (2018).
19. Hao, Z. *et al.* N6-Deoxyadenosine Methylation in Mammalian Mitochondrial DNA. *Mol Cell* **78**, 382–395.e8 (2020).
20. Stoccoro, A. & Coppedè, F. Mitochondrial DNA Methylation and Human Diseases. *Int J Mol Sci* **22**, 4594 (2021).
21. Rebelo, A. P., Williams, S. L. & Moraes, C. T. In vivo methylation of mtDNA reveals the dynamics of protein–mtDNA interactions. *Nucleic Acids Res* **37**, 6701–6715 (2009).
22. Mposhi, A. *et al.* Mitochondrial DNA methylation in metabolic associated fatty liver disease. *Front Nutr* **10**, (2023).
23. Adeva-Andany, M. M., Carneiro-Freire, N., Seco-Filgueira, M., Fernández-Fernández, C. & Mouriño-Bayolo, D. Mitochondrial β -oxidation of saturated fatty acids in humans. *Mitochondrion* **46**, 73–90 (2019).
24. Koliaki, C. *et al.* Adaptation of Hepatic Mitochondrial Function in Humans with Non-Alcoholic Fatty Liver Is Lost in Steatohepatitis. *Cell Metab* **21**, 739–746 (2015).
25. Nassir, F. NAFLD: Mechanisms, Treatments, and Biomarkers. *Biomolecules* **12**, 824 (2022).
26. Pirola, C. J. *et al.* Epigenetic modification of liver mitochondrial DNA is associated with histological severity of nonalcoholic fatty liver disease. *Gut* **62**, 1356–1363 (2013).
27. Shock, L. S., Thakkar, P. V., Peterson, E. J., Moran, R. G. & Taylor, S. M. DNA methyltransferase 1, cytosine methylation, and cytosine hydroxymethylation in mammalian mitochondria. *Proceedings of the National Academy of Sciences* **108**, 3630–3635 (2011).
28. Sharma, P. & Sampath, H. Mitochondrial DNA Integrity: Role in Health and Disease. *Cells* **8**, 100 (2019).
29. van der Wijst, M. G. P., van Tilburg, A. Y., Ruiters, M. H. J. & Rots, M. G. Experimental mitochondria-targeted DNA methylation identifies GpC methylation, not CpG methylation, as potential regulator of mitochondrial gene expression. *Sci Rep* **7**, 177 (2017).
30. Reumers, J. *et al.* Optimized filtering reduces the error rate in detecting genomic variants by short-read sequencing. *Nat Biotechnol* **30**, 61–68 (2012).
31. Schneider, V. A. *et al.* Evaluation of GRCh38 and de novo haploid genome assemblies demonstrates the enduring quality of the reference assembly. *Genome Res* **27**, 849–864 (2017).
32. Li, H. Minimap2: pairwise alignment for nucleotide sequences. *Bioinformatics* **34**, 3094–3100 (2018).

33. Li, H. *et al.* The Sequence Alignment/Map format and SAMtools. *Bioinformatics* **25**, 2078–2079 (2009).
34. Sedlazeck, F. J. *et al.* Accurate detection of complex structural variations using single-molecule sequencing. *Nat Methods* **15**, 461–468 (2018).
35. Jiang, T. *et al.* Long-read-based human genomic structural variation detection with cuteSV. *Genome Biol* **21**, 189 (2020).
36. Shao, H. *et al.* nplnv: accurate detection and genotyping of inversions using long read sub-alignment. *BMC Bioinformatics* **19**, 261 (2018).
37. Edge, P. & Bansal, V. Longshot enables accurate variant calling in diploid genomes from single-molecule long read sequencing. *Nat Commun* **10**, 4660 (2019).
38. Loman, N. J., Quick, J. & Simpson, J. T. A complete bacterial genome assembled de novo using only nanopore sequencing data. *Nat Methods* **12**, 733–735 (2015).
39. Simon Andrews. Babraham Bioinformatics - FastQC A Quality Control tool for High Throughput Sequence Data. *Soil* vol. 5 Preprint at (2020).
40. Dobin, A. *et al.* STAR: Ultrafast universal RNA-seq aligner. *Bioinformatics* **29**, (2013).
41. Love, M. I., Huber, W. & Anders, S. Moderated estimation of fold change and dispersion for RNA-seq data with DESeq2. *Genome Biol* **15**, (2014).
42. Szklarczyk, D. *et al.* STRING v11: Protein-protein association networks with increased coverage, supporting functional discovery in genome-wide experimental datasets. *Nucleic Acids Res* **47**, (2019).
43. Aryee, M. J. *et al.* Minfi: a flexible and comprehensive Bioconductor package for the analysis of Infinium DNA methylation microarrays. *Bioinformatics* **30**, 1363–1369 (2014).
44. Tian, Y. *et al.* ChAMP: updated methylation analysis pipeline for Illumina BeadChips. *Bioinformatics* **33**, 3982–3984 (2017).
45. Teschendorff, A. E. *et al.* A beta-mixture quantile normalization method for correcting probe design bias in Illumina Infinium 450 k DNA methylation data. *Bioinformatics* **29**, 189–196 (2013).
46. Zhou, Y. *et al.* Metascape provides a biologist-oriented resource for the analysis of systems-level datasets. *Nat Commun* **10**, (2019).
47. Schindelin, J. *et al.* Fiji: an open-source platform for biological-image analysis. *Nat Methods* **9**, 676–682 (2012).
48. Lam, J. *et al.* A Universal Approach to Analyzing Transmission Electron Microscopy with ImageJ. *Cells* **10**, 2177 (2021).
49. Iacobazzi, V., Castegna, A., Infantino, V. & Andria, G. Mitochondrial DNA methylation as a next-generation biomarker and diagnostic tool. *Mol Genet Metab* **110**, 25–34 (2013).
50. Naviaux, R. K. Mitochondrial control of epigenetics. *Cancer Biol Ther* **7**, 1191–1193 (2008).

51. Parmentier, C. *et al.* Evaluation of transcriptomic signature as a valuable tool to study drug-induced cholestasis in primary human hepatocytes. *Arch Toxicol* **91**, 2879–2893 (2017).
52. Bordi, M. *et al.* A gene toolbox for monitoring autophagy transcription. *Cell Death Dis* **12**, 1044 (2021).
53. Schyman, P., Xu, Z., Desai, V. & Wallqvist, A. TOXPANEL: A Gene-Set Analysis Tool to Assess Liver and Kidney Injuries. *Front Pharmacol* **12**, (2021).
54. Panzitt, K., Fickert, P. & Wagner, M. Regulation of autophagy by bile acids and in cholestasis - CholestoPHAGY or CholeSTOPagy. *Biochimica et Biophysica Acta (BBA) - Molecular Basis of Disease* **1867**, 166017 (2021).
55. Pinto, C., Ninfole, E., Benedetti, A., Marzioni, M. & Maroni, L. Involvement of Autophagy in Ageing and Chronic Cholestatic Diseases. *Cells* **10**, 2772 (2021).
56. Lüth, T. *et al.* Nanopore Single-Molecule Sequencing for Mitochondrial DNA Methylation Analysis: Investigating Parkin-Associated Parkinsonism as a Proof of Concept. *Front Aging Neurosci* **13**, (2021).
57. Goldsmith, C. *et al.* Low biological fluctuation of mitochondrial CpG and non-CpG methylation at the single-molecule level. *Sci Rep* **11**, 8032 (2021).
58. Bellizzi, D. *et al.* The Control Region of Mitochondrial DNA Shows an Unusual CpG and Non-CpG Methylation Pattern. *DNA Research* **20**, 537–547 (2013).
59. Dou, X. *et al.* The strand-biased mitochondrial DNA methylome and its regulation by DNMT3A. *Genome Res* **29**, 1622–1634 (2019).
60. Chiang, J. Y. L. Bile Acid Regulation of Gene Expression: Roles of Nuclear Hormone Receptors. *Endocr Rev* **23**, 443–463 (2002).
61. Li, F., Patterson, A. D., Krausz, K. W., Tanaka, N. & Gonzalez, F. J. Metabolomics reveals an essential role for peroxisome proliferator-activated receptor α in bile acid homeostasis. *J Lipid Res* **53**, 1625–1635 (2012).
62. Schiöth, H. B. *et al.* A targeted analysis reveals relevant shifts in the methylation and transcription of genes responsible for bile acid homeostasis and drug metabolism in non-alcoholic fatty liver disease. *BMC Genomics* **17**, 462 (2016).
63. Wiese, M. & Bannister, A. J. Two genomes, one cell: Mitochondrial-nuclear coordination via epigenetic pathways. *Mol Metab* **38**, 100942 (2020).
64. Pennisi, G. *et al.* A cholestatic pattern predicts major liver-related outcomes in patients with non-alcoholic fatty liver disease. *Liver International* **42**, 1037–1048 (2022).
65. Gottlieb, A. & Canbay, A. Why Bile Acids Are So Important in Non-Alcoholic Fatty Liver Disease (NAFLD) Progression. *Cells* **8**, 1358 (2019).
66. Ferslew, B. C. *et al.* Altered Bile Acid Metabolome in Patients with Nonalcoholic Steatohepatitis. *Dig Dis Sci* **60**, 3318–3328 (2015).

67. Van Brantegem, P., Chatterjee, S., De Bruyn, T., Annaert, P. & Deferm, N. Drug-induced cholestasis assay in primary hepatocytes. *MethodsX* **7**, 101080 (2020).
68. Xu, X. *et al.* Targeted therapeutics and novel signaling pathways in non-alcohol-associated fatty liver/steatohepatitis (NAFL/NASH). *Signal Transduct Target Ther* **7**, 287 (2022).
69. Jiao, T., Ma, Y., Guo, X., Ye, Y. & Xie, C. Bile acid and receptors: biology and drug discovery for nonalcoholic fatty liver disease. *Acta Pharmacol Sin* **43**, 1103–1119 (2022).
70. Abrigo, J. *et al.* Bile Acids Induce Alterations in Mitochondrial Function in Skeletal Muscle Fibers. *Antioxidants* **11**, 1706 (2022).
71. Abrigo, J. *et al.* Cholic and deoxycholic acids induce mitochondrial dysfunction, impaired biogenesis and autophagic flux in skeletal muscle cells. *Biol Res* **56**, 30 (2023).
72. Rolo, A. P. Bile Acids Affect Liver Mitochondrial Bioenergetics: Possible Relevance for Cholestasis Therapy. *Toxicological Sciences* **57**, 177–185 (2000).
73. Legaki, A.-I. *et al.* Hepatocyte Mitochondrial Dynamics and Bioenergetics in Obesity-Related Non-Alcoholic Fatty Liver Disease. *Curr Obes Rep* **11**, 126–143 (2022).
74. Wang, Y., Ding, W.-X. & Li, T. Cholesterol and bile acid-mediated regulation of autophagy in fatty liver diseases and atherosclerosis. *Biochimica et Biophysica Acta (BBA) - Molecular and Cell Biology of Lipids* **1863**, 726–733 (2018).
75. Pinto, C., Ninfole, E., Benedetti, A., Marzoni, M. & Maroni, L. Involvement of Autophagy in Ageing and Chronic Cholestatic Diseases. *Cells* **10**, 2772 (2021).
76. Panzitt, K., Fickert, P. & Wagner, M. Regulation of autophagy by bile acids and in cholestasis - CholestoPHAGY or CholeSTOPagy. *Biochimica et Biophysica Acta (BBA) - Molecular Basis of Disease* **1867**, 166017 (2021).
77. Ma, K. *et al.* Mitophagy, Mitochondrial Homeostasis, and Cell Fate. *Front Cell Dev Biol* **8**, (2020).
78. Ma, X., McKeen, T., Zhang, J. & Ding, W.-X. Role and Mechanisms of Mitophagy in Liver Diseases. *Cells* **9**, 837 (2020).
79. Moore, M. P. *et al.* Compromised hepatic mitochondrial fatty acid oxidation and reduced markers of mitochondrial turnover in human NAFLD. *Hepatology* **76**, 1452–1465 (2022).
80. Zhou, T., Chang, L., Luo, Y., Zhou, Y. & Zhang, J. Mst1 inhibition attenuates non-alcoholic fatty liver disease via reversing Parkin-related mitophagy. *Redox Biol* **21**, 101120 (2019).
81. Lin, D. *et al.* Wolfberries potentiate mitophagy and enhance mitochondrial biogenesis leading to prevention of hepatic steatosis in obese mice: The role of AMP-activated protein kinase α 2 subunit. *Mol Nutr Food Res* **58**, 1005–1015 (2014).
82. Choi, S. *et al.* Methyl-Sensing Nuclear Receptor Liver Receptor Homolog-1 Regulates Mitochondrial Function in Mouse Hepatocytes. *Hepatology* **71**, 1055–1069 (2020).
83. Pérez-Carreras, M. *et al.* Defective hepatic mitochondrial respiratory chain in patients with nonalcoholic steatohepatitis. *Hepatology* **38**, 999–1007 (2003).

84. Moore, M. P. *et al.* Compromised hepatic mitochondrial fatty acid oxidation and reduced markers of mitochondrial turnover in human NAFLD. *Hepatology* **76**, 1452–1465 (2022).
85. Koliaki, C. *et al.* Adaptation of Hepatic Mitochondrial Function in Humans with Non-Alcoholic Fatty Liver Is Lost in Steatohepatitis. *Cell Metab* **21**, 739–746 (2015).
86. Liu, W. *et al.* Dysregulated cholesterol homeostasis results in resistance to ferroptosis increasing tumorigenicity and metastasis in cancer. *Nat Commun* **12**, 5103 (2021).

CHAPTER VI

General discussion and future perspectives

6.1 General discussion

Metabolic associated steatotic liver disease (MASLD) is a global health problem that is still growing and becoming the main cause of liver transplantations¹. There are several reasons for this rising problem being: lack of non-invasive tests to correctly stratify patients (non-MASH vs MASH), estimating the right prognosis to give the appropriate treatment and most importantly, finding therapeutics that ameliorate all aspects of the disease including steatosis but also inflammation and fibrosis²⁻⁵. Both the nuclear receptor peroxisome proliferator activated receptor alpha (PPAR α) and mitochondria are known as crucial drivers in the disease progression because of their role in lipid metabolism^{6,7}. However clinical trials using compounds that specifically target PPAR α or mitochondria could only partially ameliorate the disease⁸. Besides, epigenetic strategies receive growing therapeutic interest since epigenetic modifications are (pharmacologically) reversible and (re)program transcriptional network changes implicated in redox homeostasis, peroxisome and mitochondria function, inflammation, insulin sensibility and homeostasis. However the regulatory pathways driving the epigenetic progression of MASLD, including the role of mitochondria and PPAR α , are still largely unknown and therefore hold promise for future therapeutic exploration⁹. Hence, the main focus of this PhD thesis was to evaluate “passenger” or “driver” functions of PPAR α and mitochondria in the epigenetic progression of MASLD, to get new perspectives on novel therapeutic targets and/or diagnostic biomarker applications.

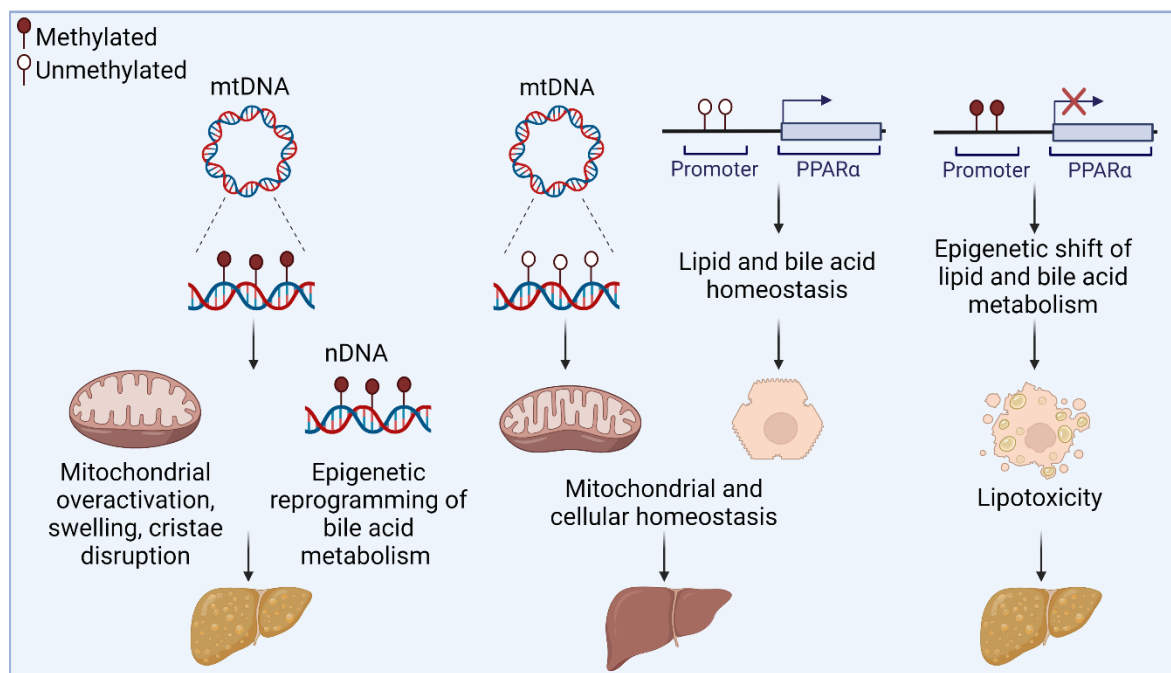


Figure 1: Schematic overview of results in thesis.

MASLD is characterized by an overall hypomethylation and a hypermethylation of PPAR α ^{10,11}. A driver in this epigenetic reprogramming of the lipid metabolism is the “western diet”. Preclinical studies showed a correlation between the consumption of a high-fat diet and DNA methylation of gene clusters including hypermethylation in promoter regions of PPAR α and hypomethylation of

the promotor of PPAR γ . Besides high levels of fructose have been associated with hypermethylation of CTP1A and PPAR α target genes¹²⁻¹⁵. However lifestyle interventions in humans, including diet changes, could only partially reverse specific DNA methylation changes¹⁶⁻¹⁸. Therefore some questions remain: is the hypermethylation of lipid metabolic genes, including PPAR α target genes, only a consequence of diet or could it also be driven by the loss of PPAR α ? Is this process epigenetically regulated by PPAR α or only induced by the loss of a transcription factor?

In Chapter 3 we explored the role of PPAR α in the epigenetic reprogramming of the lipid metabolism in MASLD via expression and methylation profile analysis of hepatocyte-specific PPAR α KO mice. Regarding the first question, we showed that a diet-induced downregulation of PPAR α strongly resembles a genetic hepatocyte-specific loss of PPAR α on a control chow diet, both inducing a MASLD gene signature. Moreover, both show a similar methylation signature inducing an epigenetic shift of the lipid and bile acid homeostasis, including hypermethylation of PPAR α target genes, to ferroptosis and pyroptosis lipotoxicity driving MASLD progression. Together these results show that, besides diet, the loss of PPAR α has an important driver function in the epigenetic shift towards lipotoxicity and MASLD progression (Figure 1). This suppressor role of PPAR α in preventing lipotoxicity by epigenetically reprogramming the lipid metabolism has also been shown in lactation research. Milk lipids will activate PPAR α in the postnatal period and thereby reprogram the lipid metabolism by demethylation of PPAR α target genes to adapt to the changes in nutritional environment^{19,20}.

Regarding the second question, remarkably PPAR α was found as one of the main transcription factors of the hypermethylated lipid-related genes, inducing a differential expression of a lot of PPAR α target genes. A few studies in colon cancer have shown an inhibitory effect of PPAR α on DNMT1 via the activation of other transcription factors including Rb1^{21,22}. Since, our data also shows a diet or genetic loss of PPAR α induced upregulation and PPRE binding motif in epigenetic regulating enzymes Uhrf1²³⁻²⁵ and E2F1²⁶, this suggest an indirect epigenetic regulatory function of PPAR α in the epigenetic reprogramming of its target genes. Besides, PPAR α has shown to interact with histone modifying enzymes (including PRMT, JMJD, SIRT, HDACs) and form a positive autoregulatory loop or reciprocal transcriptional crosstalk. For example the JMJD3- SIRT1-PPAR α complex that is formed to regulate the β -oxidation network, is abolished when one of the genes is downregulated or both the SIRT1 and PPAR α transcriptional network have been reported to depend on the interaction of both proteins²⁷. Since our data shows a downregulation of PPAR α , this could indicate that these interactions are lost and thereby change the histone modification landscape of the PPAR α transcriptional network and thereby change its expression. In addition, the upregulation of epigenetic enzymes and the disruption of the PPAR α transcriptional network by the loss of PPAR α function, suggests a reciprocal upregulation of epigenetic enzymes in order to try to restore cellular homeostasis. Recently, more investigation is focused on the interplay between histone modifications and DNA methylation, showing that histone modifications can influence DNA methylation and vice versa²⁸. Fu et al. showed a positive correlation between CpG methylation and H3K9 methylation, and a negative correlation with H3K4 methylation²⁹. Interestingly, lipid accumulation has been reported to specifically alter the H3K9 and H3K4 methylation of the PPAR α network³⁰. Therefore it is interesting to speculate that the loss of PPAR α could also change the histone modification landscape of its target genes, as well as its DNA methylation state, by crosstalk of histone modifying with DNA (hydroxy)methylation enzymes.

Altogether, our data strongly suggest an indirect epigenetic driver (suppressor) function of PPAR α

in the regulation of its target genes. Although this work was mostly focused on the effects on lipid metabolism, further characterisation of PPAR α 's epigenetic protein interaction partners responsible for reprogramming the lipid metabolism may also reveal novel insights for targeting lipid-metabolism dependent chronic inflammation. As reviewed by Christofides, A. et al., PPAR α also has a profound role in the regulation of T cell responses and macrophage mediated inflammation³¹. Interestingly, PPAR α agonists have been reported to increase Foxp3 expression in human iTreg (functional Foxp3+ regulatory T cells) through demethylation by a downregulation of DNMTs³². Therefore together with our results, it could be worth trying combination therapies of PPAR agonist with epigenetic pharmacological compounds (*e.g.* metformin, vitamin E, berberin) that have been tested before to further pave the way towards polypharmacological medicine targeting more than one aspect of the disease^{5,33}.

Mitochondrial dysfunction is a hallmark of various diseases, including MASLD³⁴. However, the pathways inducing this metabolic dysfunction are often not fully understood. Mitochondria contain their own DNA (mtDNA) which is circular, organised in nucleoids without histones and only has two promoters that generate polycistronic RNA. Since this organisation is different from that of the nuclear DNA, a lot of questions remain about the epigenetic regulation of mtDNA and its possible impact on mitochondrial function(s). In Chapter 4 and 5 we investigated whether MASLD is associated with a mtDNA methylation signature by nanopore episequencing and whether this could influence mitochondrial metabolic functions related to MASLD disease progression. Does mtDNA methylation exist in MASLD? Can mitochondrial methylation become a new biomarker for MASLD stratification? Are these changes related to changes in mitochondrial functioning? Has mtDNA methylation therapeutic possibilities for MASLD?

Different techniques have been used previously to investigate mtDNA methylation, including methylation specific PCR and pyrosequencing³⁵. However all of these techniques are based on prior bisulfite conversion, which induces overestimation of methylation percentages because of the circular structure of the mtDNA³⁶. Therefore in chapter 4, we first optimised nanopore episequencing to specifically sequence mtDNA, without prior bisulfite conversion. With this technique we showed that an *in vitro* steatosis treatment of 1mM FFA for 24h induces a clear accumulation of lipid droplets, accompanied with hypermethylation of several electron transport chain (ETC) genes and mitochondrial tRNAs. Gene body methylation of the nuclear DNA is mostly related to an upregulation of gene expression, while hypermethylation of the promotor region is mostly associated with downregulation^{37,38}. Interestingly, in mitochondria some studies have also pointed to a direct role of gene body methylation on mitochondrial gene expression, by affecting post-transcriptional modifications of polycistronic mitochondrial mRNAs^{35,39,40}. Of special note, dysregulation of post-transcriptional (epi-transcriptomic) modifications of mitochondrial RNA, but especially tRNA, have shown a role in mitochondrial dysfunction in different metabolic diseases and therefore received growing interest in the last few years^{41,42}. More specially, processing of the mitochondrial polycistronic RNA is regulated by a process called tRNA punctuation. This model is based on the principal that most of the mitochondrial encoded mRNAs and rRNAs are separated by a tRNA. After transcription, these tRNAs are specifically targeted for modifications and cleaved out of the polycistronic RNA transcripts to be further processed and matured^{43,44}. Interestingly, the latter is largely affected by both mutations and incorrect methylation that prevent correct folding and thus influence stability and recognition of tRNA. Therefore both mutations and incorrect mitochondrial tRNA methylation, induce the accumulation of unprocessed tRNAs. The latter, largely

affects correct mitochondrial protein translation and therefore disturbs mitochondrial metabolic homeostasis which is related to different diseases^{45–48}. Hence, the gene body methylation of tRNAs found in this work, could provide new insights in post-transcriptional tRNA modifications that effect RNA punctuation and thereby change mitochondrial functioning in MASLD. Besides, changes of mtDNA methylation have been proposed as potential new biomarkers in cancer research. However as reviewed by Mohd Khair et al. it seems that mtDNA methylation changes are cell type specific e.g. hypermethylation of the D-loop has been correlated with breast cancer risk, while lower mtDNA methylation was detected in cervix cancer^{49–51}. Therefore the methylation signature for MASLD we observed in our pilot study of 2 samples holds promise as potential novel mitochondrial biomarker which needs further validation in patient samples and animal models.

Our data also showed in both chapters that mtDNA is more prone to CpG than GpC methylation, although overall methylation percentages on the mtDNA are relatively low compared to the nuclear DNA. Therefore people may question the biological relevance of mtDNA methylation regulation? However, in chapter 5 we showed that an artificial increase of 20% of mtDNA methylation induces clear metabolic stress. Mitochondria showed swelling, disruption of the cristae structure and basal overactivation of mitochondrial respiration. Besides, GpC more than CpG methylation induced increase of bile acid metabolism, whereas both induced accumulation of lipid droplets and a clear upregulation of mitophagy or cholestophagy. Together, this suggests that mitochondrial methylation induces mitochondrial dysfunction (or damage) that needs to be cleared out of the cell (Figure 1). Interestingly, both mitochondrial swelling and overactivation of mitochondrial respiration are hallmarks of the progression from mitochondrial adaptation to the constant accumulation of lipids towards mitochondrial dysfunction in MASLD^{52–55}. Moreover, recently bile acid metabolism dysregulation has been associated with MASLD progression and therefore became a new topic of interest in the research towards MASLD therapeutics. Bile acids (BA) are produced from cholesterol in the liver and are a major component of bile. The primary BA cholic acid (CA) and chenodeoxycholic acid (CDCA) are further conjugated with glycine or taurine and stored as bile in the gallbladder. After food consumption, these bile acids will be released in the intestinal tract to facilitate the uptake of lipids and liposoluble vitamins. Next, in the intestine primary bile acids are converted into secondary BA (deoxycholic acid (DCA) and lithocholic acid (LCA)) by bacteria and reabsorbed by the liver via the portal vein⁵⁶. Both primary and secondary BAs interact with nuclear receptors including the farnesoid X receptor (FXR), pregnane X receptor (PXR), and vitamin D receptor (VDR) with specific affinities and thereby regulate hepatic lipid and glucose metabolism. Therefore changes in the BA size or composition will induce a different stimulation of the nuclear receptors and therefore changes in lipid metabolism⁵⁷. It has been shown that the progression of metabolic dysfunction-associated steatohepatitis (MASH) is associated with an accumulation of primary and conjugated primary BA. In contrary to secondary and unconjugated BA, these BA only weakly activate the FXR receptor⁵⁸. Therefore several FXR agonists have been tested in preclinical trials as MASLD therapy and have shown promising results, emphasizing the important role of bile acids in MASLD^{59–61}. In this cellular context, damaged mitochondria are prone to selective removal by mitophagy or bile acid induced cholestophagy via the autophagy quality control pathway to preserve metabolic homeostasis. However, mitophagy is often perturbed in metabolic diseases, including MASLD. Moreover, disruption of mitophagy has been suggested as an early hit in the progression of MASLD, because it is already clearly disrupted by a high fat diet^{62,63}. Therefore currently more therapies that promote mitophagy are tested in animal studies, showing promising

results^{62,64–66}.

Together, these results show for the first time that mitochondrial methylation is closely related to mitochondrial dysfunction and early signs of MASLD progression. Therefore, we are convinced that studying low percentages of mitochondrial methylation has significant impact on early signs of metabolic disorders. Although these changes might be more subtle, MASLD progression is known to depend on the combination of multiple hits where the combination of even subtle changes can make a big difference in the MASLD outcome⁶⁷. Moreover, the contribution of mitochondrial methylation opens new perspectives in the research toward regulatory pathways of mitochondrial dysfunction in MASLD.

Furthermore, there is a close interaction between the nucleus and mitochondria to adapt to different environmental changes and thereby maintain cellular homeostasis, called mito-nuclear communication⁶⁸. However, the exact regulatory pathways of this communication have not yet been fully resolved. Since previous results have demonstrated gene expression changes associated with mitochondrial DNA methylation, this raises the question whether there is a “driver” function for mitochondrial methylation in this communication? Previously, Vivian et al. showed that mice containing exactly the same nuclear DNA, show changes in methylation profile and gene expression when combined with mitochondria from different mouse strains containing different mutations⁶⁹. Similar, Ishikwa et al. showed that replacing mitochondria of a poorly metastatic mouse tumour cell line with mitochondria of a highly metastatic mouse tumour cell line with mutation in the mitochondrial ND6 gene, changed the metastatic potential of the cell line to highly metastatic⁷⁰. Both studies emphasize the crucial role of mitochondria in the regulation of gene expression and overall cellular homeostasis. In line, our results in chapter 5 showed that mitochondrial GpC methylation induces an upregulation of the bile acid metabolism by differential methylation of bile acid metabolic genes. It is assumed that this close interaction is regulated by changes in the metabolites produced by mitochondria. Mitochondria produce important metabolites for epigenetic regulation including α -ketoglutarate, succinate and fumarate that influence the activity of Ten-eleven Translocation (TET) demethylases, but also methionine which is essential in the methyl donor carbon cycle to keep up S-adenosyl-methionine (SAM) concentrations⁷¹. Interestingly, in chapter 5 we showed that both mitochondrial CpG and GpC change mitochondrial function, which is closely related with changes in metabolite levels. Together these results could add another regulatory layer in the complicated mito-nuclear communication whereby mitochondrial methylation determines the metabolite pool available for nuclear gene methylation and expression and thereby overall cellular homeostasis.

6.2 Conclusion and Future perspectives

The results of this dissertation open new research perspectives towards epigenetic diagnostic biomarkers and therapeutics for MASLD. We have shown that the important direct role in lipid metabolism of both PPAR α and mitochondria, is largely controlled by epigenetics but at the same time also defines the epigenetic progression of MASLD. However more in depth research is necessary to characterize the exact chromatin/methylation modifying interaction partners and to map the most predictive epigenetic biomarkers.

PPAR α has shown to be a promising epigenetic regulator in MASLD. However the exact epigenetic interaction partners that help to control the lipid metabolism could not be identified and need further investigation. Therefore some proteomic PPAR α interactome or biotin proximity ligation study could shed light on this topic. Besides, this research was performed in whole liver cell lysates including a mix of hepatocytes, Kupffer cells and stellate cells. These cells have different functions with hepatocytes as the main building blocks of the liver that maintain basic functions of the liver including lipid metabolism; Kupffer cells as the largest population of tissue macrophages that control liver inflammation; and stellate cells are responsible for lipid storage and production of extracellular matrix upon liver injury. Although PPAR α is mostly expressed in hepatocytes, the other non-parenchymal cells also express lower amounts of PPAR α ⁷². Therefore it would be interesting to check the interplay of PPAR α expression with epigenetic enzyme regulation in the different cell types and different stages of MASLD, with spatial transcriptomics. Moreover, because PPARA gradually decreases in MASLD¹¹, it is interesting to further characterize longitudinal changes in methylation of its target genes over the different stages of MASLD in patient samples. This could generate new biomarker opportunities for stratification of patients and thereby better predict therapeutic outcomes.

Although mitochondrial methylation has been a subject of discussion for many years, we have shown that mitochondrial methylation induces clear metabolic and gene expression changes that are important in MASLD progression. However, in this PhD work these results were performed on one overexpression model. Therefore follow-up studies need to define whether these metabolic changes are cell-type specific and if the effect of lower methylation percentages are similar. A follow-up study that could specifically show the impact of mitochondrial methylation effects related to MASLD, is an experiment that replaces the mitochondria of healthy cells by MASLD mitochondria. Similar to the results based on mitochondrial mutations, this would show the contribution of mitochondrial methylation in MASLD development. Moreover, this could further highlight if the amount of mitochondrial dysfunction is correlated with the percentages of methylation. In addition, although the role and presence of methylation is more characterized in both nuclear and mitochondrial DNA, hydroxymethylation forms another interesting layer of epigenetic control on expression. Hydroxymethylation has shown to effect gene expression and has been detected in a dynamic way on mtDNA⁷³. Interestingly, a recent study showed that helper T cells can be distinguished based on differences in methylation and hydroxymethylation in specific genomic loci characterised by Nanopore sequencing⁷⁴. Thus, following the results in this PhD it is interesting to also look for the role mitochondrial hydroxymethylation in mitochondrial dysfunction related to MASLD.

Besides, as shown in this work, bile acid metabolism is largely affected by the mito-nuclear communication induced by mitochondrial methylation. Although this could be largely defined by

changes in the metabolite pool, further investigation should look into the epigenetic changes of the nuclear encoded mitochondrial genes that also define mitochondrial functioning. The combination of studying this retrograde and anterograde communication, will give interesting insights into the complicated epigenetic communication between mitochondria and the nucleus.

Regarding future therapeutic strategies, MASLD is a multisystemic disease that may require precision medicine approaches to apply combination therapy by dual targeting PPAR α and mitochondrial metabolic functions. Since we found that PPAR α target genes are both epigenetically controlled by PPAR α and mitochondrial methylation, dual pharmacological targeting of PPAR α and mitochondrial functions may open new opportunities for more effective MASLD treatment.

6.3 References

1. Wang, D. *et al.* Changes in the global, regional, and national burdens of NAFLD from 1990 to 2019: A systematic analysis of the global burden of disease study 2019. *Front Nutr* **9**, (2022).
2. Dufour, J.-F., Caussy, C. & Loomba, R. Combination therapy for non-alcoholic steatohepatitis: rationale, opportunities and challenges. *Gut* **69**, 1877–1884 (2020).
3. Harrison, S. A. *et al.* A blood-based biomarker panel (NIS4) for non-invasive diagnosis of non-alcoholic steatohepatitis and liver fibrosis: a prospective derivation and global validation study. *Lancet Gastroenterol Hepatol* **5**, 970–985 (2020).
4. Mantovani, A. & Dalbeni, A. Treatments for NAFLD: State of Art. *Int J Mol Sci* **22**, 2350 (2021).
5. Francque, S. M. Towards precision medicine in non-alcoholic fatty liver disease. *Rev Endocr Metab Disord* (2023) doi:10.1007/s11154-023-09820-6.
6. Francque, S. *et al.* Nonalcoholic steatohepatitis: the role of peroxisome proliferator-activated receptors. *Nat Rev Gastroenterol Hepatol* **18**, 24–39 (2021).
7. Amorim, R., Magalhães, C. C., Borges, F., Oliveira, P. J. & Teixeira, J. From Non-Alcoholic Fatty Liver to Hepatocellular Carcinoma: A Story of (Mal)Adapted Mitochondria. *Biology (Basel)* **12**, 595 (2023).
8. Ferguson, D. & Finck, B. N. Emerging therapeutic approaches for the treatment of NAFLD and type 2 diabetes mellitus. *Nat Rev Endocrinol* **17**, 484–495 (2021).
9. Rodríguez-Sanabria, J. S., Escutia-Gutiérrez, R., Rosas-Campos, R., Armendáriz-Borunda, J. S. & Sandoval-Rodríguez, A. An Update in Epigenetics in Metabolic-Associated Fatty Liver Disease. *Front Med (Lausanne)* **8**, (2022).
10. Lai, Z. *et al.* Association of Hepatic Global DNA Methylation and Serum One-Carbon Metabolites with Histological Severity in Patients with NAFLD. *Obesity* **28**, 197–205 (2020).
11. Francque, S. *et al.* PPAR α gene expression correlates with severity and histological treatment response in patients with non-alcoholic steatohepatitis. *J Hepatol* **63**, (2015).
12. Hajri, T., Zaiou, M., Fungwe, T. V., Ouguerram, K. & Besong, S. Epigenetic Regulation of Peroxisome Proliferator-Activated Receptor Gamma Mediates High-Fat Diet-Induced Non-Alcoholic Fatty Liver Disease. *Cells* **10**, 1355 (2021).
13. Ohashi, K. *et al.* High fructose consumption induces DNA methylation at PPAR α and CPT1A promoter regions in the rat liver. *Biochem Biophys Res Commun* **468**, 185–189 (2015).
14. Li, Y. Y. *et al.* Fatty liver mediated by peroxisome proliferator-activated receptor- α DNA methylation can be reversed by a methylation inhibitor and curcumin. *J Dig Dis* **19**, 421–430 (2018).
15. Yoon, A., Tammen, S. A., Park, S., Han, S. N. & Choi, S.-W. Genome-wide hepatic DNA methylation changes in high-fat diet-induced obese mice. *Nutr Res Pract* **11**, 105 (2017).

16. Yaskolka Meir, A. *et al.* Effects of lifestyle interventions on epigenetic signatures of liver fat: Central randomized controlled trial. *Liver International* **41**, 2101–2111 (2021).
17. Maugeri, A. The Effects of Dietary Interventions on DNA Methylation: Implications for Obesity Management. *Int J Mol Sci* **21**, 8670 (2020).
18. Sokolowska, K. E. *et al.* Identified in blood diet-related methylation changes stratify liver biopsies of NAFLD patients according to fibrosis grade. *Clin Epigenetics* **14**, 157 (2022).
19. Hashimoto, K. & Ogawa, Y. Epigenetic Switching and Neonatal Nutritional Environment. *Adv Exp Med Biol* **1012**, 19–25 (2018).
20. Ehara, T. *et al.* Ligand-activated PPARalpha-dependent DNA demethylation regulates the fatty acid beta-oxidation genes in the postnatal liver. *Diabetes* **64**, 775–784 (2015).
21. Kong, R., Wang, N., Han, W., Bao, W. & Lu, J. Fenofibrate Exerts Antitumor Effects in Colon Cancer via Regulation of DNMT1 and CDKN2A. *PPAR Res* **2021**, 6663782 (2021).
22. Luo, Y. *et al.* Intestinal PPARalpha Protects Against Colon Carcinogenesis via Regulation of Methyltransferases DNMT1 and PRMT6. *Gastroenterology* **157**, 744-759 e4 (2019).
23. Lin, S. *et al.* UHRF1/DNMT1–MZF1 axis-modulated intragenic site-specific CpGI methylation confers divergent expression and opposing functions of PRSS3 isoforms in lung cancer. *Acta Pharm Sin B* **13**, 2086–2106 (2023).
24. Li, T. *et al.* Structural and mechanistic insights into UHRF1-mediated DNMT1 activation in the maintenance DNA methylation. *Nucleic Acids Res* **46**, 3218–3231 (2018).
25. Liu, X. *et al.* UHRF1 targets DNMT1 for DNA methylation through cooperative binding of hemimethylated DNA and methylated H3K9. *Nat Commun* **4**, 1563 (2013).
26. McCabe, M. T., Davis, J. N. & Day, M. L. Regulation of DNA Methyltransferase 1 by the pRb/E2F1 Pathway. *Cancer Res* **65**, 3624–3632 (2005).
27. Theys, C., Lauwers, D., Perez-Novio, C. & Vanden Berghe, W. PPAR α in the Epigenetic Driver Seat of NAFLD: New Therapeutic Opportunities for Epigenetic Drugs? *Biomedicines* **10**, (2022).
28. Li, Y., Chen, X. & Lu, C. The interplay between DNA and histone methylation: molecular mechanisms and disease implications. *EMBO Rep* **22**, (2021).
29. Fu, K., Bonora, G. & Pellegrini, M. Interactions between core histone marks and DNA methyltransferases predict DNA methylation patterns observed in human cells and tissues. *Epigenetics* **15**, 272–282 (2020).
30. Jun, H.-J., Kim, J., Hoang, M.-H. & Lee, S.-J. Hepatic Lipid Accumulation Alters Global Histone H3 Lysine 9 and 4 Trimethylation in the Peroxisome Proliferator-Activated Receptor Alpha Network. *PLoS One* **7**, e44345 (2012).
31. Christofides, A., Konstantinidou, E., Jani, C. & Boussiotis, V. A. The role of peroxisome proliferator-activated receptors (PPAR) in immune responses. *Metabolism* **114**, 154338 (2021).

32. Lei, J., Hasegawa, H., Matsumoto, T. & Yasukawa, M. Peroxisome Proliferator-Activated Receptor α and γ Agonists Together with TGF- β Convert Human CD4+CD25⁻ T Cells into Functional Foxp3+ Regulatory T Cells. *The Journal of Immunology* **185**, 7186–7198 (2010).
33. Sodum, N., Kumar, G., Bojja, S. L., Kumar, N. & Rao, C. M. Epigenetics in NAFLD/NASH: Targets and therapy. *Pharmacol Res* **167**, 105484 (2021).
34. Diaz-Vegas, A. *et al.* Is Mitochondrial Dysfunction a Common Root of Noncommunicable Chronic Diseases? *Endocr Rev* **41**, (2020).
35. Rots, M. G. Regulation of mitochondrial gene expression the epigenetic enigma. *Frontiers in Bioscience* **22**, 4535 (2017).
36. Goldsmith, C. *et al.* Low biological fluctuation of mitochondrial CpG and non-CpG methylation at the single-molecule level. *Sci Rep* **11**, 8032 (2021).
37. Wang, Q. *et al.* Gene body methylation in cancer: molecular mechanisms and clinical applications. *Clin Epigenetics* **14**, 154 (2022).
38. Jones, P. A. The DNA methylation paradox. *Trends in Genetics* **15**, 34–37 (1999).
39. Aminuddin, A., Ng, P. Y., Leong, C.-O. & Chua, E. W. Mitochondrial DNA alterations may influence the cisplatin responsiveness of oral squamous cell carcinoma. *Sci Rep* **10**, 7885 (2020).
40. Sun, X., Johnson, J. & St. John, J. C. Global DNA methylation synergistically regulates the nuclear and mitochondrial genomes in glioblastoma cells. *Nucleic Acids Res* **46**, 5977–5995 (2018).
41. Boughanem, H. *et al.* The emergent role of mitochondrial $\langle\text{sc}\rangle\text{RNA}\langle/\text{sc}\rangle$ modifications in metabolic alterations. *WIREs RNA* **14**, (2023).
42. Bohnsack, M. T. & Sloan, K. E. The mitochondrial epitranscriptome: the roles of RNA modifications in mitochondrial translation and human disease. *Cellular and Molecular Life Sciences* **75**, 241–260 (2018).
43. Temperley, R. J., Wydro, M., Lightowers, R. N. & Chrzanowska-Lightowers, Z. M. Human mitochondrial mRNAs--like members of all families, similar but different. *Biochim Biophys Acta* **1797**, 1081–5 (2010).
44. Ojala, D., Montoya, J. & Attardi, G. tRNA punctuation model of RNA processing in human mitochondria. *Nature* **290**, 470–4 (1981).
45. Helm, M. & Attardi, G. Nuclear Control of Cloverleaf Structure of Human Mitochondrial tRNALys. *J Mol Biol* **337**, 545–560 (2004).
46. Delaunay, S. *et al.* Mitochondrial RNA modifications shape metabolic plasticity in metastasis. *Nature* **607**, 593–603 (2022).
47. Idaghdour, Y. & Hodgkinson, A. Integrated genomic analysis of mitochondrial RNA processing in human cancers. *Genome Med* **9**, 36 (2017).
48. Stewart, J. B. *et al.* Simultaneous DNA and RNA Mapping of Somatic Mitochondrial Mutations across Diverse Human Cancers. *PLoS Genet* **11**, e1005333 (2015).

49. Sun, X. *et al.* Increased mtDNA copy number promotes cancer progression by enhancing mitochondrial oxidative phosphorylation in microsatellite-stable colorectal cancer. *Signal Transduct Target Ther* **3**, 8 (2018).
50. Han, X. *et al.* Maternal trans-general analysis of the human mitochondrial DNA pattern. *Biochem Biophys Res Commun* **493**, 643–649 (2017).
51. Mohd Khair, S. Z. N., Abd Radzak, S. M. & Mohamed Yusoff, A. A. The Uprising of Mitochondrial DNA Biomarker in Cancer. *Dis Markers* **2021**, 1–20 (2021).
52. Sanyal, A. J. *et al.* Nonalcoholic steatohepatitis: Association of insulin resistance and mitochondrial abnormalities. *Gastroenterology* **120**, 1183–1192 (2001).
53. Rector, R. S. *et al.* Mitochondrial dysfunction precedes insulin resistance and hepatic steatosis and contributes to the natural history of non-alcoholic fatty liver disease in an obese rodent model. *J Hepatol* **52**, 727–736 (2010).
54. Ramanathan, R., Ali, A. H. & Ibdah, J. A. Mitochondrial Dysfunction Plays Central Role in Nonalcoholic Fatty Liver Disease. *Int J Mol Sci* **23**, 7280 (2022).
55. Koliaki, C. *et al.* Adaptation of Hepatic Mitochondrial Function in Humans with Non-Alcoholic Fatty Liver Is Lost in Steatohepatitis. *Cell Metab* **21**, 739–746 (2015).
56. Di Ciaula, A. *et al.* Bile Acid Physiology. *Ann Hepatol* **16**, S4–S14 (2017).
57. Chiang, J. Y. L. Bile Acid Metabolism and Signaling. in *Comprehensive Physiology* 1191–1212 (Wiley, 2013). doi:10.1002/cphy.c120023.
58. Radun, R. & Trauner, M. Role of FXR in Bile Acid and Metabolic Homeostasis in NASH: Pathogenetic Concepts and Therapeutic Opportunities. *Semin Liver Dis* **41**, 461–475 (2021).
59. Shah, R. A. & Kowdley, K. V. Obeticholic acid for the treatment of nonalcoholic steatohepatitis. *Expert Rev Gastroenterol Hepatol* **14**, 311–321 (2020).
60. Schumacher, J. D. & Guo, G. L. Pharmacologic Modulation of Bile Acid-FXR-FGF15/FGF19 Pathway for the Treatment of Nonalcoholic Steatohepatitis. in 325–357 (2019). doi:10.1007/164_2019_228.
61. Clifford, B. L. *et al.* FXR activation protects against NAFLD via bile-acid-dependent reductions in lipid absorption. *Cell Metab* **33**, 1671-1684.e4 (2021).
62. Zhu, L., Wu, X. & Liao, R. Mechanism and regulation of mitophagy in nonalcoholic fatty liver disease (NAFLD): A mini-review. *Life Sci* **312**, 121162 (2023).
63. Sun, N. *et al.* Measuring In Vivo Mitophagy. *Mol Cell* **60**, 685–696 (2015).
64. Tian, C. *et al.* MRG15 aggravates non-alcoholic steatohepatitis progression by regulating the mitochondrial proteolytic degradation of TUFM. *J Hepatol* **77**, 1491–1503 (2022).
65. Cai, J. *et al.* The protective effect of selenoprotein M on non-alcoholic fatty liver disease: the role of the AMPK α 1–MFN2 pathway and Parkin mitophagy. *Cellular and Molecular Life Sciences* **79**, 354 (2022).

66. Dong, Y. *et al.* Hydroxytyrosol Promotes the Mitochondrial Function through Activating Mitophagy. *Antioxidants* **11**, 893 (2022).
67. Buzzetti, E., Pinzani, M. & Tsochatzis, E. A. The multiple-hit pathogenesis of non-alcoholic fatty liver disease (NAFLD). *Metabolism* **65**, 1038–1048 (2016).
68. Janssen, J. J. E., Grefte, S., Keijer, J. & de Boer, V. C. J. Mito-Nuclear Communication by Mitochondrial Metabolites and Its Regulation by B-Vitamins. *Front Physiol* **10**, (2019).
69. Vivian, C. J. *et al.* Mitochondrial Genomic Backgrounds Affect Nuclear DNA Methylation and Gene Expression. *Cancer Res* **77**, 6202–6214 (2017).
70. Ishikawa, K. *et al.* ROS-Generating Mitochondrial DNA Mutations Can Regulate Tumor Cell Metastasis. *Science (1979)* **320**, 661–664 (2008).
71. F. C. Lopes, A. Mitochondrial metabolism and DNA methylation: a review of the interaction between two genomes. *Clin Epigenetics* **12**, 182 (2020).
72. Berthier, A., Johanns, M., Zummo, F. P., Lefebvre, P. & Staels, B. PPARs in liver physiology. *Biochim Biophys Acta Mol Basis Dis* **1867**, 166097 (2021).
73. Ghosh, S., Sengupta, S. & Scaria, V. Hydroxymethyl cytosine marks in the human mitochondrial genome are dynamic in nature. *Mitochondrion* **27**, 25–31 (2016).
74. Goldsmith, C. *et al.* Single molecule DNA methylation and hydroxymethylation reveal unique epigenetic identity profiles of T helper cells. *bioRxiv* 2023.02.03.527091 (2023) doi:10.1101/2023.02.03.527091.

Academic Curriculum Vitae

PERSONALIA

Last name: Theys
First name: Claudia
Home address: Hovestraat 169, bus 15
2650 Edegem
Belgium
Date of Birth: 01/12/1996
Email: claudia-theys@hotmail.com
LinkedIn www.linkedin.com/in/claudia-theys-b15607202/

CAREER & EDUCATION

October 2019 – present

Doctor in biochemistry and biotechnology

University of Antwerp

- **PhD thesis entitled:** ‘The new epigenetic driver role of PPAR α and mitochondria in metabolic dysfunction associated liver disease (MASLD), paving the way towards new therapeutics and diagnostic biomarkers’

September 2017 - June 2019

Master of science in biochemistry and biotechnology

University of Antwerp

- Major: Molecular and cellular neuroscience
- Minor: research
- **Master thesis entitled:** ‘Methylation-based signature for detection and prognosis of prostate cancer’

Promotor: Prof. Dr. Carmen Jerónimo

Co-promotor: Prof. Dr. Wim Vanden Berghe

Graduated with great distinction

September 2014 - June 2017

Bachelor of Science in biochemistry and biotechnology

University of Antwerp

- Bachelor thesis entitled: ‘Generatie en in vivo toepassing van bioluminescente en fluorescente Leishmania stammen’

Promotor: Prof. Dr. Guy Caljon & Prof. Dr. Louis Maes

Graduated with great distinction

EDUCATIONAL ACTIVITIES / STUDENT SUPERVISIONS

Supervisor Bachelor thesis of Line De Vocht, titled: 'Optimalisatie van mitochondriale DNA isolatie om polychloorbiphenyl geïnduceerde mito-epigenetische veranderingen in NAFLD te bepalen'. Academic year 2019-2020 (Biochemistry and Biotechnology, University of Antwerp)

Supervisor Bachelor thesis of Nele Van Giel, titled: 'Karakterisatie en optimalisatie van NAFLD in HepG2 cellen'. Academic year 2020-2021 (Biochemistry and Biotechnology, University of Antwerp)

Supervisor Bachelor thesis of Jade Verreth, titled: 'Unraveling PCBs as an environmental trigger for the pathological development of NAFLD'. Academic year 2021-2022 (Biomedical sciences, University of Antwerp)

Supervisor Bachelor thesis of Cato De Baere and Max De Bisschop, titled: 'Karakterisatie van de gevolgen van mitochondriale methylatie op nucleaire methylatie en morfologie in de context van non-alcoholic fatty liver disease (NAFLD)'. Academic year 2022-2023 (Biomedical sciences, University of Antwerp)

Supervisor Master thesis of Femke Van Daele, titled: 'The dynamic interplay between DNA methylation, stress and appetite regulation'. Academic year 2020-2021 (Biomedical sciences, University of Ghent)

Supervisor Master thesis of Dorien Lauwers, titled: 'Exploring the regulatory role of peroxisome proliferator-activated receptor- α in the epigenetic alterations of NAFLD - Epigenetics and interaction with AMPK'. Academic year 2021-2022 (Biomedical sciences, University of Antwerp)

Supervisor for research stay of 6 months of PhD student Patrycja Jakubek. Academic year 2021-2022 (University of Antwerp Gdansk)

Member of OC B&B

INTERNATIONAL RESEARCH STAYS AND CONFERENCES

June 2022

Clinical Epigenetics international Conference (CLEPIC)

University of Szczecin

Szczecin, Poland

- Selected abstract talk
- Poster presentation

'Elucidation of epigenetic interplay of PPAR-alpha and mitochondrial metabolic functions in non-alcoholic fatty liver disease'

November 2022	<p>Epigenetics and Epigenomics in health and disease <i>Vrije Universiteit Brussel (VUB)</i> <i>Brussels, Belgium</i></p> <ul style="list-style-type: none"> • Poster presentation <p>'Elucidation of PPARα as an epigenetic driver in the progression of non-alcoholic fatty liver disease'</p>
June 2021	<p>Nutrigenomics summer school <i>University of Camerino</i> <i>Camerino, Italy</i> Online</p>
November 2021	<p>13th Nuclear Receptor Receptor Network <i>University of Leiden</i> <i>Leiden, Netherlands</i></p>
February 2019 – May 2019 thesis	<p>Research stay abroad for the completion of my master entitled 'Methylation-based signature for detection and prognosis of prostate cancer'.</p> <p><i>University of Porto</i> Porto, Portugal Instituto Português de Oncologia do Porto FG Research group of Prof. Dr. Carmen Jerónimo</p>

ADDITIONAL SCIENTIFIC TRAINING AND CERTIFICATES

2023	<p>Workshop on the use of the Seahorse and data analysis <i>University of Antwerp</i></p>
2020	<p>R workshop <i>StatUA, University of Antwerp</i></p>
2020	<p>Giving presentations in English <i>ADS, University of Antwerp</i></p>
2019	<p>FELASA Category C attest <i>University of Antwerp</i></p>
2019	<p>Basics of biosafety and Spill training <i>University of Antwerp</i></p>
2019	<p>Creative Problem Solving <i>ADS, University of Antwerp</i></p>

SCIENTIFIC GRANTS AND AWARDS

2015-2017	Certificate for completing the extracurricular Honours college at the University of Antwerp
2019	FBD Faculty Award of the University of Antwerp for top graduated master student

PUBLICATION LIST

1. **Theys, C.**; Ibrahim, J.; Mateiu, L.; Mposhi, A.; García-Pupo, L.; De Pooter, T.; De Rijk, P.; Strazisar, M.; İnce, İ.A.; Vintea, I.; et al. Mitochondrial GpC and CpG DNA Hypermethylation Cause Metabolic Stress-Induced Mitophagy and Cholestophagy. *Int. J. Mol. Sci.* 2023, 24, 16412. <https://doi.org/10.3390/ijms242216412>
2. **Theys C**, Lauwers D, Perez-Novo C, Vanden Berghe W. PPAR α in the Epigenetic Driver Seat of NAFLD: New Therapeutic Opportunities for Epigenetic Drugs? *Biomedicines*. 2022 Nov 25;10(12):3041. doi: 10.3390/biomedicines10123041. PMID: 36551797; PMCID: PMC9775974.
3. Mposhi A, Cortés-Mancera F, Heegsma J, de Meijer VE, van de Sluis B, Sydor S, Bechmann LP, **Theys C**, de Rijk P, De Pooter T, Vanden Berghe W, İnce İA, Faber KN, Rots MG. Mitochondrial DNA methylation in metabolic associated fatty liver disease. *Front Nutr.* 2023 May 25;10:964337. doi: 10.3389/fnut.2023.964337. PMID: 37305089; PMCID: PMC10249072.
4. Lin A, Sahun M, Biscop E, Verswyvel H, De Waele J, De Backer J, **Theys C**, Cuypers B, Laukens K, Berghe WV, Smits E, Bogaerts A. Acquired non-thermal plasma resistance mediates a shift towards aerobic glycolysis and ferroptotic cell death in melanoma. *Drug Resist Updat.* 2023 Mar;67:100914. doi: 10.1016/j.drug.2022.100914. Epub 2022 Dec 29. PMID: 36630862.
5. Rodriguez-Gonzalez JC, Hernández-Balmaseda I, Declerck K, Pérez-Novo C, Logie E, **Theys C**, Jakubek P, Quiñones-Maza OL, Dantas-Cassali G, Carlos Dos Reis D, Van Camp G, Lopes Paz MT, Rodeiro-Guerra I, Delgado-Hernández R, Vanden Berghe W. Antiproliferative, Antiangiogenic, and Antimetastatic Therapy Response by Mangiferin in a Syngeneic Immunocompetent Colorectal Cancer Mouse Model Involves Changes in Mitochondrial Energy Metabolism. *Front Pharmacol.* 2021 Dec 3;12:670167. doi: 10.3389/fphar.2021.670167. PMID: 34924998; PMCID: PMC8678272.